NTIA Report 83-120

Optimum Reception in Non-Gaussian Electromagnetic Interference Environments: II. Optimum and Suboptimum Threshold Signal Detection in Class A and B Noise

D. Middleton
A.D. Spaulding

U.S. DEPARTMENT OF COMMERCE
Malcom Baldrige, Secretary

Susan G. Stuebing, Acting Assistant Secretary
for Communications and Information

May 1983

PREFACE

This is the second in a series of studies by the present authors which addresses the critical problem of signal detection in highly nongaussian electromagnetic interference (EMI) environments. (The first in this series is the Report-OT-75-67, "Optimum Reception in an Impulsive Interference Environment", June 1975, by A.D. Spaulding and D. Middleton, for the Office of Telecommunications - U.S. Dep't. of Commerce [Ref. [1a]], subsequently published in somewhat shorter form in the IEEE Transactions on Communications in 1977, [1b].

Because of the recent development (1974-) of effective, tractable statistical-physical models of typical EMI environment ([2]-[10a]), which provide at least the complete first-order statistics of the received interference (as it appears following the initial linear stages of narrow-band receivers), it has become possible to determine and compare the limiting threshold (i.e. weak-signal) performance of both optimum and conventional receivers in such disturbances. The latter are found to be heavily degraded vis-à-vis the former, because of the highly nongaussian character of these typical telecommunication environments, where both man-made and natural "noise" can and usually do predominate. Optimality is important, since from it one can establish the limiting behaviour of suitably designed receiving algorithms, as well as evaluate the performance of current suboptimum receivers. These results, in turn, are fundamental to the technical basis of effective spectrum use and management. Included here as well, is the aforementioned construction of adequate EMI models and the explicit identification of the pertinent data bases required for both empirical and analytic applications.

These studies accordingly focus on signal detection, with particular attention to the structure of the nongaussian EMI and its "scenario", i.e. propagation laws, source distributions, signal waveforms, etc., as well as the corresponding (desired) signal scenario. In this way observables of the EMI environment are directly incorporated into the results, e.g., optimum signal processing algorithms, suboptimum procedures, and performance measures.

Among the many topics under investigation in this series are: (1), the rôle of the interference class (Class A, B noise) on detection algorithms and performance; (2), the effects of the EMI scenario on performance; (3), the various matched filters appropriate to different propagation conditions for the desired signal; (4), the effects of approximate or inaccurate EMI parameter data on structure and performance (i.e. "robustness" questions); (5), receiver structure and performance for varieties of digital signal waveforms in common usage; and many related problems, which one hopes to examine as the work progresses.

Finally, it should be stressed that, although attention is directed here primarily to (EM) telecommunication environments, the concepts, methods, and results of this work are quite generally applicable to other communication fields and physical systems. This is a direct consequence of the canonical formulation of the detection problem itself, on the one hand, and of the canonical nature of the broad spectrum of interference scenarios encompassed by the recently-developed non-gaussian noise or interference models on the other. Consequently, it is expected that the approaches and results obtained here should have impact well beyond the particular applications to EMI telecommunication systems discussed herein.

TABLE OF CONTENTS

Appendices

PART I. OPTIMAL THRESHOLD DETECTORS

PART II. SUBOPTIMUM THRESHOLD DETECTORS

LIST OF FIGURES

LIST OF TABLES

OPTIMUM RECEPTION IN NONGAUSSIAN ELECTROMAGNETIC INTERFERENCE ENVIRONMENTS: II. OPTIMUM AND SUBOPTIMUM THRESHOLD SIGNAL DETECTION IN CLASS A AND B NOISE*

by

David Middleton** and A.D. Spaulding***

ABSTRACT

In this second part of an ongoing study, the general problem of optimum and suboptimum detection of threshold (i.e. weak) signals in highly non-gaussian interference environments is further developed from earlier work ([1a],[1b];[34]). Both signal processing algorithms and performance measures are obtained canonically, and specifically when the electromagnetic interference environment (EMI) is either Class A or Class B noise. Two types of results are derived: (1), canonical analytic threshold algorithms and performance measures, chiefly error probabilities and probabilities of detection; and (2), various typical numerical results which illustrate the quantitative character of performance. Suboptimum systems are also treated, among them simple cross- and auto-correlators (which are optimum in gaussian interference), and clipper-correlators which employ hard limiters (and are consequently optimum in "Laplace noise"). The various modes of reception considered explicitly here include:(i), coherent and incoherent reception; (ii), "composite" or mixed reception (when there is a nonvanishing coherent component in the received signal; (iii), "on-off" and binary signals, as well as varieties of fading and doppler spread.

---

* Work supported under contract (first author) with the Institute of Telecommunication Sciences (ITS), Boulder Colorado, National Telecommunication and Information Administration (NTIA) of the U.S. Dep't. of Commerce, Wash. D.C. Work also partially supported by the U.S. Dep't. of Defense.

** 127 E. 91 St., New York, N.Y. 10028

***ITS/NTIA of U.S. Dep't. of Commerce, 325 Broadway, Boulder, Colorado 80303.

Both local optimality (LO) and asymptotic optimality (AO) are demonstrated, along with the critical influence of the proper bias in the optimum algorithms, which maintain their LO and AO character as sample size is increased, without having to add additional terms in the original threshold expansion (and thus produce insurmountable system complexity for the very large samples required for effective detection of weak signals). It is shown that for AO, as well as LO, two conditions may be needed to establish the largest magnitude of the minimum detectable input signal which can be permitted and still maintain the optimal character of the algorithm. In addition to the more general Bayes risk and probabilistic measures of performance, Asymptotic Relative Efficiencies (ARE's) are also included and their limitations discussed. A number of numerical examples which illustrate the determination of performance and performance comparisons are provided, with an extensive set of Appendices containing many of the analytic details developed and presented here for future use, as well.

KEY WORDS AND PHRASES:

Threshold signal detection, optimum threshold detection algorithms, performance measures, performance comparisons, electromagnetic interference environments (EMI), suboptimum detectors, locally optimum and asymptotically optimum algorithms; Class A, B noise; correlation detectors; clipper-correlators; error probabilities; minimum detectable signals, processing gain, bias, EMI scenarios; composite threshold detection algorithms; on-off binary signal detection; non-gaussian noise and interference.

1. INTRODUCTION

Nongaussian noise and interference have been recognized for some time [10], [10a] as an increasingly significant factor in the degradation of the performance of most electronic systems and of telecommunication systems in particular [1a,b]. Both natural and man-made noise contribute noticeably here, with the latter becoming the dominant component in most instances, as time goes on. At the same time, most telecommunication systems - specifically receivers - have been designed to be (approximately) optimal against gaussian noise (both internal and external). This has been accomplished by means of "matched filters" ([11],[12]), whose particular structures depend on the mode of reception, i.e., on whether or not reception is "coherent" of "incoherent" [Sec. 19.4, [12]]. Now, because of the growing presence of nongaussian interference of all kinds, these conventional or "classical" (correlation) receivers are found to be badly degraded O(20-50db) typically, and new designs (or "algorithms") for optimality are accordingly required [1a,b], [13].

Analytically quantifiable procedures for optimal signal processing at all desired signal levels in arbitrary interference are not generally possible, however. Thus, to obtain a "general" solution either one must restrict the class of signals and interference, mode of observation, etc., or one must limit the approach to threshold signals, where now there is no restriction on signal type and interference class. Such an approach is accordingly canonical, [14], with several considerable advantages over more specific but less general methods. These advantages are: (i), an explicit operational development of the required optimum signal processing algorithms (i.e. detection or signal extraction); (ii), an explicit formalism for evaluating error-probability performance directly in terms of the various first and second moments of the processing algorithm (vis-à-vis the various hypothesis states involved, e.g. H_0: interference alone, H_1: desired signal plus interference, etc.); and (iii), a similar procedure for obtaining the performance of specified sub-optimum systems in the electromagnetic interference (EMI) environment.

Optimality here is expressed in the general sense of minimum average risk or cost (i.e. Bayes risk ([12], Chapters 18,19), and in the more special sense of minimum probability of error, or maximum probability of correct

signal detection, etc., which is, of course, ultimately embedded in the more general Bayes formalism. Of course, as the signal level increases the signal threshold algorithm is no longer optimum, but it is still better on an absolute basis than it is for very small signals. Moreover, it remains better, in many instances, than the original suboptimum systems to which it is often vastly superior in the threshold régime (as noted above).

For these threshold signals optimality is achieved under the strictly mathematical condition of vanishingly small input signals. In the practical cases, however, as we show here, effective optimality is maintained as long as the small desired input signal does not exceed some upper bound (itself small). [The desired signal is, of course, nonvanishing in all practical applications.] These optimum threshold algorithms can be shown to be optimum in two senses: (i), locally optimum (LO), i.e. essentially yielding the smallest error probabilities for small signals θ, $(0<\theta<\epsilon<<1)$, with finite sample sizes $(n<\infty)$; and (ii), asymptotically optimum (AO), where for these same LO algorithms, the error probabilities (or average risk, more generally) remains minimal (and can approach zero) as sample-size increases indefinitely $(n\to\infty)$. For the latter we emphasize that the structure of these threshold optimum (LO) algorithms remains unchanged as $n\to\infty$, provided the correct bias, $B_n^*(\theta)$, is employed. Without the proper bias term in the threshold algorithm, the processing is suboptimum, and moreover, is not only not LO but is also not AO. [These questions are discussed in detail in Secs. 2.4, 6.1, 6.4, and particularly in Appendix A3 ff.]

The concept of optimum threshold reception is comparatively venerable. Perhaps the first exposition of the concept was presented for detection by Middleton in 1953, 1954, [15] and [16], where the approach was to demonstrate a series development the generalized likelihood function in various orders of cross- and autocorrelation components, mostly non-linear in the received waveform data. Among the important subsequent works are those of Rudnick in 1961 [17], who expressed the threshold detector in an alternative closed form, more useful in applications, and that of Capon [18], also in 1961, who introduced the notion of asymptotic relative efficiences (ARE's) for performance measures.

A further important step, including these earlier advances and embedding the overall approach fully in the Bayes formalism of statistical communication theory ([10]; Section 19.4, Chapter 20, of [12]), was presented by Middleton in 1966 [14]; (see also [21]). Thomas and coworkers ([21]-[24]) have applied these methods, particularly to non-parametric reception, since about 1965; at about the same time Antonov [25], 1967, and a little later Levin and his colleagues ([26]-[28], approx. 1969 and subsequently, used these concepts for signal detection and estimation. More recently (1978), Sheehy for example, has applied these ideas to acoustic signals. [See also [48] for some recent observations on the current status of work in this area.] In this present study we shall use Middleton's 1966 paper [14] as a starting point for the derivation of specific detection algorithms and performance measures, alone the lines, to some extent, of [1a,b], and particularly, [34].

Although the general threshold detection formalism has been available since 1966, cf. [14], its practical applicability has been limited until recently because of the lack of physically realistic and tractable nongaussian noise models. Most of the interference models suggested have been ad hoc attempts to represent such phenomena, without sufficient physical basis and analytic structure to apply generally. This difficulty was largely removed in the mid-70's and subsequently, by the development of statistical-physical models of interference, which are both analytically tractable and well-verified by experiment, [2]-[9]. Specifically, first-order probability distributions and densities have been obtained, with the model parameters themselves determined analytically from the physical EMI scenario involved [8],[9], or empirically [6],[7], when such information is unavailable. These models are canonical also, in the sense that the <u>form</u> of the results is independent of the particular physical mechanism involved, the principal conditions being; (i), that the potential number of possible sources producing the resultant interference be large, and (ii), that each source emits independently of the others [cf. Sec. 3 below].

Two main classes of interference are distinguished: Class A noise, which is "coherent" in the receiver in that it produces negligible transients therein; and Class B noise, which is alternatively "incoherent", producing essentially nothing but transient responses. The former is non-impulsive, while the latter is usually highly impulsive. Typical examples of Class A

interference are other, man-made telecommunications for the same channel or spectral region. Similarly, automobile ignition noise and atmospherics are common types of Class B interference, cf. [6]. We stress the fact that these interference models, and their classification, are not limited to EMI, but apply equally well (with different numerical values, of course) in other physical areas where the same basic source conditions noted above apply.

In the fullest formal sense these general signal processing algorithms (e.g. for detection and extraction) usually require nth-order statistical descriptions of the interference. Fortunately, we can greatly simplify the analysis, without serious loss in either methodology or performance, by using independent (noise) samples. Such procedures are conservative, in that they provide upper bounds on performance, in the sense of larger error probabilities for given input signal levels and sample sizes, or greater signal levels or sample sizes, for the same error probabilities, etc. At the same time we can now use the new canonical statistical-physical interference models noted above, to provide a truly realistic account of the EMI environment in which our signal processing tasks are to be carried out.

Because the parameters of these Class A and B models are themselves derivable from the underlying EMI scenario (i.e. source distribution, propagation law and fading effects, signal structure, etc., (cf. Sec. 3 ff.), we can gain further insight into the rôle of the EMI scenario on system performance, and from this predict how changes in source distributions, propagation conditions, etc., may affect receiver operation. In effect, what we have done by introducing these physically-derived interference models is to show explicitly how the underlying physical mechanisms and conditions can influence system design and behaviour.

In our present study we shall confine our attention to threshold signal detection in canonical Class A or Class B interference, reserving the extension of the analysis to general signal levels along the lines indicated in [1a]) for a subsequent study. Our specific goals are to obtain

(i). the optimum threshold signal detection algorithms for both the coherent and incoherent modes of reception,

(ii). the associated optimum performance for these algorithms, and

(iii). comparisons with selected suboptimum receivers, namely, receivers conventionally optimized against gaussian noise, viz. cross- and auto-correlation detectors, and against impulsive noise, e.g., clipper-correlators.

(iv). An important fourth goal is to study the effects of "mismatch", i.e., when approximate or incorrect parameter values and/or noise distributions are employed in system design and operation.

Accompanying this is the concept of "robustness": how little (or how much) is performance degraded by these various types of "mismatch".

Most of the results to be achieved under the above are new, although a few special cases have been obtained earlier [13]; also [1a,b]. In addition to the analysis, selected numerical results illustrate typical performance situations in typical Class A and B EMI environments. Algorithm structure is shown in a number of "flow diagrams", which indicate the organization of the various operational elements.

Specifically, among the principal new results achieved here are the demonstration of asymptotic optimality (AO) of the (optimum) threshold algorithms, when the correct bias is used, various explicit results for coherent and incoherent detection, including composite detectors when there is a nonvanishing coherent signal component, and upper bounds on the minimum detectable signal, required to preserve optimality of the threshold algorithm. Parallel results for binary signals are similarly obtained.

This Report is organized as follows: Section 2 presents a concise overview of the general threshold theory needed for both matched and mismatched, optimum and suboptimum systems, developed mainly from [14]. Section 3 summarizes the pertinent statistics and EMI scenario and parameter structures needed for the Class A and B interference treated here, based mostly on [6], [9], [13]. Section 4 considers threshold detection algorithms themselves, in detail. Section 5 treats "matched filters" and the operational interpretations of these algorithms, while Section 6 examines the performance of these various optimum and suboptimum detectors in analytic detail. In Section 7 selected numerical results are obtained and discussed, for typical classes of (desired) signal waveforms. Section 8 completes the work with a short discussion of both the principal general and specific results, as well as suggested next steps in the analysis. The Appendices provide most of the

technical details, and the computer software, needed in the main text.

We remark, finally, that the calculated great improvement of systems optimized properly to these highly nongaussian interference environments vis-à-vis conventionally optimized receivers (i.e. against gauss noise) stems fundamentally from the following conditions:

(1), the fact that the former are adaptive systems, which sense the (parameters of the) EMI environment currently with the the detection process, and

(2), the fact that the entire density function (pdf) is then suitably employed to give the correct threshold algorithm, while the latter remain sensitive only to second-moment statistics (which, of course, are sufficient when the noise is gaussian).

The degree of improvement over conventional detectors depends, as expected, on how nongaussian (in intensity and statistical structure) the interference is. When the interference reduces to gauss, so also does the (optimum) detector algorithm, again as we would expect. It should be noted, however, that the degradation of conventional (simple-correlation) receivers is greatly reduced vis-à-vis the optimum algorithm when (sub-optimum) clipper-correlators are employed. Nevertheless, optimum threshold algorithms may still provide a worthwhile improvement, O(3-10db), over the clipper-correlators, particularly when "composite" or mixed coherent and incoherent processing can be employed. In any case, the results of an optimality study are always needed in any effort to assess ultimate performance and practical departures from it. Finally, recent additional studies [49-54] are to be noted for possible extension of present work.

2. GENERAL THRESHOLD DETECTION THEORY:

Threshold detection theory, as is well-known [14], is a general sub-element of the Bayes, or (minimum) average risk theory of signal reception ([19],[12], Chap. 18, et seq.), and as such carries with it all the same general statistical structure and concepts of the latter, more comprehensive formulation. Moreover, the general Bayesian detection theory naturally provides the starting point from which the former is developed. We begin, accordingly, with a very brief summary of the general formalism for both optimum and sub-optimum detection.

2.1 Remarks on General Detection Theory:

Optimum reception, and, in particular optimum detection, is well-known to require the minimization of the probabilities of decision errors. This is achieved (in the usual context of minimizing the average risk, or cost, of decisions) by constructing the "test statistic", or reception algorithm, $\Lambda_n(\underset{\sim}{X}|S)$. Here Λ_n is the (generalized) likelihood ratio, defined in the standard way [Ref. 12, Chapter 18] by

$$\Lambda_n^{(1)} \equiv \frac{p\langle F_n(\underset{\sim}{X}|\underset{\sim}{S})\rangle_S}{q\, F_n(\underset{\sim}{X}|0)} \quad , \tag{2.1}$$

where $\underset{\sim}{X} = (X_1,\ldots,X_n)$ is the set of n samples of received data; $\underset{\sim}{S}$ represents the desired signal; $\langle\ \rangle_S$, the average over the signal or its (possibly) random parameters, while p,q (=1-p) are respectively the a priori probabilities that a received data set $\underset{\sim}{X}$ does or does not contain the desired signal. The quantity $F_n(\underset{\sim}{X}|\underset{\sim}{S})$ is the probability density function for the set $\underset{\sim}{X}$, under the condition of the presence of a signal ($\underset{\sim}{S}$) in the usual fashion. The optimum detection process, then, consists of comparing $\Lambda_n^{(1)}$ (or any monatonic function of $\Lambda_n^{(1)}$ (say, the logarithm, $\log \Lambda_n^{(1)}$)) with a suitably chosen threshold, $\mathcal{K}$, e.g.

$$\left.\begin{aligned} &\underline{\text{decide } H_0}\text{: "no signal present", if } \log \Lambda_n^{(1)} < \log \mathcal{K} \\ &\underline{\text{decide } H_1}\text{: "signal, as well as interference is present", if } \log \Lambda_n^{(1)} \geq \log \mathcal{K} \end{aligned}\right\}. \tag{2.2}$$

Similarly, for non-optimum systems, the reception algorithm, or processing of the data, is some (pre-determined) function, $g(\underset{\sim}{X})$, and the decision process has, like (2.2), the form

$$\left.\begin{aligned} &\underline{\text{decide } H_0}\text{: if } g(\underset{\sim}{X}) < \log K \text{ , e.g. noise alone} \\ &\underline{\text{decide } H_1}\text{: if } g(\underset{\sim}{X}) \geq \log K\text{, e.g. signal as well as noise,} \end{aligned}\right\} \tag{2.3}$$

where now the threshold K is $\mathcal{K}(K)$, and usually $K = a\mathcal{K}$, with a some (positive) constant.

Performance is generally expressed as some linear function of the Type I and Type II error probabilities, (α,β), e.g.

$$\alpha = \alpha(S|N) = \int_{\log \mathcal{K}}^{\infty} w_1(g|0)dg \; ; \; \beta = \beta(N|S) = \int_{-\infty}^{\log \mathcal{K}} w_1(g|S)dg, \tag{2.4a}$$

which for optimal systems, (minimizing average risk), becomes

$$\alpha^* = \int_{\log \mathcal{K}}^{\infty} w_1(g^*|0)dg^* \; ; \; \beta^* = \int_{-\infty}^{\log \mathcal{K}} w_1(g^*|S)dg^* \; . \tag{2.4b}$$

The $w_1(g^*|0)$ etc. are the (1st-order) pdf's with respect to H_0, H_1 of the optimum or suboptimum test statistic or "detection algorithm", $g^* = \log \Lambda_n^{(1)}$ or $g(\underset{\sim}{X})$. The associated average costs or risks are (cf. Secs. (2.3, 2.4, Ref. 20)

$$R^* = \mathcal{L}(\alpha^*,\beta^*) = \mathcal{R}_0 + p(C_0^{(1)} - C_1^{(1)})(\frac{\mathcal{K}}{\mu}\alpha^* + \beta^*) = A_0 + B_0(\frac{\mathcal{K}}{\mu}\alpha^* + \beta^*) \tag{2.5a}$$

$$R = \mathcal{L}(\alpha,\beta) = \mathcal{R}_0 + p(C_0^{(1)} - C_1^{(1)})(\frac{\mathcal{K}}{\mu}\alpha + \beta) = A_0 + B_0(\frac{\mathcal{K}}{\mu}\alpha + \beta) \; , \tag{2.5b}$$

$$\mathcal{K} \equiv [C_0^{(1)} - C_0^{(0)}] / [C_0^{(1)} - C_1^{(1)}] \; (\equiv \mathcal{K}_{01}) \; (>0), \tag{2.5c}$$

so that system comparisons are then logically made on a comparison of R, R^* for the same thresholds $K = \mathcal{K}$, where now $\mu \equiv p/q$. The convention here is that $C^{(j)} = C^{(H_j)}_{(\text{decision})}$: the superscripts refer to the hypothesis state (H_j), and the subscripts to the decisions actually made, and errors naturally "cost" more than correct decisions. [For a detailed development see Ref. 12, Chapter 19, Ref. 20, Chapter 2.]

The formalism above is adapted to the common situation where the alternative reception situation (Hypothesis H_1) is a "signal and noise" as opposed

to H_0: "noise alone". In many telecommunication applications the choice is between two types of signals in noise (or interference), and the test statistic (2.1) becomes now for these binary signal cases.

$$\Lambda_n^{(21)} = \frac{p_2\langle F_n(\underset{\sim}{X}|S_2)\rangle_2}{p_1\langle F_n(\underset{\sim}{X}|S_1)\rangle_1} = \Lambda_n^{(2)}/\Lambda_n^{(1)} \quad \text{with } \Lambda^{(i)} = \text{Eq. (2.1)}; \quad i = 1,2;(S_i) . \tag{2.6}$$

The decision process (2.2) is, correspondingly,

$$\left.\begin{array}{l} \underline{\text{decide } H_1}\text{: "a signal } (S_1) \text{ present in noise", if Log } \Lambda_n^{(21)} < \log \mathcal{K}_{12} \\ \underline{\text{decide } H_2}\text{: "a signal } (S_2) \text{present in noise", if } \log \Lambda_n^{(21)} \geq \log \mathcal{K}_{12} \end{array}\right\}, \tag{2.7}$$

with

$$\mathcal{K}_{12} \equiv (C_2^{(1)} - C_1^{(1)}) / (C_1^{(2)} - C_2^{(2)}) \ (>0). \tag{2.7a}$$

(It is assumed that all signals $\{S_1\}$ are distinct ("disjoint") from all signals $\{S_2\}$, so that there is no ambiguity in establishing correct and incorrect decisions. When the signal classes overlap, however, modifications in the cost assignments, i.e. the selection of the $C_i^{(j)}$ above, must be made: see Sec. 2.2, [20].)

Performance in the case of alternative signal classes is obtained as above [(2.4), (2.5)], now with the obvious notational modifications:

$$\alpha^{(*)} \to \beta_2^{(1)(*)} = \beta^{(*)}(S_2|S_1) = \int_{-\infty}^{\log \mathcal{K}_{12}} w_1(g^{(*)}|H_1)dg^{(*)} ;$$

$$\beta^{(*)} \to \beta_1^{(2)*} = \beta^{(*)}(S_1|S_2) = \int_{\log \mathcal{K}_{12}}^{\infty} w_1(g^{(*)}|H_2)dg^{(*)} , \tag{2.8}$$

where $g^{(*)}$, etc. = g* (=log $\Lambda_n^{(21)}$) or g , etc., and the various w_1 refer to the optimum and suboptimum detection algorithms and their associated error probabilities.

2.2 Threshold Detection

Thus, in the detection phase of reception - which is always the initial, or acquisition phase at least - and usually subsequently - each signal unit is to be detected, i.e., a decision made as to the presence (or absence) of the signal symbol, to form a stream of decisions, generating the signal sequence, which is then ultimately decoded into the desired message (possibly corrupted by interference, etc.). However, in the majority of practical situations, the explicit development of the optimum algorithm $\Lambda_n^{(1)}$, or log $\Lambda_n^{(1)}$, cannot be achieved, only approximated. Moreover, the evaluation of performance, via the error probabilities (α^*,β^*), cf. (2.4b), is even more difficult. Ingenious approximations are required, and even these are not sufficient. Only by a literal (i.e. purely computational) realization of Λ_n can we expect to obtain the optimum processor (as is sometimes done.)

In any case, for the important purposes of <u>predicting</u> performance, analytical methods, for all signal levels, are not generally realizable, and we must (apart from brute-force simulation) seek other approaches. Fortunately, as we have remarked in Sec. 1 above, it is possible to obtain canonical results analytically, in the critical limiting case of <u>weak signals</u>, which, also fortunately, is of very considerable interest, as it is the situation which establishes the limiting performance, i.e., the best that can be done either for optimum processors g(X)*, or for specified systems, g(X), which are suboptimal. In general, the limiting, optimal algorithm for any interference has been shown [14] to be (for additive signal and noise processes) the expansions of the (log) likelihood ratio about zero signal (θ=0):

$$\log \Lambda_n^{(1)} \doteq g(\underset{\sim}{x})^* \equiv \log \mu + \theta \underset{\sim}{\hat{y}}\underset{\sim}{\bar{s}}' + \frac{\theta^2}{2!}\left[\underset{\sim}{\hat{y}}(\underset{\sim}{\rho}_s - \underset{\sim}{\bar{s}}'\underset{\sim}{\hat{\bar{s}}}')\underset{\sim}{y} + \mathrm{trace}(\underset{\sim}{\rho}_s \underset{\sim}{\hat{z}})\right] + \hat{B}_n(\theta)^*, \tag{2.9}$$

where (cf. Sec. III, Ref. [13]):

$$\left.\begin{aligned} \theta = \sqrt{\overline{a_o^2}}\ ;\ \underset{\sim}{S} = [a_{oj}s_j\sqrt{\psi}]\ ;\ \psi = \langle N^2\rangle,\ \langle N\rangle = 0 \\ \underset{\sim}{s}' = [a_{oj}s_j/\sqrt{\overline{a_o^2}}\ ];\ \theta_j \equiv a_{oj}s_j\ ; \\ \overline{a_o^2} = \langle S^2\rangle/\psi\ ;\ \underset{\sim}{s} = [s(t_j-e)]\ ; \end{aligned}\right\}\ ;\ \mu \equiv p/q \qquad (2.9a)$$

and $\underset{\sim}{s}$ is a normalized signal wave form, such that $\langle s^2\rangle = 1$; $\overline{a_o^2}$ = input signal-to-noise power ratio; $\psi = \langle N^2\rangle$ = (total) mean square noise (or interference) power. Here, $\underset{\sim}{y}$ and $\underset{\sim}{z}$ are the column and square matrices

$$\underset{\sim}{y} = [y_i] = [-\frac{\partial}{\partial x_i}\log W_o]\ ;\ \underset{\sim}{\rho}_s \equiv [\overline{s_i's_j'}] = [\frac{\overline{a_{oi}a_{oj}\ s_is_j}}{\overline{a_o^2}}];\ \underset{\sim}{x} = \underset{\sim}{X}/\sqrt{\psi}\ ;$$

$$\underset{\sim}{z} = [z_{ij}] = [\frac{\partial^2}{\partial x_i \partial x_j}\log W_o] = \tilde{\underset{\sim}{z}}\ , \qquad (2.10)$$

with

$$\langle F_n(\underset{\sim}{X}|\underset{\sim}{S})\rangle_S = \langle W_n(\underset{\sim}{x}\sqrt{\psi} - \theta\underset{\sim}{s}')_N\rangle_S;\quad W_o = W_n(\underset{\sim}{X})_N\ ,$$

this last for the postulated additive signal and noise, so that W_o is the joint pdf of $\underset{\sim}{X}$ ($=\underset{\sim}{V}$) when there is only noise.

Here $\hat{B}_n(\theta)^*$ [$=O(\theta^3$ or $\theta^4)$] is a <u>bias</u>, which is determined from the higher order terms in the expansion (2.9), averaged with respect to the null-hypothesis, e.g. H_o: no signal. The (correct) bias is critical for optimum performance in these threshold cases, where $n>>1$ necessarily. [See Appendix A3.] The resulting bias is also required to insure the consistency of the test (H_1 vs. H_o) as sample size (n) becomes infinite (as $\theta\to 0$), or for $n<\infty$, as $\theta = e \doteq 0$. The quantity $g(\underset{\sim}{X})^*$ we call the <u>Locally</u> Optimum Bayes Detector (or LOBD), as it gives a Bayes or minimum average risk, cf. (2.5a) and Appendix A3.

The general result (2.9) for the LOBD includes correlated samples, and both <u>incoherent</u> and <u>coherent reception.</u> For the latter, strictly, we have

$\underset{\sim}{\bar{s}}' \neq 0$, e.g. $\langle s(t-\epsilon)\rangle_\epsilon \neq 0$, where ϵ is the signal epoch vis-à-vis the observer (receiver), which by definition of coherence, is now assumed to be strictly given. At the other extreme, we have so-called incoherent reception, where $\underset{\sim}{\bar{s}}' = 0$, e.g., $\langle s(t-\epsilon)\rangle_\epsilon = 0$. In between these extremes, it is possible to have what we call quasi-coherent reception, where $w_1(\epsilon)$ is non-uniform, such that $\langle s\rangle_\epsilon \neq 0$, and may be small but not ignorable compared to the terms containing $\langle s_i s_j\rangle_\epsilon$, i.e. $O(\theta^2)$, in (2.9). These distinctions are particularly pertinent when dealing with narrow-band signals, where now $w_1(\epsilon)$ is defined over an RF carrier cycle, not over the whole duration of the signal. [In such cases, feedback loops are often used to "lock-on" from the initial instance of purely incoherent reception, to the eventual stage of more or less exact phase tracking, which permits strict synchronization of the local oscillator of the receiver, with the RF phase of the desired input signal. The result is then, of course, coherent reception, vs. the incoherent reception that occurs when this "phase-learning" process is not employed.]

The critical feature of coherent vs. incoherent detection is, of course, the fact that the LOBD for the former is $O(\theta)$, while the latter is $O(\theta^2)$, $\theta \ll 1$. The structures of the optimum threshold detector, or LOBD, are then, respectively, [cf. Appendix A-I, also]:

I. Coherent Reception: (H_1 vs. H_0):

$$\log \Lambda_n^{(1)}\Big|_{coh} \doteq g(\underset{\sim}{x})^*_c = [\log \mu + \hat{B}_n(\theta)^*_{coh}] + \theta \underset{\sim\sim}{\tilde{y}}\underset{\sim}{\bar{s}}' \ , \tag{2.11}$$

while for the latter we have

II. Incoherent Reception (H_1 vs. H_0):

$$\log \Lambda^{(1)}_{n\text{-inc}} \doteq g(x)^*_{inc} = [\log \mu + \hat{B}_n(\theta)^*_{inc}] + \frac{\theta^2}{2!}[\underset{\sim}{\tilde{y}}(\rho_s)\underset{\sim}{y} + \text{trace}\ \underset{\sim}{\rho}_s \underset{\sim}{\hat{z}}], \ (\underset{\sim}{\bar{s}}=0), \tag{2.12}$$

in which $\hat{B}^*_{n\text{-inc}} \neq \hat{B}^*_{n\text{-coh}}$, generally. For mixed modes of reception (i.e. "quasi-coherent" cases), we must use a suitably modified form of (2.9), cf. Appendix A3-6.

When there are two classes of signal to be distinguished, generally

according to (2.6), (2.7), the general optimum threshold algorithm (2.9) is

$$\log \Lambda_n^{(21)} = \hat{B}_n^{(21)*} + \underset{\sim}{\tilde{y}}\, \underset{\sim}{\overline{\Delta\theta}}^{(21)} + \frac{1}{2!}[\underset{\sim}{\tilde{y}}(\underset{\sim}{\Delta\rho}_\theta^{(21)} - [\underset{\sim}{\bar{\theta}}^{(2)} \cdot \underset{\sim}{\tilde{\bar{\theta}}}^{(2)} - \underset{\sim}{\bar{\theta}}^{(1)} \cdot \underset{\sim}{\tilde{\bar{\theta}}}^{(1)}])\underset{\sim}{y}$$

$$+ \text{trace}\,(\underset{\sim}{\Delta\rho}_\theta^{(21)} \underset{\sim}{\tilde{z}})] \equiv g^{(21)*} \quad , \tag{2.13}$$

where now

$$\left.\begin{aligned} \underset{\sim}{\overline{\Delta\theta}}^{(21)} &\equiv \underset{\sim}{\bar{\theta}}^{(2)} - \underset{\sim}{\bar{\theta}}^{(1)} = [\bar{a}_{oj}^{(2)}\, \bar{s}_j^{(2)} - \bar{a}_{oj}^{(1)}\, \bar{s}_j^{(1)}] = [\bar{\theta}_j^{(2)} - \bar{\theta}_j^{(1)}] \\ \underset{\sim}{\Delta\rho}_\theta^{(21)} &\equiv \underset{\sim}{\overline{\theta^{(2)}\theta^{(2)}}} - \underset{\sim}{\overline{\theta^{(1)}\theta^{(1)}}} = [\langle a_{oj}^{(2)} a_{oj}^{(2)} s_j^{(2)} s_i^{(2)}\rangle - \langle a_{oi}^{(1)} a_{oj}^{(1)} s_i^{(1)} s_j^{(1)}\rangle] \\ &\equiv \underset{\sim}{\rho}_\theta^{(2)} - \underset{\sim}{\rho}_\theta^{(1)} \quad , \end{aligned}\right\} \tag{2.13a}$$

and $\hat{B}_n^{(21)*}$ is once more a suitable bias to insure optimality and consistency of the test H_2 vs. H_1 here. This bias is obtained, as before [cf. (2.10) et seq. and Appendix A-I] by averaging the next (non-vanishing) terms in the expansion of $\log \Lambda^{(21)}$ <u>again with respect to H_o</u>, since $\log \Lambda_n^{(21)} = \log \Lambda_n^{(2)} - \log \Lambda_n^{(1)}$ is the difference of two "on-off" detectors, viz.

$$\left.\begin{aligned} \log \mu_{21} + \hat{B}_n^{(21)*} &= \log \mu_{21} + \langle O(\theta^{(2)^3})\rangle_{H_o} - \langle O(\theta^{(1)^3})\rangle_{H_o}, \text{ or} \\ &= \log \mu_{21} + \langle O(\theta^{(2)^4})\rangle_{H_o} - \langle \Theta(\theta^{(1)^4})\rangle_{H_o} \end{aligned}\right\};$$

$$\mu_{21} = \frac{p_2/q}{p_1/q} = \frac{p_2}{p_1} \quad . \tag{2.14}$$

Thus, (2.11) and (2.12) now become, for S_2 vs. S_1 in the same interference

I. Coherent Reception ($\bar{s}^{(1,2)} \neq 0$): (H_2 vs. H_1):

$$g^{(21)}(\underset{\sim}{x})^*_c = [\log \mu_{21} + \hat{B}^{(21)}_n(\theta)^*_c] + \tilde{\underset{\sim}{y}}(\overline{\underset{\sim}{\theta}^{(2)}} - \overline{\underset{\sim}{\theta}^{(1)}}) \ , \tag{2.15}$$

and

II. Incoherent Reception ($\bar{s}^{(1,2)} = 0$): H_2 vs. H_1:

$$g^{(21)}(\underset{\sim}{x})^*_{inc} = \log \mu_{21} + \hat{B}^{(21)}_n(\underset{\sim}{\theta})^*_{inc} + \frac{1}{2!}\{\tilde{\underset{\sim}{y}}\, \underset{\sim}{\Delta\rho}^{(21)}_{\theta}\, \underset{\sim}{y} + \text{trace}(\underset{\sim}{\Delta\rho}^{(21)}_{\theta}\, \underset{\sim}{z})\}. \tag{2.16}$$

The decision process is given by (2.7), with (2.13), generally, and with (2.15), (2.16), respectively for the coherent and incoherent modes of reception. [Equations (2.11) and (2.13) apply in the "composite" or "quasi-coherent" cases, when there is enough coherence (via phased-locked loops, for example) to justify using both processing modes simultaneously, cf. II-C (Part II), (1a): These variants are reserved to a subsequent study, cf. Sec. 8.]

Finally, for suboptimum detectors we have,

$$\left.\begin{aligned} g^{(21)}(\underset{\sim}{x})^*_c \to g^{(21)}(\underset{\sim}{x})_c &= g^{(2)}(\underset{\sim}{x})_c - g^{(1)}(\underset{\sim}{x})_c \\ g^{(21)}(\underset{\sim}{x})^*_{inc} \to g^{(21)}(\underset{\sim}{x})_{inc} &= g^{(2)}(\underset{\sim}{x})_{inc} - g^{(1)}(\underset{\sim}{x})_{inc} \end{aligned}\right\}, \tag{2.7}$$

with decision rules (2.7) on replacing $\log \Lambda^{(21)}_n \to g^{(21)}(\underset{\sim}{x})^*$ by $g^{(21)}(\underset{\sim}{x})$, etc.

The decision process is, of course, carried out according to (2.3), (2.7), with $\log \Lambda_n$ replaced by g^*, cf. (2.9), (2.11)-(2.13), (2.15),(2.16).

2.3 Gaussian Interference

The threshold canonical forms of Sec. 2.2 readily reduce to the known structures when the noise or interference is gaussian. This is easily seen from (2.10) and the pdf

$$W_o(\underset{\sim}{x}) = \{(2\pi)^{n/2}(\det \underset{\sim}{k}_N)^{1/2}\}^{-1} e^{-\frac{1}{2}\tilde{\underset{\sim}{x}}\underset{\sim}{k}_N^{-1}\underset{\sim}{x}} , \tag{2.18}$$

where one has directly

$$\underset{\sim}{y} = [(\underset{\sim}{k}_N^{-1}\underset{\sim}{x})_i] \; ; \; \underset{\sim}{z} = [-\frac{\partial y_i}{\partial x_j}] = -\underset{\sim}{k}_N^{-1} . \tag{2.18a}$$

Thus, the threshold algorithms (2.10), (2.12) in the "on-off" cases become

I. Coherent Reception (H_1 vs. H_o):

$$g(\underset{\sim}{x})^*_c\Big|_{gauss} = [\log \mu + \hat{B}^*_{n\text{-}coh}]_{gauss} + \tilde{\underset{\sim}{x}}\underset{\sim}{k}_N^{-1}\underset{\sim}{\theta} \; ; \tag{2.19}$$

II. Incoherent Reception (H_1 vs. H_o):

$$g(\underset{\sim}{x})^*_{inc}\Big|_{gauss} = [\log \mu + \hat{B}^*_{n\text{-}inc} - \frac{1}{2}\langle\tilde{\underset{\sim}{\theta}}\underset{\sim}{k}_N^{-1}\underset{\sim}{\theta}\rangle]_{gauss} + \frac{1}{2!}\tilde{\underset{\sim}{x}}\underset{\sim}{k}_N^{-1}\underset{\sim}{\rho}_\theta\underset{\sim}{k}_N^{-1}\underset{\sim}{x} , \tag{2.20}$$

where

$$\underset{\sim}{\theta} = [a_{oi}s_i], \text{ cf. (2.9a)} \; ; \; \underset{\sim}{\rho}_\theta \equiv \langle[\underset{\sim}{\theta}_i\underset{\sim}{\theta}_j]\rangle = [\langle a_{oi}a_{oj}s_is_j\rangle]. \tag{2.20a}$$

These results are just those (Eq. 20.7, Eq. 20.11a, [12]) obtained many years ago for these gaussian situations.

Similarly, we find for the two-signal cases (2.15), (2.16), that the threshold algorithms reduce respectively to

I. Coherent Reception (H_2 vs. H_1):

$$g^{(21)}(\underset{\sim}{x})^*_c\Big|_{\text{gauss}} = [\log \mu_{21} + \hat{B}^{(21)*}_{n\text{-}c}]_{\text{gauss}} + \underset{\sim}{\tilde{x}}\underset{\sim}{k}_N^{-1}[\underset{\sim}{\bar{\theta}}^{(2)} - \underset{\sim}{\bar{\theta}}^{(1)}] \ , \tag{2.21}$$

and

II. Incoherent Reception (H_2 vs. H_1):

$$g^{(21)}(\underset{\sim}{x})^*_{\text{inc}}\Big|_{\text{gauss}} = [\log \mu_{21} + \hat{B}^{(21)*}_{n\text{-inc}} - \tfrac{1}{2}\{\langle \underset{\sim}{\tilde{\theta}}^{(2)}\underset{\sim}{k}_N^{-1}\underset{\sim}{\theta}^{(2)}\rangle - \langle \underset{\sim}{\tilde{\theta}}^{(1)}\underset{\sim}{k}_N^{-1}\underset{\sim}{\theta}^{(1)}\rangle\}]_{\text{gauss}}$$

$$+ \frac{1}{2!}\,\underset{\sim}{\tilde{x}}\underset{\sim}{k}_N^{-1}(\underset{\sim}{\rho}_\theta^{(2)} - \underset{\sim}{\rho}^{(1)})\underset{\sim}{k}_N^{-1}\underset{\sim}{x} \ , \tag{2.22}$$

with $\underset{\sim}{\rho}_\theta^{(2)} = [\langle a_{oi}^{(2)} a_{oj}^{(2)} s_i^{(2)} s_j^{(2)}\rangle]$, etc. [Equations (2.21), (2.22) agree, as expected, with the earlier results, Problem 20.12, p. 935, [12], and Section 20.4-5, [12], respectively, when the accompanying interference is gaussian noise.]

Thus, when the noise is gaussian, the resulting algorithms remain optimum (LOBD's) with a generalized cross- or auto-correlation structure for the processors, cf. (2.19)-(2.22). With independent noise sampling ($k_N^{(-1)} = (\delta_{ij})$), these algorithms reduce to the simpler specific LOBD structures A.1-24,25) with the biases now obtained from (4.9), (4.12).

2.4 Canonical Evaluation of Threshold Detection Performance:

By threshold detection we mean not only appropriately small input signals vis-à-vis the accompanying interference, but also appropriately large observation periods, expressed as a suitably large number $n' \leq n$) of effectively independent noise samples. Thus, for the LOBD, or g*, cf. (2.9) et seq., we consider the quasi-limiting cases of "small signals" ($\theta^2 << 1$) and large samples ($n \geq n' >> 1$), or equivalently, large time-bandwidth products $n \doteq B_e T >> 1$. Performance, in terms of the error probabilities (2.4b), is then found by direct application of the Central Limit Theorem (cf. Sec. 7.7-3, [12]) to

the detection algorithm, or test statistic g*. Accordingly g* is asymptotically normally distributed, in the "on-off" cases (H_1 vs. H_0), with the first and second moments†

$$\langle g^{(*)} \rangle_{H_0 H_1} \ , \langle (g^{(*)})^2 \rangle_{H_0,H_1} \to \text{var } g^* \Big|_{H_0,H_1} \equiv \sigma^{*2}_{o,1} \tag{2.23}$$

e.g.

$$w_1(g^*|H_0) \cong \frac{e^{-(g^*-\langle g^* \rangle_{H_0})^2/2\sigma_0^{*2}}}{\sqrt{2\pi\sigma_0^{*2}}} \ ; \ w_1(g^*|H_1) \cong \frac{e^{-(g^*-\langle g^* \rangle_{H_1})^2/2\sigma_1^{*2}}}{\sqrt{2\pi\sigma_1^{*2}}} \ . \tag{2.24}$$

In fact, applying (2.23), (2.24) to (2.4b) for "on-off" detection (H_1 vs. H_0), where the (conditional) false-alarm probability, α_F^* (or threshold $\mathcal{K}$), is preset, [the so-called Neyman-Pearson Observer, (Sec. 19.2-1, [12])], we have

$$\boxed{\alpha_F^* \simeq \frac{1}{2}\{1+\Theta[\frac{\langle g^* \rangle_0 - \log \mathcal{K}}{\sigma_0^* \sqrt{2}}]\}; \ \beta^* \simeq \frac{1}{2}\{1-\Theta[\frac{\langle g^* \rangle_1 - \log \mathcal{K}}{\sigma_1^* \sqrt{2}}]\},} \tag{2.25}$$

so that the probability, P_D^*, of correctly detecting the presence of a signal is maximized to become

$$\boxed{P_D^* = p(1-\beta^*) \simeq \frac{p}{2}\{1+\Theta[\frac{\langle g^* \rangle_1 - \langle g^* \rangle_0}{\sqrt{2}\ \sigma_1^*} - \frac{\sigma_0^*}{\sigma_1^*}\ \Theta^{-1}(1-2\alpha_F^*)]\},} \tag{2.26}$$

on eliminating threshold $\mathcal{K}$. Here

$$y = \Theta(x) \equiv \frac{2}{\sqrt{\pi}} \int_0^x e^{-t^2} dt = \text{erf } x; \quad x = \Theta^{-1}(y) \tag{2.26a}$$

are the well-known error function and its inverse. [Equation (2.16) is, of course, equivalent to minimizing the error probability ($\beta \to \beta^*$), with $\alpha = \alpha_F^*$ fixed.

---

† But, see the ultimate condition (2.29) ff, when for optimality $\sigma_1^* \to \sigma_0^*$, etc.

Similarly, when the threshold is set to $\mathcal{K} = 1$, i.e. when $(\alpha \to \alpha^*, \beta \to \beta^*)$ are jointly minimized, we have the so-called Ideal Observer [cf. Sec. 19.2-2, [12]], so that the total probability of decision error is

$$P_e^* = p\beta^* + q\alpha^* \simeq \frac{1}{2}\{1 - p\Theta[\frac{\langle g \rangle_1^*}{\sqrt{2}\,\sigma_1^*}] + q\Theta[\frac{\langle g^* \rangle_o}{\sqrt{2}\,\sigma_o^*}]\}, \quad = 1, \tag{2.27a}$$

which for symmetrical channels (i.e. p=q=1/2) reduces further to

$$\boxed{P_e^*\Big|_{sym} \simeq \frac{1}{2}\{1 - \frac{1}{2}\Theta[\frac{\langle g^* \rangle_1}{\sqrt{2}\,\sigma_1^*}] + \frac{1}{2}\Theta[\frac{\langle g^* \rangle_{H_o}}{\sqrt{2}\,\sigma_o^*}]\}, \; \mathcal{K} = 1; \; p=q=1/2 \; .} \tag{2.27b}$$

The Neyman-Pearson, or fixed false alarm observer is appropriate to the initial stages of detecting the presence of a desired signal, while the Ideal Observer ($\mathcal{K} = 1$) is the more suitable criterion (i.e. total decision error probability) when particular elements of a signal are to be detected, i.e. "marks" or "spaces" (in these "on-off" cases), in the course of message transmission, where now P_e^* is directly proportional to the bit-error rate.

Equations (2.23)-(2.27b) apply equally well, formally, for suboptimum detectors, $g(\underset{\sim}{x})$: we simply replace g^* by g, $\sigma_{1,o}^*$ by $\sigma_{1,o}$, P_D^*, P_e^* by P_D, P_e in the above. Furthermore, we have explicitly for the averages (2.18)

$$\langle h^k \rangle_{o,1} \equiv \int_{-\infty}^{\infty} w_n(\underset{\sim}{x}|H_{o,1})_N h(\underset{\sim}{x})^k d\underset{\sim}{x} \; , \; (h=g,g^*) \; , \tag{2.28a}$$

with

$$w_n(\underset{\sim}{x}|H_o)_N = W_n(\underset{\sim}{x})_N \; ; \; w_n(\underset{\sim}{x}|H_1) = W(\underset{\sim}{x}-\underset{\sim}{s})_N \quad , \tag{2.28b}$$

cf. (2.9), for the postulated additive signal and noise cases here.

The relations P_D^*, P_D, P_e^*, P_e, etc., (2.25) et seq., hold asymptotically for all input signal levels (as long as the number $(n'<n)$ of effectively

independent noise samples remains large). However, the LOBD's, g*, [(2.9), (2.11), (2.12) etc.] are then no longer optimum, in the locally optimum sense ($\theta^2<<1$, $n'>>1$), but can become drastically suboptimum as the input signal level ($\sim\theta$) becomes larger. In keeping with the concept of the LOBD, which is a truncated series development in θ, cf. (2.9), which depends on the mode of observation (or reception) i.e. coherent or incoherent [cf. (2.10) et seq.], we must be similarly consistent with respect to the appropriate power of θ in determining the above probability measures of performance. Because of the asymptotically optimum (AO) condition, cf. Appendix A3, which determines the bias $B_n^*(\theta)$ as the average of the next highest non-vanishing (H_o-) average in the series development $\log \Lambda_n = g^* + \ldots$, cf. (2.9), we must likewise require that $\sigma_1^{*2} = \sigma_o^{*2} + F_n(\theta \text{ or } \theta^2)$, where $F_n^* << 1$. This (AO) condition,

$$\boxed{|F_n^*(\theta \text{ or } \theta^2)| << \sigma_o^{*2} \ , \ \therefore \sigma_1^{*2} \doteq \sigma_o^{*2} \ , \ n >> 1,} \qquad (2.29)$$

in turn, requires that the input signal level remains appropriately small, to insure that g* (=LOBD) is indeed "locally optimum" and asymptotically optimum.

We can make the condition (2.29) somewhat more explicit by considering for these additive signal and noise cases (2.28b) the expansions

$$\langle g^{*k} \rangle_{H_1} = \int (g^*) \ w_n(\underset{\sim}{x}|H_o)\underset{\sim\sim}{dx} - \bar{a}_o \langle (g^*)^k \underset{\sim}{s} w_n'/w_n \rangle_{o,s} + \frac{\overline{a_o^2}}{2} \langle (g^*)^k \underset{\sim}{s}\underset{\sim}{s} w_n''/w_n \rangle_{o,s} + \ldots \ , \ k=1,2, \qquad (2.30a)$$

so that

$$\sigma_1^{*2} = \sigma_o^{*2} + F_n^* \doteq \sigma_o^{*2} \ , \qquad (2.30b)$$

and

$$\therefore \quad F_n^* = \bar{a}_o[2\langle g^*\rangle_o\langle g^*\underset{\sim}{\tilde{s}}\underset{\sim}{w}_n'/w_n\rangle_o - \langle (g^*)^2\underset{\sim}{\tilde{s}}\underset{\sim}{w}_n'/w_n\rangle_o]$$

$$+ \frac{\overline{a_o^2}}{2}[\langle (g^*)^2\underset{\sim}{\tilde{s}}\underset{\sim}{w}_n''\underset{\sim}{s}/w_n\rangle_{o,s} - 2\langle g^*\rangle_o\langle g^*\underset{\sim}{\tilde{s}}\underset{\sim}{w}_n'/w_n\rangle_o] + O(a_o^3) << \sigma_o^{*2}, \quad (2.30c)$$

with

$$\underset{\sim}{w}_n' \equiv [\frac{\partial}{\partial x_i} w_n(x_1,\ldots,x_n)] \; ; \; \underset{\sim}{w}_n'' = [\frac{\partial^2}{\partial x_i \partial x_j} w_n], \text{ etc.} \quad (2.30d)$$

Thus, for coherent reception the first term of (2.30c) determines the required smallness of $(\bar{a}_o)$, while the second term supplies the needed condition on (a_o^2) in the incoherent cases (since,(2.30d),$\bar{s}$=0 then, etc.). Suboptimum algorithms, g, are handled similarly, with $g^* \to g$ in the above. We shall encounter explicit examples of $F_n^* << 1$, (2.30c), later, in Section 6 ff. In any case, (2.26) and (2.27b) now reduce to

$$\left.\begin{aligned} P_D^{(*)} &\doteq \frac{p}{2}\left\{1+\Theta\left[\frac{\langle g^{(*)}\rangle_1 - \langle g^{(*)}\rangle_o}{\sqrt{2}\,\sigma_o^{(*)}} - \Theta^{-1}(1-2\alpha_F^{(*)})\right]\right\}, \quad (2.31)\\ P_e^{(*)} &\doteq \frac{1}{2}\left\{1-\frac{1}{2}\Theta\left[\frac{\langle g^{(*)}\rangle_1}{\sqrt{2}\,\sigma_o^{(*)}}\right] + \frac{1}{2}\Theta\left[\frac{\langle g^{(*)}\rangle_o}{\sqrt{2}\,\sigma_o^{(*)}}\right]\right\}_{\mu=1}, \quad (2.32)\end{aligned}\right\} \; F_n^{(*)} << \sigma_o^{(*)2},$$

Here, super (*) denotes optimum by super * alone and suboptimum otherwise, i.e. a blank superscript.

For the common telecommunication situations involving the "symmetrical" 2-signal situations H_2: S_2+N vs. H_1: S_1+N, cf. (2.13)-(2.17), performance is calculated as above with the help of (2.8). Now, however, we have $\alpha^* \to \beta_2^{(1)*}$, $\beta^* \to \beta_2^{(2)*}$, $\mathcal{K} \to \mathcal{K}_{12}$, cf. (2.7), (2.7a), and (2.24) is appropriately modified $g^* \to g^{(2)*}$, (2.13) et seq., $H_o \to H_1$; $H_1 \to H_2$, $n >> 1$. Thus, for example, (2.32) is extended to

$$P_e^{(*)(21)} \underset{\sim}{\sim} \frac{1}{2}\left\{1-p_2\Theta\left[\frac{\langle g^{(2)(*)}\rangle_2}{\sqrt{2}\,\sigma_1^{(*)}}\right]+p_1\Theta\left[\frac{\langle g^{(2)(*)}\rangle_1}{\sqrt{2}\,\sigma_1^{(*)}}\right]\right\}, \quad \dot{\mu}_{21} \equiv p_2/p_1 \;;\; p_1+p_2 = 1 \tag{2.33}$$

where $\sigma_2^{(*)2} \underset{\sim}{\sim} \sigma_1^{(*)2}$, and the higher order terms in θ(or θ^2) are dropped in the means and variances, consistent with the order of development of $g^{(21)(*)}$, as explained above in the case of the "on-off" detection algorithms, cf. (2.29). We shall see some examples of this in Sec. 6 ff., as well.

Finally, the explicit evaluation and comparison of threshold performance, by LOBD's (g*), or specified sub-optimum systems (g), may be effected by comparing P_D^* vs. P_D, or P_e^* vs. P_e, for the same perameters: observation time ($\equiv$ sample size n), input signal-to-noise ratio $\theta(=\sqrt{\overline{a_0^2}}$, or $\overline{a_0^2}$) and input signal and noise levels, etc. Comparisons may also be made using the associated error probabilities (α^*,β^*), or (α,β), in the Bayes and average risks (2.5a,b). Other useful ways of comparison include calculations of the various Asymptotic Relative Efficiencies (ARE's), and Efficacies, cf. Appendix, [14].(See also, p. 921, of [1a] and our remarks in Sec. 8.) [In addition to the results of Secs. 6,7 here, examples of comparisons based on the error probabilities are also given further in [1a], [13], [14].]

3. A SUMMARY OF CLASS A AND B INTERFERENCE MODELS: 1st-ORDER STATISTICS:

In this section we provide appropriate first-order statistics of Class A and B interference. This includes the general EMI scenario, from which the principal parameters of Class A and B models may be calculated, as well as a rather general desired signal scenario, which encompasses most practical applications.

We shall henceforth approximate the general threshold theory [Sec. 2] by restricting the analysis to independent noise or interference samples (n). As explained in Section 1 above (and as we shall see in Secs. 4-7 subsequently), this greatly simplifies the analysis, without significantly affecting the results. Moreover, it permits us to use the recently developed (and experimentally verified, [5],[6]) first-order probability models of Class A and B interference, which canonically describe most classes of noise and interference.

3.1 Desired Signal Scenarios:

The desired signals are here narrow-band input waveforms,* which appear likewise as narrow band signals at the output of the front-end stages of the receiver, i.e. before any subsequent linear or nonlinear processing. These desired signals often have the same generic form as those producing the interference (in Class A cases). One has explicitly (in sampled form)

$$\underset{\sim}{S}(t,\underset{\sim}{\theta}') = \left[\frac{a_j \hat{I}_{oS}^{1/2}(t,\phi)}{r_d^{\gamma}} \cos[\omega_o(t_j-\epsilon)-\phi_s(t_j)-\phi_o]\right] = [a_{oj}s_j\sqrt{\psi}] \ ,$$

$$\text{cf. (2.9a)}, \quad \psi = \bar{I}_N \ , \tag{3.1}$$

where $\psi(\equiv \bar{I}_N)$ is the mean total noise intensity (measured at the same point in the receiver as the desired signal). Here $r_d \equiv r_D/\hat{r}_o = c_o\lambda/\hat{r}_o$ is the normalized distance of the source to the receiver, $\hat{r}_o$ is the normalizing distance, c_o = speed of propagation, so that λ is a distance measured in units of time (secs.). The quantity a_j is a dimensionless scale factor embodying the effects of fading.

In an alternative form we may write (3.1) as

$$\underset{\sim}{S} = \left[\frac{a_j G_o(t_j,\phi)}{\lambda^{\gamma}} \cos[\omega_o(t_j-\epsilon)-\phi_j-\phi_o]\right] = [a_{oj}\ s_j\sqrt{\psi}] = \left[\frac{A_{oj}}{\sqrt{2}}\, s(t_j-\epsilon)\right] \tag{3.1a}$$

where now

$$G_o(t,\phi) \equiv \hat{I}_{os}(t,\phi)^{1/2}\hat{r}_o^{\gamma}/c_o^{\gamma} \ , \tag{3.1b}$$

and the "mean amplitude", A_o, over the sampling period $t\ ,T_o+t_o)$ is obtained from

$$A_o^2/2 = \frac{1}{T}\int_{t_o}^{t_o+T} S(t)^2 dt \ . \tag{3.1c}$$

---

* The canonical theory is in no way limited by this practical condition, cf. (2.9) et seq.

The normalized signal waveform (s_j) is likewise defined by (3.1a) with the help of (3.1c), cf. Sec. 19.4, [12], Eq. (19.49a).

In many applications digital signals may be used, with no significant amplitude modulation, so that G_o and $\hat{I}_{os}$ are no longer time-dependent. Thus, we can write (3.1a) as

$$\underset{\sim}{S} = \left[\left[\frac{a_j G_o(\phi)/\sqrt{2}}{\lambda^\gamma}\right]\sqrt{2}\cos[\omega_o(t_j-\epsilon)-\phi_j-\phi_o]\right] \equiv \left[\frac{A_{oj}}{\sqrt{2}}\, s(t_j-\epsilon)\right] = [a_{oj}s_j\sqrt{\psi}], \tag{3.2}$$

which defines the normalized signal s_j now by

$$s_j \equiv \sqrt{2}\cos[\omega_o(t_j-\epsilon)-\phi_j-\phi_o]; \therefore A_{oj} = [a_j G_o(\phi)/\lambda^\gamma], \tag{3.2a}$$

so that $\langle s_j^2\rangle_\epsilon = 1$, as required.

Since the location of the desired signal source is not necessarily known at the receiver, λ is a random variable, as is the fading parameter $\underline{a}$, and the beam-pattern function, $G_o(\phi)$, as well. For most observation periods Rayleigh fading is the expected mechanism, e.g., $\underline{a}$ obeys the pdf

$$w_1(a) = \frac{2a\, e^{-a^2/\overline{a^2}}}{\overline{a^2}}\ , \ a \geq 0\ . \tag{3.3}$$

The average effects of the (resolvable) multipath are determined by the value of the propagation exponent (γ), which, for example, is usually larger than unity for rough terrain, e.g. $\gamma = 2$ is an often-used empirical value; (γ need not be an integer, however). Moreover, the desired source may be moving (comparatively slowly), so that its location vis-à-vis the receiver is described by a random walk pdf of the form [30], [31]

$$w_1(r_d)_S = 2r_d e^{-r_d^2 - r_{oa}^2} I_o(2r_{oa}r_d), \quad (r_d, r_{oa} \geq 0), \tag{3.4a}$$

or

$$w_1(\lambda)_S = \frac{2c_o^2}{\hat{r}_o^2} \lambda e^{-\lambda^2 (c_o/\hat{r}_o)^2 - r_{oa}^2} I_o(2r_{oa}c_o\lambda/\hat{r}_o) \ , \quad (r_{oa}, \lambda > 0). \tag{3.4b}$$

When the source is not moving, but its location is unknown to the receiver, the pdf of its location can be usefully expressed alternatively by the density function [9],

$$\left.\begin{aligned} w_1(\lambda)_S = B_\mu \lambda^{1-\mu} d\lambda w_1(\phi) d\phi \quad ; \quad B_\mu = \frac{2-\mu}{\lambda_1^{2-\mu} - \lambda_o^{2-\mu}} \ ; \ (0<)\lambda_o \leq \lambda_1 (<\infty) \\ 0 \leq \phi \leq 2\pi \end{aligned}\right\} \ , \ \mu \geq 0. \tag{3.5}$$

for the simple geometry of Figure 3.1, where the possible location of the source is in the region Λ_S. Other, more complex geometries may be handled in the same fashion, but this rather simple model often gives reasonable and representative results.

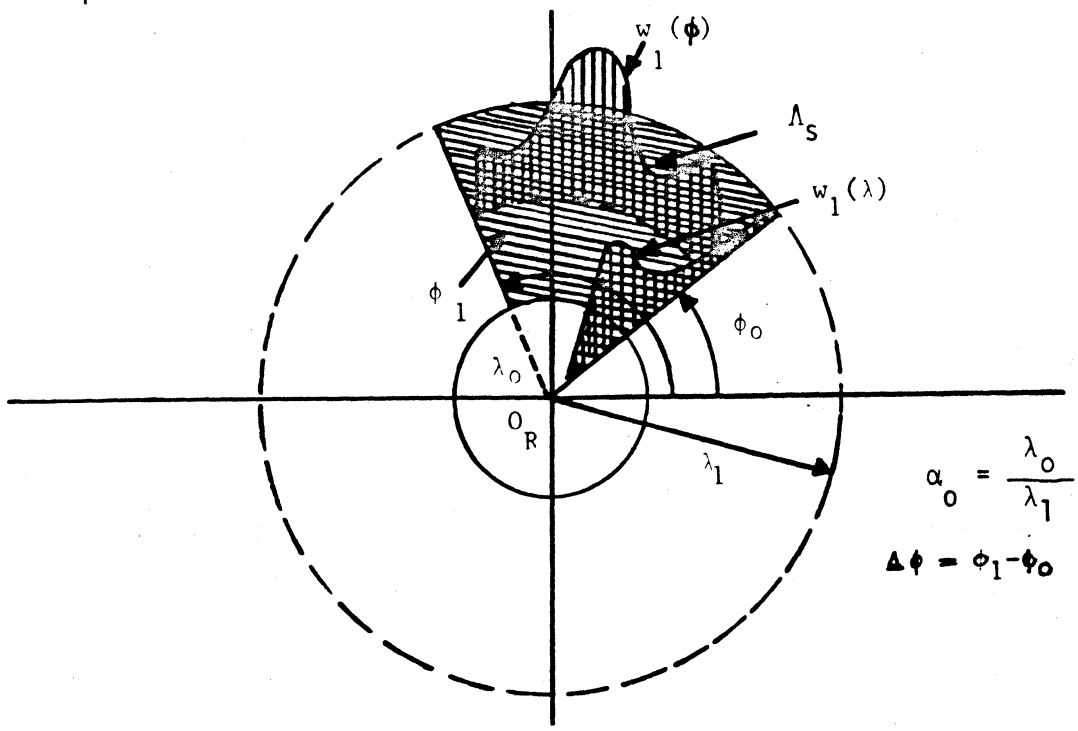

Figure 3.1. Schema of $w_1(\lambda)$, $w_1(\phi)$, Eq. (3.5); $\alpha_o (\equiv \lambda_o/\lambda_1)$ ratio of inner to outer radii.

3.2 EMI Scenarios: Calculation of Parameters:

The EMI scenario describes how a typical interfering source radiates and where it is located (statistically) in a domain (Λ_I) of such possible sources. It also provides an explicit structure for the resulting, typical waveform as seen following the linear front-end stages of the receiver. The scenario is fundamental in determining the explicit structure of the various distributions of the EMI itself, particularly when strictly canonical conditions do not hold, cf. [32], for Class A as well as Class B interference. Equally important, the EMI scenario allows us to calculate the principal parameters of these distributions, as we note below, cf. (3.10) ff.

The (first-order) EMI scenario is specifically defined by:

(3.6)

(i). the propagation law [$\lambda^{-\gamma}$, cf. (3.1a)], $\gamma>0$;

(ii). the distribution, σ_S, of sources in Λ_I; here $\sigma_S \sim \lambda^{-\mu} w_1(\phi)$;

(iii). the statistics of the fading parameter, $\underline{a}$, cf. (3.3),(3.1);

(iv). the average emission characteristics of the sources, as embodied in the "overlap index" A_A, A_B ;

(v). the structure of the wave-form-beam pattern factor

$$G_o(t,\phi)=|\mathcal{a}_{RT}(\phi)|bu_o(t,\underset{\sim}{\theta}') \ ,$$

cf. (2.17), [6]

where $\mathcal{a}_{RT}(\phi)$=composite source (T)-receiver (R) beam patterns,

u_o =normalized basic interference waveform in linear receiver output, before "processing";

b =appropriately dimensional parameter.

(vi). the statistics of any other pertinent parameters in the typical source model.

For the interfering sources we use (3.5) again, where Λ_I now is not necessarily the same domain as that for the desired signal source, Λ_S; Fig. 3.1 shows a typical domain. [We simplify without serious loss of

generality, by writing $\sigma_S(\lambda,\phi) = \sigma_s(\lambda)\sigma_S(\phi)$ here.] Note, for example, that μ=0 corresponds to a uniform source distribution $\sigma_S(\lambda,\phi) = \sigma_{oS}/\lambda^{\mu} = \sigma_{oS}$. Specifically, the envelope of a typical source at the output of the front-end stages of the receiver (to the subsequent processing) is

$$\hat{B}_o = \frac{aG_o(\phi,t)}{\lambda^{\gamma}} \quad , \text{ cf. (3.1)} , \tag{3.7}$$

where now the scenario (3.6) applies.

The global, or "macro"-parameter of Class A, or Class B, interference are $\mathcal{P}_3 = \{A,\Omega_2,\Gamma'\}_{A,B}$, defined by

(3.8)
$A_{A,B}$ = "overlap index" = (av. no. of interfering sources emitting at any given instant) x (av. duration of a typical emission);

$\Omega_{2A,B}$ = $[A\langle\hat{B}_o^2\rangle/2]_{A,B}$ = mean intensity of the nongaussian component of the EMI;

$\Gamma'_{A,B} \equiv [\sigma_G^2/\Omega_2]_{A,B}$ = gaussian factor, or ratio of the mean intensity of the gauss to the non-gauss component of the EMI;

$\bar{I}_N\big|_{A,B}$ = $(\Omega_2+\sigma_G^2)_{A,B}$ = mean total intensity of the interference.

The gauss component is itself a sum of two components:

$$\sigma_G^2 = \sigma_E^2 + \sigma_R^2 , \tag{3.9}$$

the one due to (many) unresolvable external sources (σ_E^2), the other, to receiver noise, which appears largely in the initial (linear) stages of the receiver.

From (3.5)-(3.7) we can now readily calculate Ω_2,Γ', and $\bar{I}_N$. Thus, we have

$$\Omega_2 = A\,\frac{\overline{a^2}\langle G_o^2\rangle}{2}\,\frac{1}{\langle\lambda^{2\gamma}\rangle} \quad . \tag{3.10}$$

where $\langle G_o^2\rangle = \langle G_o^2\rangle_\phi$, etc., cf. (v), (3.6). From (3.5) it follows that

$$\langle 1/\lambda^{2\gamma}\rangle \equiv C^{(2)}_{\mu,\gamma} = \frac{2-\mu}{2\gamma+\mu-2}\left(\frac{1-\alpha_o^{2\gamma+\mu-2}}{1-\alpha_o^{2-\mu}}\right)\alpha_o^{2-2\gamma-\mu}\lambda_1^{-2\gamma} \;;\; \alpha_o \equiv \lambda_o/\lambda_1 \tag{3.11}$$

with $(\mu,\gamma \geq 0)$. Similarly, Γ' and $\bar{I}_N$, cf. (3.8), become

$$\Gamma' = 2\sigma_G^2/A\,\overline{a^2}\,\overline{G_o^2}\,C^{(2)}_{\mu,\gamma} \;;\; \bar{I}_N = A\,\overline{G_o^2}\,\frac{\overline{a^2}}{2}\,C^{(2)}_{\mu,\gamma} + \sigma_G^2 \;, \tag{3.12}$$

for Class A, or B interference. Clearly, the geometry and other elements of the EMI scenario strongly influence the magnitudes of these "macro"-parameters, cf. (3.8), and as we shall note below, the specific structure of the associated probability distributions.

Finally, we remark that more complex channel characteristics can be introduced, i.e. scatter channels which introduce spreading in frequency and path delay of both the desired signal and the interfering signals which may be developed along the lines of [3], [35], [36], and in a much more general way, by Middleton, in [37], [38]. For the 1st-order EMI's no correlation structures appear (we assume independent samples, or equivalently, noise samples taken outside the (rms) delay and frequency spread intervals). On the other hand, the correlation structure of the signal is preserved in our processing, so that the effects of channel "spread", if present, will modify the received signal. (We reserve the analysis to a later study.)

3.3 Probability Densities (of the Instantaneous Amplitudes):

It has been shown [32] that the EMI scenario can noticeably influence the form of the pdf (and APD) of Class A and B noise. We summarize the pertinent results established elsewhere (Class A, [32]; Class B, [5], [6]):

I. Class A Noise:

There are two principal developments for Class A interference [32]: (1), the "strictly canonical" forms, which correspond to source distributions where the potentially interfering sources are either equidistant, or approximately equidistant, from the receiver; and (2), the "quasi-canonical cases, where the sources are widely distributed in space and $\underline{a}$ or $\underline{G}_o$ is rayleigh distributed. For the former we have the following expression for the first-order pdf (needed subsequently for locally optimum processing algorithms and performance, cf. Secs. 4-6):

(1). Strictly Canonical Class A pdf:

$$w_1(x)_{A+G} = e^{-A_A} \sum_{m=0}^{\infty} \frac{A_A^m}{m!} \frac{e^{-x^2/4\hat{\sigma}^2_{mA}}}{\sqrt{4\pi\hat{\sigma}^2_{mA}}} , \tag{3.13}$$

where

$$2\hat{\sigma}^2_{mA} \equiv \frac{m/A_A+\Gamma'_A}{1+\Gamma'_A} \quad ; \quad \Gamma'_A = \sigma_G^2/\Omega_{2A} \quad : \quad x = \frac{X}{\sqrt{\Omega_{2A}(1+\Gamma'_A)}} . \tag{3.13a}$$

Equation (3.13) is also appropriate for the "approximately" canonical cases, where the source distribution is no longer confined to sources equidistant from the receiver; [for details, see Sec. 5 of [32]].

(2). Quasi-Canonical Class A pdf:

$$w_1(x)_{A+G} \cong e^{-A_A\hat{g}_o} \sum_{m=0}^{\infty} \frac{(A_A\hat{g}_o)^m}{m!} \left\{ \frac{de^{-x^2d^2/4\sigma^2_{om}}}{\sqrt{4\pi\sigma^2_{om}}} + \hat{\Phi}(0)(xd/2\sigma_{om}) \right\} , \tag{3.14}$$

where the "correction term" $\hat{\Phi}(0)$ is specifically

$$\hat{\Phi}(0) = \sum_{n=1}^{\infty} \frac{(-1)^n}{n!}\, {}_mC_n \cdot \frac{d}{\sqrt{4\pi\sigma_{om}^2}} \cdot \frac{\Gamma(1+\frac{n\alpha}{2})}{\sqrt{\pi}} \left[\frac{\pi}{2\Gamma(\frac{3+\alpha}{2})(m+\Gamma_A' A_A d^2)^{\alpha/2}}\right]^n$$

$$\cdot e^{-x^2 d^2/4\sigma_{om}^2}\, {}_1F_1(-\tfrac{n\alpha}{2}; 1/2; x^2 d^2/4\sigma_{om}^2) \ , \qquad (3.14a)$$

and where

$$2\sigma_{om}^2 \equiv \frac{m/A_A + \hat{\Gamma}_A}{1+\Gamma_A'} \ ; \ \hat{\Gamma}_A \equiv \Gamma_A' d^2 \ ; \ d^2\Big|_{\alpha_o<<1} \doteq \frac{\alpha}{2-\alpha} \cdot \frac{1}{\alpha_o^{(2-\alpha)\gamma}} \ (>>1) \qquad (3.14b)$$

$$(0<)\alpha = \frac{2-\mu}{\gamma} \ (<2) \ , \ \alpha_o \equiv \lambda_o/\lambda_1, \ {}_mC_n = \frac{m!}{(m-n)!n!} \ , \qquad (3.14c)$$

in which (μ,γ,α_o) are parameters of the EMI scenario, cf. Sec. (3.2) above, and $\hat{g}_o$ is a numerical scaling factor obtained by a suitably analytic "fitting" process, described in Secs. 7.2, 8.4 of [32].

For Class B interference we have, similarly ([6],[13],[33]):

II. Class B Noise:

Here we use a simplified version of the general first-order case [6], which involves only three parameters, instead of the usual six. Moreover, we assume a limiting form of the EMI scenario, where now α_o $(=\lambda_o/\lambda_1) \to 0$, e.g. $\lambda_o = 0$, cf. Fig. 3.1: potentially interfering sources can be effectively co-located with the receiver. This permits a considerable mathematical simplification of the resulting pdf [6] but, in turn, gives a distribution for which none of the moments exists (because the intensity at a point source is infinite, in such models). This defect is readily overcome in practice by truncating the pdf $w_1(x)$ at sufficiently large amplitudes $(x>>1)$, or equivalently, at sufficiently small values of the APD $(P_1 \equiv \int_{x_o}^{\infty} w_1(x)dx)$, [cf. Fig. 1, [33] and discussion therein]. [For the more complete model (still with $\lambda_o=0$, but suitably approximated at large x to insure finite moments, see [5],[6],[13].]

The appropriate pdf here is thus [from Eq. (2.10a), [13]], a

(3) (Quasi-Canonical Class B pdf ($\alpha_o \to 0$):

$$w_1(x)_{B+G} \simeq \frac{e^{-x^2/\Omega_B}}{\pi\sqrt{\Omega_B}} \sum_{n=0}^{\infty} \frac{(-1)^n}{n!} \hat{A}_\alpha^n \, \Gamma(\tfrac{n\alpha+1}{2}) \; {}_1F_1(-\tfrac{n\alpha}{2}; 1/2; x^2/\Omega_B) \;, \qquad (3.15a)$$

or

$$\simeq \frac{1}{\pi\sqrt{\Omega_B}} \sum_{n=0}^{\infty} \frac{1}{n!} (-1)^n \hat{A}_\alpha^n \, \Gamma(\tfrac{n\alpha+1}{2}) \; {}_1F_1(\tfrac{1+n\alpha}{2}; 1/2; -x^2/\Omega_B) \;, \qquad (3.15b)$$

where α is given by (3.14c) and

$$\Omega_B \equiv 2\sqrt{2}\, G_B/N_I \;, \qquad (3.16a)$$

and

$$\hat{A}_\alpha = A_\alpha/2^\alpha G_B^\alpha = b_{1\alpha} A_B/[\tfrac{\Omega_{2B}}{2} \cdot (\tfrac{4-\alpha}{2-\alpha} + \Gamma_B')]^{\alpha/2} \;, \qquad (3.16b)$$

with

$$\left.\begin{aligned} A_\alpha &= 2^\alpha b_{1\alpha} A_B/[2\Omega_{2B}(1+\Gamma_B')]^{\alpha/2} \;;\; b_{1\alpha} = \frac{\Gamma(1-\frac{\alpha}{2})}{2^{\alpha/2}\Gamma(1+\frac{\alpha}{2})} \left\langle \left(\frac{\hat{B}_{oB}}{\sqrt{2}}\right)^\alpha \right\rangle \\ G_B^2 &\equiv (\tfrac{4-\alpha}{2-\alpha} + \Gamma_B')/4(1+\Gamma_B') \;. \end{aligned}\right\} \qquad (3.16c)$$

(It can be shown that $\int_{-\infty}^{\infty} w_1(x)_{A+G} dx = 1$, from the series development of ${}_1F_1$, etc., and moreover, that $w_1 \geq 0$, all x, as required of a proper pdf or directly from the characteristic function, (2.38), [6], with ($\lambda \to 0,\infty$) therein.) Thus, this model has three parameters $\mathcal{P}'_{3B} = \{\hat{A}_\alpha, \Omega_B, \alpha\}$. The parameter Ω_B is a normalizing parameter (through N_I in (3.16a), cf. (2.11c), [13]). As before, the "macro-parameters" ($A_B, \Omega_{2A}, \Gamma_B'$) are defined precisely as in the Class A cases, cf. (3.8). In practice, one uses a value of Ω_B which normalizes

the x-process to the measured intensity of the process, since the analytical second moment does not exist, for the reasons explained above. Although the more complete model ([6],[7],[13]) removes this difficulty, using (3.15a) in conjunction with empirical data does not at all limit the applicability of this simplified Class B model.

4. OPTIMUM* AND SUBOPTIMUM THRESHOLD DETECTION ALGORITHMS:

We now return to Section 2.2 above and consider both LOBD and selected suboptimum threshold detection algorithms, under the simplifying assumption of independent noise or interference samples. The correlated or "coherent" structure of the desired signal is, of course, preserved, since it is a critical element in enhancing the signal vis-à-vis the noise. For the suboptimum cases here we choose three types: I, correlation detectors, which are conventionally optimum when the noise or interference reduces to the gaussian; II, LOBD structures, where, however, there is a mismatch between the algorithm selected and the critical class of interference in which the desired signal is being received, or where the estimates of the noise parameters are noticeably imprecise, or both. And III, where correlation detectors (already suboptimum in nongaussian noise) are used in similar "mismatched" situations.

We begin with the optimum cases:

4.1 LOBD Detection Algorithms:

From (2.11)-(2.16) we obtain for independent (but not necessarily stationary) noise samples the following results

I. Coherent Reception (H_1 vs. H_0):

$$g(\underset{\sim}{x})^*_c = [\log \mu + \hat{B}^*_{n\text{-coh}}] - \sum_{j=1}^{n} \langle a_{oj} s_j \rangle \ell_j \ , \tag{4.1}$$

---

* See Appendix A-3 for a demonstration of the optimality of the LOBD and associated conditions; cf., also, Sec. 2.5, above.

where now

$$\ell_j \equiv \ell(x_j) = \left[\frac{d}{dx} \log w_1(x|H_o) \right]_{x=x_j} ; \tag{4.2a}$$

and

$$\hat{B}^*_{n\text{-coh}} = -\frac{1}{2} \sum_i^n L_i^{(2)} \langle a_{oi} s_i \rangle^2 , \quad \text{cf. Eq. (A.1-16).} \tag{4.2b}$$

Similarly, we get

Ia. Coherent Reception (H_2 vs. H_1):

$$g^{(21)}(\underset{\sim}{x})^*_c = [\log \mu_{21} + \hat{B}^{(21)*}_{n\text{-coh}}] - \sum_{j=1}^n [\langle a_{oj}^{(2)} s_j^{(2)} \rangle - \langle a_{oj}^{(1)} s_j^{(1)} \rangle] \ell_j , \tag{4.3}$$

where

$$B^{(2)*}_{n\text{-coh}} = -\frac{1}{2} \sum_i^n L_i^{(2)} \{ \langle a_{oi}^{(2)} s_i^{(2)} \rangle^2 - \langle a_{oi}^{(1)} s_i^{(1)} \rangle^2 \}, \text{ cf. (A.2-45).} \tag{4.3a}$$

[The explicit structures of the various bias terms are derived in Appendix A-1.]

II. Incoherent Reception [H_1 vs. H_o]:

$$g(\underset{\sim}{x})^*_{inc} = [\log \mu + \hat{B}^*_{n\text{-inc}}] + \frac{1}{2!} \sum_{ij}^n [\ell_i \ell_j + \ell_i' \delta_{ij}] \langle a_{oi} a_{oj} s_i s_j \rangle , \tag{4.4}$$

where

$$\hat{B}^*_{n\text{-inc}} = -\frac{1}{8} \sum_{ij}^n \langle a_{oi} a_{oj} s_i s_j \rangle^2 \{ [L_i^{(4)} - 2L_i^{(2)} L_j^{(2)}] \delta_{ij} + 2 L_i^{(2)} L_j^{(2)} \}, \tag{4.4a}$$

cf. (A.1-20a), and

IIa. Incoherent Reception [H_2 vs. H_1]:

$$g^{(21)}(\underset{\sim}{x})^*_{inc} = [\log \mu_{21} + \hat{B}^{(21)*}_{n\text{-}inc}] + \frac{1}{2!} \sum_{ij} (\ell_i \ell_j + \ell'_i \delta_{ij})[\langle (a_{oi} a_{oj} s_i s_j)^{(2)} \rangle$$

$$- \langle (a_{oi} a_{oj} s_i s_j)^{(1)} \rangle] \ , \tag{4.5}$$

where

$$\hat{B}^{(21)*}_{n\text{-}inc} = - \frac{1}{8} \sum_{ij}^{n} \{\langle a^{(2)}_{oi} a^{(2)}_{oj} s^{(2)}_i s^{(2)}_j \rangle^2 - \langle a^{(1)}_{oi} a^{(1)}_{oj} s^{(1)}_i s^{(1)}_j \rangle^2\}$$

$$\cdot \{(L^{(4)}_i - 2L^{(2)2}_i)\delta_{ij} + 2L^{(2)}_i L^{(2)}_j\}, \tag{4.5a}$$

from (A.2-5ab), and again, the bias terms here are derived in Appendix A-1. The quantity ℓ'_i is

$$\ell'_i = \ell'(x_i) \equiv [\frac{d}{dx} \ell = \frac{d^2}{dx^2} \log w_1(x|H_o)]_{x=x_i} \ ; \text{ with } \delta_{ij}=1, \ i=j; =0, i \neq j \ . \tag{4.6}$$

4.2 Selected Suboptimum Detection Algorithms: (Simple- and Clipper-) Correlation Detectors

We begin with the simple or undistorted coherent (i.e. cross-) correlation detectors, and the corresponding incoherent (or auto-) correlation detectors, which are (threshold) optimum structures when the noise is gaussian [cf. Sec. A.1-3], and which may be optimum at all signal levels when special conditions at the receiver so warrant. [For a discussion of specific examples, see Sec. 20.4-1, [12], Secs. 2.5, 2.6, [20].] For independent noise samples we obtain [from Sec. (2.3), for instance, or Sec. A.1-3]:

I. Simple-Correlators:

A. Coherent Reception [H_1 vs. H_0]:

$$g(\underset{\sim}{x})_c = B'_{coh} + \sum_{j=1}^{n} \langle a_{oj} s_j \rangle x_j \ ; \tag{4.7}$$

B. Coherent Reception [H_2 vs. H_1]:

$$g^{(21)}(\underset{\sim}{x})_c = B^{(21)'}_{coh} + \sum_{j=1}^{n} [\langle a_{oj} s_j \rangle^{(2)} - \langle a_{oj} s_j \rangle^{(1)}] x_j \ , \tag{4.8}$$

where the biases are now [cf. A.4-22] specifically

$$B'_{coh} = \log \mu - \frac{1}{2} \sum_{j=1}^{n} \langle a_{oj} s_j \ ^2 \rangle ; \ B^{(21)'}_{coh} = \log \mu_{21} - \frac{1}{2} [\sum_{j=1}^{n} \{ \langle (a_{oj} s_j)^{(2)} \rangle^2$$

$$- \langle (a_{oj} s_j)^{(1)} \rangle^2 \}] . \tag{4.9}$$

Similarly, for incoherent reception we have

C. Incoherent Reception [H_1 vs. H_0]:

$$g(\underset{\sim}{x})_{inc} = B'_{inc} + \frac{1}{2!} \sum_{ij}^{n} \langle a_{oi} a_{oj} s_i s_j \rangle x_i x_j \ ; \tag{4.10}$$

D. Incoherent Reception [H_2 vs. H_1]:

$$g^{(21)}(\underset{\sim}{x})_{inc} = B^{(21)'}_{inc} + \frac{1}{2!} \sum_{ij}^{n} [\langle (a_{oi} a_{oj} s_i s_j)^{(2)} \rangle - \langle (a_{oi} a_{oj} s_i s_j)^{(1)} \rangle] x_i x_j \ , \tag{4.11}$$

and from [A.4-55] the biases are found to be explicitly

$$B'_{inc} = \log \mu - \frac{1}{2} \sum_{j=1}^{n} \langle (a_{oj} s_j)^2 \rangle - \frac{1}{4} \sum_{ij}^{n} \langle a_{oi} a_{oj} s_i s_j \rangle^2 \tag{4.12a}$$

$$B_{inc}^{(21)'} = \log \mu_{21} - \frac{1}{2} \sum_{j=1}^{n} \{\langle \theta_j^{(2)2} \rangle - \langle \theta_j^{(1)2} \rangle\} - \frac{1}{4} \sum_{ij}^{n} [\langle \theta_i^{(2)} \theta_j^{(2)} \rangle^2$$

$$- \langle \theta_i^{(1)} \theta_j^{(1)} \rangle^2] \ , \ (\theta_j = a_{oj} s_j, \text{ etc.}). \qquad (4.12b)$$

For the energy detector, cf. (A.4-61a), (4.11), (4.12) are simply modified to

(Energy):

$$g^{(21)}(\underset{\sim}{x})_{inc} = B_{inc}^{(21)'} + \frac{1}{2} \sum_{i}^{n} [\langle a_{oi}^2 s_i^2)^{(2)} \rangle - \langle (a_{oi}^2 s_i^2)^{(1)} \rangle] x_i^2 \qquad (4.12b)$$

with the bias

$$B_{inc}^{(21)'} = \log \mu_{21} - \frac{1}{2} \sum_{i} (\langle \theta_i^{(2)2} \rangle - \langle \theta_i^{(1)2} \rangle) - \frac{1}{4} \sum_{i} (\langle \theta_i^{(2)2} \rangle^2 \langle \theta_i^{(1)2} \rangle^2) \ , \qquad (4.12c)$$

This shows, as expected, that for detection here, the signal energies must be different, and the larger the difference, the better the discrimination between the (1) and (2) states.

II. Clipper Correlators:

From Secs. A.4-3,4 we may write specifically the (suboptimum) detection algorithms when "super"-clippers are used in the correlation receivers, in contrast to the situation above (I), where there is no distortion. We summarize the results:

A. Coherent Reception [H_1 vs. H_0]:

$$g(\underset{\sim}{x})_{coh} = \log \mu - \sqrt{2} \sum_{i}^{n} \langle \theta_i \rangle^2 w_{1E}(0)_i + \sqrt{2} \sum_{i}^{n} \langle \theta_i \rangle \ \text{sgn} \ x_i \ ; \qquad (4.13)$$

B. Coherent Reception [H_2 vs. H_1]:

$$g^{(21)}(\underset{\sim}{x})_c = \log \mu - \sqrt{2} \sum_i^n [\langle\theta_i^{(2)}\rangle^2 - \langle\theta_i^{(1)}\rangle^2] w_{1E}(0)_i + \sum_i^n [\langle\theta_i^{(2)}\rangle - \langle\theta_i^{(1)}\rangle] \operatorname{sgn} x_i . \tag{4.14}$$

Similarly, for the incoherent cases we have

C. Incoherent Reception [H_1 vs. H_0]:

$$g(\underset{\sim}{x})_{inc} = \log \mu - \sum_i^n \langle\theta_i^2\rangle(1-\sqrt{2}\, w_{1E}(0)_i) - \frac{1}{4} \sum_{ij}^n \langle\theta_i\theta_j\rangle^2 [8 w_{1E}(0) w_{1E}(0)_j - \{\sqrt{2}\, w''_{1E}(0)_i + 8 w_{1E}(0)_i^2\}\delta_{ij}]$$

$$+ \sum_{ij}^n \langle\theta_i\theta_j\rangle \operatorname{sgn} x_i \operatorname{sgn} x_j , \tag{4.15}$$

and for binary signals:

D. Incoherent Reception [H_2 vs. H_1]:

$$g^{(21)}(\underset{\sim}{x})_{inc} = \log \mu - \sum_i^n [\langle\theta_i^{(2)^2}\rangle - \langle\theta_i^{(1)^2}\rangle][1-\sqrt{2}\, w_{1E}(0)_i] - \frac{1}{4} \sum_{ij}^n [\langle(\theta_i\theta_j)^{(2)}\rangle^2 - \langle(\theta_i\theta_j)^{(1)}\rangle^2]\{8 w_{1E}(0)_i w_{1E}(0)_j - [\sqrt{2}\, w''_{1E}(0)_i + 8 w_{1E}(0)_i^2]\delta_{ij}\}. \tag{4.16}$$

In the above $w_{1E}(0)_i$ is the (jth-) value of the noise pdf (A4-50b) when $x_i = 0$.

4.3 Selected Suboptimum Detection Algorithms: II-Mismatched LOBD's.

Here we indicate "mismatch" by the following device: from (4.1), (4.2) we write

$$\ell_j \to (\ell_{D|E})_j \equiv \frac{d}{dx} \log w_1(x|H_o)_{D|E} \ , \tag{4.17}$$

where D|E denotes D-class parameters, or parameter estimates, D=D', when the pdf of x is chosen (correctly or not) to be E-class. Thus, we have the following varieties of mismatched and matched conditions:

TABLE 4.1. VARIETY OF MISMATCHED AND MATCHED CONDITIONS.

Parameter Values (D)=	Selected Class of Interference (E)=	Remarks
1). D	D	Exact (or "true") parameter values are used in the same postulated class of interference.
(1a). E	E	Same as 1). E≠D, or E = D.)
2). D'	D	Class D estimates, D' (≠D) used in same postulated Class (D) of interference
3). D	E	Class D (exact) parameter values used in chosen Class (E) interference.
4). D'	E	Class D estimates (D'≠D) used in postulated Class E interference

[Interchanging D and E clearly introduces no new forms of relationship. Later, when performance is to be evaluated, along the lines of Sec. 2.4, we shall need to relate the category (E) to the actual, or true, statistical situation, with respect to which the various averages of g*, g, etc. are to be taken, cf. Sec. 6 and Appendix A-I.]

Accordingly, the various possible mismatched threshold detection algorithms follow directly from (4.1)-(4.6) on replacing ℓ_j therein by $\ell_{D|E}\big|_j$, etc., and, correspondingly, g* by the now suboptimum forms $g_{D|E}$, subject to

the combinations of Table 4.1. The bias terms in the LOBD's remain unchanged here. The (generally) suboptimum correlation detectors are not affected by the actual or assumed classes of parameter values or interference statistics.

Finally, in all cases, the complete detection algorithm requires that the number(s) produced by the processing algorithm (g*,g, etc.), as given specifically in Secs. 4.1, 4.2 above, be compared against the appropriate threshold $\log \mathcal{K}$, $\log K$, $\log \mathcal{K}^{(21)}$, cf. (2.2), (2.3), (2.7) respectively: if the threshold is equalled or exceeded, we decide H_1 (or H_2): a signal (or signal 2) is present: if the threshold is not exceeded, we choose the alternative (i.e. null, H_0), or signal 1 cases. We shall give explicit examples in Section 7 ff.

SECTION 5. MATCHED FILTER STRUCTURES: INTERPRETATION OF THE ALGORITHMS

From the earlier analyses of [20], Chapter 4, and the Appendix therein, we can establish matched filter structures for the linear portions of the threshold signal processing explicitly indicated in g,g* for both coherent and incoherent reception cf. (4.1), (4.4), (4.7), (4.10) above. This is important because such structures provide a guide to the actual realization of the physical entities which are needed to carry out the indicated processing, either directly as a computational program, or much more conveniently, usually, by building the specialized mini-computer which represents the operations involved, perhaps in chip form, etc. In the case of specific examples, we shall confine our attention here (in the incoherent cases explicitly) to the important special cases when the desired input signal is narrow-band, the usual situation in telecommunications practice. We consider again the coherent and incoherent cases in detail for the frequently encountered "on-off" (i.e. H_1 vs. H_0) detection situations. Corresponding results for the two-signal (H_2 vs. H_1) are summarized in Sec. 5.

5.1 Coherent Reception (H_1 vs. H_0);

Here we have the situation shown in Figs. 5.1a,b, for both optimum and suboptimum (i.e., cross-correlation detectors). First, in the optimum case, the input sampled data $\{x_j\}$ is non-linearly processed, to yield $y_j=\ell_j$, cf.

(4.1). This new (voltage) sample, [where $y_j=y(t_j)=\ell(x(t_j))$, etc., of course] is then passed through a (linear) "matched filter", where the weighting function of the filter is

$$h_M(T-t_j;T)\Delta t = \langle a_o(t_j)s(t_j)\rangle, \tag{5.1}$$

so that

$$\Psi_n^{(1)*} \equiv \sum_{j=1}^{n} \langle a_{oj}s_i\rangle \ell_j = \sum_{j=1}^{n} y(t_j)h_M(T-t_j;t)\Delta t, \tag{5.2}$$

(which in continuous form becomes, on (0-,T+), the linear functional

$$\Psi_n^{(1)*} \to \Psi_T^{(1)*}(x(t)) = \int_{0-}^{T+} y(t)h_M(T-t,T)dt.) \tag{5.2a}$$

The matched filters are shown in Figs. 5.1a,b. For the suboptimum situation of the cross-correlation detector of (4.7), we have

$$\Psi_n^{(1)} \equiv \sum_{j=1}^{n} \langle a_{oj}s_i\rangle x_j = \sum_{j=1}^{n} x(t_j)h_M(T-t_j;T)\Delta t, \tag{5.2}$$

and all operations here are linear, of course. The matched filter remains the same; only the prefilter processing is different. The filter, h_M, is a form of delay line filter, with suitable weighting ($\sim h_M$) and a read-out at t=T from wherever we choose to start the particular sampling for the interval (t_o,t_o+T), from which we in turn then make the decision indicated by (2.2). We have called such filters "Bayes mached filters of the 1st kind, Type 1", cf. Sec. 4.2, [20], which is, of course, recognized as a special form of (cross-) correlation filter.

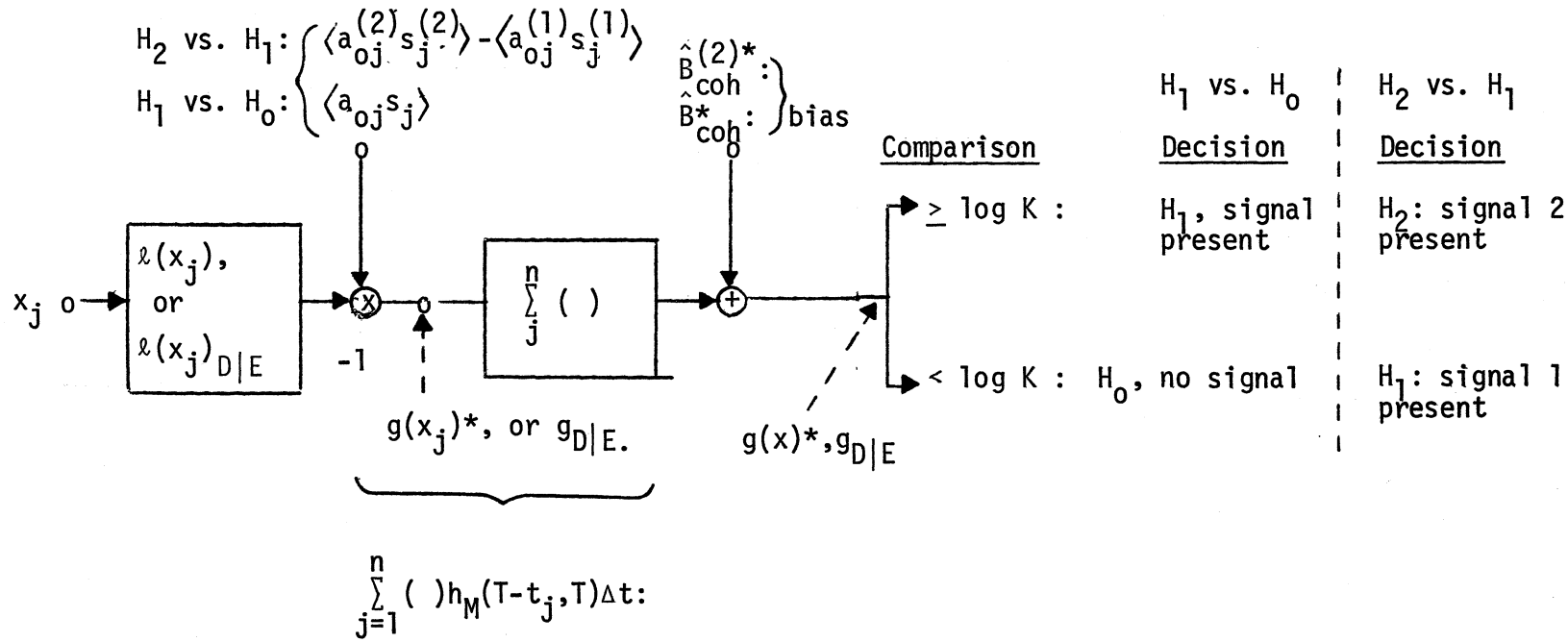

Figure 5.1a LOBD locally optimum threshold receiver, Eq.(4.1), for both "on-off" i.e. (H_1 vs. H_0) and signal 1 vs. signal 2 (H_2 vs. H_1), coherent signal detection, showing matched filter structures [cf. (5.1), (5.2)], [and (4.15), (4.18),[20]]. These are mismatched LOBD's when $\ell \to \ell_{D|E}$, Table 4.1, etc.

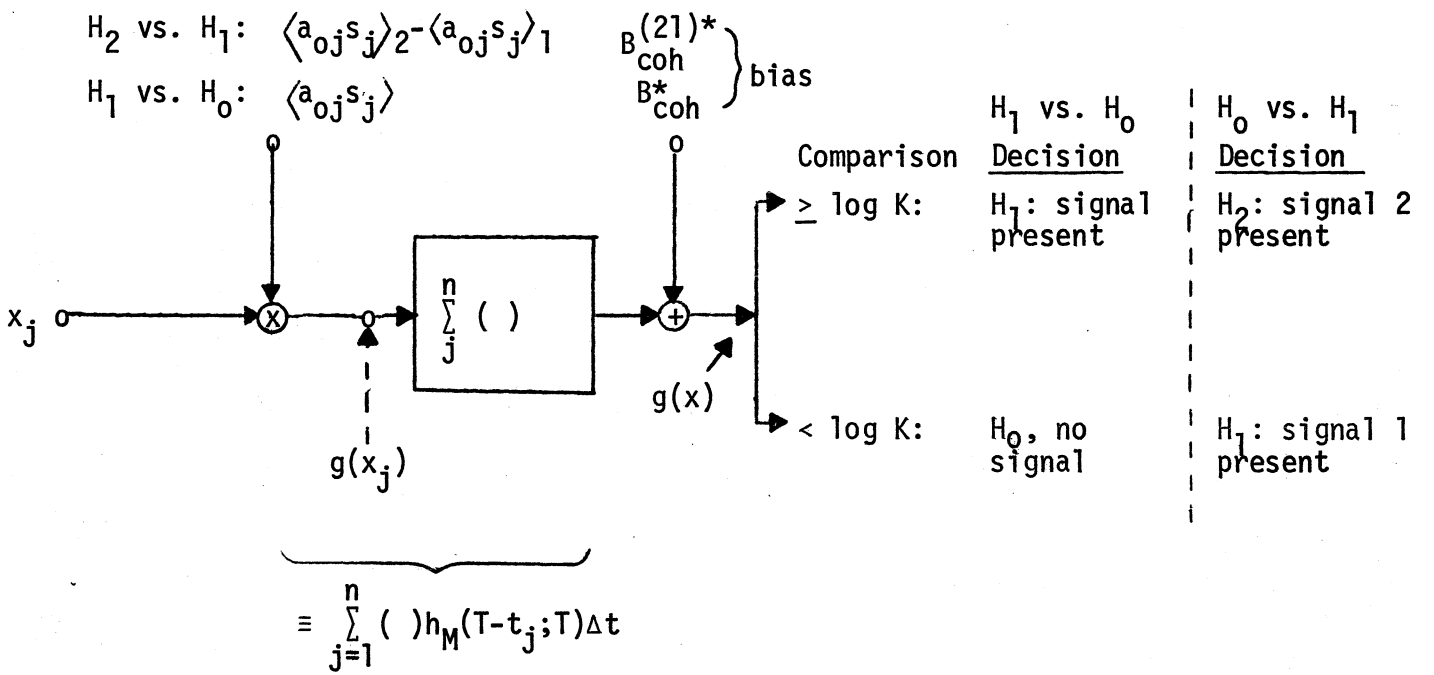

Figure 5.1b (Cross-) correlation detectors, Eq. (4.7), for "on-off" (i.e. H_1 vs. H_0) coherent signal reception showing a matched filter structure (the same as in Fig. 5.1a, cf. Eq. (5.1) et seq.), cf. [20]. Also shown is the binary signal case H_2 vs. H_1, with matched filters, (5.15).

5.2 Incoherent Reception (H_1 vs. H_0):

Here we have the same phenomenon: a highly non-linear operation on the sampled data, to obtain ℓ,ℓ', cf. (4.4), and then to pass these into a second-order nonlinear system, which in this instance can be expressed in the manner of Fig. (5.2), either as a combination of time-varying (linear) filter and zero-memory square-law device, or as another time-varying (linear) filter, and multiplication operation. The point is that the (linear) matched filter here can be represented in two realizable (i.e. operating only on the past) forms. These are:

$$h_M(t_j-t_i,t_j) \equiv \text{sol. of} \begin{cases} \sum_{\ell=1}^{n} h_M(t_\ell-t_i,t_\ell)h_M(t_\ell-t_j,t_\ell)\Delta t=\langle a_{oi}a_{oj}s_is_j\rangle, \\ \qquad\qquad 1 \le i, j \le n \\ = 0, \text{ elsewhere }, \end{cases} \tag{5.4}$$

where

$$\psi^{(2)*} \equiv \sum_{ij}^{n} y_iy_j\langle a_{oi}a_{oj}s_is_j\rangle = \sum_{j=1}^{n} y_j \sum_{i=1}^{(n,\text{or }\infty)} y_i h_M(t_j-t_i,t_j)(\Delta t)^2 \Bigg\} \tag{5.5}$$

$$= \sum_{j=1}^{n} z(t_i)^2 \, . \Bigg\} \tag{5.5a}$$

The filter, $h_M(t_j-t_i,t_j)$, is time-varying and realizable, and we call it a Bayes matched filter of the 2nd kind, type 1 (cf. Fig. 4.3, [20], also).

In the narrow-band situation we are usually forced to deal with, an equivalent, alternative form of matched filter (e.g. Fig. 5.2, where a multiplier is employed, instead of a zero-memory quadratic device). For this we have

$$\psi^{(2)*} = \sum_{ij}^{n} y_iy_j\hat{h}_M(t_j-t_i,t_j)\Delta t \; ; \quad \hat{h}_M = 0, \; t_i>t_j \, , \tag{5.6}$$

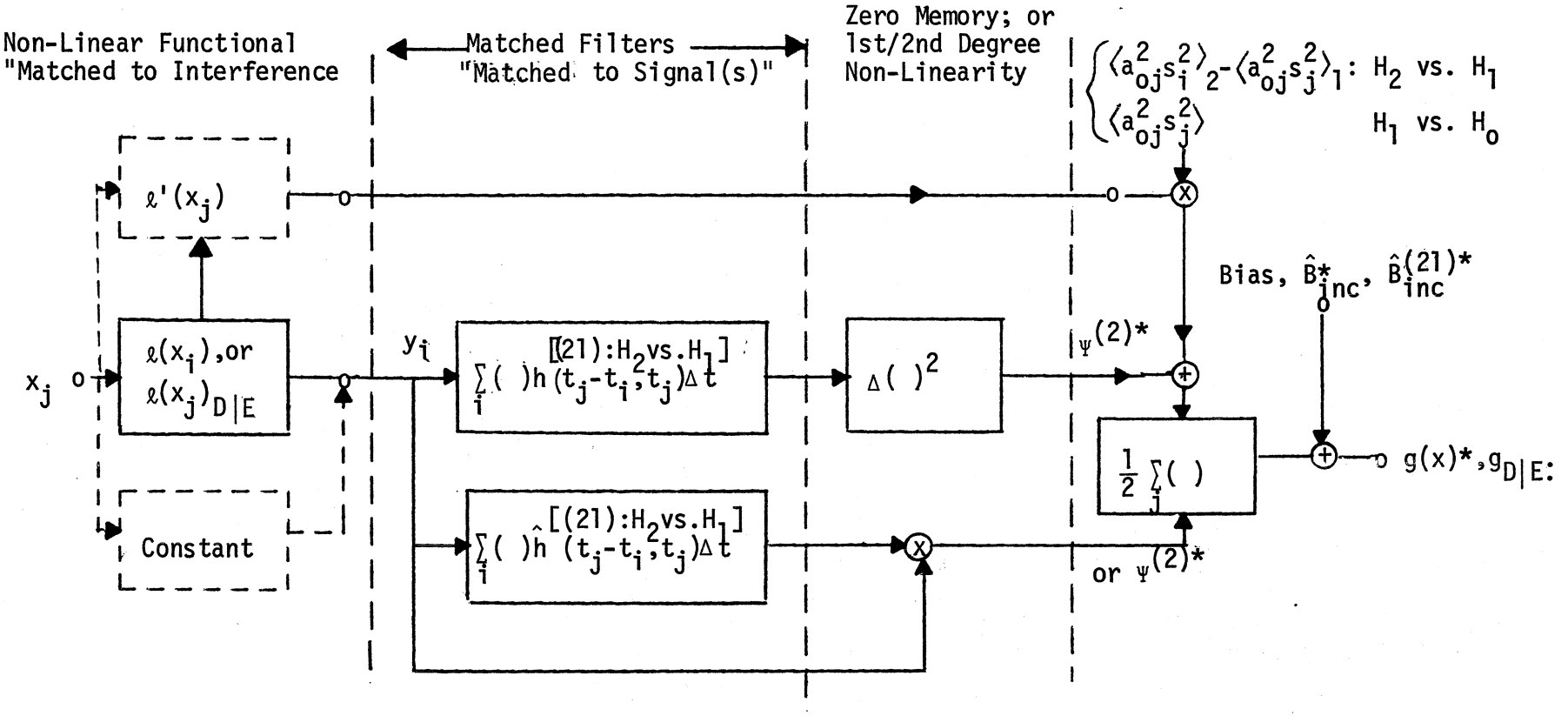

Figure 5.2 LOBD for both optimum, "on-off" (i.e. H_1 vs. H_o) and signal 1 vs. signal 2 (H_2 vs. H_1), incoherent signal detection, Eqs. (4.4), (4.5). [The dotted portion -.-., applies for the (usually) suboptimum auto-correlation detectors, Eqs. (4.10), (4.11).] The matched filters here, h, $\hat{h}$, (5.4), (5.7) are functionals of the signal auto-correlation functions $a_{oi}a_{oj}s_i s_j$ (1),(2). These are mismatched LOBD's when $\ell \to \ell_{D|E}$, Table 4.1, etc.

where explicitly

$$\hat{h}_M(t_j-t_i,t_j)\Delta t \equiv \langle Z_i Z_j^* \rangle_\theta \ , \ t_j > t_i ; \ =0, \ t_j<t_i \ , \tag{5.7}$$

in which

$$\langle Z_i Z_j^* \rangle_\theta \equiv \langle a_{oi} a_{oj} s_i s_j \rangle . \tag{5.7a}$$

This filter is discussed in Sec. 4.3, [20], also, cf. Fig. 4.4, ibid. It is realizable, time-varying, and as in the coherent cases, depends only on the signal statistics; see Sec. 5.3 ff. (The same filter, h_M, or $\hat{h}_M$, clearly applies for the suboptimum, autocorrelator of (4.10), with $y_i \to x_i$, $y_j \to x_j$, a linear transformation, cf. (5.3).)

5.3 Signal Scenarios

Using Sec. 3.1 we can provide a more detailed structure for the above matched filters, including the effects of fading (a) and propagation law (γ), cf. (3.2), (3.2a). Specifically, for narrow band signals without amplitude modulation, we have from (3.2), (3.2a)

$$s_j = \sqrt{2} \cos [\omega_o(t_j-\epsilon)-\phi_j-\phi_o] \ ; \ a_{oj} = \frac{aG_o}{\lambda^\gamma \sqrt{2\bar{I}_N}} \equiv aB_o \ ; \tag{5.8}$$

$$B_o \equiv G_o/\lambda^\gamma \sqrt{2\bar{I}_N} \ , \tag{5.8a}$$

where the fading effects are governed by the statistics of $\underline{a}$, cf. (3.3), for example.

Thus, for coherent reception the matched filter h_M, (5.1), becomes explicitly

$$h_M(T-t_j,T)\Delta t = a_{oj}\langle s_j\rangle_\epsilon = \bar{a}_{oj}\sqrt{2}\cos\,[\omega_o(t_j-\epsilon_o)-\phi_j-\phi_o],$$

$$0-<t_j<T+;\ =0,\ \text{elsewhere}, \tag{5.9}$$

since $w_1(\epsilon) = \delta(\epsilon-\epsilon_o)$. Moreover, with the assumed stationarity of all random processes here, we have $\bar{a}_{oj} = \bar{a}_o$ $(= \bar{a}\,\langle B_o\rangle)$, under the further not unreasonable assumption that a_o (and a, B_o) and ϵ are all mutually independent. This result, (5.9), is clearly independent of the fading law, whether or not it is rapid or slow, and whether or not the signal source is moving. This, in turn, is a direct consequence of the coherent mode of detection.

On the other hand, <u>with incoherent reception</u> all the above effects appear explicitly in the structure of the appropriate matched filter [e.g. h_M, $\hat{h}_M$, (5.4), (5.7)], as we might expect, because of the second-order statistics involved. Thus, for example, $\hat{h}_M$, (5.7), becomes now from (5.8)

$$\left.\begin{aligned}\hat{h}_M(t_j-t_i,t_j)\Delta t = \langle a_{oi}a_{oj}\rangle\langle s_i s_j\rangle_{\epsilon,..} &= \langle a_{oi}a_{oj}\rangle\cos[\omega_o(t_i-t_j)-\phi_i+\phi_j],\ t_j>t_i\\ &= 0 \qquad\qquad\qquad\qquad\qquad\quad t_j<t_i\end{aligned}\right\}, \tag{5.10}$$

and we have, moreover, the various situations:

(i). <u>slow fading (one-sided):</u>

$$\langle a_{oi}a_{oj}\rangle = \overline{a_o^2} = \overline{a^2}\,\langle G_o^2\rangle/\bar{I}_N\lambda^{2\gamma} \tag{5.11a}$$

(ii). <u>rapid fading (one-sided):</u>

$$\langle a_{oi}a_{oj}\rangle = \overline{a_o^2}\,\delta_{ij} + \bar{a}_o^2(1-\delta_{ij}),$$

$$= \{\overline{a^2}\,\langle G_o^2\rangle/\bar{I}_N\lambda^{2\gamma}\}\delta_{ij}+(1-\delta_{ij})\bar{a}^2\langle G_o\rangle^2/\bar{I}_N\lambda^{2\gamma} \tag{5.11b}$$

(iii). slow fading (two-sided):

$$[\overline{a_{oj}} = 0]; = \overline{a_o^2}\,\delta_{ij} = \overline{a^2}\langle G_o^2\rangle/\bar{I}_N\lambda^{2\gamma}. \tag{5.11c}$$

These results can be extended to include doppler, namely, relative motion between the desired signal source and the receiver: the normalized signal (5.8) is now

$$s_j = \sqrt{2}\cos[(\omega_o+\omega_d)(t_j-\epsilon)-\phi_j-\phi_o] \quad ; \quad \omega_d = \frac{\omega_o v_d}{c_o}\,, \tag{5.12}$$

so that [cf. III, Sec. 5.1 of [34]]

$$\rho_{s\text{-}ij} \equiv \langle s_i s_j\rangle_{\epsilon,\omega_d,\ldots} = e^{-(\Delta\omega_d)^2(t_i-t_j)^2/2}\cos[\omega_o(t_i-t_j)-\phi_i+\phi_j], \tag{5.13}$$

where $\Delta\omega_d = (\omega_o/c_o)\Delta v_d$, $t_i-t_j = (i-j)\Delta T$, and $(\Delta v_d)^2$ is the variance in relative velocity, and we have postulated a gaussian distribution of velocities; c_o is the speed of (wavefront) propagation of EM waves in the medium in question. Applying the relations (5.11) with (5.13) gives, in this more general case,

$$\left.\begin{aligned}\hat{h}_M(t_j-t_i,t_j)\Delta t = \langle a_{oi}a_{oj}\rangle e^{-(\Delta\omega_d)^2(t_i-t_j)^2/2}\cos[\omega_o(t_i-t_j)-\phi_i+\phi_j]\ , \quad & t_j > t_i,\\ = 0\ , \quad & t_j < t_i\end{aligned}\right\} \tag{5.14}$$

for this matched filter for incoherent reception. In this way, from the "anatomy" of the desired signal, from source to receiver, we can construct the desired matched filter for detection. [We remark that still more sophisticated (received) signal forms can be constructed, if the channel itself is dispersive, i.e. has time-delay and frequency spread effects as

well as fading (above), cf. [35]-[38] and remarks at the end of Sec. 3.2 above.]

5.4 Extensions: Binary Signals (H_2 vs. H_1):

The matched filters above for the "on-off" cases (H_1 vs. H_0) are directly modified in the binary signal situation (H_2 vs. H_1). Comparing (4.3), (4.5), (4.8), (4.11) with the respective "on-off" cases, we see at once that (5.1) and (5.7) are modified to

$$h_M^{(21)}{}_{\Delta t}\Big|_{coh} = \langle a_{oj}s_j\rangle_2 - \langle a_{oj}s_j\rangle_1 ; 0 \le t_j \le T; = 0 \text{ elsewhere} ; \tag{5.15a}$$

$$\hat{h}_M^{(21)}{}_{\Delta t}\Big|_{inc} = \langle a_{oi}s_{oj}s_is_j\rangle_2 - \langle a_{oi}a_{oj}s_is_j\rangle_1 , \; t_j > t_i ; = 0 \text{ elsewhere} . \tag{5.15b}$$

From the results of Sec. 5.3 we have, in detail:

$$\begin{aligned} h_M^{(21)}(T-t_j;T)\Delta T = \sqrt{2}(&\langle a_{oj}\rangle_2 \cos[\omega_{o2}(t_j-\epsilon_o)-\phi_j^{(2)}-\phi_o] \\ &-\langle a_{oj}\rangle_1 \cos[\omega_{o1}(t_j-\epsilon_o)-\phi_j^{(1)}-\phi_o]) \quad , \\ &0 \le t_j \le T \; , \end{aligned} \tag{5.16}$$

for the coherent cases (where any doppler is compensated for). For the incoherent cases (5.14) becomes

$$\begin{aligned} h_M^{(21)}(t_j-t_i,t_j)\Delta T = e^{-(\Delta\omega_d)^2(t_i-t_j)/2}\{&\langle a_{oi}a_{oj}\rangle_2 \cos[\omega_{o2}(t_i-t_j)-\phi_i^{(2)}+\phi_j^{(2)}] \\ &-\langle a_{oi}a_{oj}\rangle_1 \cos[\omega_{o1}(t_i-t_j)-\phi_i^{(1)}+\phi_j^{(1)}]\} \; , \\ &t_j > t_i \; ; = 0, \; t_i < t_j \; , \end{aligned} \tag{5.17}$$

where now the effects of doppler ($\sim \Delta\omega_d$) show up as a common damping factor (since the source of signals 1,2 is the common source). For further "anatomy" of the filter structure, we can use (5.8), (5.8a), for a_{oi}, etc.

5.5 The Generic Character of the LOBD as Adaptive Processor:

At this point it is important to point out a number of general properties of the canonical LOBD's described above. We observe that:

(1). For coherent and incoherent detection - with independent noise samples - the matched filter depends only on signal statistics and structure. Because the LOBD is a threshold system, only first and second-moment statistics of the signal amplitude are needed, Sec. (5.3). [Higher-order statistics are required, of course, for doppler, which is phase variable, cf. (5.13).]

(2). The matched filter (by definition) is always linear, but may or may not be realizable, in the sense of operating only on the "past" of the received data [cf. Chapter 4, [20]);

(3). A variety of equivalent matched filters can be obtained, to represent the data functional $\Psi^{(1)}$, $\Psi^{(2)}$, etc.;

(4). The general functional description of the LOBD is as follows:

(i). It first "matches" the receiver to the (non-gaussian, or gaussian) noise or interference, in that (a), it "adapts" - i.e., determines the Class of interference (A,B, or C) and then estimates the Class parameters, $\mathcal{P}_{3A}$, $\mathcal{P}_{3B}$, etc.- to generate a nongaussian functional, e.g. ℓ,ℓ', of the input data;

(ii). Next, the LOBD then "matches" the signal - as it is a priori known or structured at the receiver - to this new input (ℓ,ℓ', etc.), to form an appropriate correlation detector for the non-gaussian functional ℓ, etc.

These "matched" filters are, by definition, always linear and usually realizable in the causal sense [Sec. 5.2, 5.4];

(iii). For incoherent detection there is an additional, third operation, which follows the matching process, (ii), above. This is usually a nonlinear operation plus summation, where the additional nonlinearity is either a memoryless quadratic process or a multiplication;

(iv). In the mixed cases, of combined coherent and incoherent processing, (usually where there is some RF phase information in narrow-band reception), the nonlinearities following steps (i), (ii), can be more complicated (cf. [1b], Part II, IIC., for example).

Figure 5.3 illustrates the general formalism of LOBD signal detection, for either coherent or incoherent reception, in the prototypical "on-off" case (H_1 vs. H_0). The extension to the binary signal cases (H_2 vs. H_1) is immediate from Sec. 5.4.) Note the key elementsof Locally Optimum Bayes Estimation (LOBD's), of the EMI parameters. (The LOBE theory is developed in parallel concept to that of the LOBD, except that for the most part one operates under the H_1: "signal-present" condition.) The combined operation of LOBD and LOBE is clearly an adaptive process, which, of course, accounts for its usually significant superiority over conventional systems, a priori optimized against gauss noise.

Often, of course, in practice nonoptimum or finite-sample estimates of the parameters of the interfering noise are usually used, as outlined in Sec. 4.3 above. Moreover, before estimating the pertinent noise parameters, it is necessary to establish which class of interference the detector is operating against. One method of doing this is to estimate the pdf (or APD): Class A noise is always distinctively evident by an (almost) zero magnitude of the pdf (or a flat plateau in the APD) between the small-amplitude or "gaussian" region, and the large-amplitude region. In Class B interference there is no zero amplitude region (or flat plateau). [See [6], [7].) An

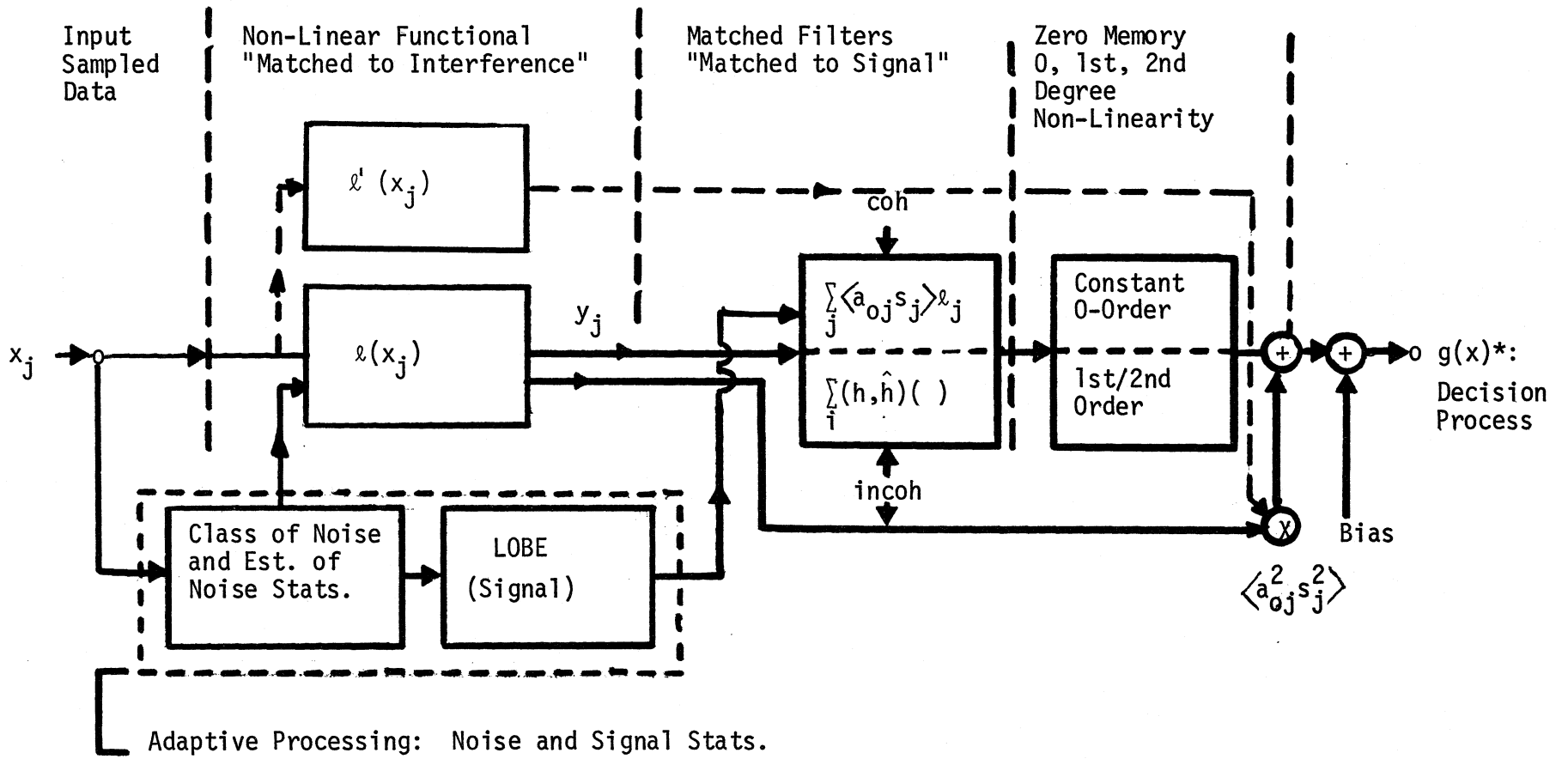

Figure 5.3. The full LOBD for optimum ("on-off", i.e. H_1 vs. H_0) threshold detection of signals in a general EMI environment, for coherent/incoherent reception, and showing the adaptive portion of the optimum receiver [cf. Figs. 5.1, 5.2].

additional advantage of these (estimated) pdf's (etc.) is that they can also be used to give (estimated) values of the Class (A, B) parameters involved, in the manner of [7], for instance. However, if the elements of the EMI scenario are known, the needed parameters can then be calculated, rather than estimated, in the manner of Sec. 3.2 above.

6. PERFORMANCE OF OPTIMUM AND SUBOPTIMUM THRESHOLD DETECTORS: MINIMUM DETECTABLE SIGNALS, PROCESSING GAINS, AND CONDITIONS OF APPLICABILITY

From the general results of Sec. 2.4 and the specific results of Appendices A1-A4, we can obtain at once explicit canonical forms for the various error and correct signal detection probabilities by which performance is most generally measured. This is discussed in Sec. 6.1, while specific structures are reviewed in Sec. 6.2, along with the joint concepts of minimum detectable signal and processing gain, in turn illustrated by the specific relations developed in Appendices A1-A4. In Sections 6.3-6.5 we examine the improvement factors of the optimum detectors over the suboptimum (correlation) detectors discussed in this paper, along with the important conditions on the strength of the input signals which permit us to employ these (analytical) performance measures, and thereby to obtain meaningful numerical results from them. It is shown (in Sec. 6.4), for example, that the set of conditions, for both coherent and incoherent reception, must be simultaneously obeyed, if one is safely to use the performance measures for either mode of reception. This coupling of the coherent and incoherent modes of detection in the evaluation of either mode is the consequence of the fact that coherent detection can never be inferior to incoherent detection under the otherwise same signal and noise conditions of observation. In any case, we emphasize the fact that our results apply generally to all signal types, broad band and narrow band, and can be immediately specialized to narrow band examples as needed, cf. Sec. 7 ff.

We proceed:

6.1 Canonical Performance Measures:

We now apply the specific results of Appendices A1-A4 to Eqs. (2.31)-(2.33), and note that regardless of the mode of detection, optimum (but not suboptimum) algorithms are asymptotically normally distributed, $G(\log \mu \mp \sigma_o^{*2}/2, \sigma_o^{*2})$, where σ_o^{*2} is the variance of the detection algorithm in question (and is the same under both hypotheses).† Here $(\mp)$ refers to: $(-)$, H_o; $(+)$, H_1 in the "on-off" cases, or to H_1, H_2, respectively in the binary signal situations ($s^{(1)}$ vs. $s^{(2)}$). The results are the canonical forms for the correct signal detection probability (Neyman-Pearson Observer) and the error-probability (Ideal Observer), used in ongoing telecommunication reception.

We have, accordingly, since for optimum (threshold) detectors

H_1 vs. H_o:

$$\langle g^* \rangle_1 - \langle g^* \rangle_o = \frac{\sigma_o^{*2}}{2} - (-\frac{\sigma_o^{*2}}{2}) = \sigma_o^{*2};$$

H_2 vs. H_1:

$$\langle g^{(21)^*} \rangle_2 - \langle g^{(21)^*} \rangle_1 = \frac{\sigma_o^{(21)^{*2}}}{2} - (-\frac{\sigma_o^{(21)^{*2}}}{2}) = \sigma_o^{(21)^{*2}} \quad , \tag{6.1}$$

the relations [from (2.31),(2.32)] for the "on-off" cases, both optimum and suboptimum††

$$\boxed{P_D^{(*)} \underset{\sim}{\cdot} \frac{p}{2}\{1+\Theta[\frac{\sigma_o^{(*)}}{\sqrt{2}} - \Theta^{-1}(1-2\alpha_F^{(*)})]\}, \quad \text{(N.P. Observer)},} \tag{6.2}$$

where $\alpha_F^{(*)}$ is the false-alarm probability and $\beta_D^{(*)}$ is the false-detection probability††

---

† The suboptimum cases yield asymptotically normal forms, but with different means and variance structures, cf. (6.3) ff.

†† We use the condensed notation $b^{(*)}$ to denote either b* or b, (* ≡ opt.; otherwise suboptimum). It is important to note that the appropriate bias terms (i.e. those for which the algorithms becomes optimum for the corresponding noise [cf. Appendix A4-1,D] are assumed here. Otherwise, one must use (2.31), (2.32) directly. See footnote, next page

$$\alpha_F^{(*)} \doteq \frac{1}{2}\{1-\Theta[\frac{\sigma_o^{(*)}}{2\sqrt{2}} + \frac{\log(\mathcal{K}/\mu)}{\sqrt{2}\,\hat{\sigma}_o}]\};\quad \beta_D^{(*)} \simeq \frac{1}{2}\{1-\Theta[\frac{\sigma_o^{(*)}}{2\sqrt{2}} - \frac{\log(\mathcal{K}/\mu)}{\sqrt{2}\,\hat{\sigma}_o}]\}, \tag{6.3}$$

with

$$\Theta(x) = -\Theta(-x) = \frac{2}{\sqrt{\pi}}\int_0^x e^{-t^2}dt\ ;\quad \Theta^{-1}(y) = x \text{ in } \Theta(x)\ . \tag{6.3a}$$

For the suboptimum cases note the presence of $\hat{\sigma}_o$, (cf. A.4-12,31), as well as σ_o, in the above (and following) expressions. In the optimum cases we have $\sigma_o, \hat{\sigma}_o \to \sigma_o^*$, of course, here†

Similarly, for the Ideal Observer (threshold $\mathcal{K}=1$) in the "on-off" cases, where one considers the error probability $P_e^{(*)} = q\alpha^{(*)}+p\beta^{(*)}$ as the measure of performance, the result here is specifically, on combining (6.3) in $P_e^{(*)}$:

$$P_e^{(*)} \doteq \frac{1}{2}\{1-p\Theta[\frac{\sigma_o^{(*)}}{2\sqrt{2}} - \frac{\log\mu}{\sqrt{2}\,\hat{\sigma}_o^*}]+q\Theta[-\frac{\sigma_o^{(*)}}{2\sqrt{2}} + \frac{\log\mu}{\sqrt{2}\,\hat{\sigma}_o^*}]\},\ \mathcal{K}=1,\ [\text{I.O.}], \tag{6.4}$$

for the general channel ($\mu=p/q\neq 1$, or $\mu=1$). This reduces to the case of the symmetrical channel ($\mu=1$) to the more familiar, simpler result for the optimum cases:†

(μ=1):
$$\boxed{P_e^{(*)} \doteq \frac{1}{2}\{1-\Theta[\frac{\sigma_o^{(*)}}{2\sqrt{2}}]\}\ ,\ \mathcal{K}=1,\ [\text{I.O.}].} \tag{6.5}$$

When binary signaling is employed we can also use a Neyman-Pearson Observer (N.P.O.) procedure, where now one of the error probabilities $\alpha_F^{(*)} \to \beta_1^{(2)(*)}$ (the [conditional] probability of incorrectly stating that signal S_2 is present when actually signal S_1 occurs) is preset and the other ($\beta^{(*)} \to \beta_2^{(1)(*)}$ is minimized or otherwise evaluated according to (6.2), which becomes now†

†Our suboptimum cases are here (and subsequently) restricted to those situations where the (nonvanishing) bias is chosen to be the appropriate bias for the class of noise for which these (suboptimum) algorithms, cf. Sec. 4.2, become optimum cf. Appendix A4-1,D. Otherwise, we must employ (2.31),(2.32) directly as performance measures.

$$P_{D-2}^{(*)} \doteq \frac{p_2}{2}\{1+\Theta[\frac{\sigma_o^{(21)(*)}}{\sqrt{2}} - \Theta^{-1}(1-2\beta_1^{(2)(*)})]\}, \qquad [N.P.O.], \quad (6.5a)$$

where (6.3) becomes

$$\alpha_F^{(*)} \to \beta_1^{(2)(*)} \doteq \frac{1}{2}\{1-\Theta[\frac{\sigma_o^{(21)*}}{2\sqrt{2}} + \frac{\log(\mathcal{K}^{(21)}/\mu_{21})}{\sqrt{2}\,\hat{\sigma}_o^{(21)(*)}}]\}, \quad \mu_{21}\equiv p_2/p_1, \; p_1+p_2 = 1. \quad (6.5b)$$

$$\beta_D^{(*)} \to \beta_2^{(1)(*)} \doteq \frac{1}{2}\{1-\Theta[\frac{\sigma_o^{(21)*}}{2\sqrt{2}} - \frac{\log(\mathcal{K}^{(21)}/\mu_{21})}{\sqrt{2}\,\hat{\sigma}_o^{(21)(*)}}]\}, \quad (6.5c)$$

and the "on-off" threshold $\mathcal{K}$ is replaced by the binary threshold $\mathcal{K}^{(21)}$. [Clearly, this is symmetrical in S_1, S_2.] Again, note that $\hat{\sigma}_o \neq \sigma_o \neq \sigma_o^*$, cf. (A.4-71-74), and in the optimum cases, $\sigma_o, \hat{\sigma}_o \to \sigma_o^*$. [See footnote, p. 55.]

A more meaningful measure of performance in the binary signal cases, however, is the Ideal Observer [I.O.] above, (6.4), (6.5). Accordingly, from (2.33) and Appendixes A.2-3,4; A.4-3, we find that in these binary threshold cases, canonically, for the "unsymmetric" channel ($\mu_{21}\neq 1$)

$$\underline{(\mu_{21}\neq 1):} \quad P_e^{(*)} \doteq \frac{1}{2}\{1-p_2\Theta[\frac{\sigma_o^{(21)*}}{2\sqrt{2}} - \frac{\log \mu_{21}}{\sqrt{2}\,\hat{\sigma}_o^{(21)*}}] + p_1\Theta[-\frac{\sigma_o^{(21)*}}{2\sqrt{2}} + \frac{\log \mu_{21}}{\sqrt{2}\,\hat{\sigma}_o^{(21)*}}]\}, \quad [I.O.], \mathcal{K}=1 . \quad (6.5d)$$

In the more common operational situations it is the symmetric channel ($\mu_{21}=1$) that is used, so that (6.5d) reduces directly to the more familiar, and simpler, threshold result:

$$\underline{(\mu_{21}=1):} \quad P_e^{(*)} \doteq \frac{1}{2}\{1-\Theta[\frac{\sigma_o^{(21)(*)}}{2\sqrt{2}}]\}, \quad [I.O., \mathcal{K}=\mu_{21}=1]. \quad (6.5e)$$

This, like (6.2)-(6.5d) above, is a canonical form; [but note the restriction, footnote, p. 55.]

Finally, as we have noted earlier and recall now, various conditions on the "smallness" of the input signals ($\wedge a_o^2 > 0$) must be satisfied if these performance measures (6.2)-(6.5e) are to predict receiver performance accurately. These conditions will be discussed in Sec. 6.4 ff. In the meantime, we note that these results above are canonical in several ways: (i), their form is independent of the mode (coherent or incoherent) of reception; (ii), they are independent, formally, of signal structure, (i.e. narrow-band as well as broad-band signal are included), and (iii), last but by no means least, they are likewise invariant, formally, for the explicit noise statistics.

6.2 Minimum Detectable Signals and Processing Gains:†

We can "anatomize" the quantities $[\sigma_o^{(*)2}, \sigma_o^{(21)(*)2}]$, identifying the "minimum detectable signal" and "processing gain" through the following definition of "output signal-to-noise ratio" when the (total) noise is stationary:

$$\boxed{\left(\frac{S}{N}\right)_{out}^{(*)2} \equiv \frac{\sigma_o^{(*)2}}{2} \equiv \Pi^{(*)}(n) f^{(*)}(\langle a_o^2\rangle_{min}^{(*)}) = \Pi^{(*)}(n) f^{(*)}[\left(\frac{S}{N}\right)_{in\text{-}min}^{2(*)}],} \quad (6.6)$$

where $\Pi^{(*)}(n)$ is the <u>processing gain,</u> and $\langle a_o^2\rangle_{min}^{(*)}$ is the minimum input detectable signal (-to-noise ratio), $\left(\frac{S}{N}\right)_{in\text{-}min}^{2(*)}$, or more loosely, the <u>minimum detectable signal.</u> Here, $f^{(*)}(\langle a_o^2\rangle_{min}^{(*)})$ is some (simple) power of $\langle a_o^2\rangle_{min}^{(*)}$, as we shall note below, cf. (6.9), (6.22b), whose structure depends on the mode of observation. The quantity $(S/N)_{out}^{(*)2}$ is an effective output signal-to-noise (intensity) ratio, after processing, which determines the performance of the detector in these threshold regimes, according to the appropriate probability measures, (6.2), (6.4), (6.5) above. The minimum detectable <u>input</u> signal-to-noise ratio $\langle a_o^2\rangle_{min}^{(*)}$ has its component signal and noise intensities measured at the same point in the receiver, usually at the output of the receiver's (linear) front-end stages, before subsequent nonlinear processing (as exhibited in the algorithms $g_n^{(*)}(\underset{\sim}{x})$, etc.). The minimum detectable signal is the least (normalized) input signal (intensity) which

---

See footnotes on pp. 54 , and p. 55, particularly.

can be sensed at the receiver, subject to the particular controls of the decision probabilities and observation time (i.e. sample-size, n).

From the assumption of "practical optimality" discussed in Sec. 2.4 above, where it is sufficient that the H_1-variance, $(\sigma^*_{in})^2$, of the threshold algorithm be effectively equal to the H_o-variance, $(\sigma^*_{on})^2$, e.g.

$$\therefore \begin{cases} (\sigma^*_{in})^2 = (\sigma^*_{on})^2 + F(n,\overline{a_o^2}) \doteq (\sigma^*_{on})^2 \ , \quad n >> 1, \\ F(n,\overline{a_o^2}) << (\sigma^*_{on})^2 \ , \end{cases}$$

cf. (2.29), we can also derive the useful concept of "minimum detectable signal", $\langle a_o^2\rangle^*_{min}$, and associated processing gain, Π^*. This is because the condition $F(n,\overline{a_o^2})/(\sigma^*_{on})^2 << 1$, establishing a maximum value for threshold signals, $\langle a_o^2\rangle$, for which the algorithms are still LO and AO, cf. Appendix A3, also establishes a non-vanishing input signal-to-noise ratio, $\langle a_o^2\rangle^*$, for all n, and particularly, large n, such that $0 < \langle a_o^2\rangle^*_{min} \leq [\langle a_o^2\rangle^*_{min}]_{max} (<<1)$, where $[\langle a_o^2\rangle^*_{min}]_{max}$ is determined by our selection of the quantitative meaning of "<<" in the above condition. This is physically consistent with our notion of input signal, which is, of course, always nonvanishing.

Accordingly, instead of minimum detectable signal we can equally well ask for the corresponding maximum detectable range, $r^{(*)}_{d\text{-}max}$, of the desired signal. This is obtained in Sec. 3.1 from (3.1), (3.2) and the definition

$$\langle a_o^2\rangle^{(*)}_{min} \equiv \langle I_S\rangle / \langle I_N\rangle = \left(\frac{S}{N}\right)^2_{TR} \frac{1}{(r^{(*)}_{d\text{-}max})^{2\gamma}} \ ;$$

$$\left(\frac{S}{N}\right)^2_{TR} = \frac{\overline{a^2}(\langle \hat{I}_o^2\rangle/2)^{1/2}}{\langle I_N\rangle} = \frac{\overline{a^2}(\overline{G_o^2}/2)(c_o/\hat{r}_o)^{2\gamma}}{\Omega_2+\sigma_G^2} \ , \qquad (6.7)$$

which incorporates the various elements of the propagation law, interference scenario (Sec. 3.2), fading, beam-pattern structure of desired source and receiver, etc. Thus, $(S/N)^2_{TR}$, in contrast to $(S/N)^2_{out}$ in (6.6), is a signal-to-noise intensity ratio which is a measure of the desired signal level

at the transmitter output, in terms of the noise or interference level at the output of the (linear) front-end stages of the receiver. From (6.6), (6.7) we see that $r_{d\text{-}max}^{(*)}$ may be obtained from the relation

$$r_{d\text{-}max}^{(*)} = [(\frac{S}{N})_{TR}^2 / \langle a_o^2 \rangle_{min}^{(*)}]^{1/2\gamma} = \{(\frac{S}{N})_{TR}^2 / f^{-1}(\sigma_o^{(*)2}/2\Pi^{(*)})\}^{1/2\gamma} , \qquad (6.8)$$

so that once $\langle a_o^2 \rangle_{min}^{(*)}$, or $\sigma_o^{(*)}$ and $\Pi^{(*)}$ are specified, along with the function f, maximum detectable range can be calculated, as well. This has been done in a recent study by Middleton [34], and will not be pursued further in the present investigation.

In order to determine $\Pi^{(*)}$ and $a_{o\ min}^{2\ (*)}$ in (6.6) we need the specific results of Appendices 2, 4. We begin with

I. Optimum Coherent Threshold Detection:

From (A.2-14), in (6.6) we have (for henceforth stationary noise processes):†

$$\sigma_{o\text{-}coh}^{*2} = 2\Pi_{coh}^* \langle a_o^2 \rangle_{min\text{-}coh}^* = 2(nL^{(2)}) \ (\frac{1}{2n} \sum_i^n \langle a_{oi} s_i \rangle^2), \text{ Eq. (A.2-14).} \qquad (6.9)$$

$$\therefore \quad \boxed{\Pi_{coh}^* = nL^{(2)} \ ; \ \langle a_o^2 \rangle_{min\text{-}coh}^* = \frac{1}{2n} \sum_i^n \langle a_o s_i \rangle^2} \ , \qquad (6.10)$$

with

$$L^{(2)} \equiv \langle \ell^2 \rangle_o = \int_{-\infty}^{\infty} \{\frac{d}{dx} \log w_1(x|H_o)\}^2 w_1(x|H_o) dx \ ,$$

$$= \int_{-\infty}^{\infty} (w_1'/w_1)^2 w_1(x|H_o) dx, \text{ Eq. (A.1-15),} \qquad (6.10a)$$

---

† See footnote, p. 102.

and $f^*(\ )$ in (6.6) is clearly $(\ )^1$, i.e., the first power of the indicated argument. Noting that here the sampling process may be adjusted for narrow-band signals so that $\langle s_i \rangle = s_{max} = \sqrt{2}$ and with no real restriction as to generality in regarding $\underline{a}$ and $\underline{s}$ to be statistically independent, so that $\langle a_o s_i \rangle = \overline{a_o}\sqrt{2}$, we see that $\langle a_o^2 \rangle^*_{min\text{-}coh} = \bar{a}_o^2$: regardless of the fading law, only the mean amplitude is relevant. [This is not the case for the maximum range, however, where both $\overline{a_o}$ and a_o^2 ($\sim a^2$) are required, cf. (6.7).] We also obtain, on solving (6.2), or (6.5), for σ_o^*, and then using (6.9), the following useful expression for the minimum detectable signal:

$$\langle a_o^2 \rangle^*_{min\text{-}coh} = (\Pi^*_{coh})^{-1} \begin{cases} \Theta^{-1}(2p_D^*-1)+\Theta^{-1}(1-2\alpha_F^*) \\ 2\Theta^{-1}(1-2P_e^*) \end{cases}^2 \begin{matrix} :[N.P.O.],\ p_D^* \equiv P_D^*/p. \\ :[I.O.]:\mu=1. \end{matrix} \tag{6.11}$$

$$= (\Pi^*_{coh})^{-1}\{C^{(*)2}_{N.P.} \text{ or } C^{(*)2}_{I.O.}\}, \tag{6.11a}$$

with

$$C^*_{N.P.} = \sqrt{B^*_{N.P.}} \equiv \Theta^{-1}(2p_D^*-1)+\Theta^{-1}(1-2\alpha_F^*) \ ; \ C^*_{I.O.} \equiv 2\Theta^{-1}(1-2P_e^*) \equiv \sqrt{B^*_{I.O.}} \tag{6.11b}$$

This relation shows how the minimum detectable signal depends on sample size and the background noise (via Π^*) and on the "controls" of the decision process in detection, e.g. p_D^*, α_F^*, P_e^*.

For binary signals we use (A.2-50a) in (6.6), to get in these stationary cases

<u>binary:</u> $$(\sigma^{(21)*}_{o\text{-}coh})^2 = 2\Pi^{(21)*}_{coh}\langle a_o^2 \rangle^{(21)*}_{min\text{-}coh}$$

$$\equiv 2(nL^{(2)})\left(\frac{1}{2n}\sum_i^n (\langle a^{(2)}_{oi} s^{(2)}_i \rangle - \langle a^{(1)}_{oi} s^{(1)}_i \rangle)^2\right), \text{ Eq. (A.2-50a)}, \tag{6.12}$$

so that

$$\therefore \quad \boxed{\Pi_{coh}^{(21)*} = nL^{(2)};\ \langle a_o^2\rangle_{min\text{-}coh}^{(21)*} \equiv \frac{1}{2n}\sum_i^n \left(\overline{a_{oi}^{(2)}}\langle s_i^{(2)}\rangle - \overline{a_{oi}^{(1)}}\langle s_i^{(1)}\rangle\right)^2.} \tag{6.13}$$

We have also, cf. (6.11a), the equivalent expression

$$\langle a_o^2\rangle_{min\text{-}coh}^{(21)*} = (\Pi_{coh}^{(21)*})^{-1}\{C_{N.P.}^{(*)2} \text{ or } C_{I.O.}^{(*)2}\}^2 . \tag{6.13a}$$

With equal amplitudes ($a_o^{(2)} = a_o^{(1)}$), a usual condition of operation, the effective minimum detectable signal becomes now

$$\langle a_o^2\rangle_{min\text{-}coh}^{(21)*} \equiv \bar{a}_o^2 \cdot \sum_i^n \left(\frac{\langle s_i^{(2)}\rangle - \langle s_i^{(1)}\rangle}{\sqrt{2n}}\right)^2 . \tag{6.14}$$

By inspection, it as once evident that choosing <u>antipodal signals</u>, e.g. $s_i^{(1)} = -s_i^{(2)}$, and selecting the t_i such that $s_i = s_{max} = \sqrt{2}$ (at least for narrow-band signals) maximizes the minimum detectable signal here [as well as $\sigma_o^{(21)*}$], and hence further minimizes P_e^*. Thus, from (6.14) we have

<u>antipodal:</u> $\langle a_o^2\rangle_{min\text{-}coh}^{(21)*} = 4\bar{a}_o^2$. (6.15a)

Similarly, for <u>orthogonal signals</u>, e.g.

$$s_i^{(2)} = \sqrt{2}\cos\omega_o t_i \ ; \ \ s_i^{(1)} = \sqrt{2}\sin\omega_o t_i \ , \tag{6.15b}$$

we see that the sum in (6.14) becomes

$$\langle a_o^2\rangle^{(21)*}_{\text{min-coh}} = \frac{\bar{a}_o^2}{n}\sum_i^n (\cos\omega_o t_i - \sin\omega_o t_i)^2 = \bar{a}_o^2\{1 - \frac{1}{n}\sum_i^n \sin(\omega_o t_i/2)\},$$

$$= 2\bar{a}_o^2 \text{ , (orthogonal),} \qquad (6.15b)$$

which is thus maximized by choosing the sampling times $t_i = k(4i-1)\pi/\omega_o$, where $k/\omega_o = 1/2\pi B = T/2\pi$, in which B is the bandwidth of the signals, which are "on" during (t_o, t_o+T) intervals. Of course, for "on-off" signalling, $s_i^{(1)}=0$ here and $\langle a_o^2\rangle^{(21)*}_{\text{min-coh}} \to \langle a_o^2\rangle^{*}_{\text{min-coh}} = \bar{a}_o^2$, cf. (6.10) et seq. Accordingly, we have obtained quite readily the well-known results that for the same total signal intensity, binary antipodal signals are superior to binary orthogonal signals, and are equivalent to "on-off" operation (this last, since $\bar{a}_o|_{\text{binary}} \to 2\bar{a}_o|_{\text{on-off}}$ under the same power conditions). By "superior" here is meant smaller error probabilities (or larger P_D's, cf. (6.2)), since $\sigma_o^{(21)*}$ is increased in the antipodal cases vis-à-vis the orthogonal signals.

II. Suboptimum Coherent Threshold Detection (Cross-Correlators)

From (A.4-52a) we obtain in the case of the suboptimum cross-correlators for "on-off" operation in the usual stationary régimes:

$$\sigma^2_{o\text{-coh}} \equiv 2\Pi_{\text{coh}}\langle a_o^2\rangle_{\text{min-coh}} = 2(n)\Big(\sum_i^n \langle a_o s_i\rangle^2/2n\Big) \qquad (6.16)$$

$$\therefore\ \Pi_{\text{coh}} = n\ ;\ \langle a_o^2\rangle_{\text{min-coh}} = \frac{\bar{a}_o^2}{2n}\sum_{i=1}^n \langle s_i\rangle^2 \to \bar{a}_o^2\ . \qquad (6.17)$$

Comparing (6.17) and (6.10) we see at once that here

$$\boxed{\Pi_{\text{coh}}/\Pi^*_{\text{coh}} \equiv \Phi^*_{\text{d-coh}} = L^{(2)^{-1}}(\leq 1)} \text{ , where } L^{(2)} = \text{Eq. (6.10a).} \qquad (6.18)$$

The quantity $\Phi^*_{\text{d-coh}}$ is the degradation factor for these cross-correlation detectors (4.7) vis-à-vis the optimum (threshold) detector (4.1), for the

same input signals, observation periods (n), and coherent (mode of) observation. Thus, $\Phi^*_{d\text{-coh}}$ is, not unexpectedly, determined by the statistical character of the noise alone, through $L^{(2)}$, (6.10a). For gauss noise $L^{(2)} = 1$, cf. A.1-3, but for the usually encountered non-gaussian noise, $L^{(2)} >> 1$. [See Sec. 8 for various values of $L^{(2)}$, etc.]

With binary signals we use (A.4-20) to write similarly

$$\sigma^{(21)^2}_{o\text{-coh}} \equiv 2\Pi^{(21)}_{coh}\langle a_o^2\rangle^{(21)}_{min\text{-}coh} = 2\cdot(n)\cdot\{\sum_i^n \left(\frac{\langle a_o^{(2)}s_i^{(2)}\rangle - \langle a_o^{(1)}s_i^{(1)}\rangle}{\sqrt{2n}}\right)^2\}\ ; \tag{6.19}$$

$$\therefore\ \Pi^{(21)}_{coh} = n;\quad \langle a_o^2\rangle^{(21)}_{min\text{-}coh} = \bar{a}_o^2 \sum_{i=1}^n \left(\frac{\langle s_i^{(2)}\rangle - \langle s_i^{(1)}\rangle}{\sqrt{2n}}\right)^2 , \tag{6.20}$$

(with $a_o^{(2)} = a_o^{(1)}$, usually), and, again, the degradation factor becomes

$$\Pi^{(21)}_{coh}/\Pi^{(21)*}_{coh} \equiv \Phi^{(21)*}_{d\text{-coh}} = 1/L^{(2)} , \tag{6.21}$$

unchanged from the "on-off" cases above. Similarly, expressions like (6.11), (6.13) for the minimum detectable signal in these suboptimum cases are

$$\langle a_o^2\rangle_{min\text{-}coh} = \Pi^{-1}_{coh}\{C^2_{N.P.} \text{ or } C^2_{I.O.}\}\ ;\ \langle a_o^2\rangle^{(21)}_{min\text{-}coh} = \Pi^{(21)^{-1}}_{coh}\{C^2_{N.P.} \text{ or } C^2_{I.O.}\} , \tag{6.21a}$$

where $C_{N.P.} = \Theta^{-1}(2p_D-1)+\Theta^{-1}(1-2\alpha_F)$, etc. are the <u>suboptimum versions</u> of the controls for the N.P. and I.O. cases, e.g. $p_D^* \to p_D$, $P_e^* \to P_e$, Sec. 6.1.

<u>III. Optimum Incoherent Threshold Detection:</u>

We proceed as above for the coherent cases. Here we apply (A.2-40) to obtain for "on-off" signalling (in the stationary régime):

"on-off": $$\sigma^{*2}_{o\text{-inc}} = \frac{1}{4}\sum_{ij}^{n}\langle a_{oi}a_{oj}s_is_j\rangle^2\{(L^{(4)}-2L^{(2)^2})\delta_{ij}+2L^{(2)^2}\} \tag{6.22a}$$

$$\equiv 2\Pi^*_{inc}(\langle a_o^2\rangle^*_{min\text{-}inc})^2 \ , \tag{6.22b}$$

so that

$$\boxed{\left\langle a_o^2\right\rangle^*_{min\text{-}inc} \equiv \{\frac{1}{2}\sum_{i}^{n}\left\langle a_{oi}^2 s_i^2\right\rangle^2\}^{1/2} \to (\frac{1}{2}\sum_{i}^{n}\overline{a_o^2}) = \overline{a_o^2}} \tag{6.23}$$

$(\overline{s_i^2} = 1$, by normalization).

Accordingly, applying (6.23) to (6.22a,b) gives directly the processing gain for these incoherent, "on-off" threshold signal detectors:

$$\boxed{\Pi^*_{inc} = \frac{nL^{(4)}}{8}\{1+\frac{2L^{(2)^2}}{L^{(4)}}(Q_n-1)\},} \tag{6.24}$$

where

$$\boxed{Q_n-1 \equiv \frac{1}{n}\sum_{ij}^{n}{}' m_{ij}^2\rho_{ij}^2 \ (\geq 0)} \ ; \ m_{ij} \equiv \langle a_{oi}a_{oj}\rangle/\overline{a_o^2} \ ; \ \rho_{ij} \equiv \langle s_is_j\rangle. \tag{6.25}$$

Here $L^{(2)}$ has been specified in (6.10a), while $L^{(4)}$, cf. (A.1-19b), is given by

$$L^{(4)} = \langle(\ell^2+\ell')^2\rangle_o = \int_{-\infty}^{\infty}(\frac{w_1''}{w_1})^2 w_1(x|H_o)dx \tag{6.26}$$

and is also expressed numerically in Sec. 7. We now observe that the processing gain (6.24) depends on signal structure, as well as on sample size (n) and noise statistics, unlike the coherent cases, cf. (6.10).

The minimum detectable signal (6.23) may also be written, by (6.22b) in (6.2) or (6.5), as

$$\langle a_o^2\rangle^*_{\text{min-inc}} = (\Pi^*_{\text{inc}})^{-1/2}\begin{cases}\Theta^{-1}(2p^*_D-1)+\Theta^{-1}(1-2\alpha^*_F) & : \text{N.P.O.}\\ 2\Theta^{-1}(1-2P^*_e) & : \text{I.O.}\end{cases} \quad ,p^*_D\equiv P^*_D/P, \tag{6.27}$$

$$= (\Pi^*_{\text{inc}})^{-1/2}\{C^*_{\text{N.P.}} \text{ or } C^*_{\text{I.O.}}\} \ , \tag{6.27a}$$

cf. (6.11): note the different exponents on Π^* and $\{\Theta^{-1}\ldots\}$, etc.

For binary signals we next use (A.2-56) with (A.2-52a), to write (in these stationary régimes)

binary:

$$(\sigma^{(21)*}_{\text{o-inc}})^2 \equiv 2\Pi^{(21)*}_{\text{inc}}(\langle a_o^2\rangle^{(21)*}_{\text{min-inc}})^2 = \frac{1}{4}\sum_{ij}^{n}(\langle a^{(2)}_{oi}a^{(2)}_{oj}s^{(2)}_i s^{(2)}_j\rangle - \langle a^{(1)}_{oi}a^{(1)}_{oj}s^{(1)}_i s^{(1)}_j\rangle)^2$$
$$\cdot\{(L^{(4)}-2L^{(2)^2})\delta_{ij}+2L^{(2)^2}\} \ , \tag{6.28}$$

so that, parallelling (6.22a)-(6.25) we get in these binary cases the following expresssions for the minimum detectable signal and associated processing gain $[\langle a_o^{(2)^2}\rangle \neq \langle a_o^{(1)^2}\rangle]$:

$$\langle a_o^2\rangle^{(21)*}_{\text{min-inc}} \equiv \{\frac{1}{n}\sum_{i}^{n}(\langle(a_o^{(2)}s_i^{(2)})^2\rangle - \langle(a_o^{(1)}s_i^{(1)})^2\rangle)^2\}^{1/2}$$
$$= \langle a_o^{(2)^2}\rangle - \langle a_o^{(1)^2}\rangle, \ (\neq 0), \tag{6.29}$$

since $\langle (s_i^{(2),(1)})^2 \rangle = 1$ by normalization, and

$$\Pi_{inc}^{(21)*} = \frac{nL^{(4)}}{8}\{1 + \frac{2L^{(2)^2}}{L^{(4)}}[Q_n^{(21)}-1]\}, \tag{6.30}$$

where specifically

$$Q_n^{(21)}-1 \equiv \sum_{ij}{}' \frac{\{\langle a_{oi}^{(2)}a_{oj}^{(2)}\rangle \rho_{ij}^{(2s)} - \langle a_{oi}^{(1)}a_{oj}^{(1)}\rangle \rho_{ij}^{(1s)}\}^2}{n\{\langle a_o^{(2)^2}\rangle - \langle a_o^{(1)}\rangle^2\}^2} \; ; \; \rho_{ij}^{(\;)} \equiv \langle s_i^{(\;)} s_j^{(\;)} \rangle . \tag{6.31}$$

$$= \sum_{ij}{}' \frac{\{\langle a_o^{(2)}\rangle^2 m_{ij}^{(2)} \rho_{ij}^{(2s)} - \langle a_o^{(1)^2}\rangle m_{ij}^{(1)} \rho_{ij}^{(1s)}\}^2}{n\{\langle a_o^{(2)^2}\rangle - \langle a_o^{(1)^2}\rangle\}^2} \tag{6.31a}$$

where we have used the definition of m_{ij} in (6.25) above.

In the important special cases where the signal amplitudes are equal, $a_o^{(2)} = a_o^{(1)} = a_o$, e.g. $\langle a_o^{(2)^2}\rangle = \langle a_o^{(1)^2}\rangle = \langle a_o^2\rangle$ ($\neq 0$), (6.28) simplifies to

$\underline{a_o^{(1)} = a_o^{(2)}:}$

$$(\sigma_{o\text{-}inc}^{(21)*})^2 = 2\Pi_{inc}^{(21)*}\langle a_o^2\rangle_{inc}^{(21)*} = \frac{\overline{a_o^2}^2 L^{(2)^2}}{2} \sum_{ij}{}' m_{ij}^2(\rho_{ij}^{(2s)} - \rho_{ij}^{(1s)})^2 , \tag{6.32}$$

so that

$\underline{a_o^{(1)} = a_o^{(2)}:}$

$$\langle a_o^2\rangle_{min\text{-}inc}^{(21)*} = \overline{a_o^2}; \; \therefore \Pi_{inc}^{(21)*} = \frac{n^2 L^{(2)^2}}{4} \sum_{ij}{}' \frac{m_{ij}^2(\rho_{ij}^{(2s)} - \rho_{ij}^{(1s)})^2}{n^2} \equiv \frac{nL^{(2)^2}}{4}(\hat{Q}_n^{(21)}-1) \tag{6.33}$$

which defines $\hat{Q}_n^{(21)}$, e.g.

$$\boxed{\hat{Q}_n^{(21)}{}_{-1} \equiv \sum_{ij}^{n} {}' \frac{m_{ij}^2(\rho_{ij}^{(2s)}-\rho_{ij}^{(1s)})^2}{n}} \quad . \tag{6.33a}$$

In all instances we have the binary analogue of (6.27), viz:

$$\langle a_o^2\rangle_{\text{min-inc}}^{(21)*} = (\Pi_{\text{inc}}^{(21)*})^{-1/2}\{C_{\text{N.P.}}^{*} \text{ or } C_{\text{I.O.}}^{*}\} \quad . \tag{6.34}$$

IV. Suboptimum Incoherent Threshold Detection (Auto-correlators):

From (A.4-58b) we now obtain for "on-off" signalling and stationary régimes when the (generally suboptimum) auto-correlators (A.4-56) are used:

$$\sigma_{\text{o-inc}}^2 \equiv 2\Pi_{\text{inc}}\langle a_o^2\rangle_{\text{min-inc}}^2 = (\sum_{ij}^{n}\langle a_{oi}a_{oj}s_is_j\rangle^2)^2 / \sum_{ij}^{n}\langle a_{oi}a_{oj}s_is_j\rangle^2 \cdot[(\overline{x^4}-3)\delta_{ij}+2] \quad , \tag{6.35}$$

cf. (6.22), so that

$$\langle a_o^2\rangle_{\text{min-inc}} \equiv \{\frac{1}{n}\sum_i\langle a_o^2\rangle^2\langle s_i^2\rangle^2\}^{1/2} = \overline{a_o^2} \quad , \text{ cf. (6.23)} \quad , \tag{6.36a}$$

and

$$\therefore \quad \Pi_{\text{inc}}|_{\text{correl}} = \frac{n^2\left(\sum_{ij}^{n}\frac{m_{ij}^2\rho_{ij}^2}{n}\right)^2}{2\sum_{ij}m_{ij}^2\rho_{ij}^2[(\overline{x^4}-3)\delta_{ij}+2]} = \frac{nQ_n^2}{2[(\overline{x^4}-1)+2(Q_n-1)]} \tag{6.36b}$$

for the minimum detectable signal and processing gain for these auto-correlation detectors. Analogous to (6.27) we have

$$\langle a_o^2 \rangle_{\text{min-inc}} = \Pi_{\text{inc}}^{-1/2} \begin{cases} \Theta^{-1}(2p_D-1)+\Theta^{-1}(1-2\alpha_F) \\ 2\Theta^{-1}(1-2P_e) \end{cases} \begin{matrix} :\underline{\text{N.P.}} \\ :\underline{\text{I.O.}} \end{matrix} = \Pi_{\text{inc}}^{-1/2}\{C_{\text{N.P.}} \text{ or } C_{\text{I.O.}}\} , \tag{6.37}$$

where again $C_{N.P.}$, etc. is the suboptimum version of the control $C^*_{N.P.}$, etc., (6.27).

Comparing (6.36b) with (6.24) gives us the <u>degradation factor</u> for these (simple) correlators in nongaussian noise

<u>"on-off":</u>

$$\Phi^*_{\text{d-inc}} \equiv \Pi_{\text{inc}}/\Pi^*_{\text{inc}} = 4Q_n^2/[\overline{x^4}-1+2(Q_n-1)][L^{(4)}+2L^{(2)^2}(Q_n-1)] , \tag{6.38}$$

where $L^{(2)}$, $L^{(4)}$ are given by (6.10a), (6.26) respectively. As expected, when the noise is gaussian, $L^{(2)} = 1$, $L^{(4)} = 2$, and $\therefore \Phi_{\text{d-inc}} = 1$: the (simpler) autocorrelator is itself threshold optimum now. Unlike the coherent cases, however, cf. (6.18), $\Phi_{\text{d-inc}}$ depends on signal structure and sample size (n), as well as on the noise statistics, $L^{(2)}$, $L^{(4)}$.

With binary signals we use (A.4-72b) in these (stationary) suboptimum incoherent situations, to write similarly, cf. (6.35):

<u>binary:</u>

$$\sigma^{(21)^2}_{\text{o-inc}} = \frac{(\sum_{ij}^{n} \{\langle (a_{oi}a_{oj}s_is_j)^{(2)}\rangle - \langle (a_{oi}a_{oj}s_is_j)^{(1)}\rangle\}^2)^2}{\sum_{ij}^{n} \{\langle (a_{oi}a_{oj}s_is_j)^{(2)}\rangle - \langle (a_{oi}a_{oj}s_is_j)^{(1)}\rangle\}^2[(\overline{x^4}-3)\delta_{ij}+2]} \tag{6.39a}$$

$$\equiv 2\Pi^{(21)}_{\text{inc}}(\langle a_o^2\rangle^{(21)}_{\text{min-inc}})^2 , \tag{6.39b}$$

and paralleling (6.29)-(6.31) we have

$$\langle a_o^2\rangle^{(21)}_{\text{min-inc}} = \langle a_o^{(2)^2}\rangle - \langle a_o^{(1)^2}\rangle \neq 0 \; ; \qquad \boxed{\Pi^{(21)}_{\text{inc}} = \frac{nQ_n^{(21)^2}}{2[(\overline{x^4}-1)+2(Q_n^{(21)}-1)]}} \; , \tag{6.40}$$

where $Q_n^{(21)}$, $a_o^{(2)} \neq a_o^{(1)}$, is given by (6.31). However, for the important situations where $a_o^{(2)} = a_o^{(1)} = a_o$, the above simplify to

$\underline{a_o^{(2)} = a_o^{(1)}:}$

$$\langle a_o^2\rangle^{(21)}_{\text{min-inc}} = \overline{a_o^2} \; ; \qquad \boxed{\Pi^{(21)}_{\text{inc}} = \frac{n(\hat{Q}_n^{(21)}-1)^2}{2[\overline{x^4}-1+2(\hat{Q}_n^{(21)}-1)]}} \; , \tag{6.41}$$

and $Q_n^{(21)}$, (6.31), is now replaced by $\hat{Q}_n^{(21)}$, (6.33a); $\langle a_o^2\rangle^{(21)}_{\text{min-inc}}$ is also given by (6.34), where $C^*_{\text{N.P.}} \to C_{\text{N.P.}}$; etc., cf. (6.21a) et seq.

Finally, the <u>degradation factor</u> $\Phi^{(21)}_{\text{d-inc}}$ becomes from (6.30) and (6.40) $[a_o^{(2)} \neq a_o^{(1)}]$, and (6.33) and (6.41), $[a_o^{(2)} = a_o^{(1)}]$:

$$\Phi^{(21)*}_{\text{d-inc}}(n)\Big| \equiv \Pi^{(21)}_{\text{inc}}/\Pi^{(21)*}_{\text{inc}} = \begin{cases} \dfrac{4Q_n^{(21)^2}}{[\overline{x^4}-1+2(Q_n^{(21)}-1)][L^{(4)}+2L^{(2)^2}(Q_n^{(21)}-1)]} \; : \\ \qquad\qquad a_o^{(2)} \neq a_o^{(1)} \qquad (6.42a) \\ \dfrac{2(\hat{Q}_n^{(21)}-1)}{[\overline{x^4}-1+2(\hat{Q}_n^{(21)}-1)]L^{(2)^2}} \; ; \; a_o^{(2)} = a_o^{(1)} \; , \\ \qquad\qquad (6.42b) \end{cases}$$

which reduce for gaussian noise ($\overline{x^4}=3$), to unity, as expected. Equations

(6.42a,b) are to be contrasted with $\Phi_d^{(21)*} = 1/L^{(2)}$, (6.21). Like the "on-off" cases, the degradation factor also depends on the noise statistics, on sample size, and signal structure. Finally, note that (6.34) applies in this suboptimum situation:

$$\langle a_o^2 \rangle_{\text{min-inc}}^{(21)} = (\Pi_{\text{inc}}^{(21)})^{-1/2} (C_{\text{N.P.}} \text{ or } C_{\text{I.O.}}). \tag{6.37}$$

It is convenient to sumarize the various results of this section 6.2 in the following two Tables: The Notes to Table 6.1a apply equally to Table 6.1b, 6.2 ff. Note that the results analogous to those shown in the text and summarized in Tables 6.1a,b, and for the clipper correlators Sec. A.4-3, are provided in Table 6.2.

TABLE 6.1a SUMMARY OF THRESHOLD DETECTION PARAMETERS: "ON-OFF" INPUT SIGNALS*

"On-off" Input Signals	Coherent Threshold Detection		Incoherent Threshold Detection	
	Optimum	Cross-correlator	Optimum	Auto-correlator
$\sigma_o^{(*)2}$	$L^{(2)}\sum_i^n \langle a_{oi}s_i\rangle^2 \to nL^{(2)}\bar{a}_o^2$ [Eq. (6.9); Eq. (A.2-14).]	$\sum_i^n \langle a_{oi}s_i\rangle^2 \to n\bar{a}_o^2$ [Eqs. (6.16), (A.4-8).]	$\frac{1}{4}\sum_{ij}^n \langle a_{oi}a_{oj}s_is_j\rangle^2 \{2L^{(2)2} + [L^{(4)} - 2L^{(2)2}]\delta_{ij}\}$ [Eqs.(6.22a),(A.2-40)]	$\left(\sum_{ij}^n \langle a_{oi}a_{oj}s_is_j\rangle^2\right)^2 \Big/ \sum_{ij}\langle a_{oi}a_{oj}s_is_j\rangle^2 (\overline{x^4}-3)\delta_{ij}+2)$ [Eqs.(6.35),(A.4-16)]
$\langle a_o^2\rangle^{(*)}_{\min\text{-}()}$	$\frac{1}{2n}\sum_i^n \langle a_{oi}s_i\rangle^2 \to \bar{a}_o^2$	=(same);Eq.(6.17)	$\{\frac{1}{n}\sum_i^n \langle a_{oi}^2 s_i^2\rangle^2\}^{\frac{1}{2}} \to \overline{a_o^2}$	= (same); Eq. (6.36)
minimum detectable signal	$=(\Pi^*_{coh})^{-1}(C^*_{N.P.}$ or $C^*_{I.O.})^2$	$=\Pi^{-1}_{coh}(C_{N.P.}$ or $C_{I.O.})^2$	$=(\Pi^*_{inc})^{-\frac{1}{2}}(C^*_{N.P.}$ or $C^*_{I.O.})$	$=\Pi^{-1/2}_{inc}(C_{N.P.}$ or $C_{I.O.})$
	Eqs.(6.10), (6.11)	Eqs.(6.17), (6.21a)	Eqs. (6.23),(6.27)	Eq. (6.37)

* See "Notes", p. 73.

TABLE 6.1a. (Cont'd.)

"On-off" Input Signals	Coherent Threshold Detection		Incoherent Threshold Detection	
	Optimum	Cross-correlator	Optimum	Auto-correlator
$\Pi^{(*)}_{(\ )}$ Processing gain	$nL^{(2)}$; Eq. (6.10)	n Eq. (6.17).	$\frac{nL^{(4)}}{8}\{1+\frac{2L^{(2)^2}}{L^{(4)}}(Q_n-1)\}$; Eq. (6.24) $Q_n-1\equiv\frac{1}{n}\sum_{ij}{}' m_{ij}^2\rho_{ij}^2 (\geq 1)$ Eq. (6.25).	$\frac{nQ_n^2}{2[(\overline{x^4}-1)+2(Q_n-1)]}$ Eq. (6.36)
$\Phi^*_{d-(\ )}$ Degradation Factor	1	$1/L^{(2)}$; Eq.(6.18)	1	$4Q_n^2 \Big/ L^{(4)}(1+\frac{2L^{(2)^2}}{L^{(4)}}Q_n-1))$ $\cdot[(\overline{x^4}-1)+2(Q_n-1)]$, Eq. (6.38).
$\hat{B}_{inc}{}^{(\ )}_{\equiv}$; Bias Terms	$-\sigma^{(*)^2}_{o\text{-}coh}/2$	Eq. (A.4-55)	$-\sigma^{(*)2}_{o\text{-}inc}/2$	Eq.(A.4-55)

TABLE 6.1a (Cont'd.)

* NOTES: (i). $C^{(*)}_{N.P.} \equiv \Theta^{-1}(2p^{(*)}_D - 1) + \Theta^{-1}(1-2\alpha^{(*)}_F)$; $C^{(*)}_{I.O.} \equiv 2\Theta^{-1}(1-2P^{(*)}_e)$; Eq. (6.11)

with $p^{(*)}_D \equiv P^{(*)}_D / p$;

(ii). Stationary noise; independent noise samples (n); symmetrical pdf's of the instantaneous noise amplitudes (x);

(iii). Data acquisition period ($\sim$n) is large, so that the various detection algorithms, $g(\ )$, are asymptotically normal under H_0, H_1.

(iv). The LOBD's here (i.e. "optimum algorithms") are AODA's as well. The generally suboptimum correlation detectors are optimum only in gauss noise. [See Appendix A.3.]

(v). For signals with incoherent structure, $Q_n \cong 1$. For signals with completely coherent structure, $Q_n \sim O(n)$; in particular, for sinusoidal wave trains, $Q_n \cong n/2$, cf. (A.2-42e).

TABLE 6.1b. SUMMARY OF THRESHOLD DETECTION PARAMETERS:

I. Binary Input Signals: $\sigma_{o-(\ )}^{(21)(*)^2}$

Coherent Threshold Detection		Incoherent Threshold Detection	
Optimum	Cross-correlator	Optimum	Auto-correlator
$L^{(2)}\sum_i^n\{\langle a_{oi}^{(2)}s_i^{(2)}\rangle - \langle a_{oi}^{(1)}s_i^{(1)}\rangle\}^2$	$\sum_i^n\{\langle a_{oi}^{(2)}s_i^{(2)}\rangle - \langle a_{oi}^{(1)}s_i^{(1)}\rangle\}^2$	$\frac{1}{4}\sum_{ij}^n(\{\langle a_{oi}^{(2)}a_{oj}^{(2)}s_i^{(2)}s_j^{(2)}\rangle - \langle a_{oi}^{(1)}a_{oj}^{(1)}s_i^{(1)}s_j^{(1)}\rangle\}^2) \cdot \{(L^{(4)}-2L^{(2)^2})\delta_{ij} + 2L^{(2)^2}\}$	$a_o^{(2)} \neq a_o^{(1)}$: $\frac{(\langle a_o^{(2)^2}\rangle - \langle a_o^{(1)^2}\rangle)^2 nQ_n^{(21)^2}}{(\overline{x^4}-1)+2(Q_n^{(21)}-1)}$ Eq. (6.40)
$a_o^{(2)}=a_o^{(1)}$: $L^{(2)}\bar{a}_o^2\sum_i\{\langle s_i^{(2)}\rangle - \langle s_i^{(1)}\rangle\}^2$ [Eq. (6.12)]	$\bar{a}_o^2\sum_i\{\langle s_i^{(2)}\rangle - \langle s_i^{(1)}\rangle\}^2$ [Eqs. (6.19),(6.20)]	$a_o^{(2)}=a_o^{(1)}$: $\frac{\overline{a_o^2}^2 L^{(2)^2}}{2}\sum_{ij}^n(\ )m_{ij}^2(\rho_{ij}^{(2s)} - \rho_{ij}^{(1s)})^2$ [Eqs. (6.28), (6.33)].	$a_o^{(2)}=a_o^{(1)}$; same as above; $Q^{(21)}\to\hat{Q}_n^{(21)}$ [Eq. (6.41)]

TABLE 6.1b. SUMMARY OF THRESHOLD DETECTION PARAMETERS:

II. Binary Input Signals: $\langle a_o^2 \rangle_{\min\text{-}(\ )}^{(21)(*)}$

Coherent Threshold Detection		Incoherent Threshold Detection	
Optimum	Cross-Correlator	Optimum	Auto-correlator
$\frac{1}{2n}\sum_i^n \{\langle a_{oi}^{(2)} s_i^{(2)} \rangle - \langle a_{oi}^{(1)} s_i^{(1)} \rangle\}^2$ [Eq. (6.13)].	→ same, cf. Eq. (6.19)	$[\frac{1}{n}\sum_i \{\langle (a_{oi}^{(2)} s_i^{(2)})^2 \rangle - \langle (a_{oi}^{(1)} s_i^{(1)})^2 \rangle\}^2]^{\frac{1}{2}}$ $= \langle a_o^{(2)2} \rangle - \langle a_o^{(1)2} \rangle$; $(a_o^{(2)} \neq a_o^{(1)})$, [Eq. (6.29)]	same; Eq. (6.39a).
$a_o^{(1)} = a_o^{(2)}$: $\rightarrow \frac{\bar{a}_o^2}{2n}\sum_i^n \{\langle s_i^{(2)} \rangle - \langle s_i^{(1)} \rangle\}^2$ Eq. (6.14).	→ same, cf. Eq. (6.20).	→ $\overline{a_o^2}$: $(a_o^{(1)} = a_o^{(2)})$. Eq. (6.33)	→ same; Eq. (6.41)
$= (\Pi_{coh}^{(21)*})^{-1} (C_{N.P.}^* \text{ or } C_{I.O.}^*)^2$ [Eq. (6.13a).]	$= \Pi_{coh}^{(21)-1} (C_{N.P.} \text{ or } C_{I.O.})^2$ [Eq. (6.13a)]	$= (\Pi_{inc}^{(21)*})^{-1/2} (C_{N.P.}^* \text{ or } C_{I.O.}^*)$ [Eq. (6.34)]	$= (\Pi_{inc}^{(21)})^{-1/2} (C_{N.P.} \text{ or } C_{I.O.})$ [Eq. (6.37)]

TABLE 6.1b. SUMMARY OF THRESHOLD DETECTION PARAMETERS

III. Binary Input Signals: $\Pi_{(\ )}^{(21)(*)}$: Processing Gain

Coherent Threshold Detection		Incoherent Threshold Detection	
Optimum	Cross-correlator	Optimum	Auto-correlator
$nL^{(2)}$ [Eq. (6.10)]	n [Eq. (6.20)]	$\underline{a_o^{(1)}=a_o^{(2)}}$: $\frac{n^2L^{(2)^2}}{4}\sum_{ij}^{n,}\frac{m_{ij}^2}{n^2}(\rho_{ij}^{(2s)}-\rho_{ij}^{(1s)})^2=\frac{nL^{(2)^2}}{4}(\hat{Q}_n^{(21)}-1)$ [Eq. (6.33), (6.33a)]	$nQ_n^{(21)^2}/2[(\overline{x^4}-1)+2(Q_n^{(21)}-1)]$ $a_o^{(1)}\neq a_o^{(1)}$: [Eq. (6.40)]
		$\underline{a_o^{(1)}\neq a_o^{(2)}}$: $\frac{nL^{(4)}}{8}\{1+\frac{2L^{(2)^2}}{L^4}(Q_n^{(21)}-1)\}$ [Eq. (6.30), see Eq.(6.31) for $Q_n^{(21)}$]	[Eq.(6.41)]: $a_1^{(1)}=a_o^{(2)}$: $\frac{n(\hat{Q}^{(12)}-1)^2}{2[(\overline{x^4}-1)+2(\hat{Q}_n^{(21)}-1)]}$

TABLE 6.1b. SUMMARY OF THRESHOLD DETECTION PARAMETERS:

IV. Binary Input Signals: $\Phi_{d-(\ )}^{(21)*}$, Degradation Factor

Coherent Threshold Detection		Incoherent Threshold Detection	
1	$1/L^{(2)}$, Eq. (6.2)	1	Eq.(6.42a): $a_o^{(1)} \neq a_o^{(2)}$ Eq. (6.42b): $a_o^{(1)} = a_o^{(2)}$

V. Binary Input Signals: $\hat{B}_n^{(\ )(*)}$: Bias

$-\frac{L^{(2)}}{2}\sum_i^n\{\langle a_{oi}^{(2)}s_i^{(2)}\rangle^2 - \langle a_{oi}^{(1)}s_i^{(1)}\rangle^2\}$	$-\frac{1}{2}\sum_i^n\{\langle a_{oi}^{(2)}s_i^{(2)}\rangle^2 - \langle a_{oi}^{(1)}s_i^{(1)}\rangle^2\}$;	$-\frac{1}{8}\sum_{ij}^n\{\langle a_{oi}^{(2)}a_{oj}^{(2)}s_i^{(2)}s_j^{(2)}\rangle^2 - \langle a_{oi}^{(1)}a_{oj}^{(1)}s_i^{(1)}s_j^{(1)}\rangle^2\} \cdot\{(L^{(4)}-2L^{(2)^2})\delta_{ij}+2L^{(2)^2}\}$	$-\frac{1}{2}\sum_i^n\{\langle(a_{oi}^{(2)}s_i^{(2)})^2\rangle - \langle(a_{oi}^{(1)}s_i^{(1)})^2\rangle\}-\frac{1}{4}\sum_{ij}^n \cdot\{\langle a_{oi}^{(2)}a_{oj}^{(2)}s_i^{(2)}s_j^{(2)}\rangle^2 - \langle a_{oi}^{(1)}a_{oj}^{(1)}s_i^{(1)}s_j^{(1)}\rangle^2\}$
[Eq.(4.3a)]	[Eq. (4.9)]	[Eqs. (4.5a),(A.2-52b)]	[Eq. (4.12b)]

TABLE 6.2 THRESHOLD DETECTION PARAMETERS: (SUBOPTIMUM) CLIPPER-CORRELATORS

I. Detector Structure: $g(\underset{\sim}{x})$

Coherent Threshold Detection		Incoherent Threshold Detection	
"On-Off" Signals	Binary Signals	"On-Off" Signals	Binary Signals
$\log \mu + \hat{B}'_{coh} + \sqrt{2} \sum_i^n \langle \theta_i \rangle \cdot \operatorname{sgn} x_i$ $[\theta_i = a_{oi} s_i]$	$\log \mu + \hat{B}'_{coh} + \sqrt{2} \sum_i^n \cdot (\langle \theta_i^{(2)} \rangle - \langle \theta_i^{(1)} \rangle) \operatorname{sgn} x_i$	$\log \mu + \hat{B}'_{inc} + \sum_{ij} \langle \theta_i \theta_j \rangle \operatorname{sgn} x_i \cdot \operatorname{sgn} x_j$	$\log \mu + \hat{B}^{(21)'}_{inc} + \sum_{ij} \Delta\rho_{ij}^{(21)} \operatorname{sgn} x_i \cdot \operatorname{sgn} x_j$ $\Delta\rho_{ij}^{(21)} =$ Eq. (2.13a)

II. Detector Variances: $\hat{\sigma}_o^2$

$2 \sum_i^n \langle \theta_i \rangle^2$ Eq. (A.4-68)	$2 \sum_i^n \{\langle \theta_i^{(2)} \rangle^2 - \langle \theta_i^{(1)} \rangle^2\}$ Eq. (A.4-73)	$\sum_{ij}^n \langle \theta_i \theta_j \rangle^2 (2-\delta_{ij})$ Eq. (A.4-68)	$\sum_{ij}^n [\langle (\theta_i \theta_j)^{(2)} \rangle - \langle (\theta_i \theta_j)^{(1)} \rangle]^2 \cdot (2-\delta_{ij})$; Eq. (A.4-73)

TABLE 6.2 THRESHOLD DETECTION PARAMETERS: (SUBOPTIMUM) CLIPPER-CORRELATORS

III. Detector Variances: σ_o^2

Coherent Threshold Detection		Incoherent Threshold Detection	
"On-Off" Signals	Binary Signals	"On-Off" Signals	Binary Signals
$4w_{1E}(0)^2 \sum_i^n \langle\theta_i\rangle^2$	$4w_{1E}(0)^2 \sum_i^n (\langle\theta_i^{(2)}\rangle - \langle\theta_i^{(1)}\rangle)^2$	$\dfrac{(\sum_{ij}\langle\theta_i\theta_j\rangle^2\{8w_{1E}(0)^2(1-\delta_{ij}) - \sqrt{2}w''_{1E}(0)\delta_{ij}\})^2}{4\sum_{ij}^n\langle\theta_i\theta_j\rangle^2(2-\delta_{ij})}$	→ same with $\langle\theta_i\theta_j\rangle^2 \to (\langle\theta_i\theta_j\rangle^{(2)} - \langle(\theta_i\theta_j)^{(1)}\rangle)^2$
Eq. (A.4-69a)	Eq. (A.4-74a)	Eq. (A.4-69b)	Eq. (A.4-74b)

IV. Minimum Detectable Signal: a_o^2 min-( )

$\bar{a}_o^2$	$\frac{1}{2n}\sum_i^n[(\overline{a_{oi}s_i})^{(2)} - (\overline{a_{oi}s_i})^{(1)}]^2$	$\overline{a_o^2}$	$\{\frac{1}{n}\sum_i^n[\langle\theta_i^{(2)2}\rangle - \langle\theta_i^{(1)2}\rangle]^2\}^{\frac{1}{2}}$
$\Pi_{coh}^{-1}(C_{N.P.}\text{ or }C_{I.O.})^2$	$\Pi_{coh}^{(21)-1}(C_{N.P.}\text{ or }C_{I.O.})^2$	$\Pi_{inc}^{-1/2}(C_{N.P.}\text{ or }C_{I.O.})$	$(\Pi_{inc}^{(21)})^{-1/2}(C_{N.P.}\text{ or }C_{I.O.})$

TABLE 6.2 THRESHOLD DETECTION PARAMETERS: (SUBOPTIMUM) CLIPPER CORRELATORS

V. $\Pi\{\ \}$, Processing Gain

Coherent Threshold Detection		Incoherent Threshold Detection	
"On-off" Signals	Binary Signals	"On-off" Signals	Binary Signals
$4w_{1E}(0)^2 n$	$4w_{1E}(0)^2 n$	$\left(\sum_{ij}^{n} m_{ij}^2 \rho_{ij}^2 \{8w_{1E}(0)^2(1-\delta_{ij}) - \sqrt{2}\, w''_{1E}(0)\delta_{ij}\}\right)^2 \Big/ 8\sum_{ij}^{n} m_{ij}^2 \rho_{ij}^2 (2-\delta_{ij})$	$(a_{o1} \neq a_{o2})$: same: $\rho_{ij} \to \rho_{ij}^{(2)} - \rho_{ij}^{(1)}$
		$= \dfrac{n[-\sqrt{2}\, w''_{1E}(0) + 8w_{1E}(0)^2 \cdot (Q_n - 1)]^2}{8\{2Q_n - 1\}}$	$\dfrac{n[-\sqrt{2}w''_{1E}(0) + 8w_{1E}(0)^2) \cdot (Q_n^{(21)} - 1)]^2}{8(2Q_n^{(21)} - 1)}$
			$a_{o1} = a_{o2}$: $\dfrac{}{8n\,[w_{1E}(0)^4(\hat{Q}_n^{(21)} - 1]}$ $Q_n \to \hat{Q}_n^{(21)}$

TABLE 6.2 THRESHOLD DETECTION PARAMETERS: (SUBOPTIMUM) CLIPPER CORRELATORS

VI. Detector Structure: $\Phi^*_{d\text{-}(\ )}(\equiv\Pi_{(\ )}/\Pi^*_{(\ )})$, Degradation Factor

Coherent Threshold Detection		Incoherent Threshold Detection	
"On-Off" Signals	Binary Signals	"On-Off" Signals	Binary Signals
$\dfrac{4w_{1E}(0)^2}{L_E^{(2)}}$	$\dfrac{4w_{1E}(0)^2}{L_E^{(2)}}$	$\left[-\sqrt{2}w''_{1E}(0)+8w_{1E}(0)^2(Q_n-1)\right]^2 \Big/ L^{(4)}\left(1+\dfrac{2L^{(2)^2}}{L^{(4)}}[Q_n-1]\right)[1+2(Q_n-1)]$ [=1: F→E; (A.4-36)-(A.4-46) in (A.4-31)	$\begin{cases}(a_{o1}=a_{o2}=a_o): \\ \rho_{ij}\to\rho_{ij}^{(2)}-\rho_{ij}^{(1)} \\ Q_n\to Q_n^{(21)}\ . \end{cases}$ F→E: = 1

VII. Detector Structure: Bias: $\hat{B}_{(\ )}$

$-2\sqrt{2}w_1(0)\sum_i^n \bar{a}_{oi}^2$ $=-2\sqrt{2}\,\bar{a}_o^2 w_{1E}(0)n$ Eq. (A.4-66a)	$-\sqrt{2}w_{1E}(0)\bar{a}_o^2$ $\cdot\sum_i^n(\langle s_i^{(2)}\rangle-\langle s_i^{(1)}\rangle)^2$	$-(1-\sqrt{2}w_{1E}(0))\sum_i^n\langle\theta_i^2\rangle$ $-\frac{1}{4}\sum_{ij}^n\langle\theta_i\theta_j\rangle^2\{8w_{1E}(0)^2$ $\cdot(1-\delta_{ij})-\delta_{ij}\sqrt{2}w''_{1E}(0)\}$ Eq. (A.4-66b).	same: $\langle\theta_i^2\rangle\to\Delta\rho_{ii}^{(21)}$ $\langle\theta_i\theta_j\rangle=\Delta\rho_{ij}^{(21)}$, etc.

TABLE 6.2 THRESHOLD DETECTION PARAMETERS: (SUBOPTIMUM) CLIPPER CORRELATORS

(Cont'd.)

NOTES: 1). Stationary noise regimes

2). When $F \to E$: the detectors are "matched" to the noise, i.e. are now (threshold) optimum for the Class E pdf $w_{1E}(x)_o$, we must use the optimum (LOBD) results of Tables (6.1a,b).

3). $Q_n\text{-}1 \equiv \frac{1}{n} \sum_{ij}^{n'} m_{ij}^2 \rho_{ij}^2 (\geq 0)$; $Q_{n-1}^{(21)} = \frac{1}{n} \sum_{ij}^{'} m_{ij}^2 (\rho_{ij}^{(2)} - \rho_{ij}^{(1)})^2$; $(a_o^{(2)} = a_o^{(1)} = a_o)$.

V. General Remarks:

From the results above we can make the following general observations:

(i). Processing gain for coherent threshold reception ($\Pi_{coh}^{(*)}$, LOBD or cross-correlator) is proportional to sample size (or observation time), i.e.,

$$\Pi_{coh}^{(*)} \sim n \; ; \; [\text{Eqs. (6.10), (6.13), (6.17),(6.20)}]. \tag{6.43a}$$

(ii). Processing gain for incoherent threshold reception ($\Pi_{inc}^{(*)}$, LOBD or auto-correlator), on the other hand, is $\sim (n^{\mu})$, $1 \leq \mu \leq 2$, e.g.:

$$\Pi_{inc}^{(*)} \sim n^{\mu} \; , \; 1 \leq \mu \leq 2: \; [\text{Eqs. (6.24), (6.25); (6.30), (6.31); (6.33), (6.36b), (6.41)}] \; . \tag{6.43b}$$

If the received signal is sufficiently decorrelated that

$$Q_n - 1 \equiv \frac{1}{n} \sum_{ij}{}' \, m_{ij}^2 \rho_{ij}^2 \; ,$$

cf. (6.25) for example, is $O(n^0)$, i.e. at most there are n significantly contributing terms in the double sum, then $\mu=1$ in (6.43b). On the otherhand, for correlated signals (observed RF- incoherently here), Q_n is $O(n)$, and $\mu=2$. Examples of the former type are independently (incoherently observed and) generated pulsed carriers, such as those modelled in Secs. 20.3-(2), 20.4-3, [12], where each received signal element s_i is independent of the others, so that $\rho_{ij} = \delta_{ij}$ in effect, and $\therefore Q_n = 1$. For the latter type, we have coherent pulse trains (observed incoherently), where $\rho_{ij}=\cos \omega_o(t_i-t_j)$, cf. (5.13) (no doppler), for instance. Then Q_n-1, (6.25), becomes $\frac{n}{2}[1+O(1/n)] \doteq \frac{n}{2}$, $(n \gg 1)$, so that $\Pi_{inc}^{(*)} \sim n^2$. Intermediate values of μ, $(1<\mu<2)$, arise when the received signals are partially decorrelated, as happens, for example, when there is carrier spreading (in frequency and therefore in time) because of randomly moving scatterers in the path of propagation, which generates a consequent doppler "smear" of the original signal waveform; Eq. (5.13), $\Delta\omega_d \gg 0$, shows a typical signal correlation function in the usual case of narrow-band signals subject to carrier doppler spread.

(iii). The minimum detectable signal for coherent threshold detection, similarly, is ,

$$\langle a_o^2 \rangle_{coh}^{(*)} \sim n^{-1} \quad , \text{(cf. Tables 6.1a,b).} \tag{6.43c}$$

(iv). The minimum detectable signal for incoherent threshold detection is, alternatively,

$$\langle a_o^2 \rangle_{inc}^{(*)} \sim n^{-\mu/2}, \quad (1 \leq \mu \leq 2), \text{ (cf. Tables 6.1a,b),} \tag{6.43d}$$

again depending on whether the received signal has an incoherent (μ=1) to coherent structure (μ=2), as determined, quantitatively by Q_n, cf. (6.25), (6.31), (6.36b), (6.41). Thus, note that it is possible for the minimum detectable signal in incoherent reception to behave like that for coherent reception, viz. $\langle a_o^2 \rangle \sim n^{-1}$, when μ=2, i.e., when completely correlated signals can be used (and observed).

(v). Maximum detectable signal range, $r_{d\text{-}max}^{(*)}$, whether for LOBD reception or the suboptimum correlation receivers, follows from (6.8) and (6.43c,d). We see at once that

$$r_{d\text{-}max}^{(*)}\Big|_{coh} \sim n^{1/2\gamma} \; ; \; r_{d\text{-}max}^{(*)}\Big|_{inc} \sim n^{\mu/4\gamma} \quad , \; 1 \leq \mu \leq 2. \tag{6.43e}$$

Thus, the larger the power law (γ), the larger must sample size (n) be to achieve a given maximum detectable range. Again, the coherent structure of the signal, if available and used, importantly aids the detection process and extends $r_{d\text{-}max}^{(*)}$.

(vi). In the important limiting situation of gaussian noise our general results do indeed reduce to the earlier, "classical" results (cited in [12]). We have

(1). On-off Coherent Detection

$\sigma^2_{o\text{-}coh} = 2n\bar{a}_o^2$, Eqs. (6.16), (6.17); ($L^{(2)}=1$);

Sec. 20.3-1;[12] : $\Phi_{\bar{s}} = \sum_i \bar{s}_i^2 = 2n$;

$\therefore\ \bar{a}_o^2\Phi_{\bar{s}} = 2n\bar{a}_o^2 = \sigma^{(*)2}_{o\text{-}coh}$, in Eqs.(20.79),(20.120) of [12]

$\therefore$ Eqs. (6.3) are identical with Eq. (20.79), (20.120) of [12] when the noise is gaussian.

(2). On-off Incoherent Detection:

$\sigma^2_{o\text{-}inc} = \frac{1}{2} n\overline{a_o^2}^2$ ($Q_n=1$: incoherent signal structure)

$L^{(4)}=2$; $L^{(2)}=1$; from Eqs. (6.22)-(6.24);(6.35)

$\sigma_{o\text{-}inc} = \sqrt{\frac{n}{2}}\ \overline{a_o^2}$ for instantaneous amplitudes; in Eqs. (6.3).

When envelope detection with independent envelope signal samples is used, we have

$$\sigma^2_{o\text{-}inc}\big|_{envelope} = n\,\overline{a_o^2}^2 \ ; \therefore \sigma_{o\text{-}inc} = \sqrt{n}\,\overline{a_o^2} \quad ,$$

and hence (20.131) of [12] agrees with (6.3). [Compare the envelope form of the threshold algorithm (20.128), [12], with (4.12) for amplitude cases.] With amplitude detection $\sigma_{o\text{-}inc} = \sqrt{n/2}\ \overline{a_o^2}$ in (6.3) gives precisely (20.91), [12], as required, where $\langle \Phi_G \rangle = n$.

[(3). Equations (20.93, p. 876,[12], are incorrect in their factors 2, following the incorrect relation between Φ_G and Φ_{oG} in the footnote on p. 875, [12]. The correct relation is

$\Phi_G = \Phi_{oG}/2$, cf. (20.29a), [12], not $\Phi_G = 2\Phi_{oG}$. Thus, wherever Φ_{oG} appears in (20.93), divide by 4.]

(vii). Corrections:

Ref. [47]: Eq. (3.27), delete factor containing $L^{(4)}$; Eq. (3.27a), replace "2" by $\sqrt{2}$ in second factor of Θ; Eq. (3.28), rewrite as $\Phi^*_{inc} = \sigma^*_{o\text{-}inc}/\sqrt{2} = \sqrt{\Pi^*}\,\langle a_o^2\rangle^*_{min\text{-}inc}$; Eq. (3.29), replace $2\Theta^*_{inc}$ by Φ^*; Eq. (3.30), replace argument of Θ by $\sigma^*_{o\text{-}inc}/2\sqrt{2} = (1/2)\sqrt{\Pi^*_{inc}}\; a_o^{2\,*}{}_{inc}$.

VI. Decibel Forms:

A convenient way of expressing our results in I-IV above is to use a decibel representation, so that factors are additive and powers are factors. This is particularly useful in numerical calculations where it is necessary to determine individual terms separately, initially before combining in the full relation. We have

$$\begin{cases} \check{\sigma}^{(*)2}_{o\text{-}coh} = 0.3010 + \check{\Pi}^{(*)}_{coh} + \langle \check{a}_o^2\rangle^{(*)}_{coh} \quad ; \check{A} \equiv 10\log_{10} A; & (6.44a) \\ \check{\sigma}^{(*)2}_{o\text{-}inc} = 0.3010 + \check{\Pi}^{(*)}_{inc} + 2\langle \check{a}_o^2\rangle^{(*)}_{inc}\,. & (6.44b) \end{cases}$$

Similarly, we get

$$\begin{cases} \langle \check{a}_o^2\rangle^{(*)}_{min\text{-}coh} = -\check{\Pi}^{(*)}_{coh} + 2[\check{C}^{(*)}_{N.P.} \text{ or } \check{C}^{(*)}_{I.O.}]\,, & (6.45a) \\ \langle \check{a}_o^2\rangle^{(*)}_{min\text{-}inc} = -\frac{1}{2}\check{\Pi}^{(*)}_{inc} + [\check{C}^{(*)}_{N.P.} \text{ or } \check{C}^{(*)}_{I.O.}]. & (6.45b) \end{cases}$$

(These relations hold for both the "on-off" and binary broad-band and narrow-band signal cases, of course.)

6.3 Performance Measures of Optimum vs. Suboptimum Threshold Reception:

Since performance, as measured by suitable probabilities of correct or incorrect decisions, $P_{D,e}^{(*)}$, can be expressed functionally for general input signals (broad- and narrow-band) by the general relation

$$P_{D,e}^{(*)} = F_{D,e}^{(*)}[\sigma_o^{(*)} = \Pi^{(*)}(n) f(\langle a_o^2 \rangle_{min}^{(*)})], \tag{6.46}$$

cf. (6.2), (6.4), etc., and (6.6), we have at least three principal ways of comparing performance, for the same signal waveforms against the same interference for the same mode of reception:

$$\begin{cases} \text{(I).} & \text{Given n and } \langle a_o^2 \rangle_{min} \text{ the same in both optimum and suboptimum cases, compare } P_{D,e} \text{ to } P_{D,e}^*; \\ \text{(II).} & \text{Given } P_{D,e} = P_{D,e}^*, \text{ same n, compare } \langle a_o^2 \rangle_{min} \text{ to } \langle a_o^2 \rangle_{min}^*; \\ \text{(III).} & \text{Given } P_{D,e} = P_{D,e}^*, \text{ same input minimum detectable signals } (\langle a_o^2 \rangle_{min} = \langle a_o^2 \rangle_{min}^*), \text{ determine the increase in sample size (n) of the suboptimum processor vis-à-vis that of the corresponding LOBD.} \end{cases} \tag{6.47a}$$

$$\text{(Ia)-(IIIa):} \quad \text{Same as (I)-(III), but for optimum coherent vs. optimum incoherent detection.} \tag{6.47b}$$

The first comparison (I) gives a probability measure of the suboptimality of the suboptimum system compared to the optimum, for identical signal, noise, and observation conditions (period of observation is n and mode, e.g. coherent, incoherent, etc.). The second and third methods of comparison (II,III) require the same performance, but now with different input signal levels or sample sizes. Again, the noise conditions are unchanged in each instance, and the signal structure is unaltered, but the input signal <u>level</u> ($\sim a_o$) or sample size may be changed.

Other modes of comparison are clearly possible. For example, for the same signals, sample sizes, modes of reception, we can compare performance for systems optimum in nongauss vs. those optimum in gauss. In fact, that is what we also do here, since the correlation detectors (with the <u>correct biases</u>) are themselves optimum in normal noise. A measure of superiority

of the proper processors in nongauss vis-à-vis gauss under these conditions is, of course, given by the degradation factor Φ_d^*, cf. (6.18), (6.38), (6.43), for example. Equivalently, we can measure this superiority by the extent to which $P_{D,e}^*$ are changed vis-à-vis $P_{D,e}$ (for the correlators), or performances can be compared based on different sample sizes. Still other possibilities arise, in the manner of Sec. 4.3 above, when algorithms optimal in one class of interference are used suboptimally against another class of noise. For the most part, we will consider the comparisons of (6.47a), as well as Φ_d^* directly.

Accordingly, from (6.47) we have

6.3.1 Comparisons, Eq. (6.47) Optimum vs. Suboptimum:

(I). Fixed Sample-Size (n) and Input Signals ($\langle a_o^2 \rangle_{min}$):

From (6.18), (6.38),

$$\Phi_{d-(\ )}^*(n) \equiv (\Pi/\Pi^*)_{coh/inc}, \quad (\text{same } n = n^*),$$

we have directly the canonical relation

$$\boxed{\sigma_o^2 = \Phi_d^* \sigma_o^{*2}} \tag{6.48}$$

for both coherent and incoherent reception. This, in turn, in (6.2) gives directly, with

$$\sigma_o^* = \sqrt{2}\,[\Theta^{-1}(2P_D^*/p-1)+A^*] \quad , A^{(*)} \equiv \Theta^{-1}(1-2\alpha_F^{(*)}), \tag{6.49}$$

on eliminating σ_o^*, the canonical form

$$P_D \cong \frac{p}{2}\{1+\Theta[\sqrt{\Phi_d^*}\{\Theta^{-1}(2\frac{P_D^*}{p}-1)+\Theta^{-1}(1-2\alpha_F^*)\}-\Theta^{-1}(1-2\alpha_F)]\} \quad , \quad (6.50)$$

$$\cong \frac{p}{2}\{1+\Theta[\sqrt{\Phi_d^*}\, C_{N.P.}^* - \Theta^{-1}(1-2\alpha_F)\}\ , \quad (6.50a)$$

for both coherent and incoherent on-off or binary signal detection. With (6.50) we can compare P_D with P_D^* directly, where usually $\alpha_F^* = \alpha_F$. Clearly, since $0 \leq \Phi_d^* \leq 1$, $P_D \leq P_D^*$ here, as expected.

Similarly, in the steady-state communication régimes, where $P_e(^*)$ is the more natural measure of performance once the desired signal has been initially established, we have from (6.48) in (6.5) for the symmetric channel ($\mu = 1$):

$$P_e \cong \frac{1}{2}\{1-\Theta[\sqrt{\Phi_d^*}\,\Theta^{-1}(1-2P_e^*)]\} \quad , \ \Theta^{-1}(1-2P_e^*) = \frac{1}{2}\, C_{I.O.}^*, \quad (6.51)$$

where now, of course, $P_e \geq P_e^*$, ($\Phi_d^* \leq 1$), as expected.

(II). Same Decision Probabilities ($P_{D,e} = P_{D,e}^*$), Sample Size (n):

Here the comparison is made between minimum detectable input signals when the decision probabilities [(6.2), (6.5), (6.6)] are equated. Thus, we have

$$P_{D,e} = P_{D,e}^* \ ; \ \therefore \ \sigma_o = \sigma_o^* \quad (6.52)$$

for all modes of operation here. From (6.9), (6.16), or (6.22b), (6.35), we get directly

$$\boxed{\langle a_o^2\rangle^*_{\text{min-coh}} = \Phi^*_{\text{d-coh}}\langle a_o^2\rangle_{\text{min-coh}} \; ; \; \langle a_o^2\rangle^*_{\text{min-inc}} = \sqrt{\Phi^*_{\text{d-inc}}}\langle a_o^2\rangle_{\text{min-coh}}}\,, \tag{6.53}$$

which in db become

$$\langle \check{a}_o^2\rangle^*_{\text{min-coh}} = \check{\Phi}^*_{\text{d-coh}} + \langle \check{a}_o^2\rangle_{\text{min-coh}} \; ; \; \langle \check{a}_o^2\rangle^*_{\text{min-inc}} = \tfrac{1}{2}\,\check{\Phi}^*_{\text{d-inc}} + \langle \check{a}_o^2\rangle_{\text{min-inc}}\,, \tag{6.53a}$$

all of which apply equally well for the on-off and binary cases, in form: of course, the specific structure of Φ^*_d depends on whether or not "on-off" or binary signals are employed, and the mode of reception, cf. Tables 6.1a,b.

(III). Same Decision Probabilities and Input Signals:

Here the input signal levels are the same, as are the probabilities of decision, so that comparisons are naturally made in terms of sample size: n vs. n*. This starts with $\sigma_o = \sigma^*_o$, cf. (6.52), and using (6.9), (6.16), and (6.22b), (6.35) we obtain now, with $\langle a_o^2\rangle_{\text{min}} = \langle a_o^2\rangle^*_{\text{min}}$:

$$\Pi^*(n^*) = \Pi(n) \tag{6.54}$$

generally, for coherent, incoherent, "on-off", binary signal reception, etc. Applying (6.10), (6.17) specifically gives for both "on-off" and binary operation:

(Opt. vs. Cross-correlator):

$$\boxed{n^*_{\text{coh}} = \Phi^*_{\text{d-coh}} n_{\text{coh}} = n_{\text{coh}}/L^{(2)}}\,, \tag{6.55a}$$

for the simple correlator, and for the clipper correlator [cf. Sec. A.4-3 and Table 6.2]:

(opt. vs. clipper-correlators):

$$n^*_{coh} = \frac{4w_{1E}(0)^2 n_{coh}}{L_E^{(2)}} \tag{6.55b}$$

in these stationary regimes.

For the incoherent cases we obtain similarly, from (6.38), (6.40), (6.42), and Table 6.2, with Sec. (A.4-3), the more complex relations where n*, n may appear implicitly, viz:

(opt. vs. auto-correlator):

(i). "on-off" $$\frac{n^*}{4}(L^{(4)}+2L^{(2)^2}[Q_{n^*}-1]) = \frac{nQ_n^2}{[(\overline{x^4}-1)+2(Q_n-1)]}\ ; \tag{6.56a}$$

(ii). binary:

$$\begin{cases} a_o^{(2)} \neq a_o^{(1)}: & \frac{n^*}{4}(L^{(4)}+2L^{(2)^2}\{Q_{n^*}^{(21)}-1\}) = \frac{nQ_n^{(21)^2}}{[\overline{x^4}-1+2(Q_n^{(21)}-1)]}\ , \quad (6.56b) \\ a_o^{(2)} = a_o^{(1)}: & \frac{n^*}{4} L^{(2)^2}\{Q_{n^*}^{(21)}-1\} = \frac{n\{Q_n^{(21)}-1\}^2}{[\overline{x^4}-1+2(Q_n^{(21)}-1)]}\ , \quad (6.56c) \end{cases}$$

cf. (6.30), (6.31), (6.33), (6.33a), (6.40), (6.41). Also, we have (6.24) vs..Table 6.2, and (6.30), (6.33), vs. Table 6.2 (binary) and Sec. (A.4-3):

(opt. vs. clipper correlator):

(i). "on-off" $$n^*[L_E^{(4)}+2L_E^{(2)^2}(Q_{n^*}-1)] = \frac{n[-\sqrt{2}\ w''_{1E}(0)+8w_{1E}(0)^2 Q_{n^*}-1)]^2}{2Q_n-1} \tag{6.57a}$$

(ii). binary:
$$\begin{cases} a_o^{(2)} \neq a_o^{(1)}: & n^*[L_E^{(4)}+2L_E^{(2)^2}\{Q_{n^*}^{(21)}-1\}) \\ & = \dfrac{n[-\sqrt{2}\, w''_{1E}(0)+8w_{1E}(0)^2(Q_n^{(21)}-1)]^2}{(2Q_n^{(21)}-1)} \\ a_o^{(2)}=a_o^{(1)}: & \frac{n^*}{2}L_E^{(2)^2}\{Q_{n^*}^{(21)}-1\} = 8n\, w_{1E}(0)^4(\hat{Q}_n^{(21)}-1). \end{cases} \quad (6.57c)$$

The relationship between n* and n in these incoherent cases is clearly not so straightforeward as in the coherent cases (6.55), and depends noticeably on the degree of signal correlation, cf. remarks in V, Sec. 6.2 above.

6.3.2 Comparisons-Optimum Coherent vs. Optimum Incoherent Threshold Detection:

Just as we have compared optimum vs. suboptimum threshold detection algorithms in the same modes (i.e., coherent, incoherent) of reception in 6.3.1, (I)-(III) above, so also is it instructive to compare optimum threshold detection for these different modes. Thus, according to Eq. (6.47b) we repeat the comparisons of (6.47a), but now for coherent vs. incoherent detection, respectively. Accordingly, we have

(Ia). Fixed Sample-Size (n) and Same Input Signals

$\langle a_o \rangle^*_{\text{min-coh}} = \langle a_o \rangle^*_{\text{min-inc}}$:

From (6.11b,6.27a) with (6.9) and (6.22a) we can write directly

$$\begin{aligned} B^*_{\text{coh}} &= (\sigma^*_{\text{on-coh}})^2/2 = \langle a_o^2 \rangle^*_{\text{min-coh}} \hat{a}_{\text{coh}} \Pi^*_{\text{coh}}; \\ B^*_{\text{inc}} &= (\sigma^*_{\text{on-inc}})^2/2 = \left(\langle a_o^2 \rangle^*_{\text{min-inc}} \right)^2 \hat{a}_{\text{inc}} \Pi^*_{\text{inc}} \end{aligned} \quad (6.48)'$$

so that we can define

$$\boxed{\Psi^* \equiv \hat{a}^2_{\text{inc}} \Pi^*_{\text{inc}} / (\hat{a}_{\text{coh}} \Pi^*_{\text{inc}})^2} \quad , \quad (6.49)'$$

where

$$\hat{a}_{coh} \equiv \sum_{i}^{n} (\bar{a}_{oi}\bar{s}_i)^2 \Big/ 2n\,\overline{a_o^2} \to \bar{a}_o^2 \Big/ \overline{a_o^2} \equiv 1 - \eta \text{ (stat. cases)}; \tag{6.49a)'}$$

$$0 \leq \eta \equiv \text{var } a_o \Big/ \overline{a_o^2} \ (<1) \ ;$$

$$\hat{a}_{inc} \equiv \left(\sum_{i}^{n} \left\langle a_{oi}^2 s_i^2 \right\rangle^2 \Big/ n\,\overline{a_o^2}^{\,2} \right)^{1/2} \to 1 \text{ (stat.cases)}, \tag{6.49b)'}$$

since $\overline{s_i^2} = 1$.

Here η represents the "fading factor" whose anatomy is examined in somewhat more detail in II, Sec.7.1 ff. Therefore, we have directly (in these stationary cases)

$$\boxed{\Psi^* = L^{(4)}\left[1 + \frac{2L^{(2)^2}}{L^{(4)}}(Q_n - 1)\right] \Big/ 8(1-\eta)^2 n L^{(2)^2}} \ , \tag{6.50)'}$$

and

$$B^*_{inc} = \Psi^*(B^*_{coh})^2 \ , \ [\text{cf. (6.11) - (6.11b)}] \tag{6.51)'}$$

Using (6.48)', (6.49)' in (6.2), (6.5), and (6.27) enables us to write these probability measures of performance respectively as

$$P^*_{D\text{-}inc} \simeq \frac{p}{2}\{1 + \Theta\,[\sqrt{\Psi^*}\,\{\Theta^{-1}(2p^*_{D\text{-}coh} - 1) + \Theta^{-1}(1 - 2\alpha^*_F)\}^2$$

$$- \Theta^{-1}(1 - 2\alpha^*_F)]\} \ ; \ \alpha^*_F = (\alpha^*_F)_{coh} \ ; \tag{6.52)'}$$

$$P^*_{e\text{-}inc} \simeq \frac{1}{2}\{1 - \Theta[2\sqrt{\Psi^*}\,\Theta^{-1}(1 - 2P^*_{e\text{-}coh})^2]\} \ ; \quad (p = q = \tfrac{1}{2}) \ . \tag{6.53)'}$$

Alternatively, we can express P^*_{coh} in terms of P^*_{inc} :

$$P^*_{D\text{-}coh} \simeq \frac{p}{2}\{1 + \Theta\,[(\Psi^*)^{1/4}\{\Theta^{-1}(2p^*_{D\text{-}inc} - 1) + \Theta^{-1}(1 - 2\alpha^*_F)\}^{1/2}$$

$$- \Theta^{-1}(1 - 2\alpha^*_F)]\} \ ; \ \alpha^*_F = (\alpha^*_F)_{coh} \tag{6.54)'}$$

$$P^*_{e\text{-}coh} \simeq \frac{1}{2}\{1 - \Theta[\frac{(\Psi^*)^{1/4}}{\sqrt{2}}\Theta^{-1}(1 - 2P^*_{e\text{-}inc})^{1/2}]\} \quad ; \quad (p = q = \tfrac{1}{2}) \ , \tag{6.55)'}$$

where Ψ^* in the common stationary cases is given by (6.50)' above.

(IIa). Same Decision Probabilities and Sample Size:

In this case we may expect different values of the respective (minimum) input signal (-to-noise ratios). Thus (6.52) is modified to

$$P^*_{D,e\text{-}coh} = P^*_{D,e\text{-}inc}; \ \therefore \ \sigma^*_{o\text{-}coh} = \sigma^*_{o\text{-}inc}; \ \therefore \ B^*_{coh} = B^*_{inc}; \ n^*_{coh} = n^*_{inc} \tag{6.56)'}$$

so that from (6.48)' it follows directly that

$$\left\langle a_o^2 \right\rangle^*_{inc} = (\hat{a}_{coh}\Pi^*_{coh}/\hat{a}_{inc}\hat{\Pi}_{inc})^{1/2}\sqrt{\left\langle a_o^2 \right\rangle^*_{coh}} \ ,$$

$$[\left\langle a_o^2 \right\rangle^*_{coh} = \left\langle a_o^2 \right\rangle^*_{inc} \ , \text{ etc.}] \ , \tag{6.57a}$$

$$= \left\{\frac{8(1 - \eta)L^{(2)}}{L^{(4)} + 2L^{2)^2}(Q_n - 1)}\right\}^{1/2}\sqrt{\left\langle a_o^2 \right\rangle^*_{coh}} \ . \tag{6.57b)'}$$

In the case of coherent signal waveforms (large n), we have [cf. (A.2-42e)]

$$Q_n \doteq \frac{n}{2} \ \text{(slow fading)} \ ; \ Q_n \doteq \frac{n}{2}(1 - \eta)^2 \ \text{(rapid fading)} \tag{6.58)'}$$

and since $L^{(4)} = O(2L^{(2)^2})$ in the highly nongaussian situations [cf. Figs. 7.7, 7.8 (Class A), and Figs. 7.11, 7.12 (Class B)], we see that (6.57)' reduces to

$$\left\langle a_o^2 \right\rangle^*_{inc\text{-}slow} \simeq \sqrt{\frac{8(1 - \eta)}{nL^{(2)}}}\left(\left\langle a_o^2 \right\rangle^*_{coh}\right)^{1/2} \ , \tag{6.59a)'}$$

$$\left\langle a_o^2 \right\rangle_{inc\text{-}fast} \simeq \sqrt{\frac{8}{nL^{(2)}(1 - \eta)}}\left(\left\langle a_o^2 \right\rangle^*_{coh}\right)^{1/2} \ , \tag{6.59b)'}$$

respectively for slow and rapid fading.

(IIIa). Same Decision Probabilities and Input Signals:

For this case, the comparison is between processing gains, or in more detail, between sample sizes n^*_{coh}, n^*_{inc}, needed to achieve the same performance in the two modes of threshold detection, when the minimum detectable signals are required to be the same. Accordingly, from (6.48)' again we have now

$$\hat{a}_{coh}\Pi^*_{coh} = \left\langle a_o^2 \right\rangle^*_{coh} \hat{a}^2_{inc}\Pi^*_{inc} \text{ , or } B^*_{coh} = (\Psi^*)^{-1}, \text{ cf. (6.51)'} \qquad (6.60)'$$

Since $\left\langle a_o^2 \right\rangle^*_{coh} = B^*_{coh} \hat{a}_{coh}\Pi^*_{coh}$, cf. (6.48)', we get finally

$$n^*_{coh} = \frac{1}{L^{(2)}} \left\{ n^*_{inc} B^*_{coh} \left[L^{(4)} + 2L^{(2)2} \left(Q^{-1}_{n^*\text{-inc}} \right) \right] \Big/ 8(1-\eta)^2 \right\}^{1/2} . \qquad (6.61)'$$

With slow or rapid fading and coherent signal waveforms ($n >> 1$), as before, cf. (6.58)', (6.61)' reduces to

$$n^*_{coh\text{-slow}} \simeq n^*_{inc} \sqrt{B^*_{coh}} \Big/ 2\sqrt{2}(1-\eta) \; ; \; n^*_{coh\text{-fast}} \simeq n^*_{inc} \sqrt{B^*_{coh}/8} . \qquad (6.62)'$$

(We note that slow fading works to the relative disadvantage of coherent vis-à-vis incoherent detection.)

6.3.3 Asymptotic Relative Efficiences:

It is a comparatively simple matter now to determine another frequently used measure of performance, namely, the Asymptotic Relative Efficiency (ARE), (for example, see [14], p. 242, Eqs. (78b, 80).) This is defined for nonzero signal ($\theta>0$) and the same decision (i.e. probability) controls [$C_{N.P.}$, $C_{I.O.}$, etc., cf. (6.11b) etc.], as the limit as sample sizes become infinite, of the ratio of the normalized "distances" of the two receiver characteristics under comparison when the same input signals are employed, in the same noise backgrounds. Thus, for receiver 1 vs. receiver 2 we have (in the "on-off" cases):

$$\text{ARE}\Big|_{\text{"on-off"},\theta>0} = \lim_{n_1,n_2\to\infty} \left\{ \frac{\langle g^{(1)}\rangle_1 - \langle g^{(1)}\rangle_0}{\hat{\sigma}_0^{(1)}} \Big/ \left(\frac{\langle g^{(2)}\rangle_1 - \langle g^{(2)}\rangle_0}{\hat{\sigma}_0^{(2)}} \right) \right\}$$

$$= \lim_{n_1,n_2\to\infty} \{\sigma_0^{(1)}/\sigma_0^{(2)}\}, \tag{6.58}$$

where $\sigma_0^{(1),(2)}$ are defined in (A.4-12), (A.4-13) [(A.4-72), (A.4-74) also] for general (most of the time) suboptimum systems, where $\hat{\sigma}_0^{(1),(2)}$ are the respective variances of the receiver algorithms $g^{(1)}$, $g^{(2)}$ under H_0, cf. (A.4-9), (A.4-29); (A.4-71), (A.4-73). For binary signals (6.58) becomes directly

$$\text{ARE}\Big|_{\text{binary},\theta>0} = \lim_{n_1,n_2\to\infty} \left\{ \frac{\sigma_{01}^{(21)}}{\sigma_{02}^{(21)}} \right\} . \tag{6.58a}$$

Applying the general relation (6.6) in its canonical form (6.48) here to (6.58), we see at once that the ARE for comparison against the optimum detector become simply

$$\boxed{\text{ARE}^*\Big|_{\theta>0} \equiv \lim_{n,n^*\to\infty} \left(\frac{\sigma_0}{\sigma_0^*}\right) = \lim_{n,n^*\to\infty} \sqrt{\Phi_{d^-(\ )}^{(*)}} \quad (\leq 1),} \tag{6.59}$$

for "on-off" and binary signalling. In the case of suboptimum system comparisons (6.59) becomes

$$\text{ARE}_{1/2}\Big|_{\theta>0} = \lim_{n_1,n_2\to\infty} \Phi_{d^-(\ )}^{*\frac{1}{2}} = \lim_{n_1,n_2\to\infty} \frac{\sigma_0^{(1)}}{\sigma_0^{(2)}} \quad (\leq 1) , \tag{6.59a}$$

where systems 1, 2 are so chosen that this limiting ratio is always equal to or less than unity. (Of course, if systems 1 and 2 are both optimum, the ARE is unity.)† Again, we remark that narrow-band as well as broad-band signal types are included canonically here.

From the text above (cf. Tables 6.1a,b, 6.2) we easily establish the following useful examples:

I. Coherent Reception:

(i). simple correlator: optimum

(ii). clipper correlator: optimum

(iii). simple correlator: clipper correlator

$$ARE^{*}_{coh} = \sqrt{1/L^{(2)}} \quad (\leq 1); \qquad \text{["on-off";binary]} \tag{6.60a}$$

$$ARE^{*}_{coh} = \sqrt{4w_{1E}(0)^2/L^{(2)}} \quad (\leq 1); \qquad \text{["on-off"; binary]} \tag{6.60b}$$

$$ARE_{(1/2)coh} = 1/4w_{1E}(0) \quad (\leq 1); \qquad \text{["on-off", binary]} \tag{6.60c}$$

II. Incoherent Reception:

(i). simple-correlator: optimum

$$ARE^{*}_{inc}\Big|_{\text{on-off}} = \lim_{n\to\infty}\{4Q_n^2/(L^{(4)}+2L^{(2)^2}\{Q_n-1\}) \cdot (\overline{x^4}-1+2\{Q_n-1\})\}^{\frac{1}{2}}, \text{ cf. Eq. (6.38);} \tag{6.61a}$$

$a_o^{(1)} \neq a_o^{(2)}$:

$$ARE^{*}_{inc}\Big|_{\text{binary}} = \lim_{n\to\infty}\{4Q_n^{(21)^2}/(L^{(4)}+2L^{(2)^2}\{Q_n^{(21)}-1\}) \cdot (\overline{x^4}-1+2\{Q_n^{(21)}-1\})\}^{\frac{1}{2}}, \text{cf. Eq. (6.42a)} \tag{6.61b}$$

$a_o^{(1)} = a_o^{(2)}$:

$$ARE^{*}_{inc}\Big|_{\text{binary}} = \lim_{n\to\infty}\left\{\frac{2(\hat{Q}_n^{(21)}-1)}{L^{(2)^2}[\overline{x^4}-1+2(\hat{Q}_n^{(21)}-1)]}\right\}^{1/2}, \quad \text{cf. Eq. (6.42b).} \tag{6.61c}$$

†Note, however, that ARE = 1 does not necessarily mean both algorithms are optimum, cf. last ¶ of III.

(ii). clipper-correlator / optimum

$$\mathrm{ARE}^{*}_{\mathrm{inc}}\Big|_{\text{on-off}} = \lim_{n\to\infty}\left(\frac{[-\sqrt{2}\,w''_{1E}(0)+8w_{1E}(0)^2\{Q_n-1\}]^2}{(2Q_n-1)[L_E^{(4)}+2L_E^{(2)2}\{Q_n-1\}]}\right)^{\frac{1}{2}}; \tag{6.62a}$$

$a_o^{(1)}\neq a_o^{(2)}$: $$\mathrm{ARE}^{*}_{\mathrm{inc}}\Big|_{\text{binary}} = \lim_{n\to\infty}\left(\frac{[-\sqrt{2}\,w''_{1E}(0)+8w_{1E}(0)^2\{Q_n^{(21)}-1\}]^2}{(2Q_n^{(21)}-1)(L_E^{(4)}+2L_E^{(2)2}\{Q_n^{(21)}-1\})}\right)^{\frac{1}{2}}; \tag{6.62b}$$

$a_o^{(1)}=a_o^{(2)}$: $$\mathrm{ARE}^{*}_{\mathrm{inc}}\Big|_{\text{binary}} = (4w_{1E}(0)^2/L_E^{(2)2}) \quad ; \tag{6.62c}$$

Here the signal factors $Q_n, Q_n^{(21)}$, $\hat{Q}_n^{(21)}$, are defined specifically by

"on-off": $$Q_n \cong 1+\frac{1}{n}\sum_{ij}{}' m_{ij}^2\rho_{ij}^2;\ \text{cf. Eq.(6.25)};\ m_{ij}\equiv\overline{a_{oi}a_{oj}}/\overline{a_o^2};$$

$$\rho_{ij} = \langle s_i s_j\rangle; \tag{6.63a}$$

$a_o^{(1)}\neq a_o^{(2)}$: $$Q_n^{(21)} = \frac{\sum_{ij}^{n}{}'(\langle a_o^{(2)2}\rangle m_{ij}^{(2)}\rho_{ij}^{(2s)}-\langle a_o^{(1)2}\rangle m_{ij}^{(1)}\rho_{ij}^{(1s)})^2}{n(\langle a_o^{(2)2}\rangle-\langle a_o^{(1)2}\rangle)^2}\quad;$$

Eq. (6.31); (6.63b)

$a_o^{(1)}=a_o^{(2)}$: $$\hat{Q}_n^{(21)} = 1+\frac{1}{n}\sum_{ij}{}' m_{ij}^2(\rho_{ij}^{(2s)}-\rho_{ij}^{(1s)})^2\ ;\ \text{Eq. (6.33)}\ . \tag{6.63c}$$

The noise parameters are $L^{(2)} = \langle \ell^2\rangle$, $L^{(4)} = \langle(\ell^2+\ell')^2\rangle_o$, cf. (A.1-15, 19b), as before.

We have also the comparison of suboptimums here, cf. (6.60c):

(iii). simple-correlator / clipper correlator:

$$\mathrm{ARE}_{\mathrm{inc}}\Big|_{\text{on-off}} = \lim_{n\to\infty}\left(\frac{4Q_n^2\{2Q_n-1\}}{[\overline{x^4}-1+2(Q_n-1)][-\sqrt{2}w_{1E}(0)''+8w_{1E}(0)^2\{Q_n-1\}]^2}\right)^{\frac{1}{2}}$$

$$= \text{Eq. (6.61a)/Eq. (6.62a);} \qquad (6.64a)$$

$\underline{a_0^{(1)}\neq a_0^{(2)}}$:

$$\mathrm{ARE}_{\mathrm{inc}}\Big|_{\text{binary}} = \lim_{n\to\infty}\left(\frac{4Q_n^{(21)2}\{2Q_n^{(21)}-1\}}{[\overline{x^4}-1+2(Q_n-1)][-\sqrt{2}w_{1E}(0)''+8w_{1E}(0)^2\{Q_n^{(21)}-1\}]^2}\right)^{\frac{1}{2}}$$

$$= \text{Eq. (6.61b)/Eq.(6.62b)} \qquad (6.64b)$$

$\underline{a_0^{(1)}=a_0^{(2)}}$:

$$\mathrm{ARE}_{\mathrm{inc}}\Big|_{\text{binary}} = \lim_{n\to\infty}\left(\frac{(\hat{Q}_n^{(21)}-1)}{8[\overline{x^4}-1+2(\hat{Q}_n^{(21)}-1)]w_{1E}(0)^4}\right)^{\frac{1}{2}}$$

$$= \text{Eq. (6.61c)/Eq.(6.62c).} \qquad (6.64c)$$

(We remember that when the clipper correlator is optimum, i.e. when the noise is Laplace noise, cf. Sec. A.4-3, we must use the optimum forms $L_{F:E} \to L_E$, etc., cf. (A.4-39)-(A.4-46), where $\hat{L}^{(4)} \to L^{(4)} \to L_E^{(4)}$, etc., so that in the incoherent cases specifically the ARE* = 1, as required.)

As some simple examples, let us consider coherent reception (for general signals) when (1), the noise is gaussian, and (2), when it is LaPlacian, e.g.:

$$w_{1E}(x)_{gauss} = \frac{e^{-x^2/2}}{\sqrt{2\pi}} \; ; \begin{cases} L_E^{(2)}=1; \overline{x^2}=1; \\ \text{Eq. (A.1-22).} \end{cases} \tag{6.65a}$$

$$w_{1E}(x)_{Laplace} = \frac{1}{\sqrt{2}} e^{-|x|\sqrt{2}} \; ; \begin{cases} L_E^{(2)}=2; \; (\overline{x^2}=1). \\ \text{Eq. (A.4-65a)} \; . \end{cases} \tag{6.65b}$$

We have at once from (6.65) into (6.60) the simple results

$$\text{(i).} \quad \underline{\text{simple correlator:}}_{\text{opt.}} \quad ARE^*_{coh}\Big|_{gauss} = 1; \; ARE^*_{coh}\Big|_{Laplace} = 1/\sqrt{2} \tag{6.66a}$$

$$\text{(ii).} \quad \underline{\text{clipper correlator:}}_{\text{opt.}} \quad ARE^*_{coh}\Big|_{gauss} = \sqrt{\frac{2}{\pi}}; \; ARE^*_{coh}\Big|_{Laplace} = 1; \tag{6.66b}$$

$$\text{(iii).} \quad \left(\frac{\text{simple-correlator}}{\text{clipper correlator}}\right)^{-1}: \quad ARE^*_{coh}\Big|_{gauss} = \sqrt{\frac{2}{\pi}} \; ; \; \frac{\text{simple correl.}}{\text{clipper correl.}}\Big|_{Laplace} = \frac{1}{\sqrt{2}} \; . \tag{6.66c}$$

Equation (6.66) shows that there is not much difference $0(< 2db)$ between simple and clipper correlators in these threshold cases when they operate in gaussian and Laplace noise, to which they are respectively optimum. However, when the usual Class A or B interference is the principal noise mechanism, the simple correlators (although optimum in gauss) have been found to be very suboptimum here $0(20\text{-}40db$ or more), [13], whereas the superclipper correlators (at least in the coherent régimes) remain only slightly degraded $0(1.0$ dB) from the proper optimum processor [42], [45].

We recall from Sec. 6.3, V above, that depending on the coherence of the signal during the data acquisition period $(0,T)$, the signal factors Q_n, etc., cf. (6.63), are $0(n^{\mu})$, $0 \leq \mu \leq 1$. Thus, for incoherent reception and signals made comparatively incoherent (by combinations of rapid fading and doppler or by the mode of observation: independent signal samples,

for example), we have $\mu \doteq 0$, i.e. Q_∞ is essentially independent of n, and then the results (6.61)-(6.64) remain unchanged. However, when the signal remains highly correlated during the observation period, $Q_\infty \to 0 (n \to \infty)$, and (6.61)-(6.64) reduce to the somewhat simpler forms:

III. Incoherent Reception; Coherent Signals:

(i). $\underset{\text{optimum}}{\underline{\text{simple correlator}}}$: $ARE^{*}_{inc} = 1/L^{(2)}$; (on-off and binary) (6.67a)

(ii). $\underset{\text{optimum}}{\underline{\text{clipper correlator}}}$: $ARE^{*}_{inc} = [4w_{1E}(0)^2/L^{(2)}]$; (on-off and binary); (6.67b)

(iii). $\underset{\text{clipper correlator}}{\underline{\text{simple correlator}}}$: $ARE_{inc} = [1/4w_{1E}(0)^2]$; (on-off and binary). (6.67d)

Comparing these results (6.67) for the incoherent cases with those for the coherent situations (6.60), we see that the ARE's for the former are just the square of the ARE's for the latter in their respective comparisons, when the desired signals are fully coherent in structure and are so observed. On the other hand, when this coherent signal structure is partially or totally destroyed, the corresponding ARE's, Eqs. (6.61)-(6.64), are further reduced, as we would expect. We also observe that signal level symmetry $[a_o^{(1)}=a_o^{(2)}]$ considerably simplifies the result, cf. (6.61c), (6.62c), (6.64c), vis-à-vis the asymmetric cases $[a_o^{(1)} \neq a_o^{(2)}]$, including the "on-off" situation. The ARE's for coherent reception are larger (and sometimes much larger) then their incoherent counterparts: (6.60) vs. (6.67).

Finally, we remark that although the ARE's, like output signal-to-noise ratios $(\sigma_o^{(*)})^2$, (6.6), processing gains $(\Pi^{(\ )})$, and minimum detectable signals $(\langle a_o^2 \rangle_{min})$, are useful measures of receiver performance and performance comparisons, they are not directly (or linearly) related to actual performance, as measured by the appropriate decision probabilities (P_D, P_e, etc.). Furthermore, the ARE's are <u>limiting forms</u> $(n \to \infty)$, whereas in practice one deals with finite n (>>1).

Moreover, closely related to the essentially second-moment character of the ARE's (cf. 6.58)), is the fact that they can be ambiguous measures of performance. This may be demonstrated, for example, in the case of coherent threshold detection, Sec. 6.2, I, II, where for the suboptimum detector we choose the optimum form (4.1), but without the bias, $\hat{B}^*_{n\text{-coh}}$. Thus, $\sigma_o^2=\sigma_o^{*2}$, $(\langle g\rangle_1-\langle g\rangle_o)^{(*)} = \sigma_o^{*2}$, so that the ARE = 1. This says that on the basis of the ARE the two algorithms are equivalent. But $\langle g\rangle_1 = \sigma^{*2}+\log\mu$, $\langle g\rangle_o = \log\mu$, so that (2.32) becomes (μ=1) $P_e \doteq \frac{1}{2}\{1-\frac{1}{2}\Theta(\sigma_o^*/\sqrt{2})\}$ which is to be compared with $P_e^* \doteq \frac{1}{2}\{1-\Theta(\sigma_o^*/2\sqrt{2})\}$. Since $\Theta(x/2) < \frac{1}{2}\Theta(x)$, $x > 0$, clearly $P_e > P_e^*$ in this example. In fact, $P_e \doteq 1/4$ for the usually large σ_o^*. Thus, on the basis of the more comprehensive probability measures, the algorithm without the (correct) bias can be clearly inferior. Furthermore, this suboptimum algorithm is not asymptotically optimum (AO), since it is (μ=1) $G(\sigma_o^{*2},o;\sigma_o^{*2})$, under H_o, H_1, which does not obey the n.+s. conditions (A.3-8,9).

For all these reasons, then, these latter quantities (i.e., P_D^*, etc.) are the more complete and unambiguous descriptors of performance and are ultimately to be preferred to the ARE's when receiver performance is to be assessed and compared under the practical constraint of finite sample size ($1<<n<\infty$), not only for the threshold conditions postulated here, but for all input signal levels.

6.4 Input Signal Conditions for (Optimum) Threshold Algorithms and Performance

There are <u>two</u> conditions on the maximum level of the input signal $a_o^2(>0)$ which must be obeyed† if the detection algorithms g_n^* are to remain not only LOBD's but AODA's as well (as sample size becomes larger).

As we have already noted (cf. Sec. 2.4, Secs. A.2-1,2,3,4, etc.), the <u>first condition</u> is to insure that $\text{var}_{1,\theta} g_n^* \doteq \text{var}\, g_{o,o} g_n^*$, cf. (2.29), (A.2-14), (A.2-40), (A.2-50b), which in turn is required for asymptotic optimality (AO), cf. (Appendix) Section A.3-3, as well as consistency of the test (detection) as $n\to\infty$ and for providing the associated proper bias, $\hat{B}_n^*$.

---

†In the limiting case of <u>continuous sampling</u> on the observation interval! we shall discuss this point and its relation to the <u>discrete</u> sampling cases of our current analysis in Sec. 6.4 III, following.

The second condition stems from the fact that the coherent LOBD is a truncated expansion of log Λ_n, which omits the "incoherent" term $O(\theta^2)$, so that it is possible in some nongaussian noise situations that, mathematically, incoherent LOBD's perform better than coherent LOBD's. Of course, physically this appears to be a contradiction†: coherent detection should always be at least no worse than incoherent detection under otherwise the same conditions, since the former employs the additional relevant information about the signal phase (or epoch). Consequently, there can also be an upper limit on input signal level (a_o^2) beyond which the truncation [i.e., omission of the incoherent terms, $O(\theta^2)$] of the coherent algorithm leads to this contradiction in performance, and hence beyond which the associated performance measures are not used.

Of course, the algorithms themselves are employable at all signal levels ($0<a_o^2$), but are no longer optimal as a_o^2 is increased outside the lesser of the two limits indicated. Their performance must then be re-evaluated: if $n>>1$, the Central Limit Theorem still applies, but $\sigma_{1n}^{*2} \neq \sigma_{on}^{*2}$, i.e., $\text{var}_{1,o} g_n^* \neq \text{var}_{o,o} g_n^*$, and it is then possible for "coherent" detection by these now suboptimum algorithms to be inferior to the corresponding "incoherent" detectors.

I. "On-off" Detection:

Let us look further at the "second condition" noted above: viz., from (6.2), (6.5) (as well as (6.5a), (6.5e) in the binary signal cases):

(Opt.) Coherent Det $\geq$ (Opt.) Incoherent Det:

$$\sigma_{o\text{-coh}}^* \geq \sigma_{o\text{-inc}}^*, \quad \text{(large n)}. \tag{6.68a}$$

This insures (for sufficiently large n, where (6.2) etc. apply) that (optimum) coherent performance is never worse than (optimum) incoherent performance under otherwise the same conditions. For the "on-off" cases

† See footnote, page 102.

from (6.9) and (6.22b) we can write (6.68a) as

$$\sqrt{\Pi^*_{coh}\langle a_o^2\rangle^*_{min\text{-}coh}} \geq \sqrt{\Pi^*_{inc}}\,\langle a_o^2\rangle^*_{min\text{-}inc}\ , \tag{6.68b}$$

and, using (6.10), (6.24) we get at once

$$\langle a_o^2\rangle^*_{min\text{-}coh} \geq \frac{\Pi^*_{inc}}{\Pi^*_{coh}}\langle a_o^2\rangle^{*2}_{min\text{-}inc} = \left\{\frac{L^{(4)}+2L^{(2)^2}(Q_n-1)}{8L^{(2)}}\right\}\langle a_o^2\rangle^{*2}_{min\text{-}inc}\ . \tag{6.68c}$$

Equation (6.68c) is to be used in conjunction with the first condition (on $\overline{a_o^2}$), i.e., that $var_{1,\theta}g_n^* \doteq var_{o,o}g_n^*$, here (A.2-15a), which is specifically in the stationary noise régime:

Eq. (A.2-15a): coherent:

$$\langle a_o^2\rangle^*_{min\text{-}coh} << x_o^* \equiv \frac{L^{(2)}\sum_i \hat{a}_{oi}^2\bar{s}_i^2}{\left|\sum_i \bar{s}_i^2\hat{a}_{oi}^2\{\frac{L^{(2,2)}}{2}(\overline{a_{oi}^2}/\overline{a_o^2})-L^{(2)^2}\hat{a}_{oi}^2\}+L^{(2)^2}\sum_{ij}{}'(\hat{a}_{oi}\hat{a}_{oj}(m_{ij}-\hat{a}_{oi}\hat{a}_{oj})\bar{s}_i\bar{s}_j\right|} \tag{6.69}$$

$$\hat{a}_{oi} \equiv \bar{a}_{oi}/\sqrt{\overline{a_o^2}}\ ; \tag{6.69a}$$

Eq. (A.2-42): incoherent:

$$\langle a_o^2\rangle^*_{min\text{-}inc} << y_o^* \equiv \frac{L^{(4)}+2L^{(2)^2}(Q_n-1)}{\left|\frac{L^{(6)}}{2}+6L^{(2)}L^{(2,2)}Q_n+L^{(2)^3}R_n\right|}\ . \tag{6.70}$$

In the important special cases of slow and no fading ($\bar{a}_{oi}=a_o, \overline{a_{oi}^2}=a_o^2$;

$\therefore m_{ij} = 1$), or <u>rapid fading</u> ($\overline{a_{oi}a_{oj}} = \overline{a_{oi}}\ \overline{a_{oj}}$), Eq. (6.69) simplifies directly to

$$x_o^* = \frac{L^{(2)}}{\left|L^{(2,2)}/2-(1-\eta)L^{(2)^2}\right|} = \frac{\langle \ell^2 \rangle_o}{\mathrm{var}_o \ell^2} \quad . \tag{6.71}$$

Similarly, with incoherent signal structures (A.2-42b), or totally coherent signal structures (A.2-42f), we have

$$(\underline{\text{Incoherent}}\ \underline{\text{structure}}): \quad y_o^* = \frac{L^{(4)}}{\left|\frac{L^{(6)}}{2} + 6L^{(2)}L^{(2,2)}\right|} \ ;$$

$$(\underline{\text{coherent}}\ \underline{\text{structure}}): \quad y_o^* = \frac{L^{(2)}}{3L^{(2,2)}+2L^{(2)^2}} \quad , \quad (Q_n \doteq n/2; R_n \doteq 2n) \ , \tag{6.72}$$

where we take the maximum value of F_n^{-1} in (A.2-42f), for the strictest condition on $0<a_o^2 << 1$. [Some numerical values of (x_o^*, y_o^*) are shown in Figs. 7.20-7.22 ff.]

Then, as the second condition, (6.68c) is used to set additional upper bounds on the input signal ($\sim a_o^2$). Letting

$$x \equiv \langle a_o^2 \rangle^*_{\text{min-coh}} \ ; \ y \equiv \langle a_o^2 \rangle^*_{\text{min-inc}} \ ; \ \Pi^* \equiv \Pi^*_{\text{inc}}/\Pi^*_{\text{coh}} \ , \tag{6.73}$$

we have for (6.68c)

$$\underline{\text{2nd condition:}} \quad \boxed{x \gtrsim \Pi^* y^2} \quad ; \text{ with: } \underline{\text{1st. condition:}} \begin{cases} x << x_o^*, \text{Eqs. (6.69), (6.71)} \\ y << y_o^*, \text{Eqs. (6.70), (6.72)} \end{cases} \tag{6.74}$$

The points y=x, or $1/\pi^* \geq x = y$, which at $(1/\pi^*)$ or below the curve $x = \pi^* y^2$, and which are within the region of individual constraints on (x,y), e.g., the dotted lines in Fig. 6.1, are all permissable values of $\langle a_o^2 \rangle^*_{\text{min-coh,inc}}$. The curves $y^2\pi^* = x$ represent the limiting condition $P^*_{\text{e-coh}} = P^*_{\text{e-inc}}$, or $P^*_{\text{D-coh}} = P^*_{\text{D-inc}}$. When we require coherent and incoherent performance to be equal, i.e. when we specify the limiting probabilities ($P^*_{\text{D-coh}} = P^*_{\text{D-inc}}$, etc.) which we can accept, that portion of the parabola $x = \pi^* y^2$ which lies within the rectangle (x,y) [$<<(x_o,y_o)$] determines the acceptable values of $\langle a_o^2 \rangle^*_{\text{min-coh,inc}}$.

Accordingly, to use the various relations in Section 6.1-6.3 to obtain minimum detectable signal (or maximum range, cf. [34]), when either a purely coherent or incoherent threshold detection algorithm is employed, we calculate the appropriate quantities, cf. (6.74), for both the coherent and incoherent régimes, in order to obtain physically acceptable results, even though we may be interested in only one or the other mode of detection. Thus, we may proceed as follows for minimum detectable signals (in these stationary cases):

A. Minimum Detectable Signals:

(1). Calculate $\langle a_o^2 \rangle^*_{\text{min-coh}}$ from (6.11) for coherent reception;

(2). Calculate $\langle a_o^2 \rangle^*_{\text{min-inc}}$ from (6.27) for incoherent detection;

(3). Use (6.69) or (6.71) for x_o; (6.70), or (6.72) for y_o, to determine the coherent/incoherent conditions for equal threshold variances;

(4). Compute $x = \pi^* y^2$, (6.74), for the various $\langle a_o^2 \rangle^*_{\text{min}_2}$ and locate the results of (1), (2) within the region $x \geq \pi^* y^2$, cf. Fig. 6.1. Physically acceptable results here are (usually) those for which the calculated values fall within the bounded (i.e. shaded) region [but see remarks in III ff.].

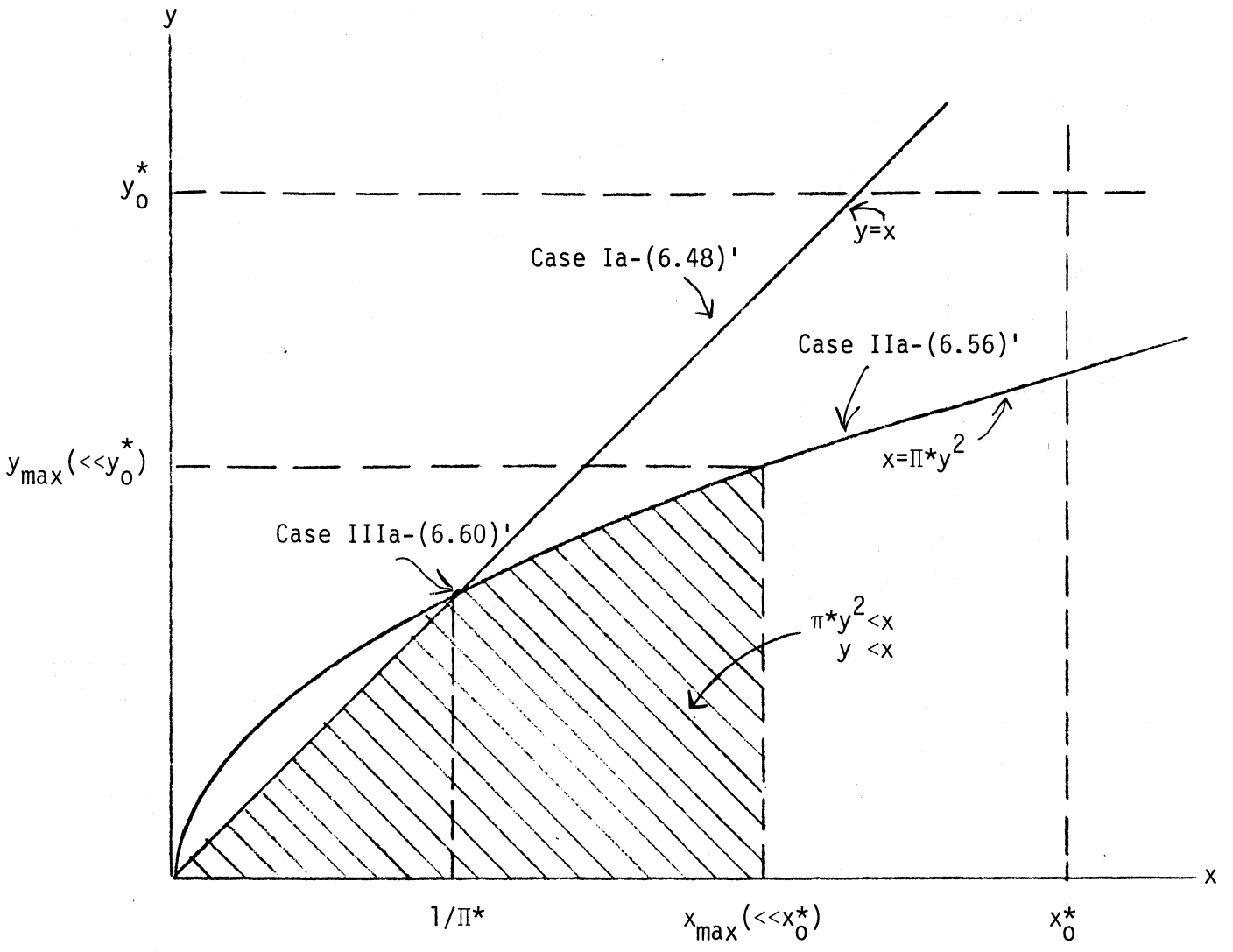

Figure 6.1. Sketch of the relationship between $x\left(=\left\langle a_o^2\right\rangle^*_{\text{min-coh}}\right)$ and $y\left(=\left\langle a_o^2\right\rangle^*_{\text{min-inc}}\right)$, showing the domain (shaded) wherein "coherent reception" $\geq$ "incoherent reception," for physical applications (same sample size, n).

II. Binary Signal Detection:

The same considerations apply for optimum binary signal reception as above for the cases of "on-off" detection, e.g., in addition to the condition of equality of variances ($\text{var}_{1,\theta} g_n^{(21)*} = \text{var}_{o,o} g_n^{(21)*}$) we must satisfy (6.68a) as well. Here, of course, we replace Π^*_{coh} by $\Pi^{(21)*}_{coh}$, etc., $\langle a_o^2 \rangle^*_{min}$ by $\langle a_o^2 \rangle^{(21)*}$, etc., and Q_n by $Q_n^{(21)}$ in (6.68b,c), where specifically we employ (6.12), (6.13), (6.29)-(6.31). The first "small-signal" (or equal variance) conditions, analogous to (6.69) etc., are now given (in the stationary régimes) by

Eq. (A.2-50a) (coherent) :

$$\left\{ \begin{array}{l} \langle a_o^2 \rangle^{(21)*}_{\text{min-coh}} \\ \text{Eq. (6.14)} \end{array} \right. \ll x_o^{(21)*}$$

$$\equiv \frac{L^{(2)} \left(\sum_i^n \langle \Delta\theta_i \rangle^2 \right)^2}{\left| \sum_i \langle \Delta\theta_i \rangle^2 \{ \langle (a_{oi}^{(2),(1)})^2 \rangle L^{(2,2)}/2 - (\langle a_{oi}^{(2),(1)} \rangle)^2 L^{(2)^2} \right.}$$

$$+ L^{(2)^2} \sum_{ij}{}' \langle \Delta\theta_i \rangle \langle \Delta\theta \rangle_j \cdot (\bar{s}_i \cdot \bar{s}_j)^{(2),(1)} \{ \overline{a_{oi} a_{oj}}^{(2),(1)}$$

$$\left. - [(\langle a_{oi} \rangle)(\langle a_{oj} \rangle)]^{(2),(1)} \} \right|, \qquad (6.75)$$

$$\langle \Delta\theta_i \rangle \equiv \langle a_{oi}^{(2)} s_i^{(2)} \rangle - \langle a_{oi}^{(1)} s_i^{(1)} \rangle, \qquad (6.75a)$$

cf. (6.69), (6.69a), and

Eq. (A.2-57) (incoherent):

$$\left\{ \langle a_o^2 \rangle^{(21)*}_{\text{min-inc}} \;\text{Eq. (6.69)} \right. \ll y_o^{(21)*} \equiv \frac{L^{(4)} + 2L^{(2)^2}(Q_n^{(21)} - 1)}{\left| \frac{L^{(6)}}{2} + 6L^{(2)}L^{(2,2)}Q_n^{(21)} + L^{(2)^3}R_n^{(21)} \right|} \quad , \tag{6.76}$$

(Eq. A.2-59) ,

for slow or no fading and stationary noise, in which $Q_n^{(21)}$, $R_n^{(21)}$ are given by (A.2-60a,b) explicitly.

For the important special cases of signals with no fading, in symmetrical channels, we have (A.2-50e) for $x_o^{(21)*}$, viz.

$$\underline{\text{[no fading; sym.]:}} \quad x_o^{(21)*} = \frac{L^{(2)} \sum_i (\bar{s}_i^{(2)} - \bar{s}_i^{(1)})^2}{\left| \{L^{(2,2)}/2 - L^{(2)^2}\} \sum (\bar{s}_i^{(2)} - \bar{s}_i^{(1)})^2 \bar{s}_i^{(2),(1)} \right|} \quad , \tag{6.77}$$

and from (A.2-62), for both coherent and incoherent signal structures

$$y_o^{(21)*} \doteq \frac{L^{(4)}}{\left| L^{(6)}/2 + 6L^{(2)}L^{(2,2)} \right|} \quad , \tag{6.78}$$

cf. (6.71), (6.72) above. Still other forms can be obtained from (6.75), (6.76), depending on channel conditions. In any case, (6.73), (6.74) apply generally, with $x_o^* \to x_o^{(21)*}$, etc., now. The domain of input signal levels for applicability of the optimum algorithms is likewise sketched in Fig. 6.1, where, of course, $x = \langle a_o^{(2)^2} \rangle^*_{\text{min-coh}}$ or $\langle a^{(1)^2} \rangle^*_{\text{min-coh}}$, etc.: there are thus a pair of (x,y)'s now, when $a_o^{(2)} \neq a_o^{(1)}$, but only a single set (x,y) when the channel is symmetrical: $a_o^{(2)} = a_o^{(1)} = a_o$. The general procedure for determining minimum detectable signals is again given by A. above, suitably modified, e.g.:

A. Minimum Detectable Signals:

(1). Calculate $\langle a_o^2 \rangle^{(21)*}_{\text{min-coh}}$, from (6.14);

(2). Calculate $\langle a_o^2 \rangle^{(21)*}_{\text{min-inch}}$ from (6.29); (or 6.33);

(3). Use (6.75) or (6.77) for x_o^*; (6.76) or (6.78) for y_o^*, (e.g., the equal variance conditions on both coherent and incoherent reception;

(4). Compute $x = \pi^{(21)*} y^2$, (6.74), $\pi^* \to \pi^{(21)*}$, where $\pi^{(21)*} = \Pi^{(21)*}_{\text{inc}} / \Pi^{(21)*}_{\text{coh}}$, cf. (6.13), (6.30).

III. The Second Input Signal Condition -- Optimum Incoherent vs. Coherent Detection: Discussion

Our starting point is Figure 6.1. For the moment let us impose the "coherent-vs-incoherent" condition posited in (6.68a) above, here, of course, for discrete sampling such that the noise samples are statistically independent--our universal condition in this study, cf. Sec. 2.4 et seq.

Then, we can make the following observations about Figure 6.1:

(i) The parabola (6.74) is the contour of Case IIa, Eq. (6.56)' et seq., for optimum incoherent threshold performance being equal to optimum coherent performance.

(ii) The straight line (y=x) embodies Case Ia, Eq. (6.48)' et seq., where coherent performance is better (i.e., smaller error probabilities) than incoherent performance, with the same sample sizes, when $\langle a_o^2 \rangle^*_{\text{min-coh}} (\equiv x) = y \equiv \langle a_o^2 \rangle^*_{\text{min-inc}} \leq 1/\pi^*$. For x=y larger than $x_{III}=y_{III}=1/\pi^*$ coherent performance is inferior to incoherent performance.

(iii) At $x=y=1/\pi^*=x_{III}=y_{III}$ we have Case IIIa, (6.60)' et seq., where $n^*_{\text{inc}} > n^*_{\text{coh}}$ ($>>1$) usually.

(iv) Here x_o^*, y_o^* are bounding values obtained from the basic Condition I, namely the "equal variance" condition which is necessary to insure asymptotic optimality at small but non-vanishing signals.

(Explicit examples relating x_o^*, y_o^* to the associated minimum detectable signal $\langle a_o^2 \rangle^*_{\text{min}}$ are given by Eqs. (6.69)-(6.72) above.) If $x_{\text{max}}, y_{\text{max}}$ are the largest input signal values permitted, the allowed minimum detectable

signals (x,y) must obey the inequalities $x \leq x_{max} << x_o^*$ or $y \leq y_{max} << y_o^*$. Here the usual quantitative choice of the inequality (<<) is 13 dB or 15 dB in practice. (Of course, the value given to "<<" is arbitrary, dependent on a reasonable choice of what is meant by "small" signals.) Accordingly, the rectangular (shaded) region bounded by x_{max}, y_{max}) in Figure 6.1 is the domain wherein the AO, or equal-variance condition holds practically.

Now, from Figure 6.1 it is clear that it may be possible for these threshold algorithms to be AO (as well as LOB) and have coherent detection with larger minimum detectable signals, or larger error probabilities (inferior performance), or both, than (AO) incoherent detection. When this happens, we call the region of (x,y) values an anomalous region, with respect to the conditions $\left\langle a_o^2 \right\rangle^*_{\text{min-coh}} \leq \left\langle a_o^2 \right\rangle^*_{\text{min-inc}}$, and coherent performance $\geq$ incoherent performance. Thus, in the region formed by y=x and the parabola (within x_{max}, y_{max}) we have the "anomalous" situation y>x, with incoherent performance better than coherent. The region bounded by the line y=x, the parabola, x_{max}, and y=o is the non-anomalous region, as shown in Figure 6.1.

The results of Figure 6.1 show that for both optimum coherent and incoherent threshold detectors which are AO (as well as LOB) one can have any combination of minimum detectable signal and performance inequalities for the same data sample size. This, in turn, means that the so-called Condition II, defined by Eq. (6.74) is not (for discrete, independent noise samples) an ultimate constraint on the validity of "practical" optimality: we can disregard Condition II as long as Condition I--the equal variance condition--is obeyed. Thus, there is ultimately only Condition I, which sets a bound on the largest value of input minimum detectable signal for which the AO still obtains (cf. Appendix A3). Moreover, we may expect Condition II to be automatically satisfied in the limit of continuous sampling. The formal use of Condition II in the discrete case, however, is helpful in identifying the apparently anomalous regions of behavior. Of course, with continuous sampling only the "regular" region is occupied, because then coherent detection cannot be any less effective than incoherent detection for otherwise the same conditions of operation.

This follows in as much as more signal information (i.e., epoch) is used in the coherent cases than in incoherent reception, while all the noise data, viz. those contained in the n-th order pdf's $w_n(\underset{\sim}{x})_N$ as $n\to\infty$, are employed in either observation mode. [We note that the derivatives of $w_n(\underset{\sim}{x})_N$, as $n\to\infty$, contain no additional noise information.]

The explanation for the anomalous behavior of the optimim incoherent vis-à-vis the optimum coherent detector lies in the different effective amount of relevant signal and noise information available under independent (noise) samples. Although all signal (i.e., waveform) information is used in both detection modes, with only the epoch information lacking in the incoherent cases†, more relevant noise information is available in the incoherent cases. This is apparent from the fact that for coherent detection we require $\ell(=\frac{d}{dx}\log w,(x))$ in the algorithm and $L^{(2)}(\equiv\langle \ell^2 \rangle_o)$ in the performance measure, whereas both ℓ and ℓ' are needed in the incoherent algorithm, and $L^{(4)}$ $(\equiv \langle(\ell^2+\ell')^2\rangle_o)$ as well as $L^{(2)}$, in its performance. In addition, there is further information embodied in the way $L^{(2)}$ and $L^{(4)}$ appear in $\sigma^*_{o\text{-inc}}$, along with their combination with signal structure (Q_n), cf. (6.24); for example, the functional form of Π^*_{inc}, as well as its individual $L^{(2)}$, $L^{(4)}$, and Q_n components.

Whether or not the use of this added information is enough to offset the loss of epoch information in the signal will depend, of course, on the specific nature of the nongaussian noise, signal structure, the signal's interaction with the noise, and on the probability controls (P^*_D, α^*_F, etc.) under which the receiver is set to operate. For signals which maintain their structure (e.g., no doppler smearing) we may have "anomalous" behavior, i.e., the incoherent minimum detectable signals are smaller than for the corresponding

---

† For simplicity, we confine the argument to the important limiting cases where total waveform information is available to the receiver. This, however, is not a restriction on our general argument. We note, also, that with proper choice of epoch and sampling intervals in the coherent cases, discrete signal sampling is fully equivalent to continuous signal sampling on the observation interval (O.T.).

coherent cases (under the same performance measures). On the other hand, incoherent reception of "incoherent" signals is always inferior (in the sense of larger minimum detectable signals for the same controls) to coherent reception of coherent waveforms, as we would expect. Specific examples of these behaviors are presented in Sec. 7.4 ff. Finally, even in the gauss noise cases ($L^{(2)}=1$, $L^{(4)}=2$) we may expect anomalous behavior for the same reasons. [An academic exception is the case of the completely known signal, for the reasons cited in Sec. A.3-6, I, esp. p. A66.] The general magnitude of the anomalies in $\langle a_o^2 \rangle^*_{min}$ appears to be O(2-3 dB), cf. Sec. 7.4 ff. All our comments here apply equally to the earlier results Sec. 5.1, V, [34].

IV . Remarks on Suboptimum Receivers:

Similar conditions on the largest "small-signal" inputs to suboptimum receivers, giving equal variances under H_0, H_1, etc. are derived in Appendix A.4, cf. (A.4-10) for the coherent cases and (A.4-30) for the incoherent detectors, generally. In the case of simple correlators these equal variance conditions are given by (A.4-59), and for energy detectors, by (A.4-63), while for hard-limiting or "super-clipper" correlators, these conditions are given in (A.4-70). For binary signals, see the remarks in Sec. A.4-4.

However, when these receivers are suboptimum [as they will be in most instances unless they are operating in the noise for which they are "matched," i.e., become optimum, viz., gauss noise (A.4-50a) for the simple correlators, "Laplace noise" (A.4-50b) for the hard-limiter correlators], there is no reason to assume that coherent reception will necessarily always be better than incoherent reception for otherwise the same reception conditions. Such a situation will depend on the detectors themselves vis-à-vis noise and signal. Consequently, we do not impose the second condition, cf. Eqs. (6.68), on the magnitude of the input signal, so that only the conditions on equal variances referenced above are needed in the evaluation of performance using the (suboptimum) results of Section 6.1, etc.

Of course, these suboptimum algorithms can be used at all input signal levels, but then $\mathrm{var}_{1,\theta} g \neq \mathrm{var}_{o,o} g$ and the large-sample ($n \gg 1$) expressions for P_D, P_e, etc., cf. Sec. 6.1, must be appropriately modified, along the lines of (2.23)-(2.27), cf. (2.26), (2.27) specifically.

6.5 The Composite LOBD:

We have shown (in Appendix A.3-6) that the composite LOBD, which includes both coherent ($\bar{\theta} \geq 0$) and incoherent processing ($\overline{\theta^2} > 0$, $\bar{\theta} = 0$), is also an AODA, and in the "on-off" cases is given explicitly by

$$\begin{aligned} g^*_{n\text{-comp}} &= \log \mu + \hat{B}^*_{comp} + \frac{1}{2} \sum_{ij}^{n} [-2\ell_i \langle \theta_i \rangle \delta_{ij} + (\ell_i \ell_j + \ell_i' \delta_{ij}) \langle \theta_i \theta_j \rangle] \\ &= \log \mu + \mathrm{LOBD}_{coh} + \mathrm{LOBD}_{inc} , \end{aligned} \tag{6.79a}$$

where the bias is

$$\begin{aligned} \hat{B}^*_{n\text{-comp}} &= -\frac{1}{8} \sum_{ij}^{n} \{4L_i^{(2)} \langle \theta_i \rangle^2 \delta_{ij} + \langle \theta_i \theta_j \rangle^2 [(L_i^{(4)} - 2L_i^{(2)2}) \delta_{ij} + 2L_i^{(2)} L_j^{(2)}]\} \\ &= \hat{B}^*_{n\text{-coh}} + \hat{B}^*_{n\text{-inc}}, \end{aligned} \tag{6.79b}$$

and the variance $\sigma^{*2}_{on\text{-comp}}$ ($=\mathrm{var}_{o,o}\, g^*_{n\text{-comp}}$) is given by

$$\begin{aligned} \sigma^{*2}_{on\text{-comp}} &= \frac{1}{4} \sum_{ij}^{n} \{4L_i^{(2)} \langle \theta_i \rangle^2 \delta_{ij} + \langle \theta_i \theta_j \rangle^2 [(L_i^{(4)} - 2L_i^{(2)2}) \delta_{ij} + 2L_i^{(2)} L_j^{(2)}]\} \\ &= \sigma^{*2}_{on\text{-coh}} + \sigma^{*2}_{on\text{-inc}} . \end{aligned} \tag{6.79c}$$

The equal-variance, or "small-signal" condition that $\sigma^{*2}_{1n} \doteq \sigma^{*2}_{on}$ here is given by (6.69) or (6.70), whichever is the stricter. Note that there

is here no "second-condition", cf. Sec. 6.4, I , II above, since there is now no question of a purely coherent processor in possible competition with an incoherent algorithm to produce possibly inferior performance vis-à-vis the incoherent algorithm: there is just a single, albeit composite algorithm.

Performance, as measured by the probabilities P_D^*, or P_e^*, cf. (6.2) -(6.5), follows at once on applying $\sigma^*_{\text{on-comp}}$ therein; (cf. Footnote p. 55).

With binary signals [cf. II, Appendix A.3-6] we have the extensions of (6.79), viz:

$$g^{(21)*}_{\text{n-comp}} = \log \mu + \hat{B}^{(21)*}_{\text{n-comp}} + \frac{1}{2}\sum_{ij}^{n}\{-2\ell_i[\langle a^{(2)}_{oi}s^{(2)}_i\rangle - \langle a^{(1)}_{oi}s^{(1)}_i\rangle]\delta_{ij}$$

$$+[\ell_i\ell_j+\ell'_i\delta_{ij}][\langle a_{oi}a_{oj}s_is_j\rangle^{(2)} - \langle a_{oi}a_{oj}s_is_j\rangle^{(1)}]\}, \qquad (6.80)$$

in which the bias and associated variance $\sigma^{(21)*2}_{\text{on-comp}}$ are specifically

$$\hat{B}^{(21)*}_{\text{n-comp}} = -\frac{1}{8}\sum_{ij}^{n}[4L^{(2)}_i\{\langle a^{(2)}_{oi}s^{(2)}_i\rangle^2 - \langle a^{(1)}_{oi}s^{(1)}_i\rangle^2\}\delta_{ij}$$

$$+[\langle a^{(2)}_{oi}a^{(2)}_{oj}s^{(2)}_is^{(2)}_j\rangle^2 - \langle a^{(1)}_{oi}a^{(1)}_{oj}s^{(1)}_is^{(1)}_j\rangle^2]$$

$$\cdot[(L^{(4)}_i - 2L^{(2)2}_i)\delta_{ij} + 2L^{(2)}_iL^{(2)}_j]], \qquad (6.80a)$$

$$= \hat{B}^{*(21)}_{\text{n-coh}} + \hat{B}^{*(21)}_{\text{n-inc}}$$

$$\sigma^{(21)*2}_{\text{on-comp}} = \frac{1}{4}\sum_{ij}^{n}(4L_i^{(2)}\{\langle a_{oi}s_i\rangle^{(2)}-\langle a_{oi}s_i\rangle^{(1)}\}^2\delta_{ij}$$

$$+[\langle a_{oi}a_{oj}s_is_j\rangle^{(2)}-\langle a_{oi}a_{oj}s_is_j\rangle^{(1)}]^2$$

$$\cdot[(L_i^{(4)}-2L_i^{(2)^2})\delta_{ij}+2L_i^{(2)}L_j^{(2)}]) \ ,$$

$$= \sigma^{(21)*2}_{\text{coh}} + \sigma^{(21)*2}_{\text{inc}} \ , \qquad (6.80b)$$

cf. (A.3-35,36). The "small-signal" condition ($\sigma^*_{\text{n-comp}} \doteq \sigma^*_{\text{on-comp}}$) is given here by the stricter of (6.75), (6.76), or the more special cases, (6.77) vs. (6.78). Performance (P_D^*, P_e^*) is obtained by applying (6.80b) to (6.5a), (6.5e).

--- --- ---

Various suboptimum composite algorithms are suggested as extensions of the previously developed simple and clipper-correlators discussed earlier in this Section (and in Appendix A.4). Thus, parallelling the optimum examples above, we have from A, B of Sec. 4.2 above:

I. Composite Simple Correlators (H_1 vs. H_0):

$$g_{\text{n-comp}} = \log\mu+\hat{B}_{\text{n-comp}}+\frac{1}{2}\sum_{ij}^{n}\{2x_i\langle\theta_i\rangle\delta_{ij}+\langle\theta_i\theta_j\rangle x_ix_j\}, \qquad (6.81a)$$

where

$$\hat{B}_{\text{n-comp}} = -\frac{1}{4}\{\sum_{ij}^{n}(2\{\langle\theta_i\rangle^2+\langle\theta_i^2\rangle\}\delta_{ij}+\langle\theta_i\theta_j\rangle^2). \qquad (6.81b)$$

The H_o-variance of $g_{\text{n-comp}}$ is the sum of the variances (A.4-57), viz.

$$\hat{\sigma}^2_{\text{on-comp}} = \sum_{ij}^{n} \left(\{\langle\theta_i\rangle^2+\left(\frac{\overline{x_i^4}-3}{4}\right)\langle\theta_i\theta_j\rangle^2\}\delta_{ij}+2\langle\theta_i\theta_j\rangle^2\right) \qquad (6.81c)$$

II. Composite Clipper-Correlators (H_1 vs. H_0):

$$g_{\text{n-comp}} = \log\mu + \hat{B}_{\text{n-comp}} + \sum_{ij}^{n}(\delta_{ij}\sqrt{2}\langle\theta_i\rangle \operatorname{sgn} x_i+\langle\theta_i\theta_j\rangle \operatorname{sgn} x_i \operatorname{sgn} x_j), \qquad (6.82a)$$

where

$$\hat{B}_{\text{n-comp}} = -\frac{1}{4}\sum_{ij}^{n}[4\{(\langle\theta_i\rangle^2-\langle\theta_i^2\rangle)\sqrt{2}\, w_{1E}(0)_i+\langle\theta_i^2\rangle\}\delta_{ij}$$

$$+\langle\theta_i\theta_j\rangle^2[8w_{1E}(0)_i w_{1E}(0)_j-\{\sqrt{2}\, w''_{1E}(0)_i+8w_{1E}(0)_i^2\}\delta_{ij}]] \; . \qquad (6.82b)$$

The H_0-variance is the sum of the variances (A.4-68), viz:

$$\hat{\sigma}^2_{\text{on-comp}} = \sum_{ij}^{n}(\{2\langle\theta_i\rangle^2-\langle\theta_i^2\rangle^2\}\delta_{ij}+2\langle\theta_i\theta_j\rangle^2) \; . \qquad (6.82c)$$

The "small-signal" conditions here are the stricter of (A.4-59) for the simple correlators, and the stricter of (A.4-70) in the case of the clipper-correlators.

For performance in the above (and generally), we need both $\hat{\sigma}^2_{\text{on-comp}}$ and the quantity $\sigma_{\text{o-comp}}$, defined by

$$\frac{\langle g_{\text{comp}}\rangle_1-\langle g_{\text{comp}}\rangle_0}{\sqrt{2}\,\hat{\sigma}_{\text{on-comp}}} = \frac{[\text{numerator of (A.4-12a,b)+numerator of A.4-31a,b)}]}{\sqrt{2}\,[\{\text{Eq. (A.4-9)+Eq.(A.4-29)}\}=\hat{\sigma}^2_{\text{on-comp}}]^{1/2}}$$

$$\equiv \frac{\sigma_{\text{o-comp(F)}}}{\sqrt{2}} \; , \qquad (6.83a)$$

and

$$\frac{\langle g_{comp}\rangle_1}{\sqrt{2}\,\hat{\sigma}_{on\text{-}comp}} = \frac{-\langle g_{comp}\rangle_0}{\sqrt{2}\,\hat{\sigma}_{on\text{-}comp}} = \frac{\sigma_{o\text{-}comp(F)}}{2\sqrt{2}} \,. \tag{6.83b}$$

Then, in particular, for these composite correlation detectors we use the results of Appendices A.4-2,3 to obtain the specific values of $L^{(2)}_{F:E}$, $\hat{L}^{(2)}_{F:E}$, etc. which appear in both σ_0,(6.83a,b),and in $\hat{\sigma}^2_{on\text{-}comp}$ (cf. (6.81c), (6.82c)). Performance is then calculated using these values in (6.2)-(6.5), as appropriate. [We recall [D, Sec. A.4-1] that these suboptimum algorithms become optimum against the appropriate noise, e.g. gauss for the simple correlators, "Laplace" noise for the clipper-correlators.

All these (optimum) algorithms are, of course, LOBD's: each gives the minimum error probabilities for all values of input signal ($\theta = \sqrt{\overline{a^2}}$) in some finite range $0 < \theta < \epsilon(<<1)$. But each LOBD has a different range, e.g. $\epsilon_{coh} \neq \epsilon_{inc} \neq \epsilon_{comp}$; in fact, $\epsilon_{comp} \geq \epsilon_{coh} \geq \epsilon_{inc}$, since $LOBD_{comp}(\bar{\theta}\geq 0)$ is never worse than $LOBD_{coh}$, which in turn is never inferior to $LOBD_{inc}$, for the same common channel conditions, provided the input signal level ($\sim a_o^2$) is not too great (i.e. the "small-signal" conditions). For very small signals we may expect that $LOBD_{comb} \to (LOBD)_{coh}$, $(\bar{\theta}>0)$, since the incoherent component $(0<\theta^2<<\bar{\theta})$ is now negligible vis-à-vis the coherent contribution. On the other hand, if $\bar{\theta}=0$, $\therefore (LOBD)_{coh}=0$, and $LOBD_{comp}=(LOBD)_{inc}$, with the range ϵ_{inc}.

Finally, the composite LOBD is generally recommended, provided the complexity of the processing occasioned by the additional algorithmic component ($LOBD_{inc}$, or $LOBD_{coh}$) can be tolerated practically. Otherwise, in the coherent cases we omit the $(LOBD)_{inc}$-component; hence the considerable attention to the coherent algorithm ($\bar{\theta}>0$) now and previously. [It is, of course, analytically much simpler than $(LOBD)_{inc}$, which can be an additional reason to focus on $(LOBD)_{coh}$ when $\bar{\theta}>0$.] As noted in Sec. A.3-(I,II), a rare special situation arises in the gaussian case for the completely known signals: the

composite LOBD is replaced by the exact, $(\text{LOBD})_{coh}$ form. When the noise is non-gaussian, we proceed as above.

III. Composite Threshold Detectors: Minimum Detectable Signals:

We conclude Sec. 6.5 with a derivation of the minimum detectable signal for these optimum composite threshold cases. Combining (6.9) and (6.22b), for example, remembering from (6.79c) that $\sigma^{*2}_{\text{on-comp}} = \sigma^{*2}_{\text{on-coh}} + \sigma^{*2}_{\text{on-inc}}$, we can define at once (in these "on-off" cases with stationary noise) $\left\langle a_o^2 \right\rangle^*_{\text{min-comp}}$ by

$$\sigma^{*2}_{\text{on-comp}} \equiv 2 \left\langle a_o^2 \right\rangle^*_{\text{min-comp}} \hat{a}_{coh} \Pi^*_{coh} + 2 \left\langle a_o^2 \right\rangle^*_{\text{min-comp}} \hat{a}^2_{inc} \Pi^*_{inc} \tag{6.84}$$

From (6.2) or (6.4) we get directly

$$\frac{\sigma^*_{\text{on-comp}}}{\sqrt{2}} = 2\Theta^{-1}(1-2P^*_e) \text{ , or } \{\Theta^{-1}(2p^*_D-1)+\Theta^{-1}(1-2\alpha^*_F)\} \equiv C_{I.O.} \text{ or } C_{N.P.}, \tag{6.85}$$

$$\equiv \sqrt{B^*_{I.O.}} \qquad\qquad \equiv \sqrt{B^*_{N.P.}}$$

respectively for the Ideal Observer or the Neyman-Pearson Observer, cf. (6.11b). Applying (6.85) to (6.84), we obtain the desired expression for the minimum detectable signal associated with this "on-off" composite detector, viz.

$$\left\langle a_o^2 \right\rangle^*_{\text{min-comp}} = \frac{1}{2} \frac{\hat{a}_{coh} \Pi^*_{coh}}{\hat{a}^2_{inc} \Pi^*_{inc}} \left\{ \sqrt{1+4B^* \frac{\hat{a}^2_{inc} \Pi^*_{inc}}{\hat{a}_{coh} \Pi^*_{coh}}} - 1 \right\}, \tag{6.86}$$

$$B^* = C^2_{I.O.} \text{ or } C^2_{N.P.} ,$$

or, using (6.10), (6.24), with (6.49)', we get explicitly in these stationary cases

$$\left\langle a_o^2\right\rangle^*_{\text{min-comp}} = \frac{4L^{(2)}(1-\eta)}{L^{(4)}+2L^{(2)^2}(Q_n-1)} \left\{\sqrt{1+\frac{B^*\{L^{(4)}+2L^{(2)^2}(Q_n-1)\}}{2nL^{(2)^2}}} - 1\right\} . \quad (6.86a)$$

For example, in the case of signals with incoherent structure, $Q_n=1$, and $\therefore\ \Pi^*_{coh}\to 0$:

$$\therefore\ \left\langle a_o^2\right\rangle^*_{\text{min-comp}} = \sqrt{\frac{B^*}{\Pi^*_{inc}}} = \left\langle a_o^2\right\rangle^*_{\text{min-inc}} \quad (6.87a)$$

$$= \sqrt{B}\,\frac{4}{\sqrt{2L^{(4)}_n}} \quad . \quad (6.87b)$$

Similarly, for signals with coherent structures, e.g., sinusoidal pulse trains where $Q_n \doteq n/2$, or $\doteq n(1-\eta)^2/2$, cf. (A.2-42e), for slow or rapid fading respectively and large sample ($n>>1$), we get from (6.86a)

Coh. struct.:

$$\therefore\ \left\langle a_o^2\right\rangle^*_{\substack{\text{min-comp}\\ \text{slow}}} \cong \frac{4(1-\eta)}{nL^{(2)}}\left\{\sqrt{1+B^*/2(1-\eta)^2} - 1\right\} \quad (6.88a)$$

$$\cong \frac{4}{nL^{(2)}}\left\{\sqrt{\frac{B^*}{2}} - (1-\eta)\right\} \quad ;\ B^*>>2(1-\eta)^2 ,$$

$$\left\langle a_o^2\right\rangle^*_{\substack{\text{min-comp}\\ \text{rapid}}} \cong \frac{4}{nL^{(2)}(1-\eta)}\{\sqrt{1+B^*/2} - 1\} \cong \frac{4}{nL^{(2)}(1-\eta)}\left(\sqrt{\frac{B^*}{2}} - 1\right), \quad (6.88b)$$

$$B^*>>2 .$$

Note the expected relations $\left\langle a_o^2\right\rangle^*_{\text{min-comp}\,|\,\text{incoh.struct}} \sim 1/\sqrt{n}$, while $\left\langle a_o^2\right\rangle^*_{\text{min-comp coh.struct.}} \sim 1/n$ cf. remarks in Sec. 6.2, V, (iii), (iv).

The above relation (6.86) also applies for minimum detectable signals in the binary signal cases when $a_o^{(1)} = a_o^{(2)} = a_o$, and no or slow fading with suitable adjustments for $\Pi^*_{coh} \to \Pi^{(21)*}_{coh}$, etc., cf. Table 6.1b. We have explicitly

Binary "Symmetrical" Signals:

$$\langle a_o^2 \rangle^{(21)*}_{min\text{-}comp} = \frac{2(1-\eta)}{L^{(2)}[\hat{Q}_n^{(21)}-1]} \left\{ \sqrt{1+\frac{4B^*(\hat{Q}_n^{(21)}-1)}{n}} - 1 \right\} \tag{6.89}$$

with reductions similar to (6.87b), (6.88), depending on $\hat{Q}_n^{(21)}$, cf. (6.33a), (A.6-5c).

Finally, we observe in these optimum threshold cases that the only condition on the AO character of these LOBD's is the equal-variance condition: $x_{max} << x_o^*$; $y^*_{max} << y_o^*$, cf. Fig. 6.1 and Sec. 6.4. Usually, $y_{max} << y_o^*$ is the stricter constraint; i.e., $y_o^* < x_o^*$. (This observation is also consistent with our discussion of III, Sec. 6.4.)

A. Remarks on Suboptimum Composite Threshold Detectors:

This situation is more complex than in the optimum cases above. To obtain the minimum detectable signal when the composite threshold detection is not optimum, we start with (6.83a), to write

$$\sigma^2_{o\text{-}comp}/2 = \frac{[(A.4\text{-}12a)numerator+(A.4\text{-}31a)numerator]^2}{2[(A.4\text{-}9)+(A.4\text{-}29)]^2 \equiv (2\hat{\sigma}^2_{o\text{-}comp})} \tag{6.90}$$

$$= \frac{\langle g_{comp} \rangle_1 - \langle g_{comp} \rangle_2}{2\hat{\sigma}^2_{o\text{-}comp}} ,$$

which defines $\sigma^2_{o\text{-}comp}$. Specifically, for the stationary cases we have

$$\sigma_{o\text{-comp}}/\sqrt{2} = \frac{L^{(2)}_{F:E} \sum_i \langle \Theta_i \rangle^2 + \frac{1}{4} \sum_{ij} \langle \Theta_i \Theta_j \rangle^2 \left[\left(\hat{L}^{(4)} - 2L^{(2)^2} \right) \delta_{ij} + 2L^{(2)^2} \right]_{F:E}}{\sqrt{2} \left\{ \hat{L}^{(2)}_{F:E} \sum_i \langle \Theta_i \rangle^2 + \frac{1}{4} \sum_{ij} \langle \Theta_i \Theta_j \rangle^2 \left[\left(L^{(4)} - 2\hat{L}^{(2)^2} \right) \delta_{ij} + 2\hat{L}^{(2)^2} \right]_{F:E} \right\}}, \quad (6.91)$$

where $\sigma_{o\text{-comp}}/\sqrt{2}$ is used in (6.2) or (6.5) to obtain performance for these suboptimum composite cases. [See Sec. C of Appendix A.4-1 for the $L_{F:E}$'s.]

Now, since $\langle \Theta_i \rangle = \bar{a}_o \sqrt{2}$, $\langle \Theta_i \Theta_j \rangle = \overline{a_o^2} m_{ij} \rho_{ij}$, here, Eq. (6.91) can be written

$$\frac{\sigma_{o\text{-comp}}}{\sqrt{2}} = \frac{\overline{a_o^2} A_1 + \overline{a_o^2}^2 A_2}{\sqrt{2} \left(\overline{a_o^2} B_1 + \overline{a_o^2}^2 B_2 \right)^{1/2}} = \sqrt{B^*} \quad , \quad \text{cf. (6.11, 6.11a,b).} \quad (6.92)$$

To obtain the associated minimum detectable signal $\langle a_o^2 \rangle_{\text{min-comp}}$ $(= \overline{a_o^2})$ we must solve (6.92) for $z = \overline{a_o^2}$, e. g.

$$\boxed{z^3 A_2^2 + 2A_1 A_2 z^2 + (A_1^2 - B_1 B_2) z - B^* B_1 = 0} \quad , \quad (6.93)$$

which we leave to a subsequent study. The associated processing gain here is now defined by

$$\Pi_{\text{comp}} \equiv B^* / \langle a_o^2 \rangle^2_{\text{min-comp}} \quad ,$$

since (6.94)

$$\sigma^2_{o\text{-comp}} \equiv 2 \langle a_o^2 \rangle^2_{\text{min-comp}} \Pi_{\text{comp}} \quad .$$

7. QUANTITATIVE EXAMPLES: DETECTOR PERFORMANCE

In this Section we examine some specific examples, to illustrate the general results of the preceeding sections, in particular, Section 6. Our general aim is to provide a reasonable catalogue of common signal types, channel conditions, reception modes, and noise models from which to select representative applications.

We begin with a (partial) summary of the results of Sec. 5.3 preceding:

7.1 Statistical-Physical Components of the Receiver Algorithms:

Both to implement the various optimum and suboptimum detection algorithms and to evaluate and compare their performance, we need the structural elements of signal and noise which determine how the received data are to be processed and how these various receivers perform. Accordingly, we note the following typical relations:

I. Common Signal Types

(i). "On-off": $s_i^{(2)}=\sqrt{2}\cos(\omega_o t_i-\phi_o)=\sqrt{2}\cos\omega_o t_i$ (7.1)

$s_i^{(1)}=0$

(ii). Orthogonal: $s_i^{(2)} = \sqrt{2}\cos\omega_o t_i$; (7.2)

$s_i^{(1)}=\sqrt{2}\sin\omega_o t_i \ (=\sqrt{2}\cos(\omega_o t_i-\pi/2))$

(iii). Antipodal: $s_i^{(2)}= -s_i^{(1)}(=-\sqrt{2}\cos\omega_o t_i)$. (7.3)

} for coherent reception

For incoherent reception we cannot use these RF phase distinctions, and most simply we change the frequency:

$$s_i^{(1)} = \sqrt{2}\cos\omega_{o1}t_i \ ; \ s_i^{(2)} = \sqrt{2}\cos\omega_{o2}t_i \quad . \tag{7.3a}$$

II. Common Channel Conditions:

(1). Fading :

(i). no fading:

$$m_{ij}\,\overline{a_o^2} = a_o^2 = G_o^2/\bar{I}_N\lambda^{2\gamma}\ ;\ (m_{ij}=1) \tag{7.4a}$$

(ii). slow fading (one-sided):

$$m_{ij}\,\overline{a_o^2} = \overline{a_o^2} = \overline{a^2}\langle G_o^2\rangle/\bar{I}_N\lambda^{2\gamma};\ (m_{ij}=1)\ ; \tag{7.4b}$$

(iii). rapid fading (one-sided):

$$m_{ij}\overline{a_o^2} = \overline{a_o^2}[\delta_{ij}+[\bar{a}_o^2/\overline{a_o^2})(1-\delta_{ij})]\ , \tag{7.4c}$$

$$= [\overline{a^2}\ \delta_{ij}+\bar{a}^2(1-\delta_{ij})]\langle G_o^2\rangle/\bar{I}_N\lambda^{2\gamma}\ ; \tag{7.4d}$$

(iv). rapid fading (two-sided):

$$m_{ij}\overline{a_o^2} = \overline{a_o^2}\delta_{ij} = \overline{a^2}\langle G_o^2\rangle/\bar{I}_N\lambda^{2\gamma}\ \ ;\ \bar{a}_o = 0, \tag{7.4e}$$

cf. (5.8), (5.8a), and where the fading effects are represented by the statistics of $\underline{a}$ [cf. (3.3) for rayleigh fading]; $\bar{I}_N$ is the mean intensity of the accompanying noise (cf. Sec. 3.2). Fading is usually the result of unresolvable multipath effects. [For random signal source locations we replace $\lambda^{-2\gamma}$ by $\langle\lambda^{-2\gamma}\rangle$ in (7.4), cf. (3.4),(3.5).]

(2). Doppler:

$$s_i = \sqrt{2}\cos[(\omega_o+\omega_d)t_i-\phi_o]\ ; \tag{7.5a}$$

$$\therefore\ \overline{s_i} = \sqrt{2}\,e^{-(\Delta\omega_d t_i)^2/2}\cos(\omega_o t_i-\phi_o)\ ;\ \Delta\omega_d=\omega_o\Delta v/c_o\ , \tag{7.5b}$$

$$\rho_{ij} = \overline{s_i s_j} = e^{-[\Delta\omega_d(t_i-t_j)]^2/2}\cos\,\omega_o(t_i-t_j),\ \text{cf.(5.13)}, \tag{7.5c}$$

these last two relations on the assumption that the doppler shift (ω_d) is governed by a gaussian process, cf. Sec. 5.3, Eqs. (5.12) et seq. Without doppler, (7.5) reduce directly to simpler forms, where $\omega_d=0$; $\Delta\omega_d=0$.

(3). Propagation Law (γ):

This will depend on the mean propagation conditions, including the relevant geometry. For instance, simple spherical spreading is represented by $\gamma=1$, while cylindrical spreading (associated with "wave-guide" modes of propagation) is usually $\gamma= 1/2$. Resolvable multipath effects give $\gamma>1$: $\gamma=2$ is typical of rough terrain, cities, etc.; for very rough terrain with multiple reflections, $\gamma>2$. [See Sections 3.1-3.3 above.]

III. Common Modes of Reception:

We distinguish: (i), coherent; (ii), incoherent; and (iii), "mixed" or "composite". "Coherent" reception here implies complete knowledge of the signal epoch (ϵ) [or phase ($\omega_0\epsilon_0$) in the narrow-band cases] at the receiver, and is usually achieved after the desired signal has been originally detected, and "lock-on" in phase has been accomplished. Initial signal detection, of course, is done incoherently, where the ignorance of signal epoch or phase is such that $\langle s \rangle_\epsilon = 0$, with $\rho_{ij} \neq 0$ generally. The composite mode of reception combines both coherent and incoherent processing whenever $\bar{s} \neq 0$, i.e., whenever there is enough phase coherence to provide a non-vanishing mean signal. This occurs both at the intermediate stages of detection and after the coherent mode has been established by successful "lock-on". If one is willing to support the added complexity of the incoherent processing after coherency has been achieved, then "composite" processing (of the kind discussed in Sec. 6.5) provides improved performance over purely coherent (or incoherent) detection alone, cf. the examples (Sec. 7.5) below. Various schema of signal processing are shown in Sec. 5 earlier.

IV. Common Noise Models:

The principle noise or interference models of practical importance are the Class A and B noise models, described in some detail in Sec. 3.3 preceding. The former is "coherent", i.e., produces negligible transients

in the receiver, while the latter is "impulsive", generating essentially nothing but overlapping transient responses. Included with both these primary nongaussian noise mechanisms is an additive gaussian component, partially internal and partially external. The gauss noise model is itself a limiting case of either the Class A or B sources, when the number of independently emitting sources becomes large, or when no individual source stands out above the general gaussian background. It is the Class A and B models which most effectively represent real-world EMI environments and which we consider here specifically below in the application of our general threshold theory to typical EMI examples, both for detector design, i.e. specification of the optimum threshold algorithms, and for the evaluation of performance, including that of suboptimum systems like the simple- and clipper-correlators of conventional practice.

In a compact way, we can summarize typical <u>received</u> narrow-band signal waveforms in common use by the normalized expression

$$s_i^{(\ )} = \sqrt{2}\, a_d(t_i)\cos[(\omega_{o(\ )}+\omega_d)t_i-\phi_o],\ (\ ) \equiv (1),(2), \tag{7.6}$$

where

$$\begin{cases} \phi_o=0\ (\text{"on-off"}) \text{ and } s_i^{(1)}=0;\ =\pi/2\ (\text{"orthogonal"});\ =\pi(\text{"antipodal"}), \\ \qquad \text{cf. Eqs. (7.1)-(7.3), in the coherent cases when } \bar{s}_i\neq 0, \text{ only.} \qquad (7.6a) \\ a_d(t_i) = 1\ [\text{no doppler spread}),\ \omega_d=0 \text{ or } \omega_d\neq 0.] \\ \qquad = e^{-(t_i\Delta\omega_d)^2/2} \quad (\text{gauss doppler spread},\ \bar{\omega}_d=0). \qquad (7.6b) \end{cases}$$

The effects of fading (cf. B above) are embodied in the first and second order amplitude statistics $\bar{a}_o$, $\overline{a_o^2}$, viz., $\overline{a_o^2}m_{ij}^{(\ )}$, where $m_{ij}^{(\ )} \equiv \langle a_{oi}^{(\ )}a_{oj}^{(\ )}\rangle/\overline{a_o^2}^{(\ )}$. In all the binary signal cases henceforth we shall employ the same signal levels, so that $a_o^{(2)} = a_o^{(1)} = a_o$, [but $s^{(2)} \neq s^{(1)}$, of course]. Thus, from (7.4) we have

$$\left.\begin{aligned} m_{ij} &= 1\text{: (no fading, slow, one-sided fading)} ; \\ m_{ij} &= \delta_{ij}+(\bar{a}_o^2/\overline{a_o^2})(1-\delta_{ij})\text{: (rapid fading)}; \\ m_{ij} &= \delta_{ij}\text{: (rapid, two-sided fading)}. \end{aligned}\right\} \tag{7.7}$$

Also, for the signal correlation function $\rho_{ij}^{(\ )}$ we have various possibilities:

$$\left.\begin{aligned} \rho_{ij}^{(\ )} &= \bar{s}_i^{(\ )}\bar{s}_j^{(\ )}\text{: (coherent reception, no doppler, } a_d=1, \omega_d=0); \\ &= \cos \omega_{o(\ )}(t_i-t_j)\text{: (incoherent reception, no doppler)}; \\ &= \exp\{-[\Delta\omega_d\ (t_i-t_j)]^2/2\} \cos \omega_o(t_i-t_j): \\ &\quad \text{(doppler spread, coherent or incoherent reception; } \bar{\omega}_d=0) \end{aligned}\right\} \tag{7.8}$$

Various combinations of (7.6)-(7.8) provide a wide range of typical received signal structures, to be used in obtaining both the algorithmic structure (Secs. 4, 5) and performance results (Sec. 6) when specific numerical results are desired.

7.2 Optimum Structures:

These are described in canonical form in Sections 4, 5. Using A.- D. above in these structural forms, along with $\ell(x_i|A)$, $\{x_i\}$, gives the desired algorithm when combined with a suitable threshold. Thus, ℓ_i exhibits the basic input-output relation for the sampled data $\{x_i\}$.

For Class A interference we have directly

$$\ell(x_i|A) \equiv \frac{d}{dx} \log w_1(x)_{A+G}\Big|_{x=x_i}, \tag{7.9}$$

where $w_1(x)_{A+G}$ is given by (3.13) or (3.14).

Class B interference requires some adjustments, to account for the fact that the parameter Ω_B, cf. (3.15), normalizes the data to the measured value of the (total) intensity, rather than to the calculated value $(\Omega_{2B}+\sigma_G^2)$, which is not obtainable in finite magnitude from the approximation $w_1(x)_{B+G}$, (3.15). Thus writing

$$\hat{x} \equiv x/\sqrt{\Omega_B} = X/\sqrt{(\Omega_{2B}+\sigma_G^2)} \cdot \sqrt{\Omega_B} \ , \tag{7.10}$$

we have $\hat{x}$ now the normalized data (X) with respect to the measured intensity. The pdf (3.15) becomes

$$w_1(\hat{x})_{B+G} \cong \frac{e^{-\hat{x}^2}}{\pi} \sum_{n=0}^{\infty} \frac{(-1)^n}{n!} \hat{A}_\alpha^n \Gamma(\tfrac{n\alpha+1}{2}) {}_1F_1(-\tfrac{n\alpha}{2}; 1/2; \hat{x}^2) \tag{7.11a}$$

$$\cong \frac{1}{\pi} \sum_{n=0}^{\infty} \frac{(-1)^n}{n!} \hat{A}_\alpha^n \Gamma(\tfrac{n\alpha+1}{2}) {}_1F_1(\tfrac{1+n\alpha}{2}; 1/2; -\hat{x}^2) \ . \tag{7.11b}$$

The (macro-) parameters here are $\hat{A}_\alpha \sim A_B^{1-\alpha/2}$, cf. (3.16b), and $\alpha(=\frac{2-\mu}{\gamma})$, cf. (3.14c), where (μ,γ) are parameters associated with the EMI scenario, cf. (3.6). The basic input-output relation ℓ_i is now

$$\ell(x_i|B) \equiv \frac{d}{dx} \log w_1(x)_{B+G}\Big|_{x=x_i} \tag{7.12}$$

for these Class B cases.

Figures 7.1 and 7.2 show $\ell(x_i|A)$, $\ell(x_i|B)$ for typical parameter values: $\mathcal{P}_{2A}(A_A, \Gamma_A')$, $\mathcal{P}_{2B}(\hat{A}_\alpha, \alpha)$; see Sec. 7.5 for some further comments.

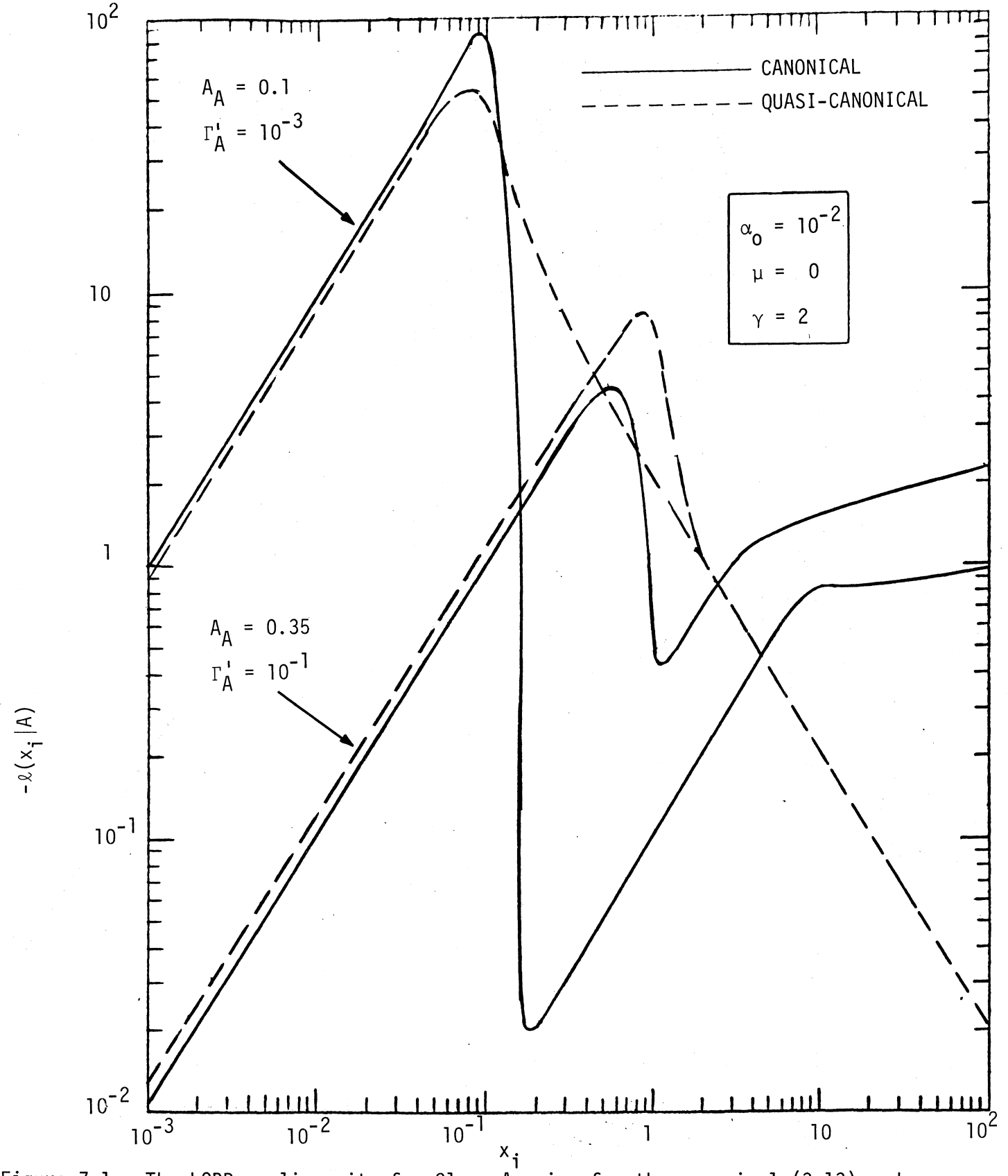

Figure 7.1. The LOBD nonlinearity for Class A noise for the canonical (3.13) and quasi-canonical (3.14) models.

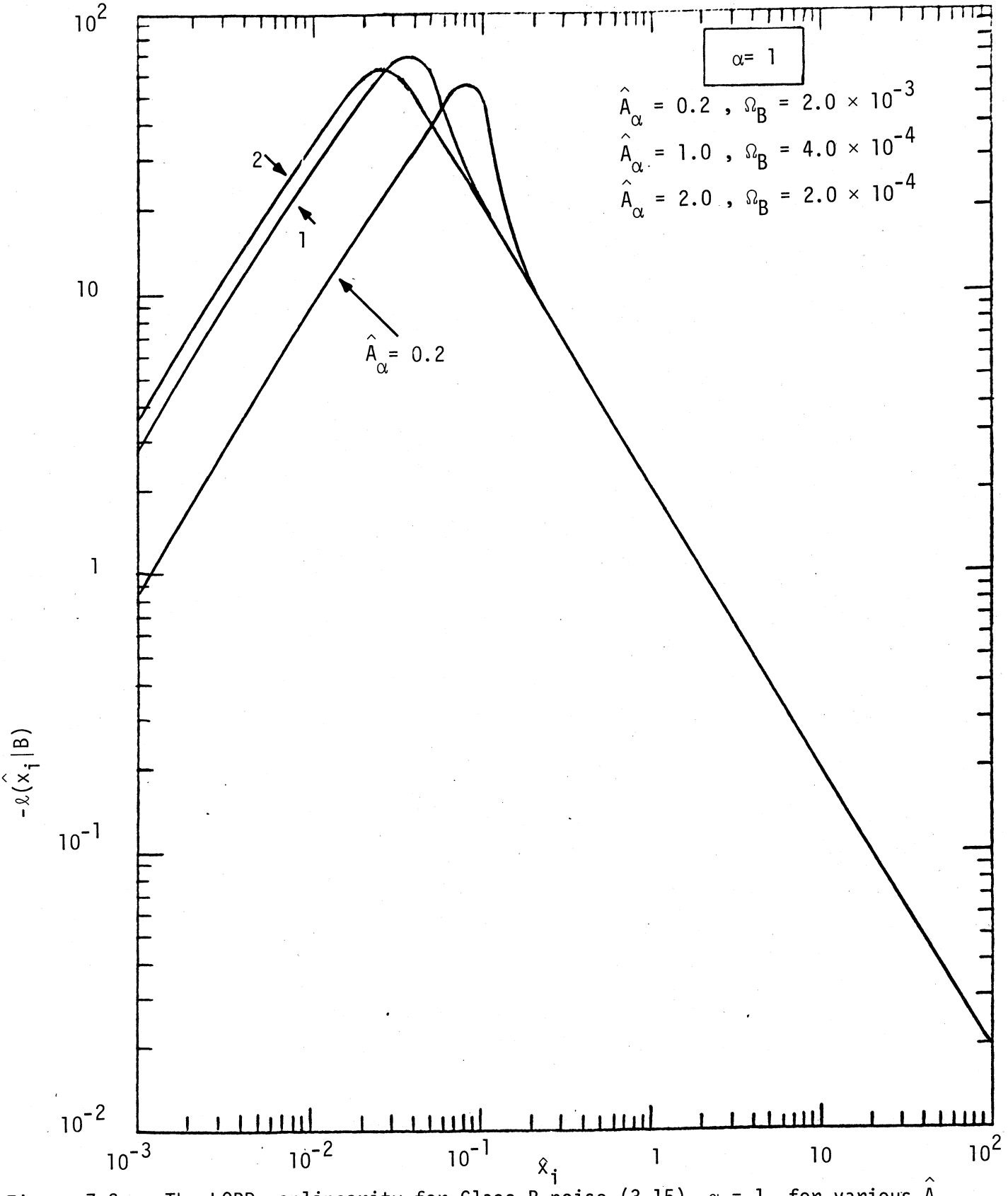

Figure 7.2a. The LOBD nonlinearity for Class B noise (3.15), $\alpha = 1$, for various $\hat{A}_\alpha$.

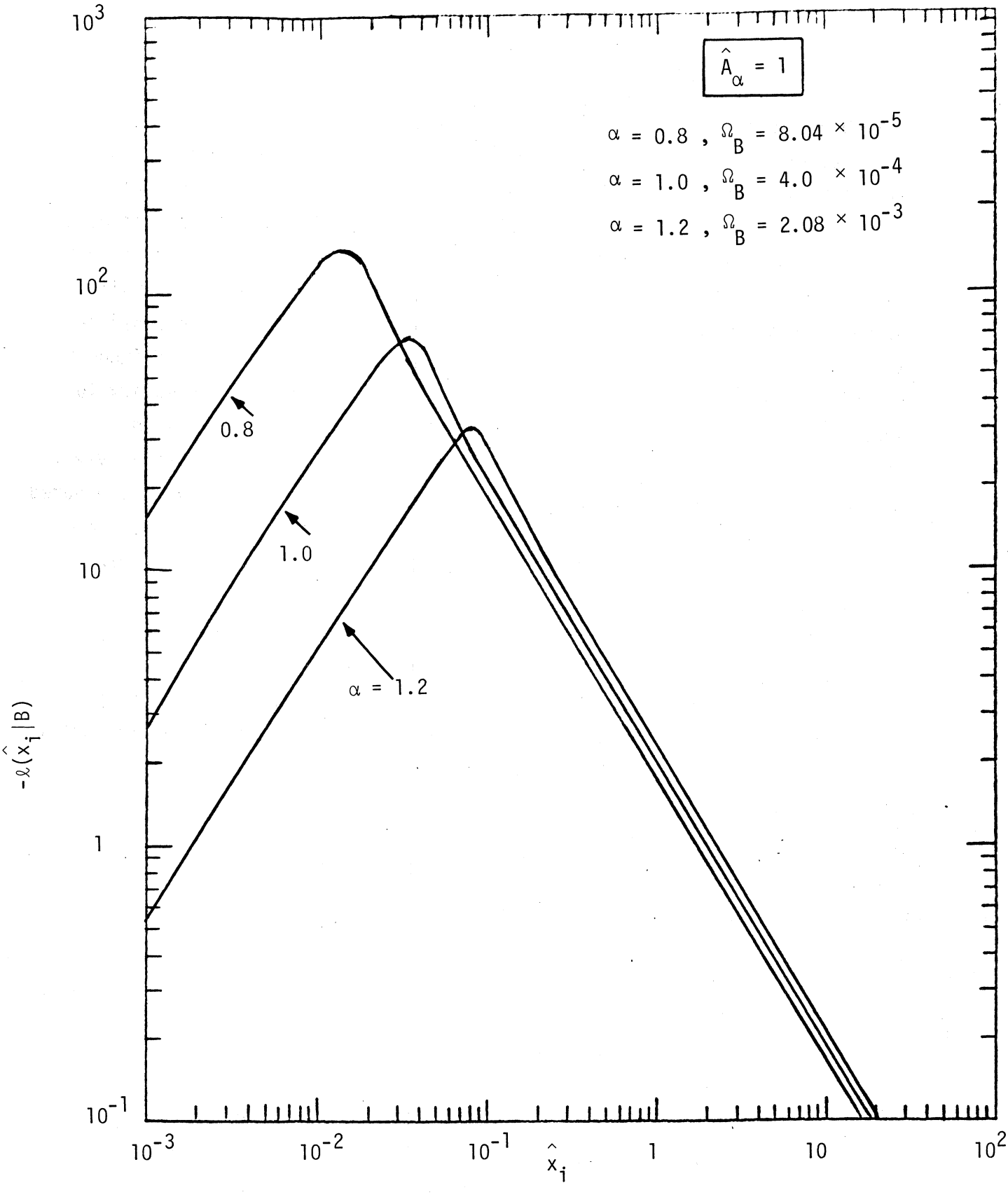

Figure 7.2b. The LOBD nonlinearity for Class B noise (3.15), $\hat{A}_\alpha = 1.0$, for various α.

7.3 Optimum Threshold Detectors: Performance Elements:

Rather than attempting an exhaustive (and expensive) enumeration of all combinations of typical signal, noise, and observational procedures (reviewed in Sec. 7.1 above), we shall adopt the following general approach to obtaining specific numerical results: We shall calculate various canonical relations and "basic ingredients" (e.g., $L^{(2)}$, $L^{(4)}$, etc.), including processing gains (per unit sample) and the appropriate (upper) "bounds" on the magnitude of the input signal associated with both coherent and incoherent detection, as well as such special relations as appear necessary to enhance the usefulness of these results. This procedure we repeat in Section 7.4 for the two classes of suboptimum receiver discussed here, viz., the simple correlator and the clipper-correlator. Thus Section 7.5 is devoted to selected numerical illustrations of performance, including detector comparisons, for typical EMI and signal situations, showing how one may use the canonical results and "basic ingredients" computed initially.

I. Various Useful Canonical Performance Relations:

Independent of the particular noise and signal structures are the probability measures of optimum threshold performance (in large sample régimes), given in Sec. 6.1. Accordingly, we have [cf. footnote, p. 55].

$$P_D^{(*)} \underset{\sim}{=} \frac{p}{2}\left\{1+\Theta\left[\frac{\sigma_{on}^{(*)}}{\sqrt{2}} - \Theta^{-1}(1-2\alpha_F^{(*)})\right]\right\} \quad ;$$

$$P_e^{(*)} \underset{\sim}{=} \frac{1}{2}\left\{1-\Theta\left[\frac{\sigma_{on}^{(*)}}{2\sqrt{2}}\right]\right\} \quad ; \ (\alpha=\mu=1) \qquad (7.13)$$

from (6.2), (6.5), (6.5e), where the quantity $\sigma_{on}^{(*)}$ $[=(\mathrm{var}_0 g_n^{(*)})^{1/2}]$ is determined in detail according to Sections 6.2-6.5, for both optimum and suboptimum detectors (* ≡ opt., (-) ≡ sub-opt.), and where the particular

signal and noise structures are specifically introduced. Examples of the latter calculations are given in Sec. 7.5 ff. Figures 7.3, 7.4 show typical curves for $(p_D^*/2)$ $(\equiv P_D^*/p)$ and $P_e^{(*)}$, respectively. Binary as well as the "on-off" signal cases are included. As expected, decreasing the false alarm probability $(\alpha_F^{(*)})$ increases the magnitude of $\sigma_{on}^{(*)}$ needed to obtain a given $P_D^{(*)}$.

Another set of canonical relations are the probability controls, $C_{N.P.}^{(*)}$, $C_{I.O.}^{(*)}$, cf. (6.11), (6.21a), (6.27) etc., which appear in the various expressions for the minimum detectable signals (Sec. 6.2 et seq.). These are

$$C_{N.P.}^{(*)} \equiv \Theta^{-1}(2p_D^{(*)}-1)+\Theta^{-1}(1-2\alpha_F^{(*)}) \; ; \; C_{I.O.}^{(*)} \equiv 2\Theta^{-1}(1-2P_e^*) \; , \tag{7.14}$$

respectively for the Neyman-Pearson and Ideal Observers. Figures 7.5, 7.6 illustrate these quantities.

II. "Basic Ingredients":

These are the various non-linear statistics of the accompanying (non-gaussian + gauss) noise, which are particular elements of the processing gains $(\Pi^{(*)})$, minimum detectable signals, $\sigma_{on}^{(*)}$, etc. and bounds on the acceptable size of the input signals $(a_o^2 << 1)$. From (A.2-42a) we have specifically

$$L^{(2)} \equiv \left\langle \left(\frac{w_1'}{w_1}\right)^2 \right\rangle_o = \left\langle \ell^2 \right\rangle_o = \int_{-\infty}^{\infty} \ell^2 w_1(x)dx \; (>0); \; \ell \equiv \frac{d}{dx} \log w_1(x), \text{ etc.}; \tag{7.15a}$$

$$L^{(4)} \equiv \left\langle \left(\frac{w_1''}{w_1}\right)^2 \right\rangle_o = \left\langle (\ell' + \ell^2)^2 \right\rangle_o = \int_{-\infty}^{\infty} (\ell' + \ell^2)^2 w_1(x)dx \; (>0), \tag{7.15b}$$

$$L^{(2,2)} \equiv 2\left\langle \left(\frac{w_1'}{w_1}\right)^4 \right\rangle_o = 2\left\langle \ell^4 \right\rangle_o = 2\int_{-\infty}^{\infty} \ell^4 w_1(x)dx \; (>0), \tag{7.15c}$$

$$L^{(6)} \equiv \left\langle \left(\frac{w_1''}{w_1}\right)^3 \right\rangle_o = \left\langle (\ell' + \ell^2)^3 \right\rangle_o = \int_{-\infty}^{\infty} (\ell' + \ell^2)^3 w_1(x)dx \; \left(\gtrless 0\right). \tag{7.15d}$$

All these quantities are positive, except the last, which for certain noise parameters can be zero or negative. These relations (7.15) hold for Class A, B noise, or for any noise, with pdf $w_{1:E}$, for that matter. Figures 7.7-7.10 show $L^{(2)},\ldots,L^{(6)}$, (7.15a-d), respectively (in db), for strictly and approximately canonical Class A noise,* cf. (3.13). Similarly, Figures 7.11-7.14 give $L^{(2)},\ldots,L^{(6)}$ for the Class B noise of (3.15), (7.11) above (in db) for various $\alpha[=(2-\mu)/\gamma]$, as a function of $\hat{A}_\alpha$.

In the Class A cases these "elements" all approach their gaussian limits as $A_A \to \infty$, viz:

$$\underline{\text{(gauss):}} \quad L^{(2)}=1 \; ; \; L^{(4)} = 2; \; L^{(2,2)} = 6 \; ; \; L^{(6)} = 8 \; , \text{ cf. (A.1-22a).} \qquad (7.16)$$

For the Class B noise, we have the results of Figures 7.11-7.14, for example. Of course, when A_B ($\sim \hat{A}_\alpha$, cf. (3.16c)) $\to \infty$, we have again gaussian noise, so that (7.16) applies here equally well in the limit. See Sec. 7.5 for further comments on Figs. 7.3-7.14.

---

* Preliminary calculations show that these results are not appreciably different when quasi-canonical Class A noise is used, with $\alpha_0^2 \ll 1$, cf. (3.14) et seq. A complete investigation of this phenomenon, however, remains to be carried out.

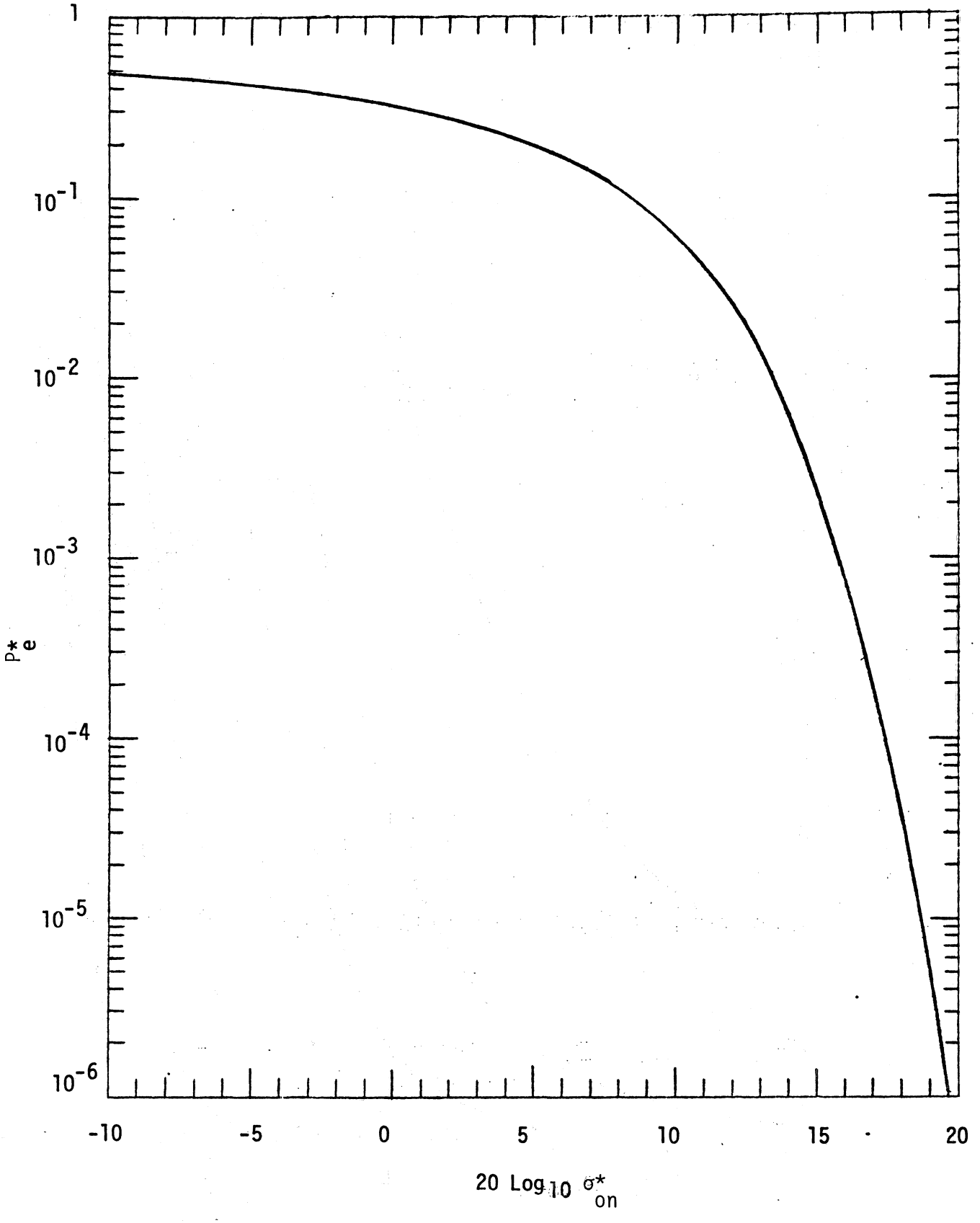

Figure 7.3. **Probability of binary error, P_e^*, as canonical function of the variance σ_{on}^{*2},** Eq. (7.13).

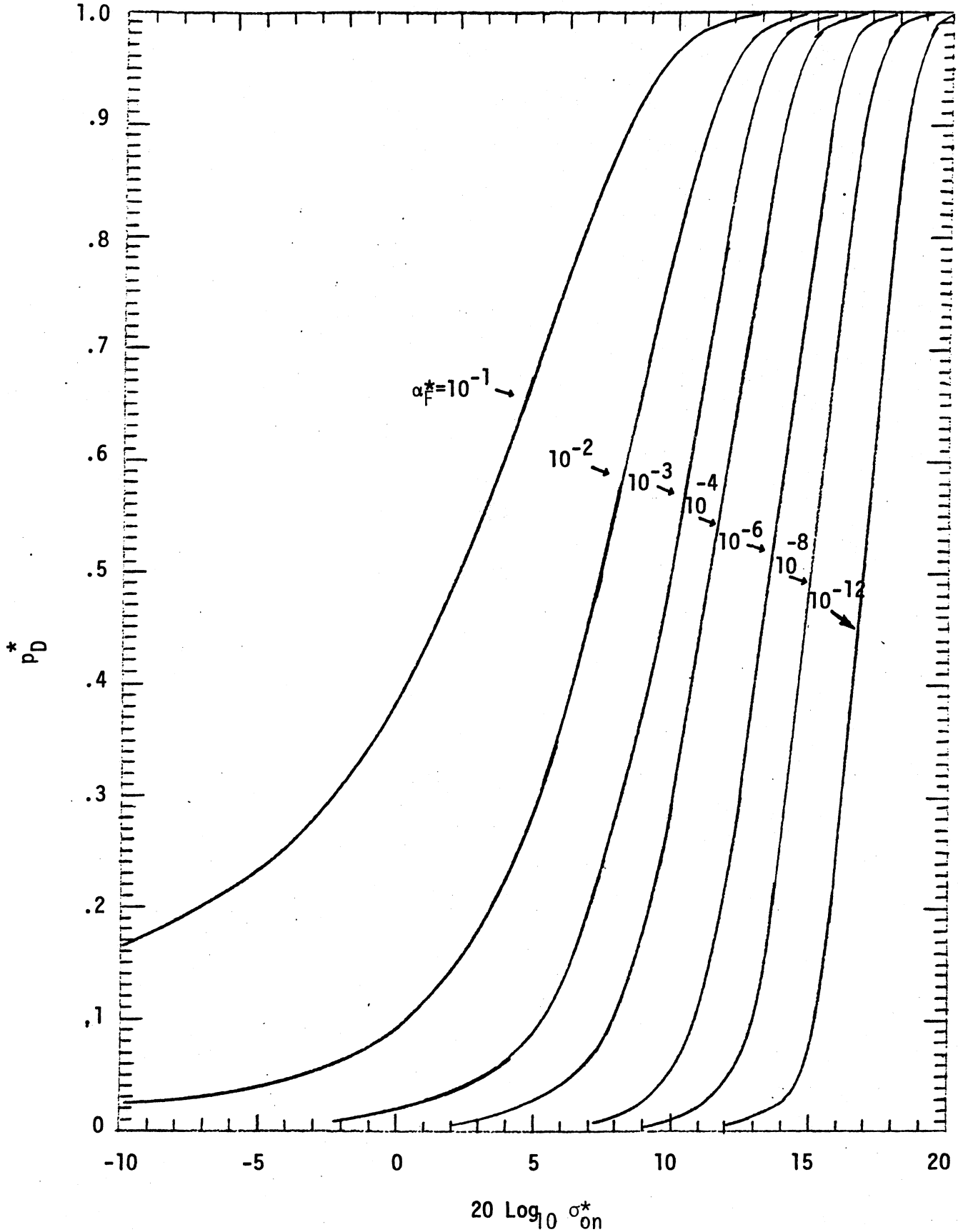

Figure 7.4. **Probability of detection, p_D^*, as canonical function of the variance σ_{on}^{*2},** Eq. (7.13).

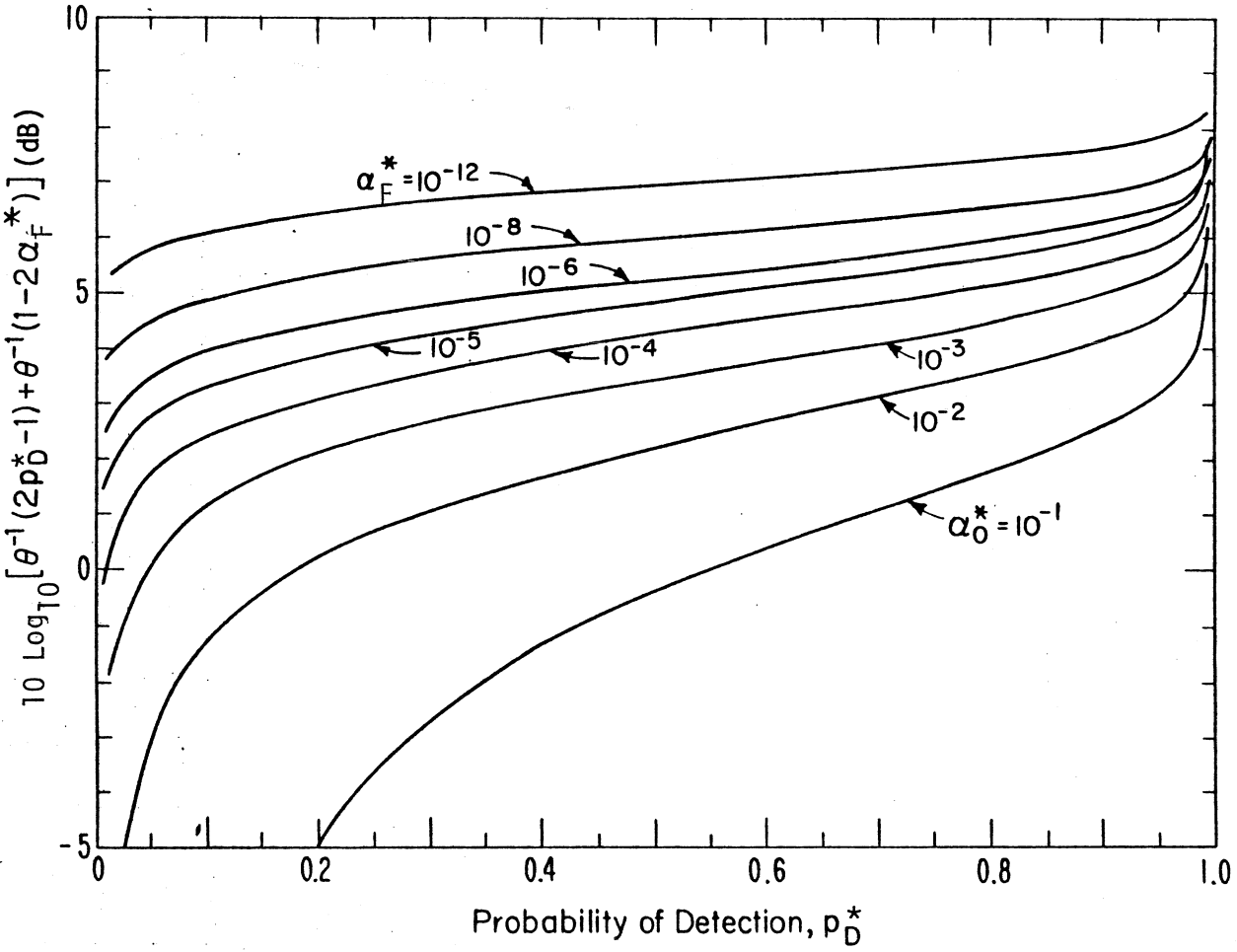

Figure 7.5. **Probabilistic controls on detection, C_{NP}^* vs p_D^* ($=P_{D/P}^*$) probabilities of false alarm, α_F^*, Eq. (7.14).**

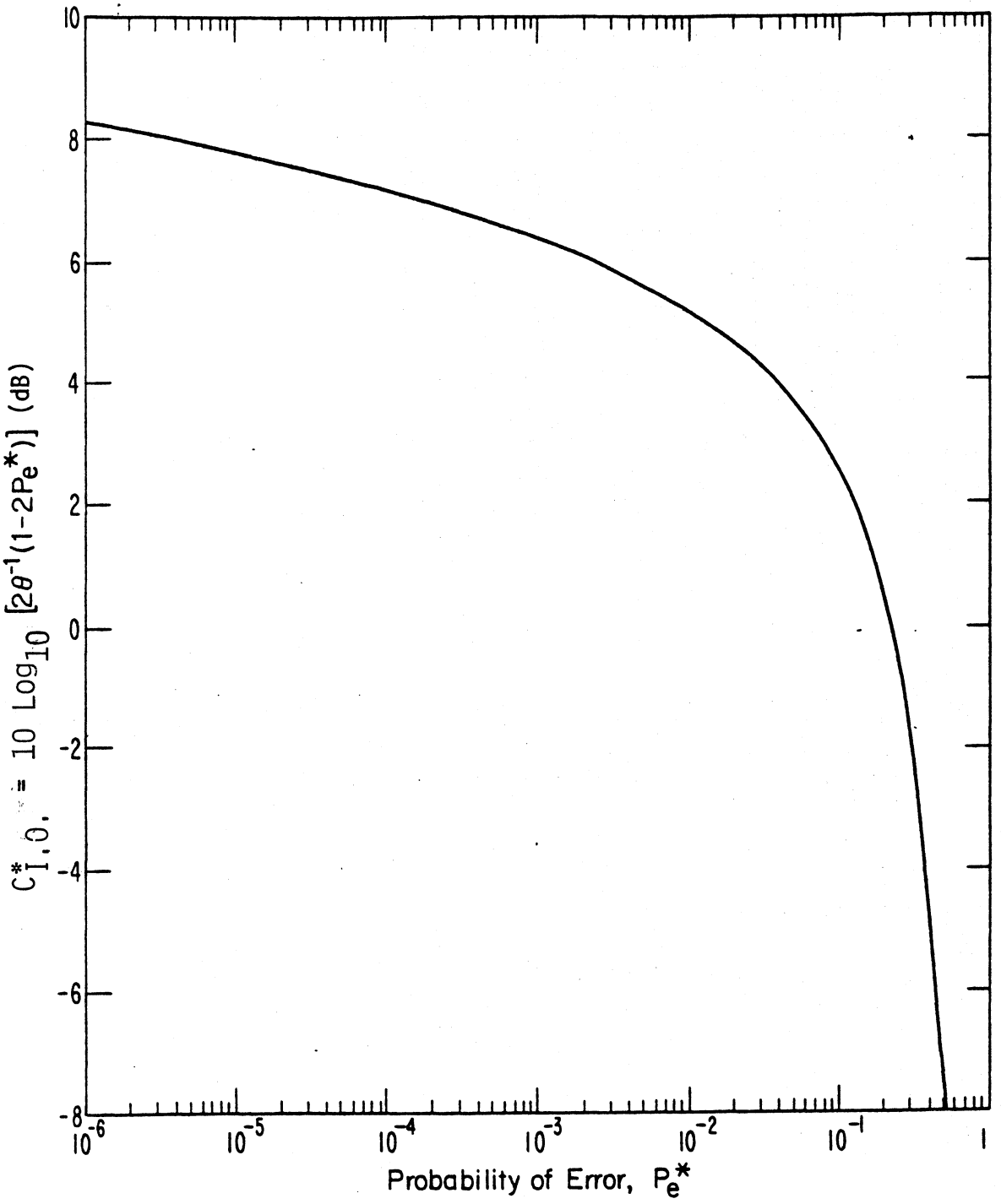

Figure 7.6. **Probabilistic controls on detection, $C^*_{I.O.}$ VS P^*_e, Eq. (7.14).**

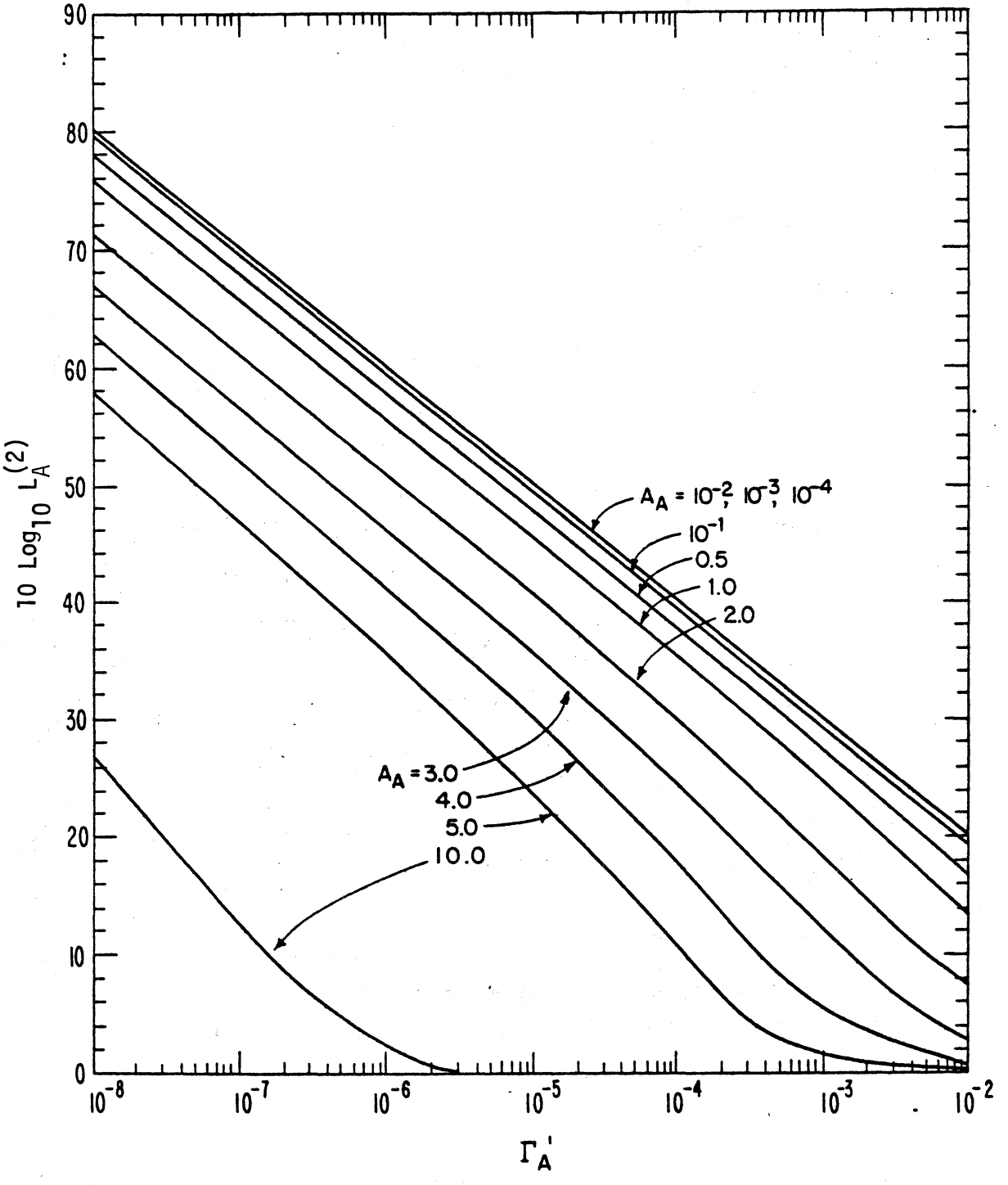

Figure 7.7. Processing gain (Π^*_{coh}/n) per sample, in dB, for optimum coherent threshold detection in Class A EMI, Eq. (7.15a).

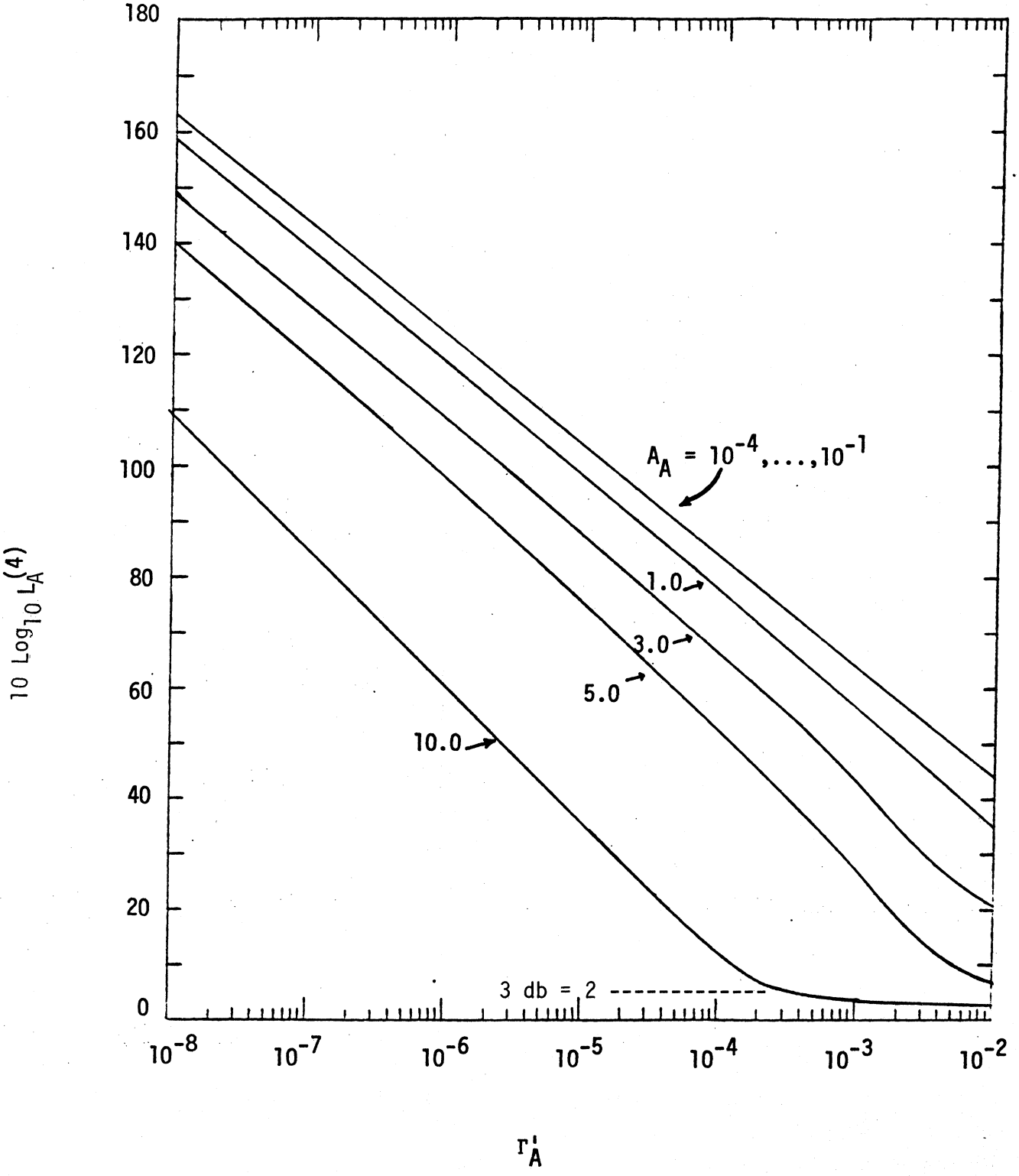

Figure 7.8. $L^{(4)}$ $(=\langle(\ell' + \ell^2)^2\rangle_0)$, in dB, for Class A EMI, Eq. (7.15b).

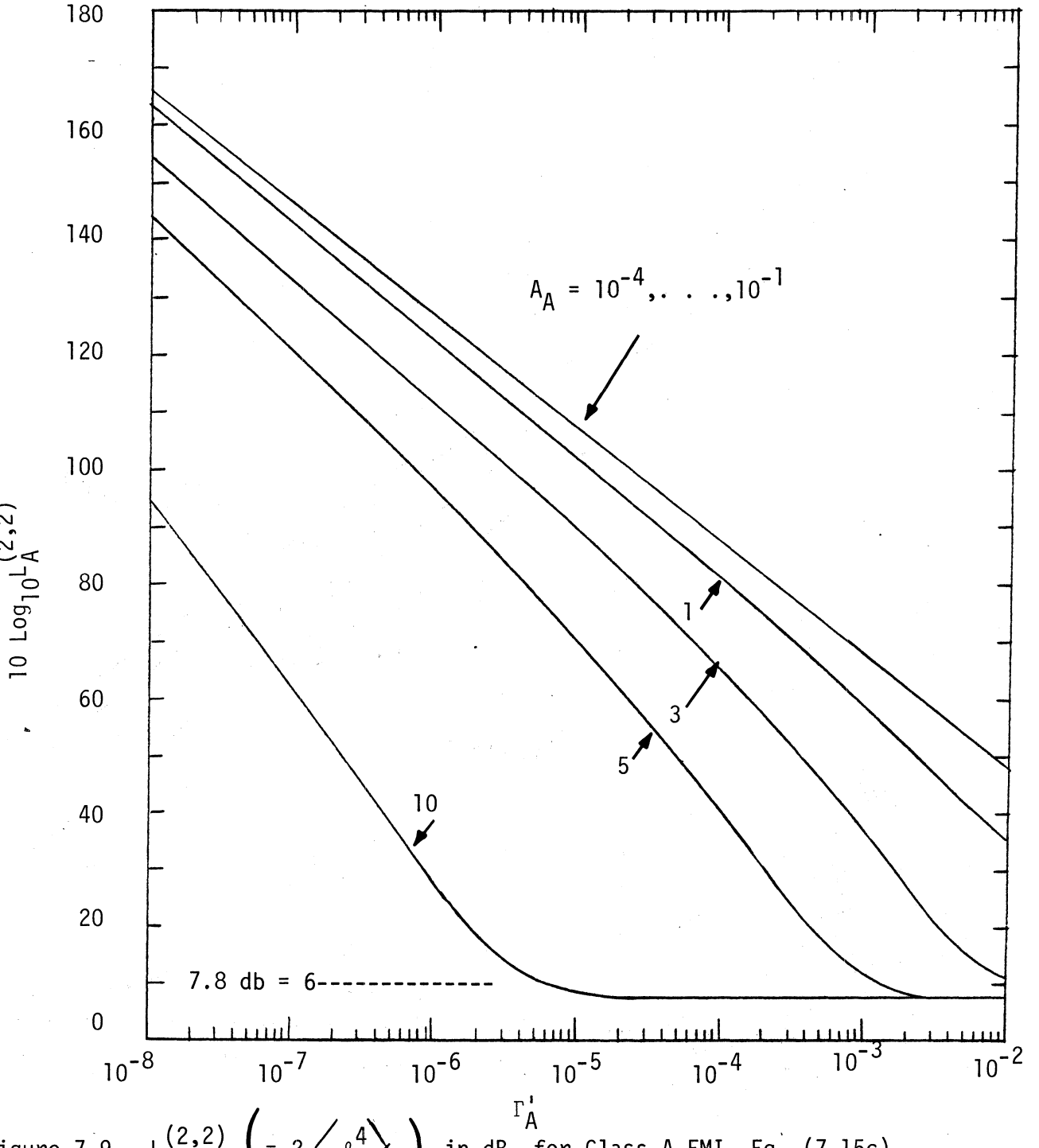

Figure 7.9. $L^{(2,2)}\left(=2\left\langle \ell^4\right\rangle_0\right)$ in dB, for Class A EMI, Eq. (7.15c).

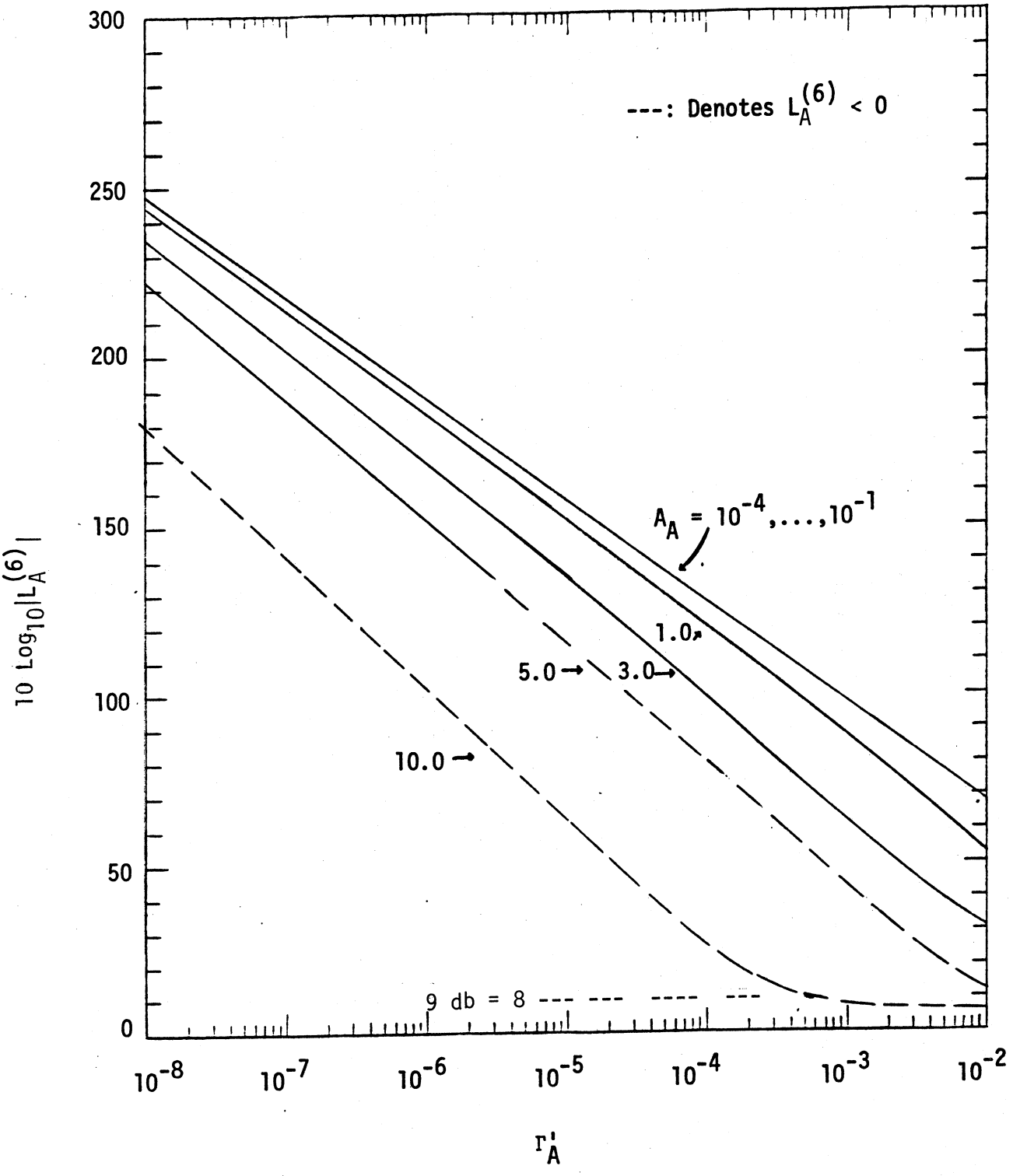

Figure 7.10. $L_A^{(6)}$ $(=\langle(\ell' + \ell^2)^3\rangle_o)$, magnitude in dB, for Class A EMI, Eq. (7.15d).

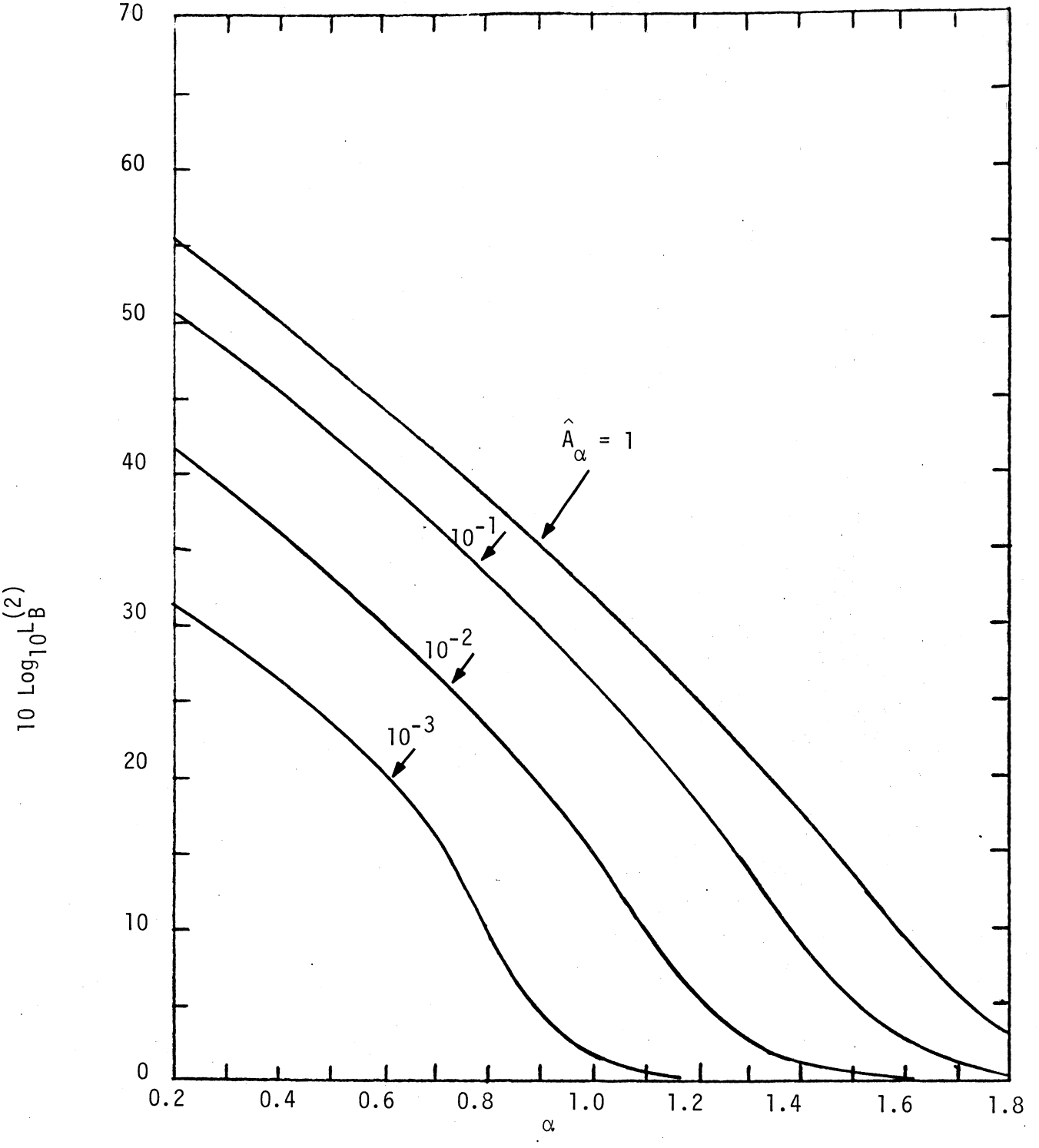

Figure 7.11. Processing gain (Π^*_{coh}/n) per sample, $L_B^{(2)}$, in dB, for optimum coherent threshold detection in Class B EMI, Eq. (7.15a).

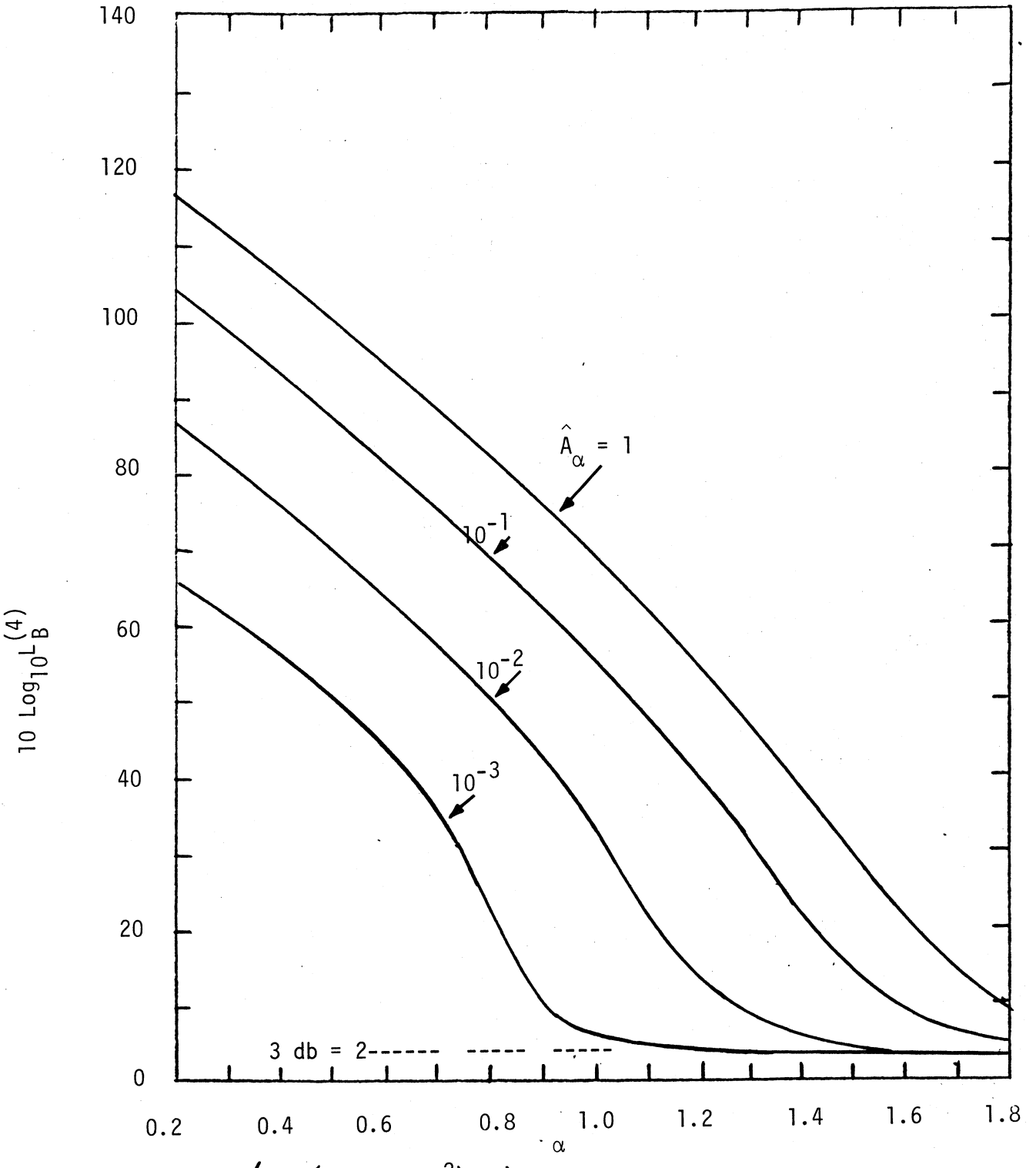

Figure 7.12. $L_B^{(4)}$ $\left(= \left\langle (\ell' + \ell^2)^2 \right\rangle_o \right)$, in dB, for Class B EMI, Eq. (7.15b).

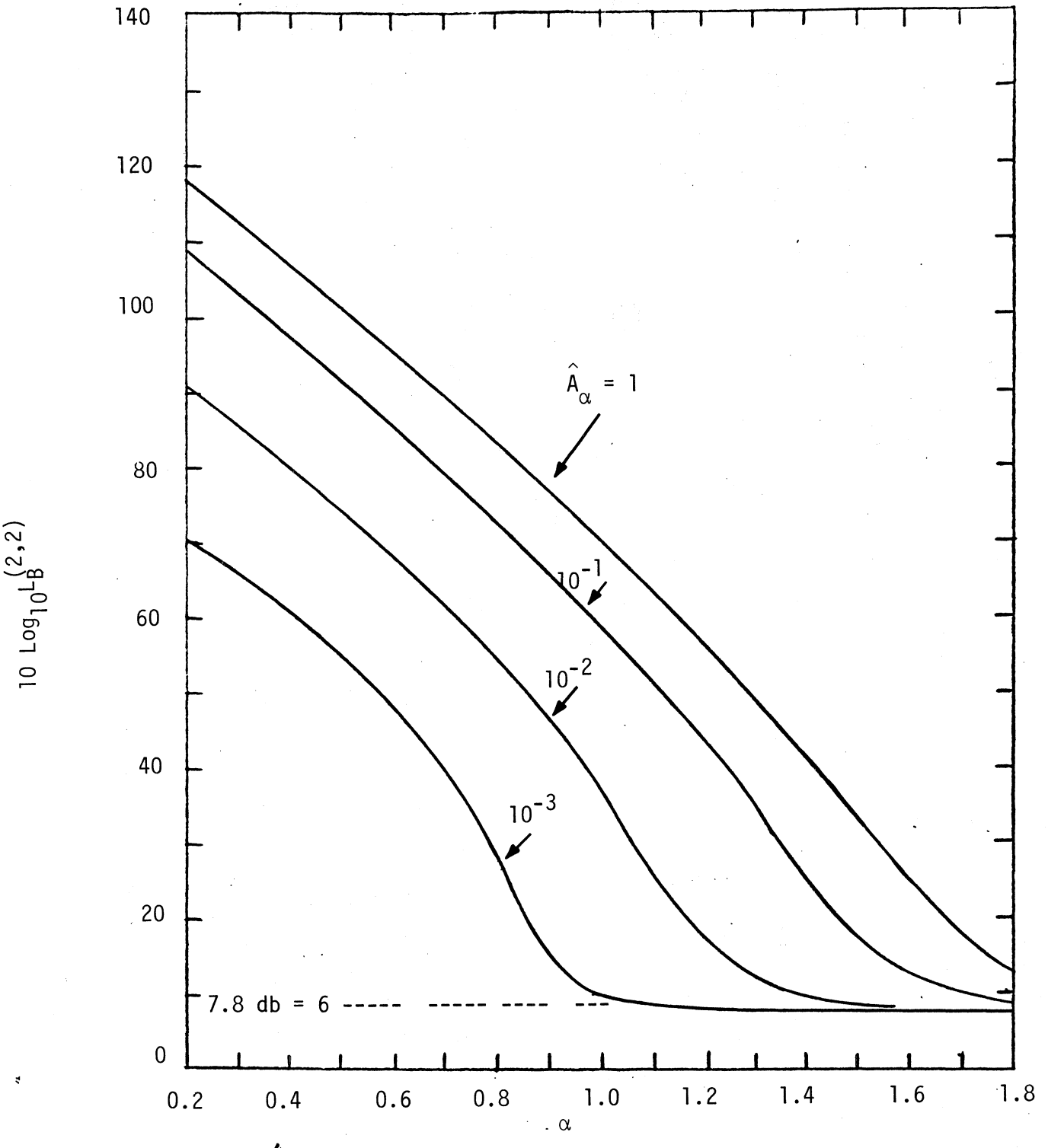

Figure 7.13. $L_B^{(2,2)} \left(= 2\langle \ell^4 \rangle_o \right)$, in dB, for Class B EMI, Eq. (7.15c).

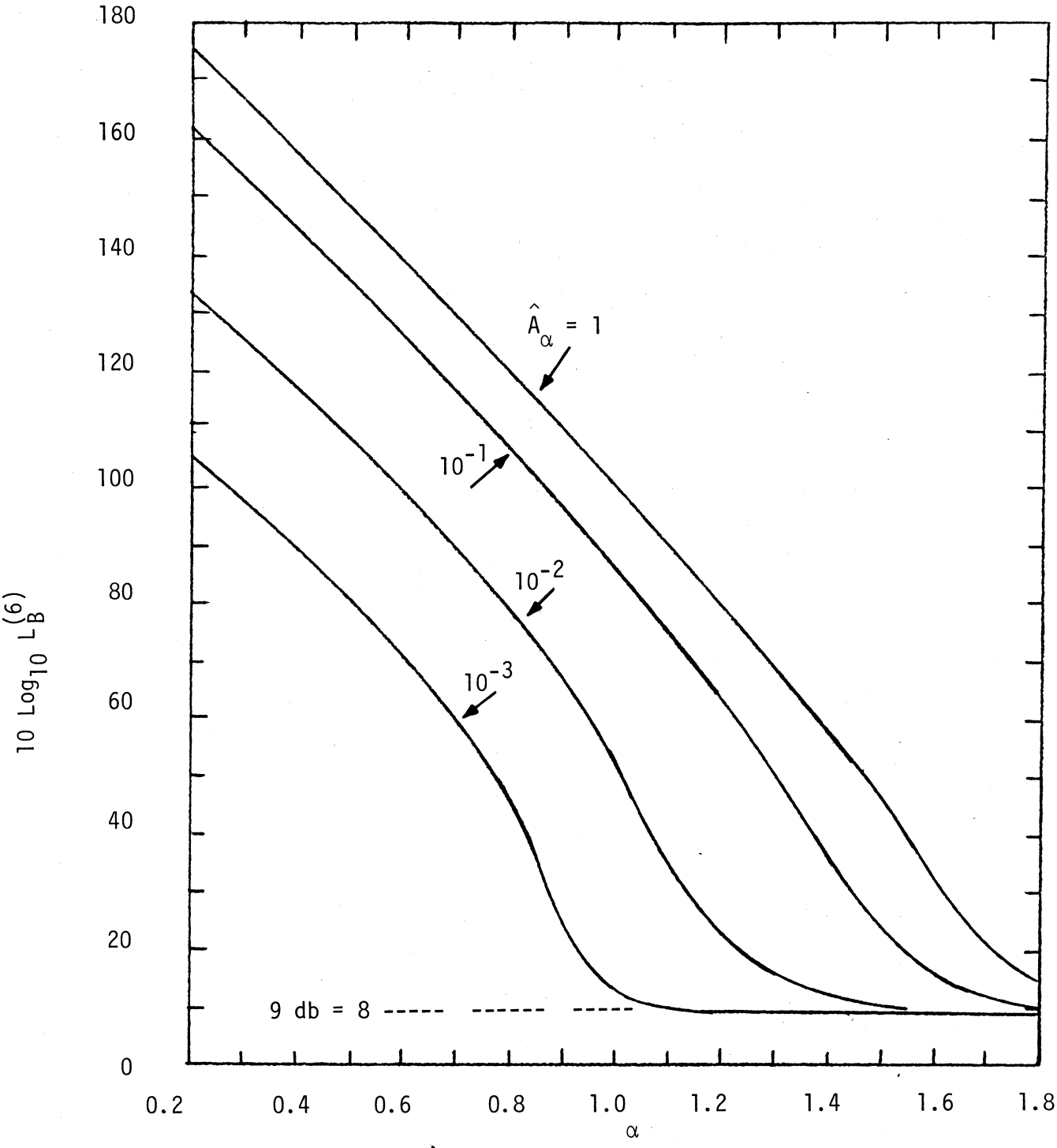

Figure 7.14. $L_B^{(6)}$ $\left(= \left\langle \left(\ell' + \ell^2 \right)^3 \right\rangle_o \right)$, in dB, for Class B EMI, Eq. (7.15d).

III. Processing Gains/per Sample:

The processing gain per sample, $\Pi^{(*)}/n$, are also needed in the evaluation of (optimum) performance. From (6.10), (6.13); (6.24), (6.33) we can write [cf. Tables 6.1a, 6.1b]:

$$\Pi^{*}_{coh/n} = L^{(2)} = \Pi^{(21)*}_{coh}/n \ ;$$

$$\Pi^{*}_{inc}/n = \frac{1}{8}\{L^{(4)}+2L^{(2)^2}(Q_n-1)\}, = \frac{L^{(4)}}{8}, \ (Q_n=1\text{:incoh.signal structure})$$

$$\simeq nL^{(2)^2}/8 \ , \ (Q_n = \frac{n}{2} \ (>>1);$$

sinusoids; Eq. (A.2-42e)) (7.17a)

(binary symmetric):

$$\Pi^{(21)*}_{inc} = \frac{L^{(2)^2}}{4}(\hat{Q}^{(21)}_n-1) = 0, \qquad (\hat{Q}^{(21)}_n=1\text{: incoherent structure})$$

$$\simeq nL^{(2)^2}/4, \ (\hat{Q}^{(21)}_n=n(>>1),$$

sinusoids, Eq. (A.2-61a) (7.17b)

explicitly for no, or slow-fading, e.g. $m_{ij}=1$, cf. (7.4a,b) above, and binary symmetric channels, when indicated. We also note from (6.14), (6.15) that in the coherent cases the minimum detectable signal $\langle a_o^2\rangle^{(21)*}_{min\text{-}coh}$ is increased vis-à-vis that of the "on-off" cases; by a factor 4 for orthogonal signals (7.3) and by a factor 2 for antipodal signals, (7.2), according to the definition (6.13), while the processing gain ($\Pi^{(21)*}_{coh}$) remains unchanged. On the

other hand, for incoherent detection, $\langle a_o^2 \rangle^{(21)*}_{\text{min-inc}} \equiv \overline{a_o^2}$, (a_o^2), (symmetrical channels), cf. (6.33), and the processing gain is increased vis-à-vis the "on-off" cases by a factor 2 to the extent that the binary signals have coherent waveform structures, cf. (7.17b) vs. (7.17a), n>>1. Figures 7.7, 7.11 show $\Pi^*_{\text{coh/n}}$ (db) for Class A and B noise respectively in the coherent cases. Figures 7.8, 7.12 show $(\Pi^*_{\text{inc/n}})$ (db) + 9.0 db (= 10 $\log_{10}$ 8), also for Class A and B noise, when Q_n = 1 for the "on-off" cases. Figures 7.15, 7.16 illustrate $\Pi^*_{\text{inc/n}}$ for Q_n = 10, Class A and Class B noise respectively. The limiting cases (n>>1, coherent signal structure) are readily calculated form (7.17a,b) with the help of the data of Figs. 7.7, 7.11. Generally, as the noise becomes more gaussian, these processing gains approach their gaussian limits (as expected) where now $L^{(2)} \to 1$, $L^{(4)} \to 2$. (See Sec. 7.5 for comments on Figs. 7.15, 7.16.)

IV. The Optimum H_o- Variances σ^{*2}_{on} :

These quantities, σ^{*2}_{on}, appear as the argument of the probabilistic performance measures, P^*_D, P^*_e, cf. (7.13), and are consequently a principal goal of our computations. Specifically, from Tables 6.1a,b we can write in summary:

A. Coherent Detection:

$$\left.\begin{array}{l} \sigma^{*2}_{\text{on-coh}} = \bar{a}_o^2 nL^{(2)} \\ \left\{ \begin{array}{l} (\sigma^{(21)*}_{\text{on-coh}})^2 = 2\bar{a}_o^2 nL^{(2)} \\ \quad " \qquad\quad = 4\bar{a}_o^2 nL^{(2)} \end{array} \right. \end{array}\right| \begin{array}{l} \equiv 2\langle a_o^2 \rangle^*_{\text{min-coh}} \Pi^*_{\text{coh}}, \text{ [Eq.(6.9)],"on-off" signals} \\ \text{: orthogonal signals, [Eq. (6.15b)]} \\ \text{: antipodal signals, [Eq. (6.15a)] ,} \end{array} \qquad (7.18)$$

these last for symmetrical channels ($a_o^{(1)} = a_o^{(2)} = a_o$), ($p_1 = p_2 = 1/2$), and no or stationary fading small or large, rapid or slow ($\bar{a}_o = a_o$, $\bar{a}_{oi} = \bar{a}_o$), all n ($\geq$ 1).

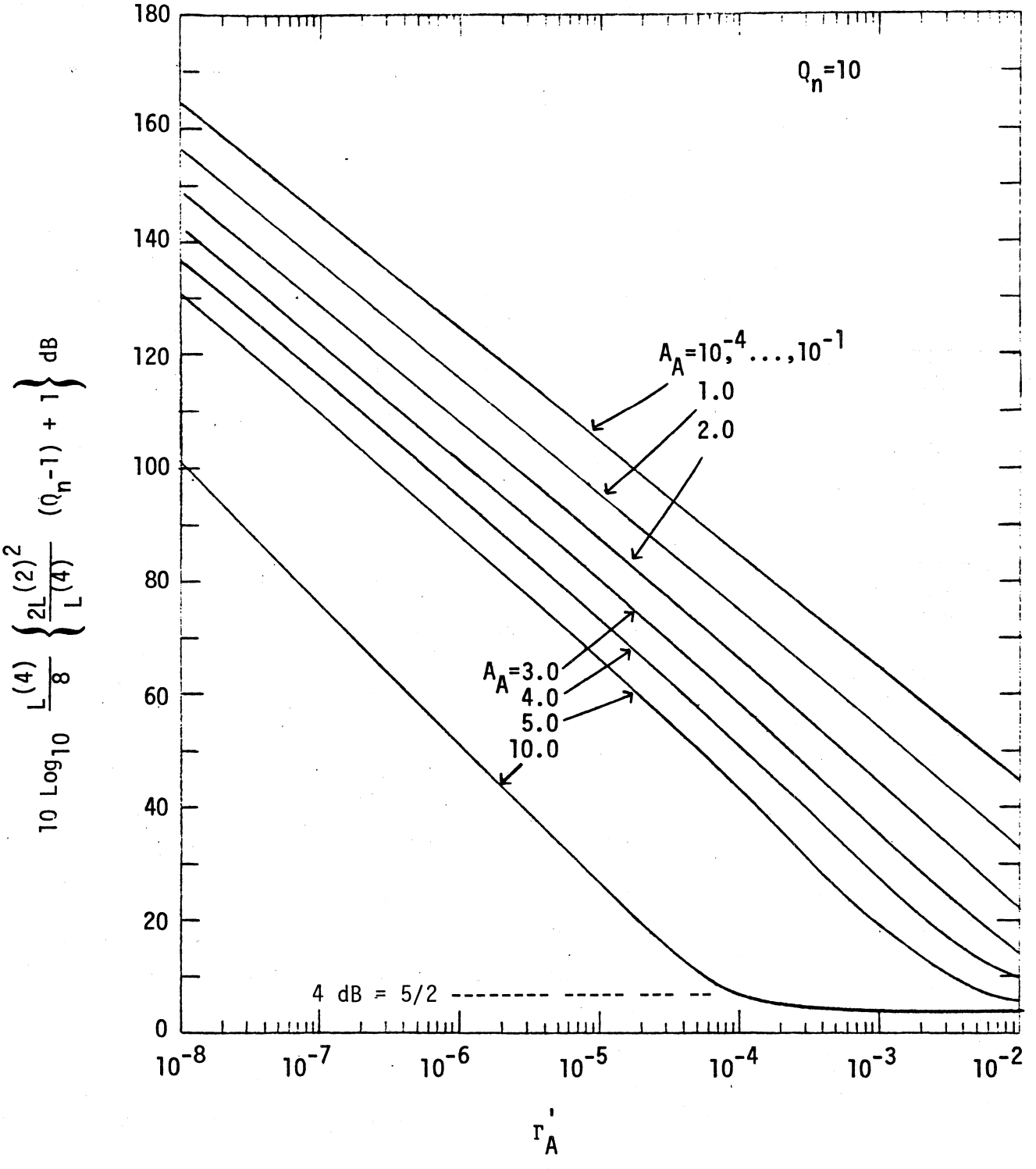

Figure 7.15. Processing gain (Π^*_{inc}/n) per sample, in dB, for optimum incoherent threshold detection in Class A EMI, for signals with partially incoherent structure (Q_n=10), Eq. (7.17a).

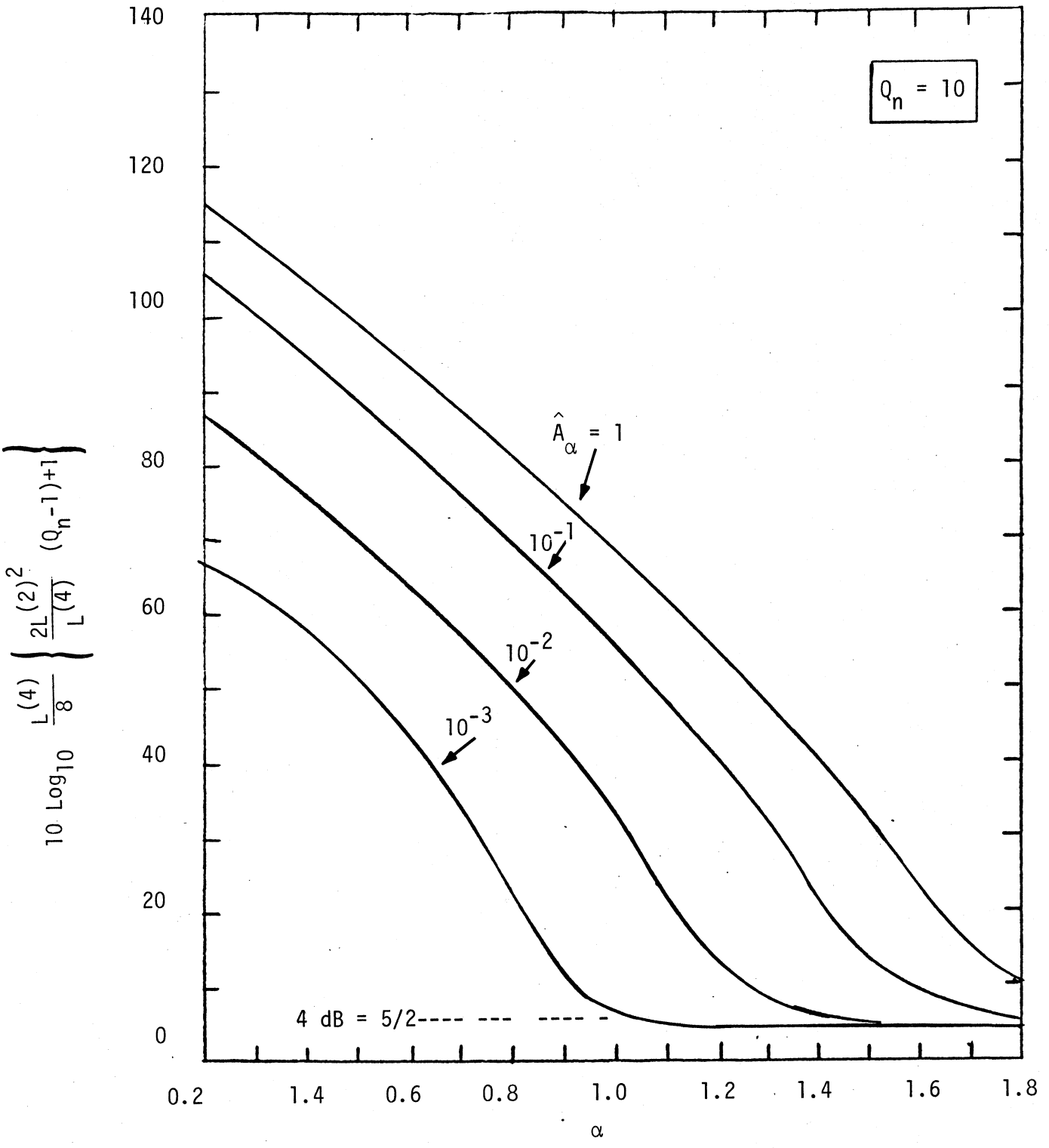

Figure 7.16. Processing gain (Π^*_{inc}/n) per sample, in dB, for optimum incoherent threshold detection in Class B EMI, for signals with partially incoherent structure (Q_n = 10), Eq. (7.17a).

B. Incoherent Detection:

$$\sigma^{*2}_{\text{on-inc}} = \frac{\overline{a_o^2}}{4}\, n\{L^{(4)} + 2L^{(2)^2}(Q_n - 1)\} \equiv 2\langle a_o^2\rangle^{*2}_{\text{min-inc}}\, \Pi^{*}_{\text{inc}} : \text{"on-off"} \tag{7.19a}$$

$$\sigma^{*(21)^2}_{\text{on-inc}} = \frac{\overline{a_o^2}\, nL^{(2)^2}}{2}\,(\hat{Q}_n^{(21)} - 1) \equiv 2(\langle a_o^2\rangle^{(21)*}_{\text{min-inc}})^2\, \Pi^{(21)*}_{\text{inc}} : \text{binary symmetrical} , \tag{7.19b}$$

where $m_{ij} = 1$, $a_o^{(2)} = a_o^{(2)} = a_o$, etc., now for slow or no fading, which is more restricted than the above, (7.18). Here we have

$$Q_n - 1 \equiv \frac{1}{n} \sum_{ij}{}' \rho_{ij}^2 \quad ; \quad \hat{Q}_n^{(21)} - 1 \equiv \frac{1}{n} \sum_{ij}{}' [\rho_{ij}^{(2)} = \rho_{ij}^{(1)}]^2, \; n \geq 1, \tag{7.19c}$$

cf. (6.25), (6.33), (6.33a), and Table 6.1b. Special results are

(i). incoherent signal structure:

$$(\sigma^{*}_{\text{on-inc}})^2 = \overline{a_o^2}\, nL^{(4)}/4 , \quad (n \geq 1)$$

(iii). coherent (sinusoidal) signal structure:

$$(\sigma^{*}_{\text{on-inc}})^2 = \overline{a_o^2}\, n^2 L^{(2)^2}/4, \; [Q_n \cong \tfrac{n}{2}] \; (n \gg 1) \quad \Big\} : \text{"on-off" signals} , \tag{7.20a}$$

and in the case of the binary symmetric channel above, these are [cf. (7.17a,b) in (7.19a,b)]

(i). incoherent signal structure:

$$(\sigma^{*(21)}_{\text{on-inc}})^2 = 0\text{: [detection of two equal energy signals: no distinction between } H_1 \text{ and } H_2.]$$

(ii). coherent (sinusoidal) signal structure:

$$(\sigma^{*(21)}_{\text{on-inc}})^2 = \overline{a_o^2}\, n^2 L(2)^2/2 \ , \ [\hat{Q}_n^{(21)} - 1 \overset{\sim}{=} n \ (>>1)].$$

} "binary signals" (7.20b)

The advantage of operation with coherent signal structures in the incoherent, "on-off" mode of detection vis-à-vis incoherent signal structures is at once apparent from (7.20a):

$$\frac{(\sigma^{*}_{\text{on-inc}})^2_{\text{coh st.}}}{(\sigma^{*}_{\text{on-inc}})^2_{\text{inch. st.}}} = \frac{nL(2)^2}{L^{(4)}} \ (>>1), \ (n>>1) \ . \qquad (7.21)$$

Although $1 > L^{(2)^2}/L^{(4)} \geq 0$, $L^{(2)^2} \sim L^{(4)}$ within O(10 db), so that for the customary large values of sample-size n, the advantage of being able to employ coherent signal structures, i.e. having channels with little or no doppler spread and/or rapid fading, is essentially $\sim n$, which is considerable where n is at all large, cf. V, Section 6.2 above. With binary (symmetric) signal operation coherent signal structure is critical, cf. (7.20b), if we are to avoid having to distinguish between two essentially equal "energy signals", whose original frequency structures are no longer distinct, because of the time- and frequency "smearing" (i.e. spreading) produced in the channel. Thus, for sufficiently "widely-spread" channels it becomes necessary to employ the "on-off" transmission mode, cf. (7.20a), where now at least, we are required to distinguish a non-vanishing (desired) signal

however distorted, from the condition of noise alone. Quantitatively, the larger the magnitudes of Q_n, $Q_n^{(21)}$, the larger the variance $(\sigma_{on}^*)^2$ and the better the detector performance, cf. (7.13).

C. The Composite Detector:

$$\sigma_{o\text{-comp}}^{*2} = \sigma_{o\text{-coh}}^{*2} + \sigma_{o\text{-inc}}^{*2}$$

$$= n\{\bar{a}_o^2 L^{(2)}[\frac{1}{2n}\sum_i \langle s_i\rangle^2] + \frac{1}{4}\overline{a_o^2}\{L^{(4)} + 2L^{(2)^2}[Q_n - 1]\}\} : \underline{\text{"on-off"}} \quad . \tag{7.22a}$$

$$(\sigma_{o\text{-comp}}^{(21)*})^2 = n\{\bar{a}_o^2 L^{(2)} \frac{1}{2n}\sum_i [\langle s_i^{(2)}\rangle - \langle s_i^{(1)}\rangle]^2 + \frac{\overline{a_o^2}}{2} L^{(2)^2}(\hat{Q}_n^{(21)} - 1)\} : \underline{\text{"binary symmetric"}} \quad . \tag{7.22b}$$

Here the sum in (7.22b) reduces to (2,4), respectively for completely coherent received orthogonal, or antipodal binary signals, cf. (7.18). The sum in (7.22a) likewise reduces to unity. Again, we assume no or slow fading here, and stationary noise and channel characteristics. Frequently, we do not have full coherence at the receiver, so that $\rho_{ij} = \langle s_i s_j\rangle \neq \bar{s}_i\bar{s}_j$, $(\bar{s}_{i,j} \neq 0)$, and we must use both first- and second-order statistics of the signal, as indicated above. We shall use (7.22) in (7.13) in Section 7.5, when we come to calculate performance.

V. Bounds on Input Signal Size:

The bounds (x_0^*, y_0^*) on the maximum input signal for which $\text{var}_1 g_n^* \doteq \text{var}_0 g_n^*$, required both for the LOBD and AOD character of these optimal threshold detection algorithms, are given in Section 6.3. We summarize the results for the usual conditions (above). We start with the "on-off" signal cases:

A. Coherent Detection:

$$x_0^* = L^{(2)} \Big/ \left(L^{(2,2)} \Big/ 2 - (1-\eta) L^{(2)^2} \right) = \frac{\langle \ell^2 \rangle_0}{\text{var}_0 \ell^2} \tag{7.23}$$

[rapid fading, for no or slow fading, $\eta \sim 0$, Eq. (6.71)].

B. Incoherent Detection:

$$y_0^* \Big|_{\text{incoh.sig.struct.}} = \frac{L^{(4)}}{\left| \frac{L^{(6)}}{2} + 6L^{(2)} L^{(2,2)} \right|};$$

$$y_0^* \Big|_{\text{coh. sig. struct.}} = \frac{L^{(2)}}{3L^{(2,2)} + 2L^{(2)^2}} \quad , \text{[Eqs. (6.72)]}. \tag{7.24}$$

For the binary symmetric channel, with no, slow or rapid, fading, we refer back to Eqs. (6.77), (6.78). Finally, when the composite detector is used [cf. Sec. 6.5], we choose the stricter of the two bounds (x_0^*, y_0^*), usually that for incoherent detection. Figures 7.17-7.19 show (7.23), (7.24) for Class A noise, while Figures 7.20-7.22 give (x_0^*, y_0^*) for various Class B cases.

7.4 Performance Elements for Suboptimum Threshold Detectors:

Just as we have established the "elements" needed to determine the performance of optimum threshold detection systems in Sec. 7.3 above, we can proceed to do the same here for suboptimum systems. As before, we

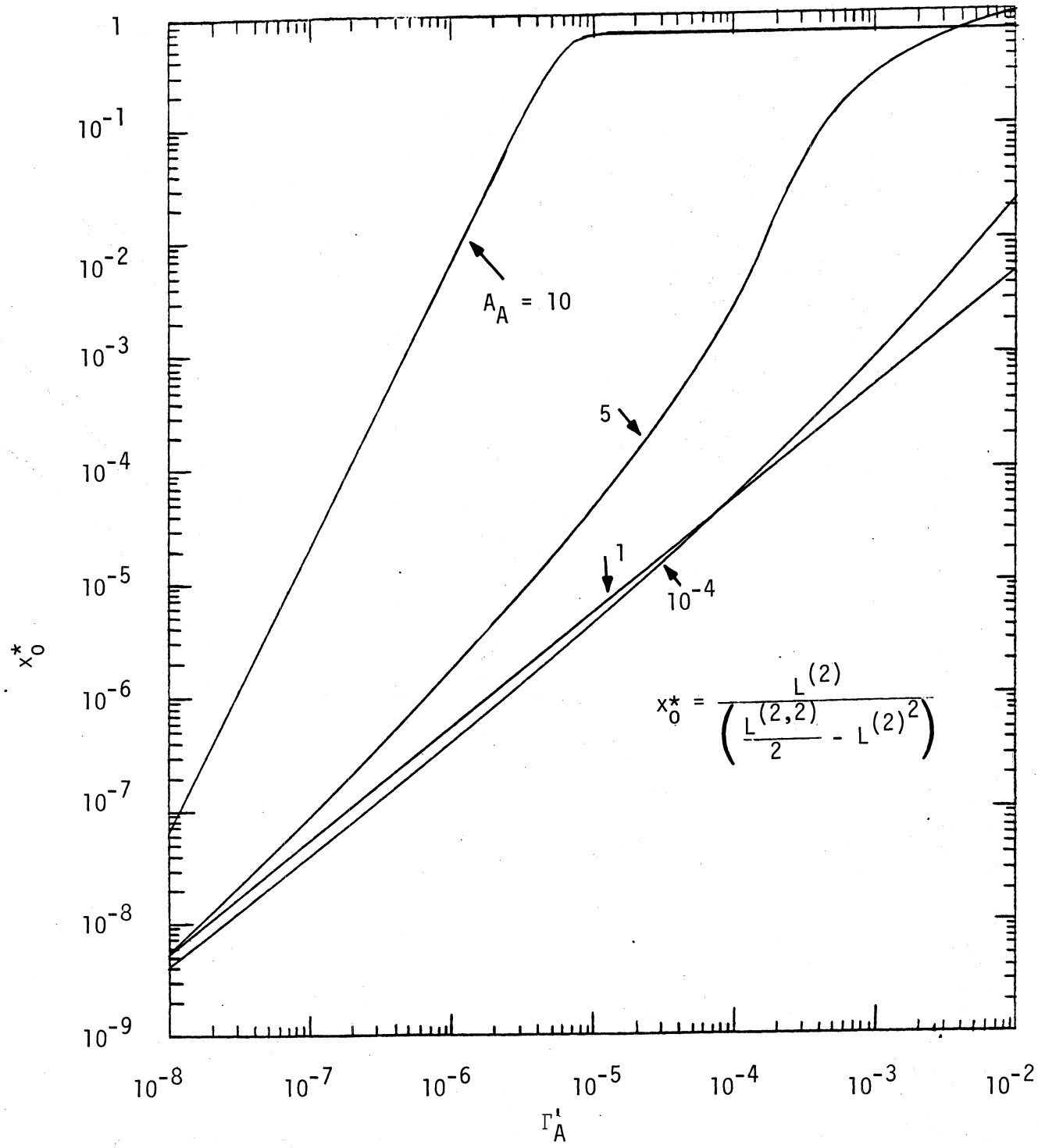

Figure 7.17. The bound, x_0^*, for coherent detection of (coherent) signals in Class A EMI, Eq. (7.23) (No or little fading: $\overline{a_0^2} \doteq \overline{a_0}^2$).

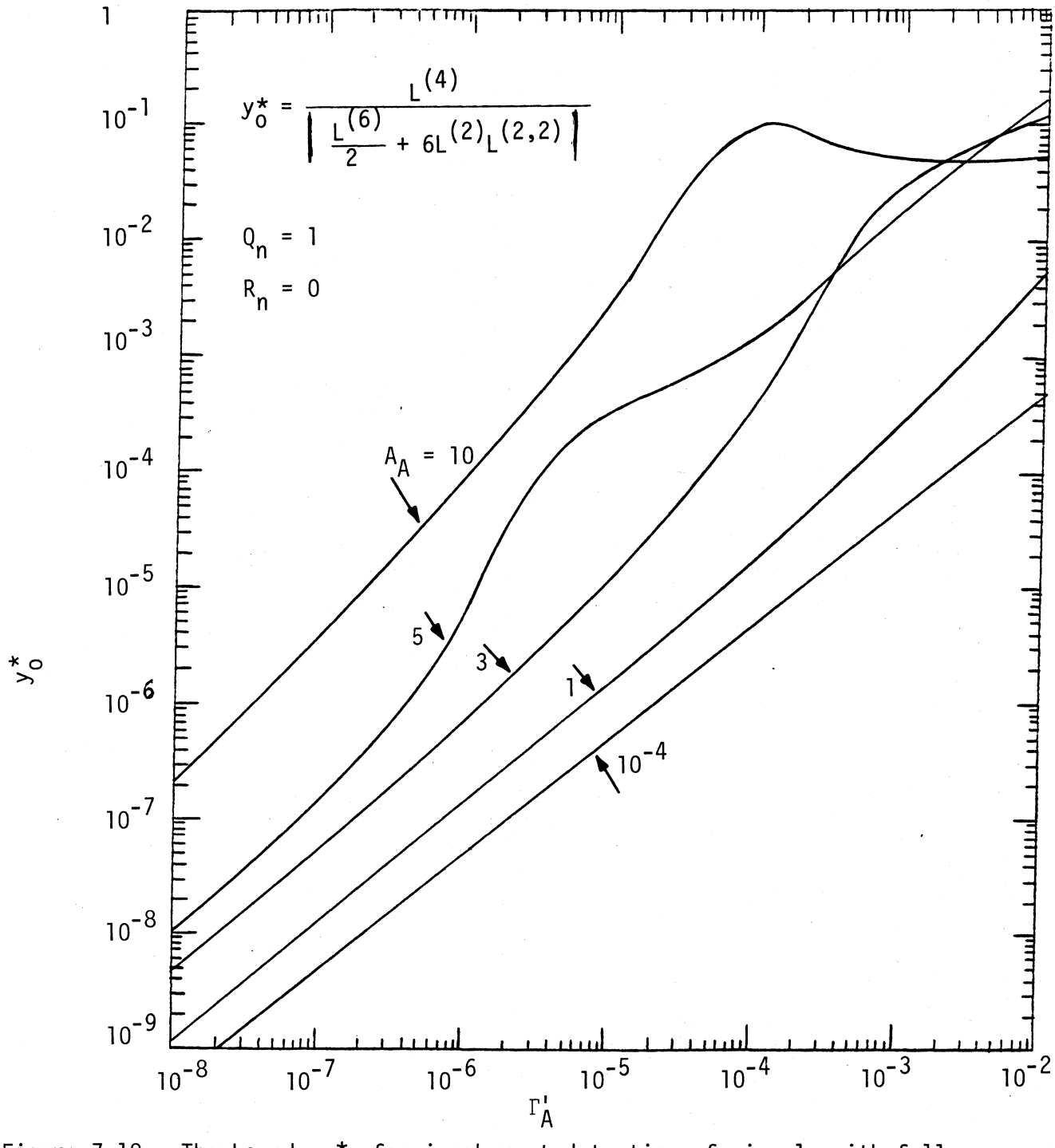

Figure 7.18. The bound, y_o^*, for incoherent detection of signals with fully incoherent structure in Class A EMI ($Q_n = 1$, $R_n = 0$), Eq. (7.24), arbitrary fading.

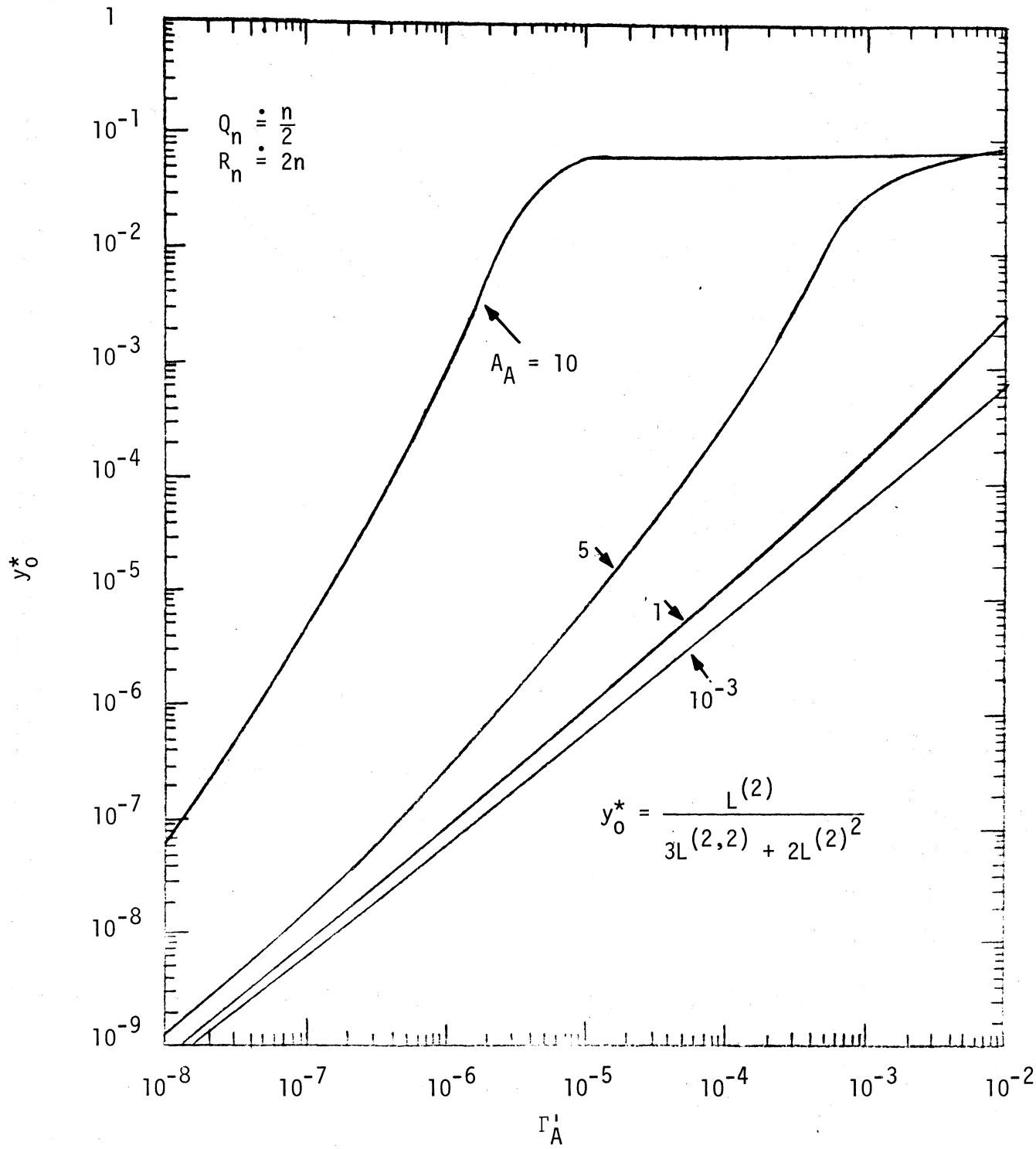

Figure 7.19. The bound, y_o^*, for incoherent detection of signals with fully coherent structure, in Class A EMI: ($Q_n \doteq n/2$, $R_n \doteq 2n$, $n \gg 1$, no, slow, or rapid fading); Eq. (7.24).

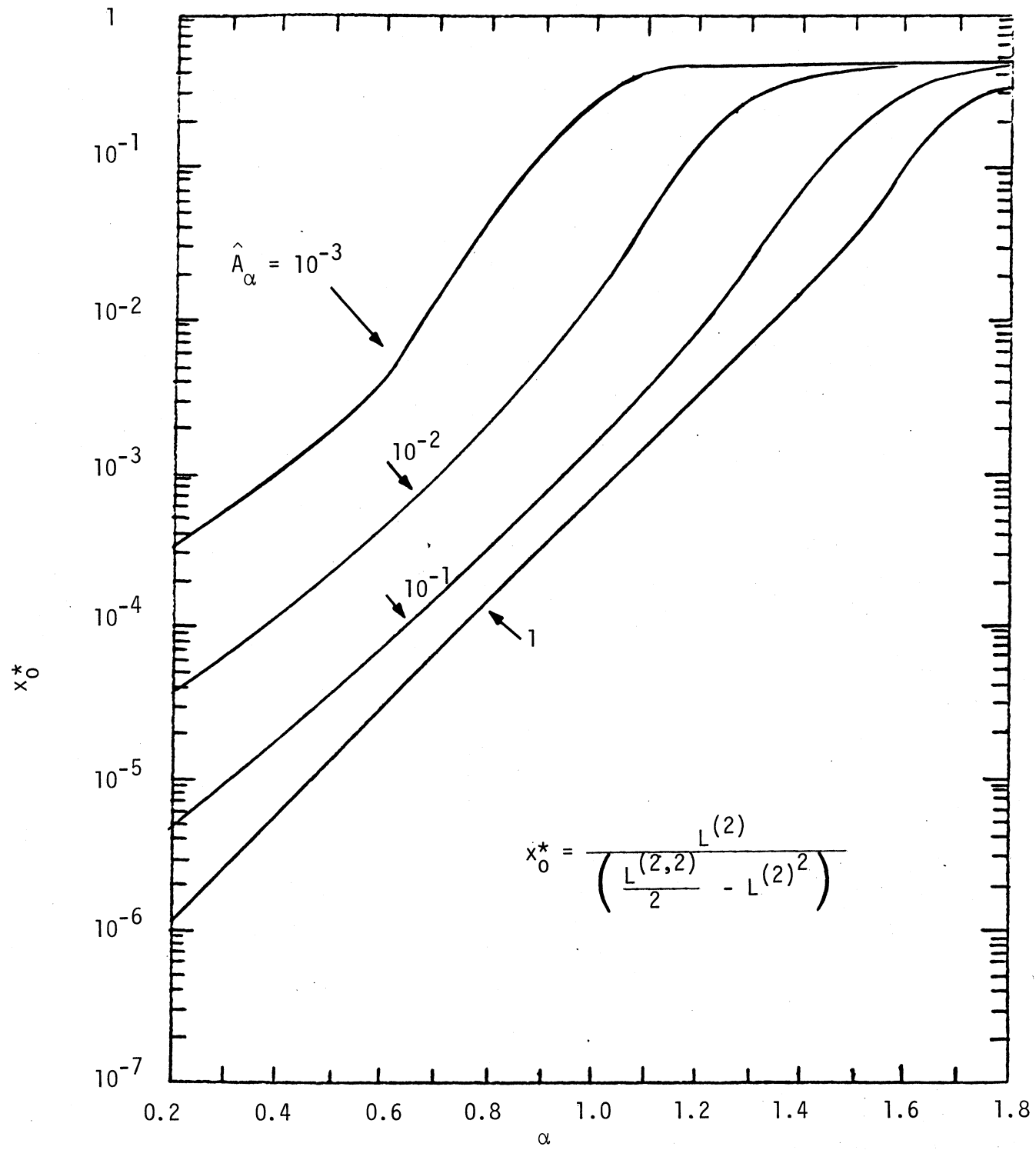

Figure 7.20. The bound, x_o^*, for coherent detection of (coherent) signals in Class B EMI, Eq. (7.23); (No or little fading: $\overline{a_o^2} \doteq \overline{a}_o{}^2$).

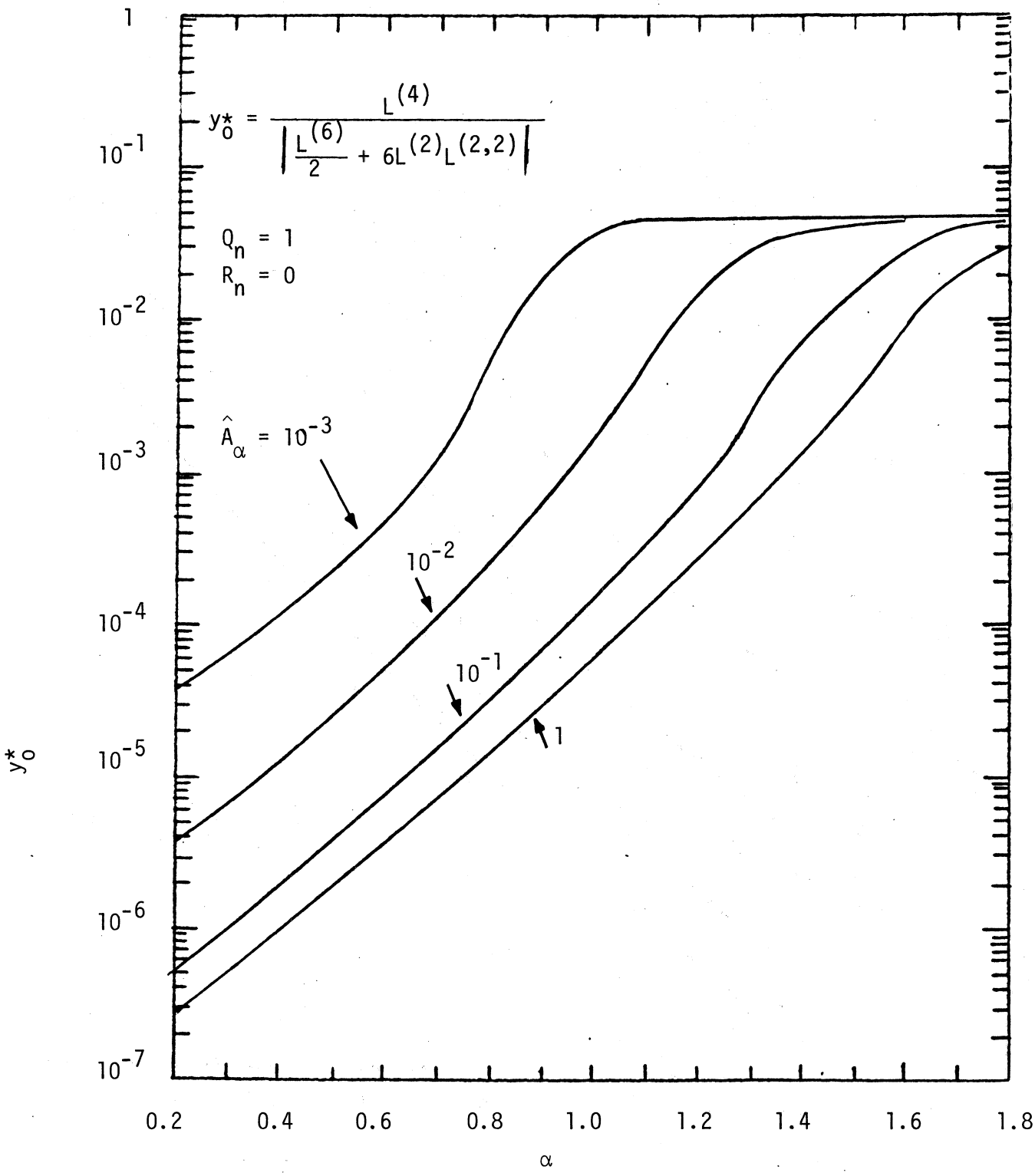

Figure 7.21. The bound, y_o^*, for incoherent detection of signals with fully incoherent structure in Class B EMI ($Q_n = 1$, $R_n = 0$), Eq. (7.24), arbitrary fading.

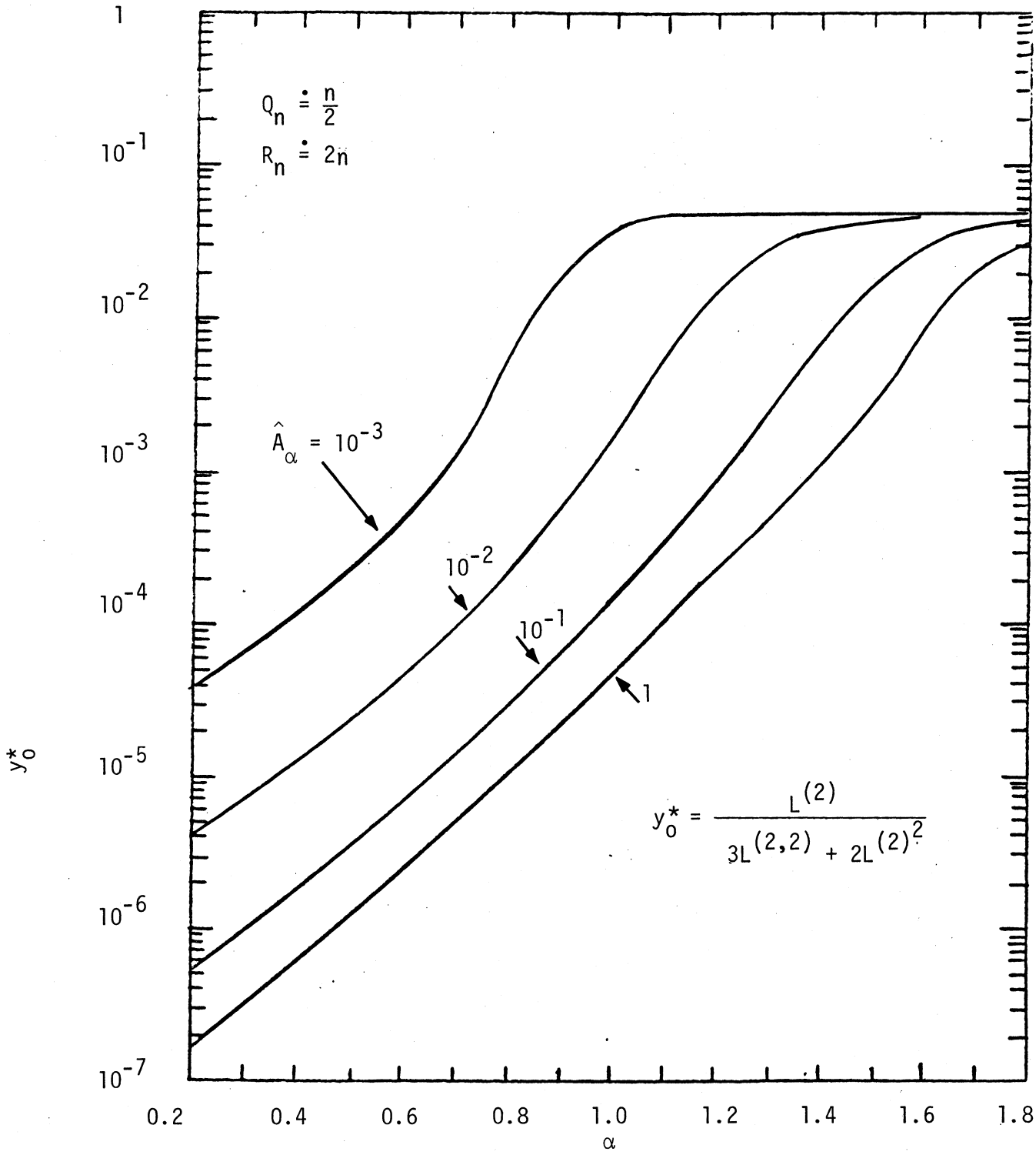

Figure 7.22. The bound, y_o^*, for incoherent detection of signals with fully coherent structure, in Class B EMI; ($Q_n \doteq n/2$, $R_n \doteq 2n$, $n >> 1$, no, slow, or rapid fading) Eq. (7.24).

seek a combination of canonical performance results with specific elements whereby particular numerical values may be obtained, as in Section 7.5 following.

I. Canonical Suboptimum Performance Measures:

Analogous to (7.13) we can write directly from Eqs. (6.50), (6.51) in suboptimum threshold situations [cf. footnote p. 55].

$$P_D \cong \frac{p}{2}\{1+\Theta[\sqrt{\Phi_d^*}\, C^*_{N.P.} - \Theta^{-1}(1-2\alpha_F)]\} \ , \quad [\text{Eq. (6.50)}] \ , \tag{7.25}$$

and

$$P_e \cong \frac{1}{2}\{1-\Theta[\tfrac{1}{2}\sqrt{\Phi_d^*}\, C^*_{I.O.}]\} \ , \quad [\text{Eq. (6.51)}] \ , \tag{7.26}$$

respectively for correct signal detection, and error probability in the subsequent "communication" phase of detection decisions. Figures 7.23 and 7.24 give the canonical relations between P_D, P_e and the degradation factor, Φ_d^*, cf. Tables 6.1a,b, 6.2; (6.18), (6.38), (6.42a,b), etc. The relations (7.25), (7.26) are canonical equivalents of (7.13).

II. Various Degradation Factors, Φ_d^*:

In order to use (7.25), (7.26) in relation to specific signal, noise, and reception conditions we need the explicit forms of the degradation factor, Φ_d^*. These are readily summarized below, from Tables 6.1a,b, 6.2. We have

A. Simple Correlators: Φ_d^*, "on-off" signals:

(i). coherent reception:

$$\Phi_d^* = 1/L^{(2)} \ , \ [\text{Eq. (6.18)}]. \tag{7.27a}$$

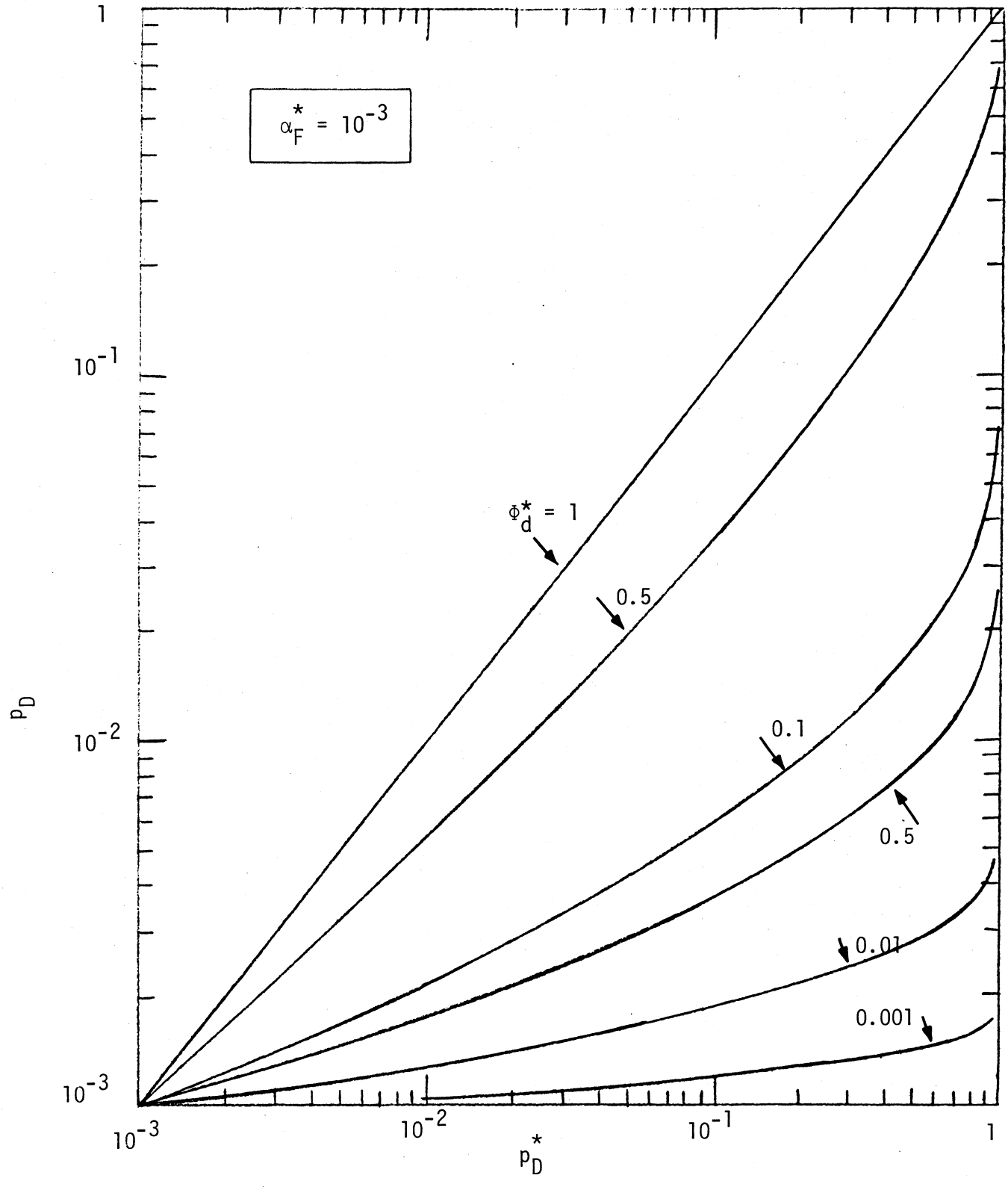

Figure 7.23a. Probability of detection versus optimum probability of detection for a false alarm probability of 10^{-3} and various degradation factors Φ_d^*, Equation (7.25).

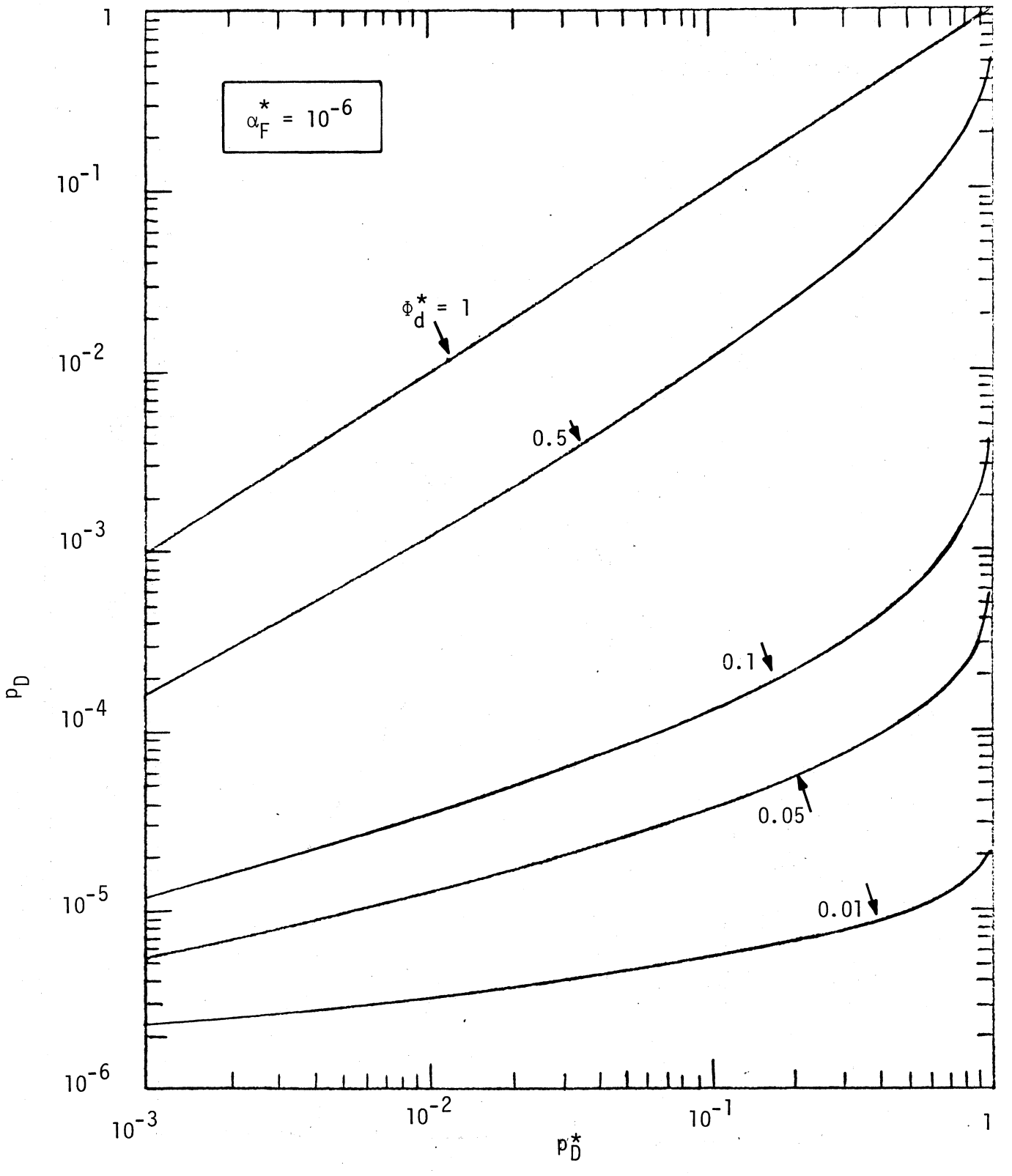

Figure 7.23b. Probability of detection versus optimum probability of detection for a false alarm probability of 10^{-6} and various degradation factors Φ_d^*, Equation (7.25).

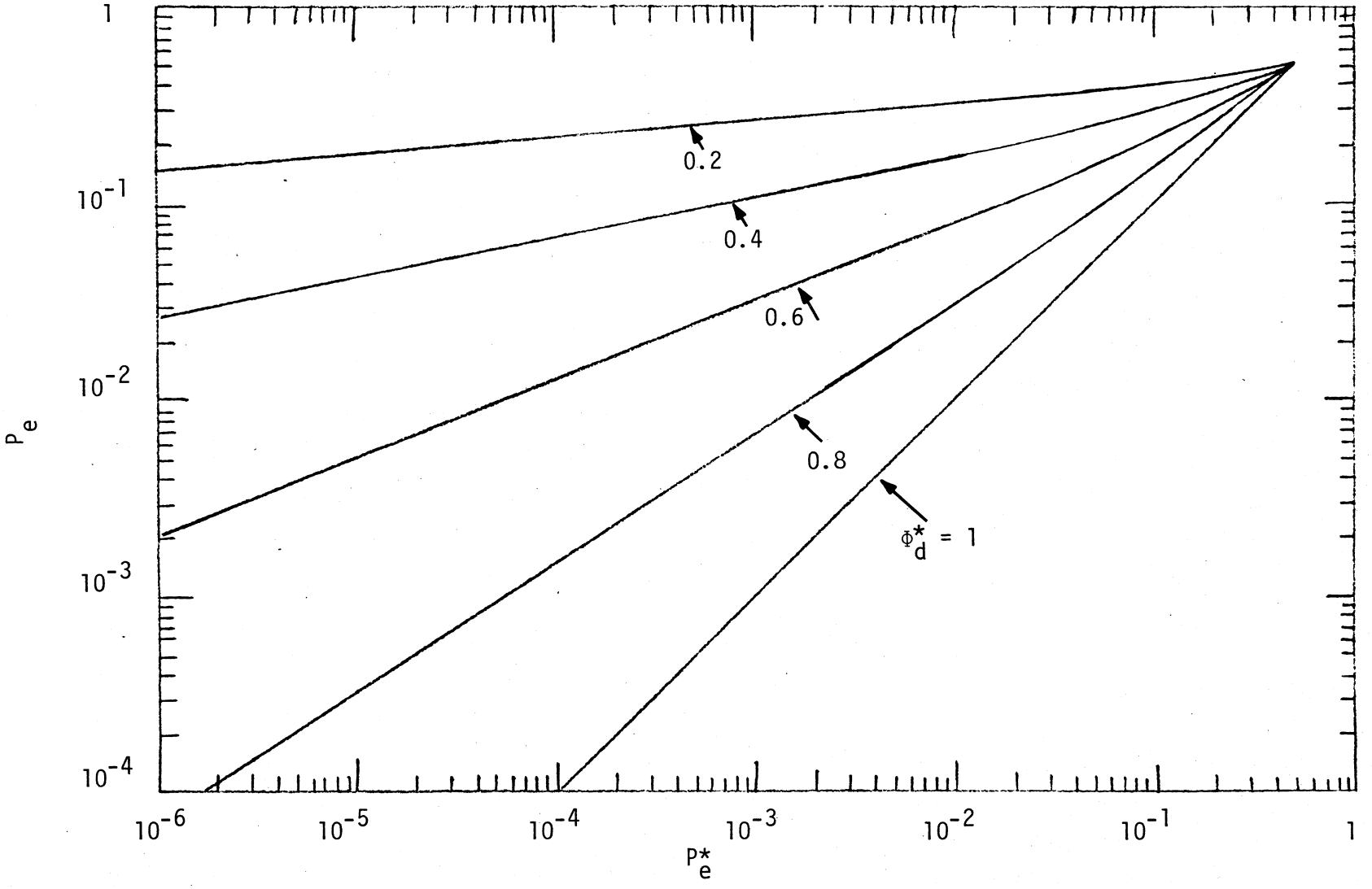

Figure 7.24. Probability of binary bit error versus optimum probability of error for various degradation factors Φ_d^*, Equation (7.26).

(ii). incoherent reception:

$$\begin{cases} \Phi_d^*\big|_{\text{incoh.struct.}} = 4/L^{(4)}(\overline{x^4}-1); \ [Q_n=1]; & (7.27b) \\ \Phi_d^*\big|_{\text{coh. struct.}} = 1/L^{(2)^2} \ ; \ [Q_n \underset{\sim}{=} n/2 >>1, \text{ sinusoids}] \ . & (7.27c) \end{cases}$$

[For intermediate values of Q_n use Eq. (6.38).] For binary signals, we get

(iii). coherent reception

$$\Phi_d^{(21)^*} = 1/L^{(2)} \ , \text{ Eq. (6.21)] .} \qquad (7.28a)$$

(iv). incoherent reception

$$\begin{cases} \Phi_d^{(21)^*}\big|_{\text{incoh.struct.}} = 0, \text{ [Eq. (6.42b)]: (degenerate case: indistinguishable signals)} & (7.28b) \\ \Phi_d^{(21)^*}\big|_{\text{coh.struct.}} = 1/L^{(2)^2} \ , \ [Q_n^{(21)} \sim n; \text{ sinusoids.}] & (7.28c) \end{cases}$$

[Again, for intermediate values of $\hat{Q}_n^{(21)}$, $Q_n^{(21)}$, use (6.42a,b).]

B. Clipper-Correlators: Φ_d^*, "on-off" signals:

(i). coherent reception:

$$\Phi_d^* = \frac{4w_{1E}(0)^2}{L^{(2)}} \ ; \ [E = A,B \text{ here; Table 6.2}] \qquad (7.29a)$$

(ii). incoherent reception:

$$\begin{cases} \Phi_d^*\Big|_{\text{incoh.struct.}} = [2w''_{1E}(0)]^2/L^{(4)}; \ [Q_n=1]; & (7.29b) \\ \Phi_d^*\Big|_{\text{coh. struct}} = \left\{\dfrac{4w_{1E}(0)}{L^{(2)}}\right\}^2, \ [Q_n \approx n/2 \gg 1, \text{ sinusoids}]. & (7.29c) \end{cases}$$

Again, for intermediate values of Q_n, see Table 6.2. Similarly, from Table 6.1d, 6.2 we get for binary signals

(iii). coherent reception:

$$\Phi_d^* = \left\{\frac{4w_{1E}(0)^2}{L^{(2)}}\right\}^2, \quad [E = A,B, \text{ here}], \text{ cf. (7.29a)} ; \qquad (7.30a)$$

(iv). incoherent reception:

$$\begin{cases} \Phi_d^*\Big|_{\text{incoh.struct.}} = 0, \text{ cf. Sec. 2.4-4 [indistinguishable signals]} & (7.30b) \\ \Phi_d^*\Big|_{\text{coh.struct.}} = \left[\dfrac{4w_{1E}(0)^2}{L^{(2)}}\right]^2, \ [Q_n^{(21)} \approx n \gg 1, \text{ sinusoids}]. & (7.30c) \end{cases}$$

To implement the Φ_d^*'s numerically we need next $\overline{x^4}$, and $w_{1A}(0)$, $w_{1B}(0)$, and, similarly $w''_{1A}(0)$, $w''_{1B}(0)$. These are, for the 4th moment of Class A and B interference

$$\overline{x^4}\Big|_{A,B} = \frac{3}{8}\left\{\frac{\Omega_{4A,B}}{\Omega^2_{2A,B}(1+\Gamma'_{A,B})^2}\right\} + 2 \quad ; \quad \Omega_{4A,B} = \frac{A_{A,B}}{4}\left\langle \hat{B}^4_{oA,B}\right\rangle, \qquad (7.31)$$

where we may use the EMI scenario (3.6) to determine Ω_4, viz.

$$\Omega_{4A,B} = A_{A,B}\left\langle \frac{a^4 G_o^4}{4\lambda^{4\gamma}} \right\rangle = A_{A,B}\left\{ \frac{\overline{a^4}\langle G_o^4\rangle}{4} \left\langle \frac{1}{\lambda^{4\gamma}} \right\rangle \Big|_{A,B} \right\}. \tag{7.32}$$

From (3.11) we get directly

$$\left\langle \frac{1}{\lambda^{4\gamma}} \right\rangle \equiv C_{\mu,\gamma}^{(4)} = \left(\frac{2-\mu}{4\gamma+\mu-2}\right)\left(\frac{1-\alpha_o^{4\gamma+\mu-2}}{1-\alpha_o^{2-\mu}}\right) \alpha_o^{2-4\gamma-\mu}\lambda_1^{-4\gamma};\ \alpha_o \equiv \lambda_o/\lambda_1 \text{ [cf. Fig. (3.1)]} \tag{7.33}$$

for this general class of scenario. With the help of (3.10) we can then write

$$\overline{x^4}\Big|_{A,B} = \frac{3}{8}\left\{ \frac{A\,\frac{\overline{a^4}\langle G_o^4\rangle}{4}\, C_{\mu,\gamma}^{(4)}}{\left(A\,\frac{\overline{a^2}}{2}\langle G_o^2\rangle C_{\mu,\gamma}^{(2)} + \sigma_G^2\right)^2} + 2 \right\}_{A,B}. \tag{7.34}$$

[For example, with the scenario of Sec. 7 of Ref. [9], where $\underline{a}$ (or G_o) is rayleigh distributed, say $\underline{a}$ is, we have $\overline{a^4} = 2\overline{a^2}^2$, $\langle G_o^4\rangle = \langle G_o^2\rangle^2$, etc., with $\gamma = 2$, $\mu = 0$ and (7.34) reduces to

$$\overline{x^4}\Big|_{A,B} = \frac{3}{8}\left\{ \frac{2C_{\mu,\gamma}^{(4)}}{A\, C_{\mu,\gamma}^{(2)^2}(1+\Gamma')^2} + 2 \right\}_{A,B} \doteq \left.\frac{1}{4A\alpha_o^2}\right|_{A,B} \quad (>>1);\ \alpha_o^2 << 1,\ \Gamma' << 1.] \tag{7.34a}$$

Similarly, we get from the noise pdf's (3.13), (3.14), (7.11):

$$\underline{\text{(Canonical):}}\quad w_{1A}(0)_{A+G} = e^{-A_A} \sum_{m=0}^{\infty} \frac{A_A^m\,(1+\Gamma_A')^{1/2}}{m!\sqrt{2\pi}(m/A_A+\Gamma')^{1/2}},\ \text{cf. (3.13)} \tag{7.35a}$$

(quasi-canonical):

$$w_{1A}(0)_{A+G} = e^{-A_A \hat{g}_o} \sum_{m=0}^{\infty} \frac{(A_A \hat{g}_o)^m}{m!} \left\{ \frac{d}{\sqrt{4\pi\sigma_{om}^2}} + \hat{\Phi}^{(0)}(0) \right\}, \text{ cf. (3.14),(3.14a).} \tag{7.35b}$$

For the Class B noise we have directly

$$w_1(0)_{B+G} \simeq \frac{1}{\pi\sqrt{\Omega_B}} \sum_{n=0}^{\infty} \frac{(-1)^n}{n!} \hat{A}_\alpha^n \, \Gamma\left(\frac{n\alpha+1}{2}\right) . \tag{7.36}$$

The second derivatives of the pdf's, w_1 above, are found similarly to be, for example,

(canonical):

$$w_1''(0)_{A+G} = -e^{-A_A} \sum_{m=0}^{\infty} \frac{A_A^m}{m!\, 2\hat{\sigma}_{mA}^2} \frac{1}{\sqrt{2\pi}\sqrt{2\hat{\sigma}_{mA}^2}} \tag{7.37}$$

$$w_1''(0)_{B+G} = -\frac{4}{\pi\Omega_B^{3/2}} \sum_{n=0}^{\infty} \frac{(-1)^n}{n!} \hat{A}_\alpha^n \, \Gamma\left(\frac{n\alpha+3}{2}\right) . \tag{7.38}$$

Figures 7.25, 7.26 show $w_1(0)_{A+G\ (canon.)}$, $w_1(0)_{B+G}$, Eqs. (7.35a), (7.36), for various ranges of parameters of these EMI models.

III. ARE's:

These are the Asymptotic Relative Efficiencies (ARE's) defined and derived in Sec. 6.3, IV above. We give here only the more important, limiting cases:

TABLE 7.1 ASYMPTOTIC RELATIVE EFFICIENCIES.

	ARE^2: coherent reception (Φ_d^*) ["on-off" + binary]	ARE^2: incoherent reception ["on-off"]
(1) $\frac{\text{simple correlator}}{\text{optimum}}$	$1/L^{(2)}$	$4/L^{(4)}(\overline{x^4}-1)$: incoh. sig. structures $1/L^{(2)2}$: coh.sig. struct. (n>>1)
(2) $\frac{\text{clipper correlator}}{\text{optimum}}$	$4w_{1E}(0)^2/L^{(2)}$	$2w''_{1E}(0)^2/L^{(4)}$: incoh. sig. struct. $\{4w_{1E}(0)^2/L^{(2)}\}^2$: coh. sig. struct. (n>>1)
(3) $\frac{\text{simple correlator}}{\text{clipper correlator}}$	$1/4w_{1E}(0)^2$	$2/w''_{1E}(0)^2(\overline{x^4}-1)$: incoh. sig. struct. $1/[4w_{1E}(0)^2]^2$: coh. sig. struct. (n>>1)

In the case of (symmetrical) binary reception (no or slow fading) in the incoherent detection mode, (1) and (2) above are zero, and (3) is 0/0 (indeterminate). For coherent signal structures, however, these ARE's are the same as for the "on-off" cases. We note, also, that here the $(ARE)_{inc} = (ARE)^2_{coh}$, and further, that in these limiting situations of large sample size (incoherent reception), the $(ARE)_{inc} = \Phi^*_{d,coh}$, $(n>>1)$, as well, cf. (7.27)-(7.30) above. (For intermediate cases where Q_n, $Q_n^{(21)}>1$ but are less than $(n/2, n)$ we must use the more complex formulae of Sec. 6.3, IV directly.)

Finally, Figures 7.27-7.30 show the (square of the) ARE's ($=\Phi^*_d$'s) here, for (1) and (2) of Table 7.1, for (canonical) Class A and Class B noise. The ARE ($=\sqrt{\Phi^*_d}$) for (3): [simple correlator/clipper correlator] may be obtained at once by subtracting, viz: $ARE_{(3)}(db) = [ARE_{(1)} - (ARE)_{(2)}]$ db. In general the clipper-correlators are much closer to optimum performance than are the simple correlators, when, as is the case here, the EMI is Class A or B noise. [But, regarding the use of ARE's as comparative performance measures, see the caveat at the end of Sec. 6.3.3, III.]

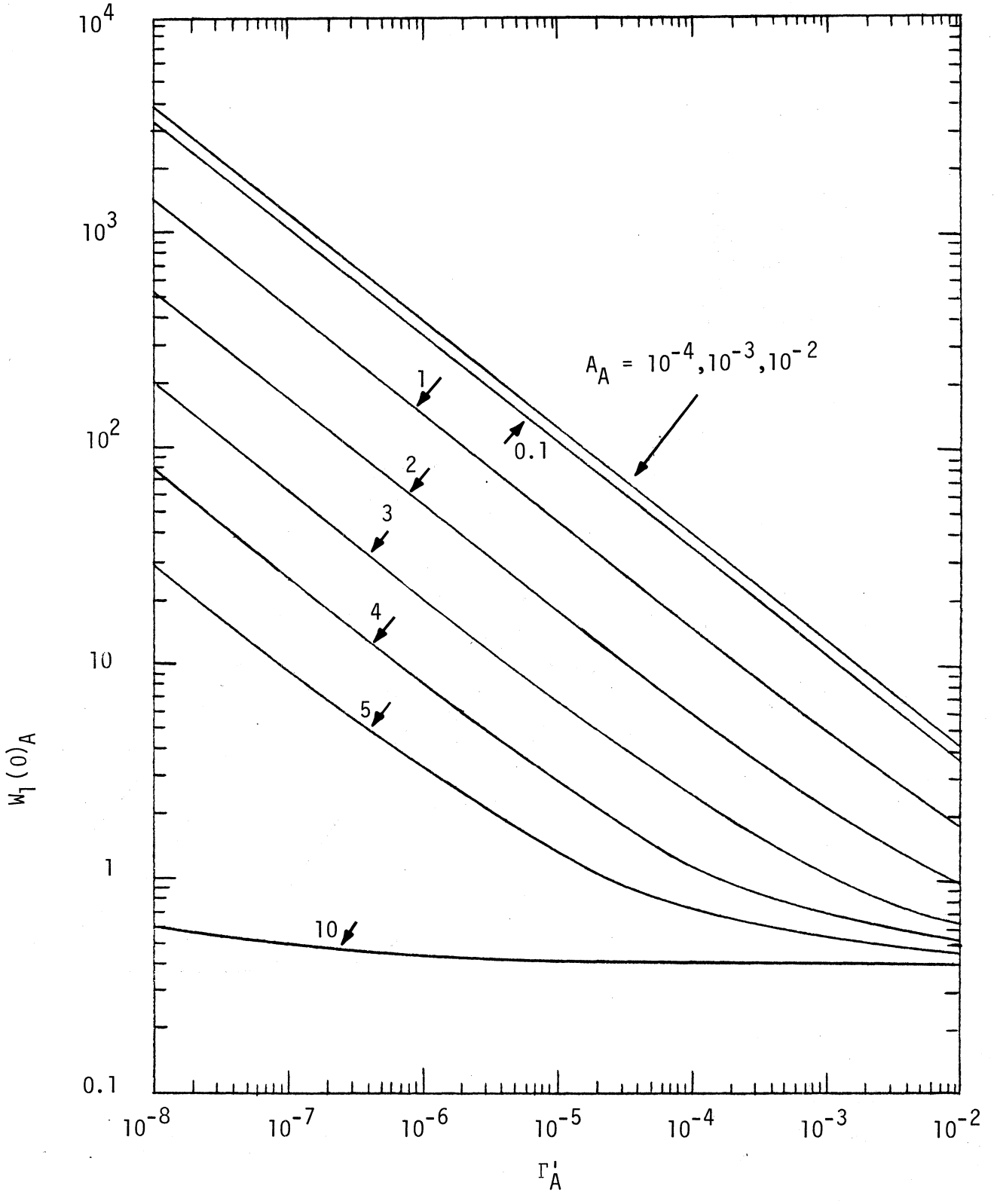

Figure 7.25. The probability density function, evaluated at zero, for Class A noise, Equation (7.35a).

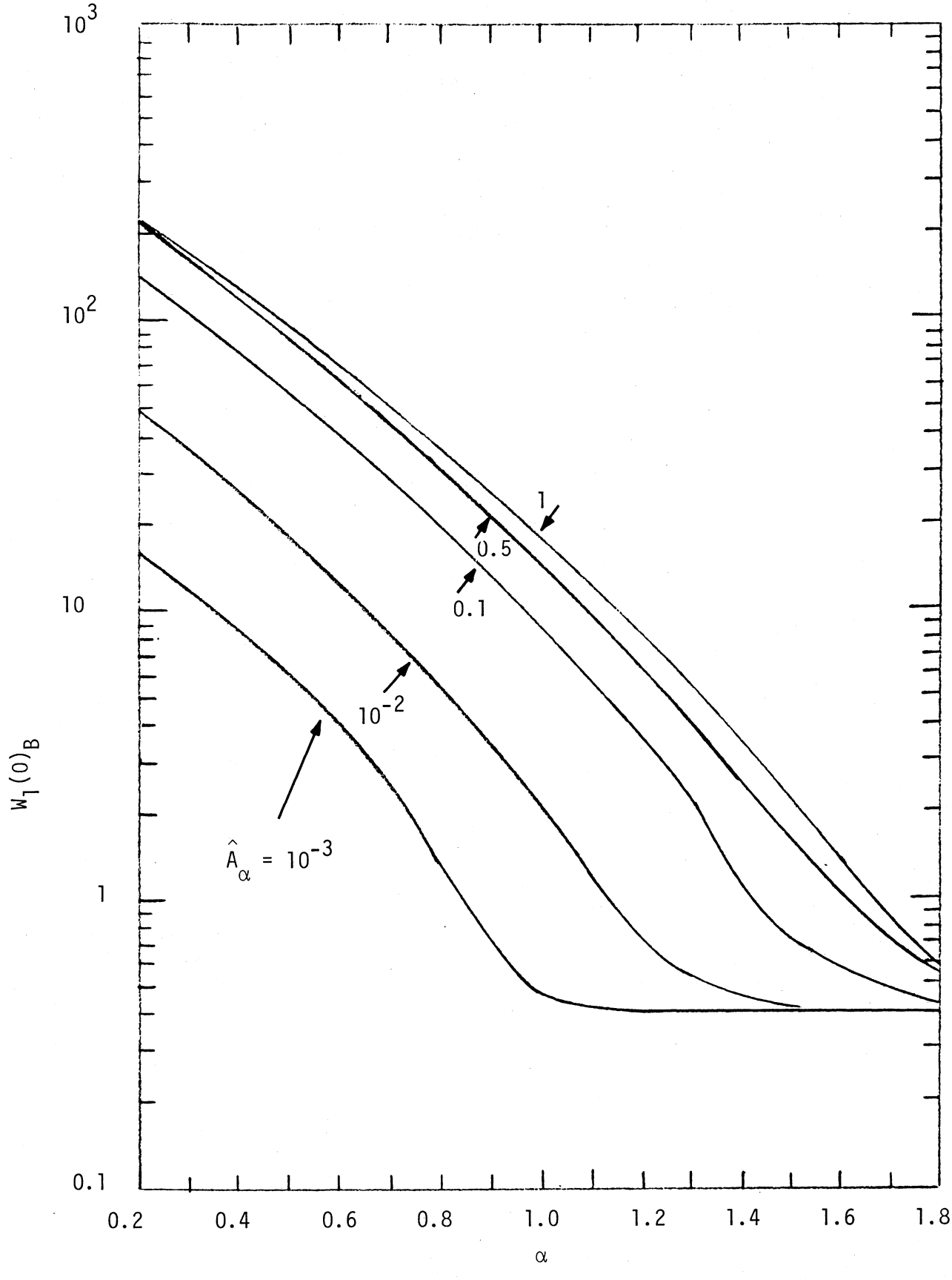

Figure 7.26. The probability density function, evaluated at zero, for Class B noise, Eq. (7.36).

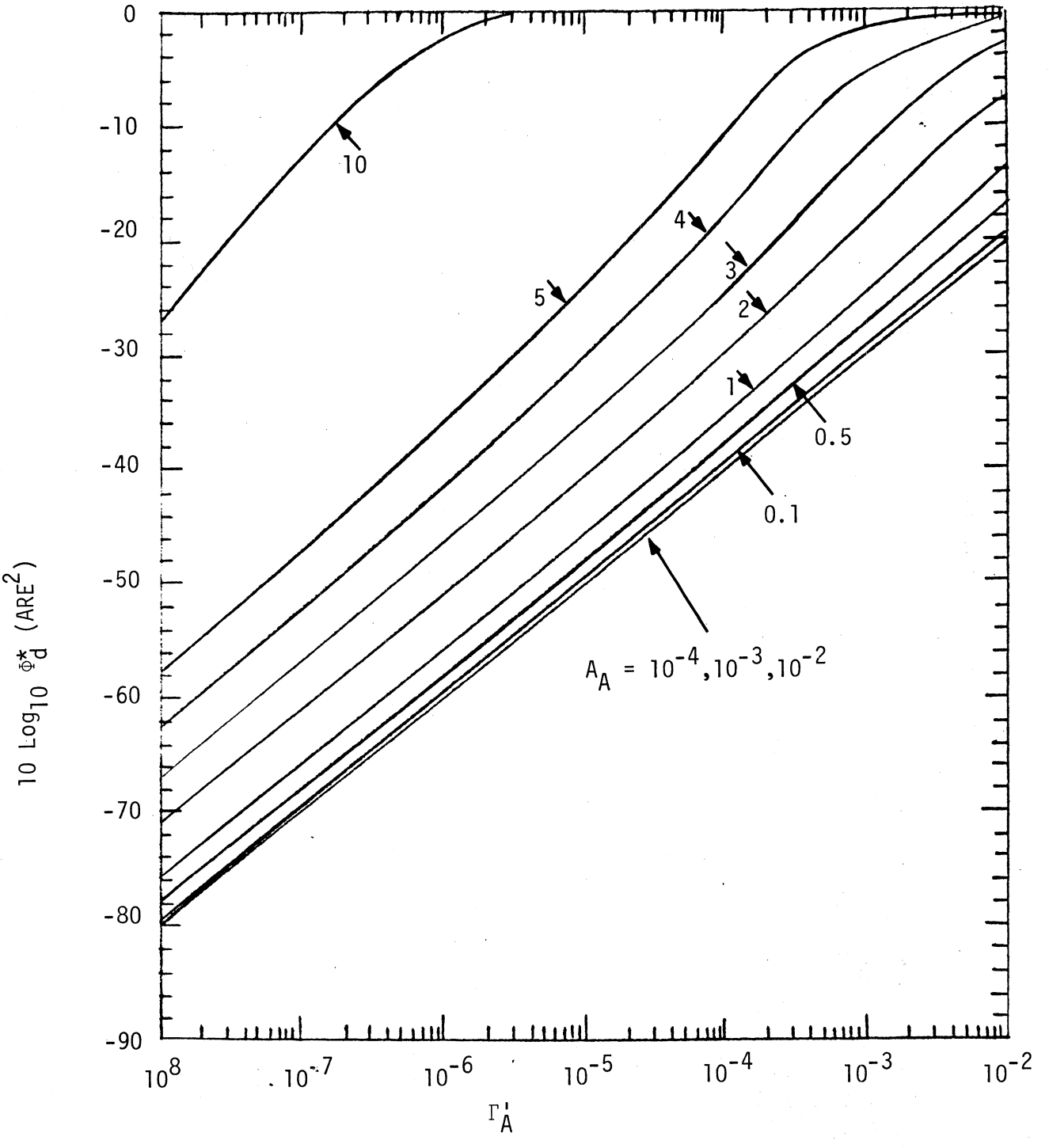

Figure 7.27. The square of the asymptotic relative efficiency, $ARE^2(\Phi_d^*)$, of the simple correlator versus the locally optimum detector for coherent reception, (1) of Table 7.1, for Class A noise.

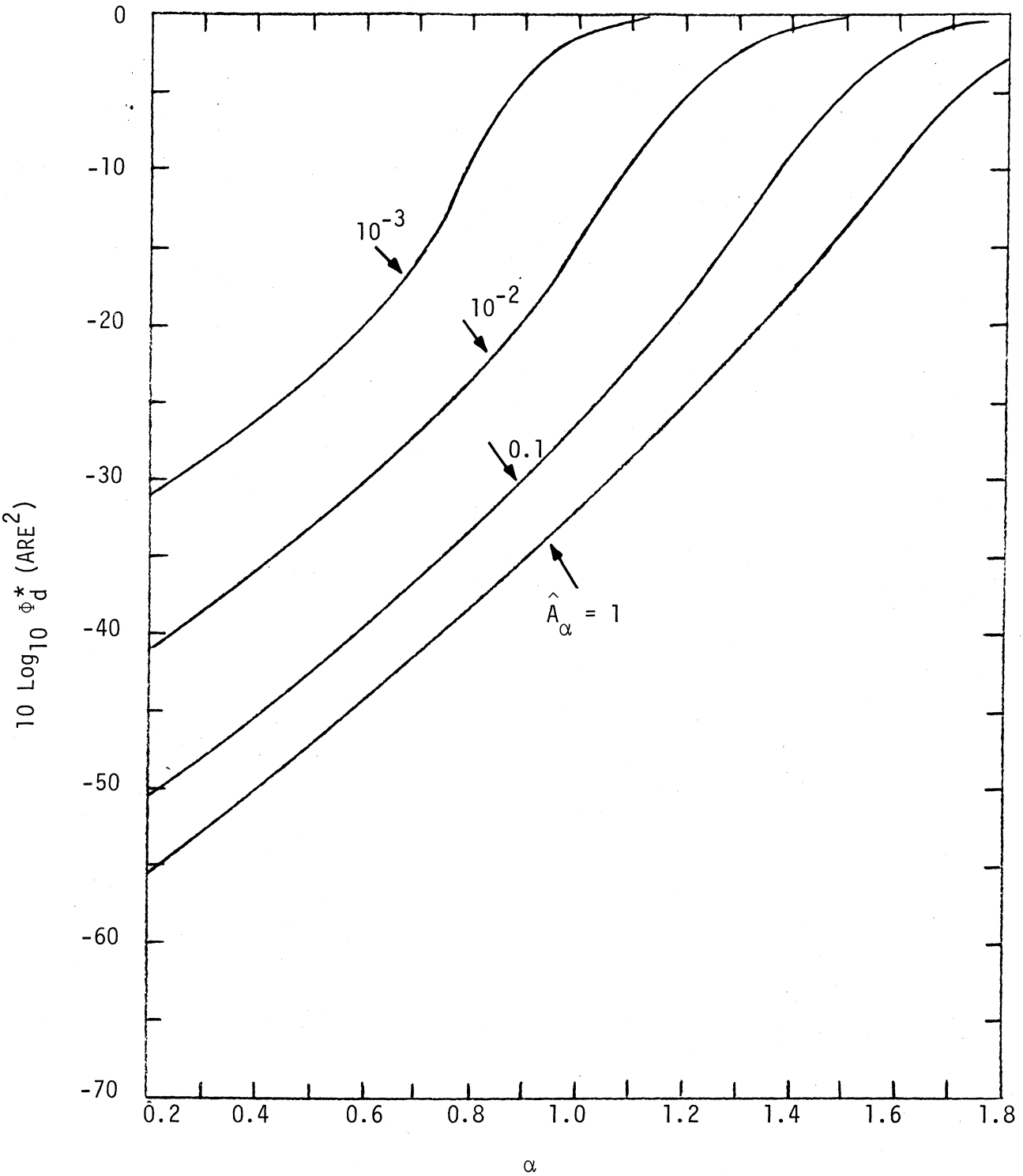

Figure 7.28. The square of the asymptotic relative efficiency, $ARE^2 (\Phi_d^*)$, of the simple correlator versus the locally optimum detector for coherent reception, (1) of Table 7.1, for Class B noise.

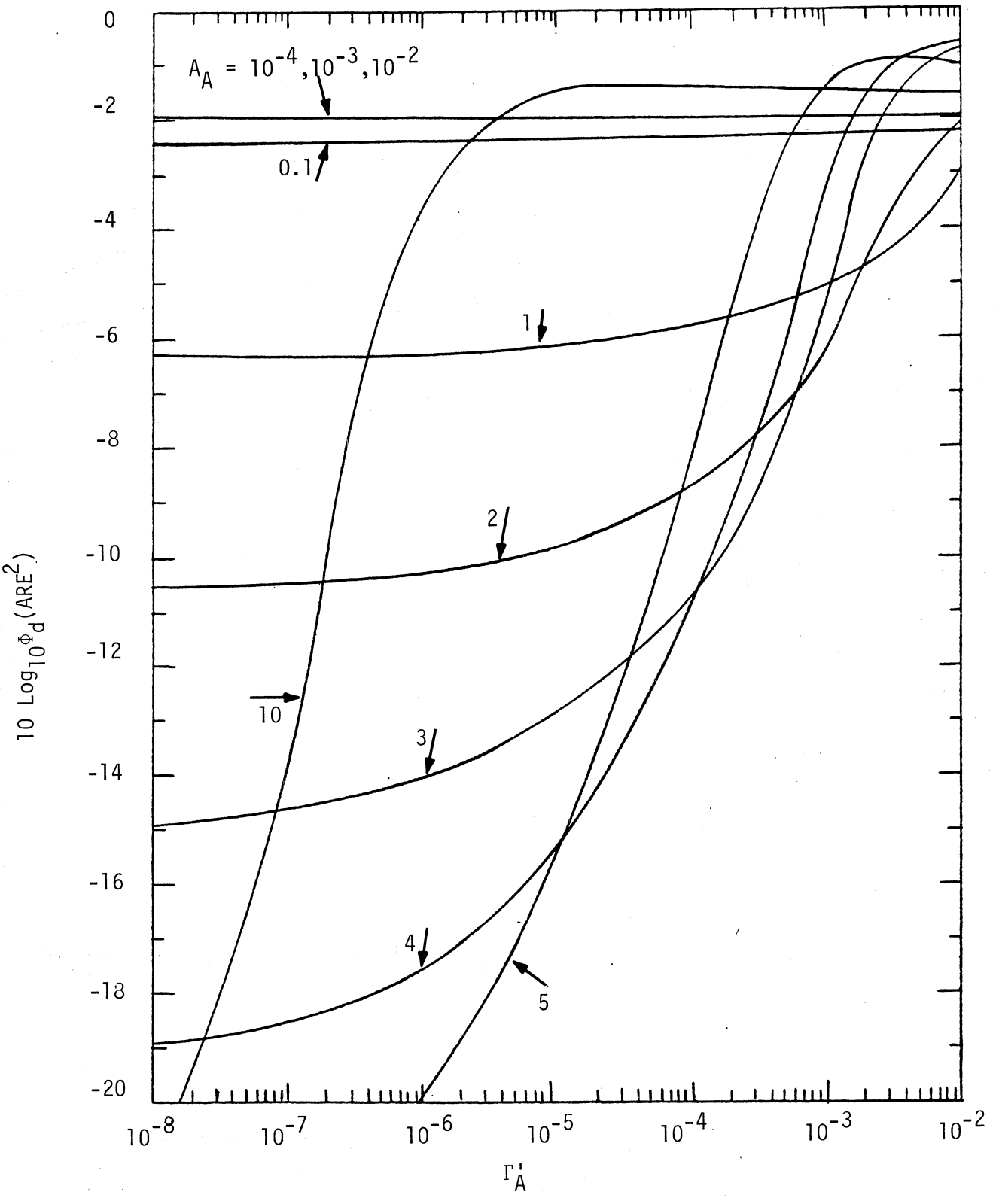

Figure 7.29. The square of the asymptotic relative efficiency, ARE^2 (Φ^*_d), of the clipper correlator (hard limiter) versus the locally optimum detector for coherent reception, (2) of Table 7.1, for Class A noise.

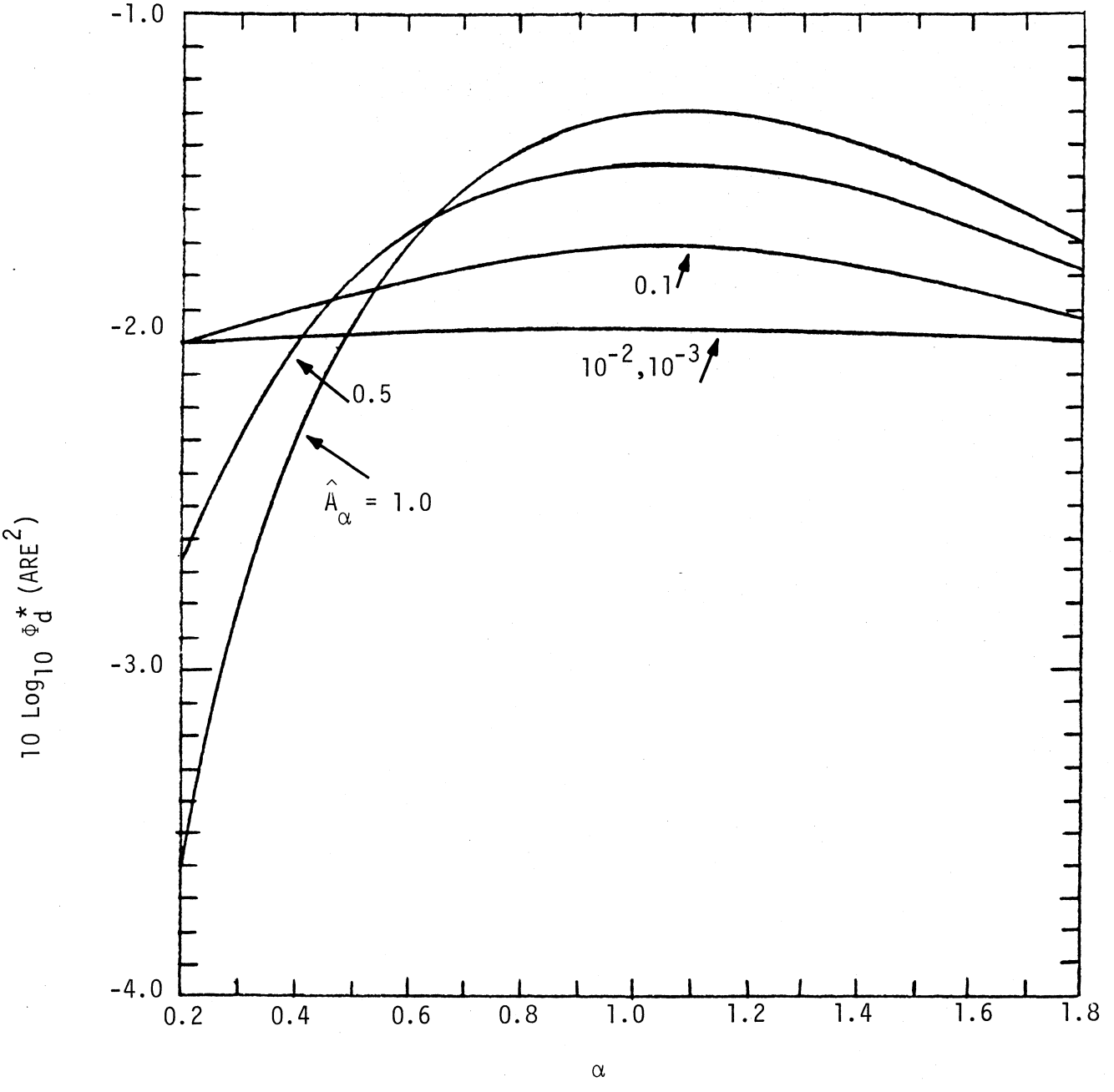

Figure 7.30. The square of the asymptotic relative efficiency, $ARE^{*}(\Phi_d^*)$, of the clipper correlator (hard limiter) versus the locally optimum detector for coherent reception, (2) of Table 7.1, for Class B noise.

7.5 Brief Remarks on Figures 7.1-7.30:

Figures 7.1, 7.2 show the (zero-memory) dynamic characteristics of the LOBD's for several specific Class A and Class B noise cases. Both Class A and B noise require a combination of linear amplifier, and clipper-suppression (negative gain) for the larger amplitudes. The Class A characteristics are, however, somewhat more complex, with a second amplifying-limiting region, cf. Figure 7.1 vs. 7.2. In the Class B cases the characteristic is a clipper-suppressor which is rather insensitive to the nongaussian nature ($\sim\hat{A}_\alpha$) and to the source distribution and propagation conditions ($\sim\alpha$) of the noise.

Figures 7.3-7.6 are essentially self-explanatory: increasing variances (σ_o^{*2}) lead to smaller error probabilities and larger probabilities of correct signal detection, with smaller false alarm probabilities (α_F^*) requiring larger σ_o^{*2}, all of which is entirely expected. Similarly, the tighter the controls the better the performance, as shown in Figures 7.5, 7.6.

In Figures 7.7-7.10 all these Class A nongaussian noise statistics $L_A^{(2)}$, $L_A^{(4)}$, etc., approach their respective limiting gaussian values as $A_A\to\infty$, as expected ($\Gamma_A'>0$); i.e., $L_A^{(2)}\to 1$, $L_A^{(4)}\to 2$, $L_A^{(2,2)}\to 6$, $L_A^{(6)}\to 8$, cf. (7.16). Moreover, when $A_A\to 0$, $\Gamma_A'\to 0$, we also obtain the gaussian limits, as expected, due to the nonvanishing gaussian component $\sigma_G^2>0$ (i.e., $\Gamma_A'\to\infty$). And, of course, the more highly nongaussian is the noise $A_A \doteq \varepsilon(>0)$ the larger is the magnitude of the statistic in question.

The behavior of the corresponding Class B statistics (Figures 7.11-7.24) is similar, although plotted differently. For $\hat{A}_\alpha(\sim A_B)\to\infty$, the curves for $L_B^{(2)}$ etc., fold back on each other, approaching zero db for $L_B^{(2)}\to 1$, 3 db for $L_B^{(4)}\to 2$, etc., cf. (7.16). Similarly, as $\hat{A}_\alpha\to 0$ (i.e., $A_B\to 0$) with $\sigma_G^2>0$, one again has a gaussian pdf, cf. (7.11a), which becomes $w_1(\hat{x})_G=e^{-\hat{x}^2}/\sqrt{\pi}$, as expected, with $\hat{x}\to X/\sigma_G\sqrt{\Omega_B}$, (7.10). Smaller values of α represent more effectively nongaussian interference; i.e., larger values of $L_B^{(2)}$, etc., consistent with the more radical departures of the pdf form gaussian behavior as $|\hat{x}|\to\infty$ [cf. Figure 3.4(II) of [6], for the APD P_{1B} $(\varepsilon\geq\varepsilon_o)$].

The processing gains (per independent sample), as shown in Figures 7.15,7.16, for signals with partially incoherent structure ($Q_n=10$, $n\gg 1$) show the same type of behavior as the various nongaussian noise moments

$L_A^{(2)}$, $L_B^{(2)}$, etc., in Figures 7.7-7.14, and for the same reasons. [For coherent threshold reception, see Figures 7.7,7.11.]

Figures 7.17-7.22 show various bounding values for minimum detectable signals under the equal variance condition (I), Sec. 6.4, for coherent and incoherent reception; see also Figure 6.1 and the discussion of III, Sec. 6.4 above. In general, as the noise becomes more gaussian, these bounds become looser, and vice versa as the interference becomes more nongaussian; e.g., A_A, $\hat{A}_\alpha$, Γ'_A, α, etc. This is consistent with our general observation that the more nongaussian the noise, the smaller, i.e., the tighter the upper bound on the maximum minimum detectable signal $\langle a_o^2 \rangle^*_{min}$ permitted under the AO or equal variance condition.

Figures 7.23a-7.24 compare suboptimum performance against the corresponding optimum performance measures, with the degradation factor, Φ_d^*, as parameter. These curves are entirely canonical in that they apply for any nongaussian (and gaussian) noise, common mode of reception (i.e., coherent, incoherent, or composite), cf. (6.48), and (6.84) vs. (6.90), as long as sample size (n) is large and the AO condition (equal-variance conditions) is obeyed. Thus, once Φ_d^* is properly determined, specific performance measures are at once obtained from these figures.

Figures 7.25,7.26 show typical pdf's at x=o for Class A and B noise, needed in the calculation of the performance of clipper-correlators and comparisons with other optimum and suboptimum threshold detection algorithms, cf. Table 7.1 above.

Finally, Figures 7.27-7.30 show typical Asymptotic Relative Efficiencies[2] (ARE's)[2], viz. Φ_d^*'s, of suboptimum detectors vs. the optimum for the noise in question and the particular mode of observation, in these threshold situations, discussed throughout this study. Characteristically, since the simple correlator is optimum in gaussian noise, as the noise becomes more gaussian, the ARE's for the simple correlator in both Class A and B noise becomes larger (i.e., closer to unity), cf. Figures 7.27,7.28, including $\alpha \to 2$ in the latter (i.e., larger α means less nongaussian, with a fold-over effect in Class B noise as $\hat{A}_\alpha \to \infty$ (not shown in the figures). The ARE's for the clipper-correlator, however, display a fold-over effect as the noise

becomes more nongaussian, until for small A_A, $O(\leq 10^{-1})$, close to the maximum value (0 db) is attained. This maximum cannot be reached here, of course, since the clipper-correlator is never optimum in Class A as gauss noise, although the difference is small, viz., $\frac{2}{\pi}$ = -2 db, cf. Eq. (6.66). A similar behavior is also noted for the clipper-correlator in Class B noise, cf. Figure 7.30, although the range of the fold-over effect as the noise goes from very nongaussian to gauss is much smaller, on the scale of a 10th the amount of the corresponding Class A effect. This shows that the super-clipper (i.e., clipper-correlator) is much less sensitive to impulsive noise (Class B) than to the "coherent" (Class A) noise. Thus, the clipper-correlator makes a comparatively robust processor against Class B noise, and can be fairly close O(4 db to 1.5 db) to the optimum processor in performance, cf. Figure 7.30.

7.6 Numerical Examples (Threshold Detection):

In this (sub) Section, we present a few numerical examples to illustrate the use of the general results of the preceding text. Typical Class A and B noise parameters and scenarios are selected; our attention here is given mainly to the on-off-cases, for comparative simplicity. Thus, we have

$$\underline{\text{Class A Interference}}: \quad A_A = 0.35; \ \Gamma_A' = 5 \times 10^{-5} \quad \text{(canonical, [9])} \tag{7.39a}$$

$$\underline{\text{Class B Interference}}: \quad \hat{A}_\alpha = 1.0; \ \alpha = 1.2; \ \Omega = 0.00207, \quad \text{("Saipan Noise," [33])}^\dagger \tag{7.39b}$$

with the various other parameters of observation being $n = 10^4$, $p_D^* = 0.90$, $P_e^* = 10^{-4}$, $\alpha_F^* = 10^{-4}$, typically; symmetrical channels are also assumed: $p = q = 1/2$, $\gamma_{I.0} = 1$. Typical results follow below.

---

†The value of $L^{(2)}$ in [33] is 4.5 db higher as a result of different intensity normalization and scaling.

I. Optimum Detection

Example 1: Performance Probabilities:

From Figures 7.3,7.4 we find at once for the values of P_D^*, P_e^*, α_F^* above that

$$\sigma_o^{*2}\Big|_{I.O} = 17.3 \text{ db } (p_e^* = 10^{-4}); \quad \sigma_o^{*2}\Big|_{N.P.} = 14.2 \text{ db} \qquad (7.40)$$

$$(\alpha_F^* = 10^{-4},\ p_D^* = 0.9);\ n>>1 \ .$$

These results apply directly, also, to suboptimum detectors (σ_o^2, etc.), for values of $P_e = P_e^*$, etc., again, provided the sample size is large ($n>>1$) and that $\sigma_1^2 \doteq \sigma_o^2$: the equal variance condition holds (so that Eq. (7.13) remains valid).

Related to the above are the results of Figures 7.5,7.6, for $\sqrt{B^*} = C^*$, etc. For the performance measures of our example above, we find at once that

$$\sqrt{B^*} = C_{N.P.}^* = 5.6 \text{ db } (= 3.63)\ ;\ C_{I.O}^* = 7.2 \text{ db } (= 5.25) \qquad (7.41)$$

Example 2: Coherent Detection in Class A Noise:

Here we wish to establish the minimum detectable signal $\left\langle a_o^2 \right\rangle_{\text{min-coh}}^*$ associated with the above operating conditions when the Class A noise of (7.39a) above embodies the interference. From (6.10) in (6.11a,b) we get directly

$$\boxed{\left\langle a_o^* \right\rangle_{\text{min-coh}}^2 = \frac{B^*}{nL_A^{(2)}(1-\eta)}} \quad ; \quad (1-\eta \equiv \bar{a}_o^2 \Big/ \overline{a_o^2}\ ;\ 0 \leq \eta < 1). \qquad (7.42)$$

For no or shallow fading, i.e., $\eta \sim 0$, but complete signal coherence ($\bar{s}_i = \sqrt{2}$), the upper bound, $x_{max} << x_{OA}^*$ on the permitted values of minimum detectable signal which still preserve the AO character of this optimum threshold algorithm is given by (6.71)

$$\overset{v}{x}_{max} = \overset{v}{x}^*_{OA} - 15 \text{ db} \quad ; \quad \overset{v}{x}^*_{OA} = 10 \log 3 \times 10^{-5} = -45 \text{ db (Fig.7.17)}, \quad (7.43)$$

so that the upper bound here is $\overset{v}{x}_{max} = -45-15 = -60$ db. [The "<<" in $x_{max} << x^*_{OA}$ is usually taken to be 15 db.]

Next we use (7.42), $\overset{v}{n} = 40$ db, with $L_A^{(2)} = 41.5$ db from Figure 7.7 and $B^* = 11.2$ db for the N.P. detector from (7.41), so that

$$\left\langle \overset{v}{a}_o^2 \right\rangle^*_{min\text{-}coh} \Big|_{N.P.} = 11.2 - 40 - 41.5 = -70.3 \text{ db}, \quad (7.44a)$$

which is substantially below the x_{max} bound (-60 db), so that the AO condition is amply satisfied. Likewise, from (7.41) for the I.O. we obtain

$$\left\langle \overset{v}{a}_o^2 \right\rangle^*_{min\text{-}coh} \Big|_{I.O.} = 14.4 - 40 - 41.5 = -67.1 \text{ db}. \quad (7.44b)$$

If the fading is moderately deep, e.g., $\eta = 0.99$, $(1 \overset{v}{-} \eta) = -20$ db, then the x^*_{OA} obtained from (6.71) using $L^{(2)}$ and $L^{(2,2)}$ from Figures 7.7 and 7.9, $L^{(2)} = 41.5$ db, $L^{(2,2)} = 90$ db, is $x^*_{OA} = 2.8 \times 10^{-5}$ or $\overset{v}{x}_{max} = -45.5-15 = -60.5$ db. Again from (7.41) and (7.42), with $(1 \overset{v}{-} \eta) = -20$ db, we obtain

$$\left\langle \overset{v}{a}_o^2 \right\rangle^*_{min\text{-}coh} \Big|_{N.P.} = 11.2-40-41.5+20 = -50.3 \text{ db},$$

and $\quad (7.44c)$

$$\left\langle \overset{v}{a}_o^2 \right\rangle^*_{min\text{-}coh} \Big|_{I.O.} = 14.4-40-41.5+20 = -47.1 \text{ db},$$

which are above the x_{max} bound, so that the estimate of $\left\langle a_o^2 \right\rangle^*_{min}$ may be suspect.

Example 3: Coherent Detection in Class B Noise:

For this example we repeat the calculations of $\left\langle a_o^2 \right\rangle^*_{min\text{-}coh}$, (7.42), in the manner of Example 2, but now with the values of $L_B^{(2)}$, $\overset{v}{x}^*_o$ appropriate to our particular Class B case (7.39b). From Figures 7.11 and

7.13 we get $L_B^{(2)} = 25$ db and $L_B^{(2,2)} = 56$ db. For no or shallow fading ($\eta = 0$), $\overset{v}{x}{}_o^* = -25$ db (Figure 7.20), and for moderate or deep fading ($\eta \geq 0.99$), $\overset{v}{x}{}_o^* = -28.2$ db. From (7.41) in (7.42), with $n = 10^4$, we obtain, for no or little fading

$$\left\langle a_o^2 \right\rangle^*_{\text{min-coh}} \Big|_{\text{N.P.}} = 11.2\text{-}40\text{-}25 = -53.8 \text{ db}, \tag{7.45a}$$

$$\left\langle a_o^2 \right\rangle^*_{\text{min-coh}} \Big|_{\text{I.O.}} = 14.4\text{-}40\text{-}25 = -50.6 \text{ db}, \tag{7.45b}$$

with $\overset{v}{x}_{max} = -25\text{-}15 = -40$ db. With even moderately deep fading [O(20db)], $\overset{v}{x}_{max} = -43.2$ db and $a_o^{2\,*}_{\text{min-coh}} = -33.8$ db and -30.6 db, respectively, for N.P. and I.O., so that even moderate fading cannot be tolerated.

Example 4: Incoherent Detection in Class A Noise:

We parallel Example 2, for the conditions as before, but now using (6.24) and (6.25) in (6.27), or (7.19a) with (7.20a) above in conjunction with (6.27), to write for the minimum detectable signal in Class A noise, when threshold detection is incoherent:

$$\left\langle a_o \right\rangle^*_{\text{min-inc}} = \left\{ 8\, B^* \Big/ nL^{(4)} \left[1 + \frac{2L^{(2)^2}}{L^{(4)}} (Q_n - 1) \right] \right\}^{\frac{1}{2}} \tag{7.46}$$

Now, from (6.58)' we have for coherent sinusoidal waveforms

$$Q_n \doteq \frac{n}{2} \text{ (slow fading)} \; ; \; Q_n \doteq \frac{n}{2} (1-\eta)^2 \text{ (rapid fading)}. \tag{7.46a}$$

For incoherent signal waveforms, $Q_n - 1 \doteq 0$. Accordingly, for the large samples ($n \gg 1$) required for (AO) threshold detection, (7.46) reduces to

(i) coherent signals:

$$\left\langle a_o^2 \right\rangle^*_{\text{min-inc}} \Big|_{\text{slow}} = \sqrt{8B^*}/nL^{(2)} \ ,$$

and (7.47a)

$$\left\langle a_o^2 \right\rangle^*_{\text{min-inc}} \Big|_{\text{rapid}} = \sqrt{8B^*}/nL^{(2)}(1-\eta), \ \frac{n}{2}(1-\eta)^2 >> 1 \ ,$$

since $L^{(2)^2}/L^{(4)} = O(1)$. (In fact, from Figures 7.7 and 7.8, $L^{(2)} = 41.5$ db, $L_A^{(4)} = 86$ db, so that $L^{(2)^2}/L^{(4)} = -3$ db.)

With incoherent signal structure ($Q_n = 1$), (6.46) reduces, for both slow and rapid fading, to

(ii) incoherent signals:

$$\left\langle a_o^2 \right\rangle_{\text{min/inc}} \doteq \sqrt{8B^*/nL^{(4)}} \ . \tag{7.47b}$$

Specific numerical results may be obtained at once for the postulated observation conditions above. We have [cf. (7.41)]:

$$\left\langle a_o^2 \right\rangle^*_{\text{min-inc}} \Big|_{\substack{\text{coh.sig.} \\ \text{slow} \\ \text{N.P.}}} = 4.5+5.6-40-41.5 = -71.4 \text{ db}, \tag{7.48a}$$

$$\left\langle a_o^2 \right\rangle^*_{\text{min-inc}} \Big|_{\substack{\text{coh.sig.} \\ \text{rapid} \\ \text{N.P.}}} = -71.4-(1\overset{v}{-}\eta) \text{ db}, \quad \text{and} \tag{7.48b}$$

$$\left\langle a_o^2 \right\rangle^*_{\text{min-inc}} \Big|_{\substack{\text{inc.sig.} \\ \text{any} \\ \text{N.P.}}} = 4.5+5.6-20-43 = -52.4 \text{ db} \ . \tag{7.48c}$$

The corresponding results for the I.O. are 1.6 db greater (=7.2-5.6) from (7.41). As expected, incoherent signal waveforms result in truly incoherent

detection, with a $\sqrt{n}$ -dependence on sample size vs. the n-dependence obtainable with coherent waveforms. Thus, a channel which destroys signal coherence greatly reduces the detectability of the resultant signal (O(20 db) here), as is well-known.

To complete our analysis, we need to establish the bound $y_{max} << y_o^*$. From Figure 7.19 for coherent waveforms, and Figure 7.18 for the incoherent waveform cases, we get respectively for y_o^*,

$$y_{OA}^* \Big|_{\text{coh-sig}} = -52.5 \text{ db} \; ; \; y_{OA}^* \Big|_{\text{inc-sig}} = -54 \text{ db} . \tag{7.49}$$

Our results (7.48a,c) above for the coherent signals fall acceptable below $y_{max} = -52.5-15 = -67.5$ db, as long as the rapid fading is not too deep, but for the incoherent signals sample-size is not sufficiently large to put $\langle a_o^* \rangle^*_{\text{min-inc}}$ below y_o^* to insure the AO character of the algorithm (and that the performance measures are themselves the required good approximations). Thus, this last result, (7.48c), really represents a suboptimum threshold algorithm, with a suspect estimate of $\langle a_o^2 \rangle_{\text{min}}$, and performance.

Finally we note the "anomalous" behavior here of (optimum) coherent versus incoherent detection: $\langle a_o^2 \rangle^*_{\text{min-coh}} > \langle a_o^2 \rangle^*_{\text{min-inc}}$ for otherwise the same reception conditions†. For a discussion of this effect, see Section 6.4,III and Figure 6.1.

---

† We note that the "anomalies" are not due to the particular values of $L^{(2)}_{A,B}$, but rather reside analytically in the quantities $B^*_{N.P.}$ or $B^*_{I.O.}$; i.e., from (7.42) and (7.47a),

$$\langle a_o^2 \rangle^*_{\text{min-coh}} - \langle a_o^2 \rangle^*_{\text{min-inc}} = (B^* - \sqrt{8B^*})/nL^{(2)}(1-\eta) .$$

From Figures 7.5 and 7.6 we see that $B^* - \sqrt{8B^*} < 0$, i.e., $\langle a_o^2 \rangle^*_{\text{min-coh}} < \langle a_o^2 \rangle^*_{\text{min-inc}}$, for those P_e^* or p_D^* where $C^* = \sqrt{B^*} < \sqrt{8} = 4.5$ db, i.e., when $P_e^* > 2\times 10^{-2}$, or when $p_D^* < 0.62 (\alpha_F^* = 10^{-4})$. Physically, as discussed in Section 6.4, III, this "anomalous" behavior stems from the different amounts of signal and noise information lost and gained for incoherent vis-à-vis coherent detection.

Example 5: Incoherent Detection in Class B Noise:

The analytic results (7.47) apply equally well here, with now $L_B^{(2)} = 25$ db and $L_B^{(4)} = 53.5$ db from Figure 7.12. From Figures 7.21,7.22 we get the limits

$$y_{0B}^* = -35.5 \text{ db (inc.sig.)} \; ; \; y_{0B}^* = -36.6 \text{ db (coh. sig.)} \quad . \tag{7.50}$$

We summarize the results for the corresponding minimum detectable signals:

$$\left\langle a_o^2 \right\rangle^* \begin{cases} = -54.9 \text{ db} & \text{(coh.sig.,slow,N.P.)}, \\ = -54.9 - (1 \overset{v}{-} \eta) \text{ db} & \text{(coh.sig.,rapid,N.P.)}, \\ = -36.1 \text{ db} & \text{(inc.sig.,any,N.P.)}, \end{cases} \tag{7.50a}$$

again with the I.O. results 1.6 db greater. With $y_{max} \ll y_{0B}^*$, or $y_{max} = -50.5$ db for coherent signal structures, the minimum detectable is acceptably below y_{max}. On the other hand, larger sample sizes are needed to make the minimum detectable signals fall within acceptable AO limits when the signal waveform is incoherent.

Example 6: Composite Detection in Class A and B Noise:

From the results of Section 6.5 (6.88a,b) we may write for the minimum detectable signal when an (optimum) composite threshold detection is used, the following special results for coherent signal waveforms:

$$\left\langle a_o^2 \right\rangle^*_{\text{min-comp}}\Big|_{\text{slow}} \doteq \frac{\sqrt{8B^*} - 4\,(1-\eta)}{nL^{(2)}} \quad , \quad B^* \gg 2(1-\eta)^2 \quad , \tag{7.51a}$$

$$\left\langle a_o^2 \right\rangle^*_{\text{min-comp}}\Big|_{\text{rapid}} \doteq \frac{\sqrt{8B^*} - 4}{nL^{(2)}(1-\eta)} \quad , \; B^* \gg 2, \; Q_n \gg 1 \quad . \tag{7.51b}$$

[For incoherent signal waveforms ($\Pi_{coh}^* \to 0$), the composite detector, of course, reduces to the purely incoherent detector of (7.47a), discussed in Examples 4,5 above.]

Comparing (7.51a,b) with (7.47a) we see that $\langle a_o^2 \rangle^*_{\text{min-comp}} < \langle a_o^2 \rangle^*_{\text{min-inc}}$ always for slow or rapid fading: there is no "anomalous" behavior here. Moreover, it is easy to demonstrate this; for example, let $x=B^*$, so that (7.51a) vs. (7.47a) becomes

$$\begin{aligned} \sqrt{8x}-4(1-\eta) &\overset{?}{\leq} \frac{x}{1-\eta} \\ 0 &\leq \frac{x^2}{(1-\eta)^2} + 16(1-\eta)^2, \quad \text{all } x \geq 0 \quad , \end{aligned} \tag{7.52}$$

and similarly for (7.51b).

One important feature of the composite (threshold) detector to be noted is its insensitivity to slow fading, vis-à-vis the coherent detector, i.e., (7.51a) vs. (7.42). A second is the possibly strong superiority over either the coherent or incoherent detector, as expressed by smaller minimum detectable signals, particularly when there is significant fading. This superiority vs. the incoherent detector is O(1.5 db) and is 0 (3 db) vs. the coherent detector with no fading, as the numerical results below indicate, and is 0 (10-20 db) when there is moderate fading (η=0.99).

For the specific noise and signal examples assumed here we have for no fading:

$$\underline{\text{Class A}}: \quad \langle a_o^2 \rangle^*_{\text{min-comp}} = \frac{2.83 \times 3.63 - 4}{10^4 \times 1.41 \times 10^4} = -73.6 \text{ db} \quad \text{(N.P.)} \quad , \tag{7.53a}$$

with the corresponding result for the I.O. of -71.1 db.

$$\begin{aligned} \underline{\text{Class B}}: \quad \langle a_o^2 \rangle^*_{\text{min-comp}} = \frac{2.83 \times 3.63 - 4}{10^4 \times 3.16 \times 10^2} &= -57 \text{ db} \quad \text{(N. P.)} \\ &= -54.7 \text{ db} \quad \text{(I.O.)} \quad . \end{aligned} \tag{7.53b}$$

These figures are to be compared with (7.44a,b) and (7.45a) for the corresponding coherent detector results and with (7.48a) for the corresponding incoherent detector results.

For moderate slow fading (η=0.99), (7.51a) gives:

$$\underline{\text{Class A}}: \quad \left\langle a_o^2 \right\rangle^*_{\text{min-comp}} = \frac{2.83 \times 3.63 - 4(.01)}{10^4 \times 1.41 \times 10^4} = -71.4 \text{ db (N.P.)} \qquad (7.53c)$$

with the corresponding result for the I.O. of -69.8 db.

$$\underline{\text{Class B}}: \quad \left\langle a_o^2 \right\rangle^*_{\text{min-comp}} = \frac{2.83 \times 3.63 - 4(.01)}{10^4 \times 3.16 \times 10^2} = -54.9 \text{ db (N.P.)}$$
$$= -53.3 \text{ db (I.O.)} \quad . \qquad (7.53d)$$

The corresponding fading results are given by (7.44c) for the coherent detector (Class A).

In general, the composite detector is to be recommended for its comparative insensitivity to slow fading. Observe that the stricter of the two possible bounds (x_o^*, y_o^*) is that for incoherent detection, i.e., from examples 2,3 and (7.49),(7.50) we have y_{OA}^* = -52.5 db (coh.sig. structure) and y_{OB}^* = -36.6 db, similarly. The results (7.53a,b) are accordingly within the limits $y_{\text{max-A}}$ = -52.5 - 15 = -67.5 db, and $y_{\text{max-B}}$ = -36.6 - 15 = -51.6 db.

Still other numerical examples can be readily constructed along these lines.

II. Suboptimum Detection and Comparisons:

Here let us use the results of Section 7.4, especially (7.25)-(7.38) and Table 7.1. We shall consider only a few examples here, by way of illustration.

For the two specific Class A and B noise cases, and reception conditions postulated here above, we begin by obtaining specific degradation factors (Φ_d^*) and ARE's from Figures 7.27-7.30 for coherent waveforms.

$$\underline{\text{Class A}}: \quad \begin{aligned} \Phi_d^* &= -41.5 \text{ db} \quad \text{(Figure 7.27, simple correlator)}, \\ \Phi_d^* &= -\ 3.5 \text{ db} \quad \text{(Figure 7.29, clipper correlator)}, \end{aligned} \tag{7.54}$$

$$\underline{\text{Class B}}: \quad \begin{aligned} \Phi_d^* &= -25.0 \text{ db} \quad \text{(Figure 7.28, simple correlator)}, \\ \Phi_d^* &= -\ 1.3 \text{ db} \quad \text{(Figure 7.30, clipper correlator)}. \end{aligned} \tag{7.55}$$

Now, Φ_d^* measures the <u>increase</u> required for the (input) minimum detectable signal (n>>1) in suboptimum <u>coherent</u> threshold detection to obtain the same performance as the corresponding optimum threshold detector. Thus, we see that simple correlators are strongly degraded in Class A noise: 41.5 db in $\langle a_o^2 \rangle_{\text{min-coh}}$ for our particular example. On the other hand, the degradation is a much less severe, though a noticeable 3.5 db, when the suboptimum clipper-correlator is used. Similar behavior is noted in our Class B example here: 25.0 db and 1.3 db, respectively.

When <u>incoherent</u> reception (of coherent signals) is employed, the degradation in $\langle a_o^2 \rangle_{\text{min}}$ is halved (in db) cf. (6.53), viz. -20.8, -1.8 db (Class A), and -12.5 db, -0.7 db (Class B), respectively, again for the same performance and sample sizes.

On the other hand, the more limited ARE's, (Sec. 6.3.3), (III, Sec. 7.4), (6.60), and Table 7.1, show that $(\text{ARE})_{\text{inc}} = (\text{ARE})^2_{\text{coh}} = \Phi^*_{\text{d-coh}}$ (for coherent signal waveforms). For example, in the coherent cases, ARE of clipper-correlator to optimum = $\frac{1}{2}(-3.5) = -1.8$ db, cf. (7.54) in Class A noise, and is -0.7 db in our Class B noise above, cf. (7.55). In contrast, the ARE of the simple correlator is -20.8 db, and -12.5 db, respectively, in Class A and B interference [cf. (7.54),(7.55)]. Of course, the more complete and revealing measures of performance are the error probabilities (P_e^*, P_e) and the probabilities of correct signal detection (p_D^*, p_D) themselves, or the associated minimum detectable signals (which are implicit functions of these probability controls, through B* or B, cf. (7.41), or (6.11b), and Figures 7.5, 7.6.

Other related comparisons may be made the same way. For example, for the same minimum detectable signal and probability control [Case III, Sec. 6.3] we can determine how much longer data acquisition must be for various suboptimum algorithms vis-à-vis the corresponding optimum algorithm (i.e., how much larger sample size n is vs. n*). For our particular example above (coherent detection) we find that:

(i.) Optimum vs. Simple-Correlator:

$$n_{coh} = n^*_{coh}/\Phi^*_d = n^*_{coh} L^{(2)}_{A,B} \quad , \tag{7.56}$$

or

$$n_{coh} = 1.41 \times 10^4 \times n^*_{coh} \qquad \text{(Class A)} \ ,$$

and

$$n_{coh} = 3.2 \times 10^2 \times n^*_{coh} \qquad \text{(Class B)} \ . \tag{7.56a}$$

Likewise,

(ii.) Optimum vs. Clipper-Correlator:

$$n_{coh} = 2.24 \times n^*_{coh} \qquad \text{(Class A)},$$

and

$$n_{coh} = 1.35 \times n^*_{coh} \qquad \text{(Class B)}. \tag{7.56b}$$

Again, the simple-correlator is much inferior to the corresponding optimum processor, requiring a much larger sample (or observation time), whereas the clipper-correlator is considerably closer to optimum, requiring only about a factor of two (or less) increase in sample size (n). Similar behavior is encountered in the noncoherent cases, cf. (6.56),(6.57), where we must implement Eqs. (7.31)-(7.38) for specific numerical results.

Many other comparisons between optimum and suboptimum threshold algorithms can be carried out in similar fashion based on the analytic and computational results in this study. We reserve such to a subsequent investigation.

8. SUMMARY OF RESULTS AND CONCLUDING REMARKS:

Here we briefly summarize the principal general results of this study, reminding the reader that the detailed quantitative, analytic results are developed principally in Sections 2 through 7, and in the various Appendices following, as a review of the Table of Contents reveals.

Sections 2 through 4 are mainly an overview of recent earlier work, needed for the subsequent developments of Sections 6 and 7, containing some new material on suboptimum detection algorithms. Section 5 focuses on the structural form of the various optimum threshold detectors, which, like the analytic theory herein described, is canonical; i.e., independent of specific signals and noise. The principal result here is the observation that these threshold algorithms require a double matching process--the earlier, and more familiar linear matched filter for the signal, against a nonlinear transformation of the input noise (and possibly weak signal)--and an initial matching of the receiver to the noise itself: namely, the above-mentioned nonlinear transformation of the (sampled) input data $\underset{\sim}{x}$. The specifics of this transformation dynamics depends, of course, on the pdf of the noise. The overall character of the receiver is adaptive--to the noise, and to the desired signal, as we note more fully below in (11).

Sections 6 and 7, along with the appendices, contain the bulk of the many new results, in particular for incoherent and composite detection. Let us now briefly list the principal general results:

(1) The optimum coherent threshold detector is superior (in the sense of smaller minimum detectable signal, etc.) to the corresponding incoherent detector when the signal waveform is incoherent, as often happens, for instance, when there is a doppler spreading produced in the channel. On the other hand, for coherent signal waveforms, these coherent and incoherent detectors are essentially comparable in threshold detection [cf. Section 6.4, III; Examples 2-5, Section 7.6].

(2) Threshold optimum systems are superior to (threshold) suboptimum systems, as expected. The former can be very much better O(20 db or more) than conventional detectors, optimized against gaussian system noise; e.g., simple correlation detectors. They are less dramatically superior O(2-6 db or so) to clipper-correlation detectors (which employ hard limiters). The

degree of superiority is also greater for Class A noise than it is for the "impulsive" Class B interference (cf. Section 7.6). These results support the use of simple, approximate detector structures, like the clipper-correlation detector, vis-à-vis the exact characteristics (cf. Figures 7.1,7.2a,b) in many instances, because of the much greater complexity of the latter.

(3) We remark that the optimum threshold detectors themselves become suboptimum for input signal levels above some limiting value, where the condition for asymptotic optimality (AO), namely, (approximately) equal variances of the test statistic under H_0 and H_1, is no longer satisfied. It is then not guaranteed that they will remain superior to the aforementioned (or any other) suboptimum detector. However, performance, on an absolute basis, improves for both as the input signal level rises. This means, of course, that even if the AO condition no longer holds, we can still adequately use the originally optimum threshold algorithm.

(4) For these threshold detectors to maintain their optimality for the large data sample sizes ($n>>1$) needed to achieve adequately small decision error probabilities for the very small input signals which are encountered, it is critical that the algorithm include the proper bias term, $\hat{B}_n^*$. This bias is obtained by terminating (under H_0) the basic expansion of the generally optimum likelihood ratio about the null signal ($\theta=0$), cf. Section 2. This bias is solely a function of rms input signal level (a_0^2), sample size (n), the basic noise statistics and second-order signal statistics. In fact, it is shown that $\hat{B}_n^*$ is $-\frac{1}{2}\,\mathrm{var}_0 g_n^* = \frac{1}{2}\left[\langle g_n^{*2}\rangle_{H_0} - \langle g_n^*\rangle_{H_0}^2\right] = -\frac{1}{2}\sigma_0^{*2}$, cf. Appendix, Section A.3-6. Without this proper bias term (lacking in most analyses of the threshold detection problem [48]), performance can be far from optimum [cf. end of Section 6.3].

(5) For best operation, the composite detector is proposed: this is the sum of the coherent and (purely) incoherent algorithms [cf. Section 6.5]. When it is possible to take advantage of the coherent mode as well as the incoherent one, the result is an improvement in performance O(2 db or more) over incoherent reception, and markedly so O(10 db+, η=0.9+) against fading to which (slow or rapid) the coherent detection is particularly vulnerable, as is the incoherent detector to rapid fading, cf. Example 6, Section 7.6. These observations apply generally to both the optimum and suboptimum threshold detectors.

(6) A very important feature of the analysis generally is its canonical character: this is true equally of the statistical-physical noise models employed and of the (optimum) threshold forms of detection algorithm. The formal structure of both algorithm and performance measure is independent of specific physical models. This gives the threshold theory its very considerable breadth: it is possible to indicate the basic functional elements of the algorithms' operations without having to choose a specific physical, numerical example.

(7) Another important feature of the present approach is its definition and use of the concepts of minimum detectable signal and processing gain [cf. Section 6.2 et seq.]. These, in turn, require a nonvanishing input signal, which is certainly the case practically. The AO condition [cf. (3)] is really a condition of small but nonzero input signals, sometimes referred to as "vanishingly small": we call it here "practically small"; i.e., small enough that the AO condition is practically approximated; e.g., $\overset{v}{x}_{max},\overset{v}{y}_{max} = \overset{v}{x}^*_o,\overset{v}{y}^*_o$ - 15 db, say, so that $\sigma_1^{*2} \doteq \sigma_o^{*2}$, where $\sigma_1^{*2} = \sigma_o^{*2} + F(n,\theta)$ and $\therefore$ $|F(n,\theta)| << (\sigma^*_o)^2$ or $|F_n|/\sigma_o^{*2} << 1$, cf. Sections 6.2, 6.4. The minimum detectable signal and processing gain permit a variety of useful system comparisons, both between optimum detectors in different modes of operation and between optimum and suboptimum receivers.

(8) The concept of Asymptotic Relative Efficiency (ARE), cf. Section 6.3, IV, though useful here, is not a complete nor necessarily reliable measure of system comparisons. A more effective measure is the degradation factor, $\Phi^*_{d\text{-}coh}$, $\Phi^*_{d\text{-}inc}$, etc., which specifies the increase needed in the minimum detectable signal of suboptimum (threshold) detectors to achieve the same performance as the corresponding optimum detector [cf. Section 7.6, II, also]. Since the minimum detectable signal is an implicit function of the performance probabilities, as well as sample size, noise statistics, etc., it is itself a "complete" performance measure also, while the ARE is not. Error probabilities (and/or probabilities of correct signal detection) are likewise the corresponding "complete" measures of performance, vis-à-vis signal-to-noise ratio, and the ARE, which is of the same level of statistical incompleteness.

(9) The rôle of discrete vis-à-vis continuous sampling is also examined here, in sufficient detail to explain the often "anomalous" behavior of incoherent threshold detectors (for the same P_e^* or p_D^* and sample size, n), giving smaller minimum detectable signals than the corresponding coherent threshold detectors, under discrete sampling, cf. Section 6.4, III. Although these effects are noticeable, they are small O(1-3 db).

(10) Another canonically important feature of the threshold theory is that it provides both structural and performance limits in the optimum cases. Such limits are critical if one is to decide what practical (usually rather suboptimum) systems are to be employed, within the available economy. Often the sacrifice of a few db in $\langle a_o^2 \rangle_{inc}$ is more than compensated for by the resulting simplicity and comparative inexpensiveness of the realization of the algorithms.

(11) In the larger sense, as well as in the particular, these threshold detection algorithms represent adaptive systems: the often very considerable superiority of the optimum algorithms over their various corresponding suboptimum alternatives stems from the fact that the former are basically adaptive. The principal area of adaptivity is the noise. In practice this takes the form of establishing (i), the class of noise--Class A vs. Class B, for example; and (ii), the three (or more) statistical-physical parameters of the particular noise environment of the class in question. Of course, in practice only estimates based on finite samples are possible, so that it is also important to determine how sensitive both the algorithms and their performance are to departures from the actual (infinite-sample) values of the parameters. This involves a robustness study. Preliminary analysis [42],[45] indicates a reasonable lack of sensitivity to small and moderate changes in parameter estimates. A second area of adaptivity lies in the signal domain: estimation of various signal parameters (amplitude, waveform, frequency, etc.) which may only be known statistically at the receiver, or even estimation of such statistics themselves. Some preliminary work employing locally optimum Bayes estimators (LOBE's), which are also AO, is now available [51].

A concise (and incomplete) overview of the material of this report is given in [49]; a much more comprehensive, invited review paper is scheduled [50].

Many further topics need to be studied in the context of the present approach: for example, along the lines of using appropriate estimator-correlators to simplify the realizations of these AO LOBD's, [52], including the proper biases (4) above; and the effects of weakly-dependent noise samples, cf. [53], but along the present lines of "parametric" models, rather than non-parametric ones, [21]-[24]. A parallel derivation for AO LOBE's of specific signal elements, extending the work of [51] in detail, is also needed. Finally (but not necessarily only), is further work along the lines of [54], specifically addressed to multiple-element arrays and beam-forming in nongaussian noise fields. Still other, associated threshold reception problems will suggest themselves in the course of the above, among them the further development of analytical and numerical results for the binary signal cases, which are initiated here.

REFERENCES

[1a]. A.D. Spaulding and D. Middleton, "Optimum Reception in an Impulsive Interference Environment", OT Report 75-67, June, 1975, Office of Telecommunications, U.S. Dep't. of Commerce, NTIS Acces. No. COM75-11097/AS.

[1b]. A.D. Spaulding and D. Middleton, "Optimum Reception in an Impulsive Interference Environment: Part I, Coherent Detection; Part II, Incoherent Reception", IEEE Trans. on Communications Vol. COM-25, Sept., 1977, pp. 910-934. (This is a shortened version of [1a].)

[2]. D. Middleton, "Statistical-Physical Models of Urban Radio-Noise Environments, Part I: Formulations", IEEE Trans. Electromagnetic Compat. Vol. EMC-14, pp. 38-56, May, 1972.

[3]. _____, "Probability Models of Received, Scattered, and Ambient Fields", Proc. IEEE-1972 Int'l. Conf. on Engineering in the Ocean Environment, Newport, R.I., Sept. 13-16, 1972, IEEE Pub. 72-CHO--660-1-OCC, pp. 8-14, "Ocean '72".

[4]. _____, "Statistical-Physical Models of Man-made Radio Noise, Part I: First-order Probability Models of the Instantaneous Amplitude", OT Report 74-36, April, 1974. Office of Telecommunications, U.S. Dep't. of Commerce, NTIS Acces. No. COM75-10864/AS.

[5]. _____, "Statistical-Physical Models of Man-made and Natural Radio Noise, Part II: First-order Probability Models of the Envelope and Phase", OT Report 76-86, April, 1976, Office of Telecommunications, (U.S. Dep't. of Commerce), NTIS Acces. No. PB253949. See [6] below:

[6]. _____, "Statistical-Physical Models of Electromagnetic Interference", IEEE Trans. on Electromagnetic Compatibility, EMC-19, No. 3, pp. 106-127, Aug. 1977. (This is a condensed version of [5].)

[7]. _____, "Procedures for Determining the Parameters of the First-Order Canonical Models of Class A and Class B Electromagnetic Interference", IEEE Trans. on Electromag. Compat. EMC-21, No. 3, pp. 190-208, Aug., 1979.

[8]. _____, "New Results in the Development of Canonical and Quasi-Canonical EMI Probability Models", paper B-1, pp. 25-32, in Proceedings of the 4th Int'l. Symposium on Electromagnetic Compatibility, March 10-12, 1981, Zurich, Switz. (See [9] for a corrected account of Sec. 4.1.)

[9]. _____, "Performance of Telecommunications Systems in the Spectral-Use Environment: VII. Interference Scenarios and the Canonical and Quasi-Canonical (First-Order) Probability Models of Class A Interference", Contractor Report 82-18, March 1982, NTIA, U. S. Dep't. of Commerce, Wash. D.C., NTIS Acces. No. PB82-226861. also, IEEE Trans. on EMC, Vol. 25, May 1983.)

[10]. A.D. Spaulding, "Man-made Noise: The Problem and Recommended Steps toward Solution", OT Report 76-85 (pp. 173), April, 1976, Office of Telecommunications (U.S. Dep't. of Commerce), NTIS Acces. No. PB 253745/AS.

[10a]. (Chemical Rubber Co.,) Handbook of Atmospherics, Ed. by Hans Vollon Vol. II, 1982 (esp. articles by G.H. Hagn); CRC, 2000 N.W. 24th St., Boca Raton, Florida 33431.

[11]. J.H. Van Vleck and D. Middleton, "A Theoretical Comparison of the Visual, Aural, and Meter Reception of Pulsed Signals in the Presence of Noise", J. Appl. Physics, Vol. 17, pp. 940-971, Nov., 1946. (See, in particular, Part I, Sec. II, and p. 944. See, also, D. Middleton, IEEE Communications Soc. Magazine, pp. 9,10, July, 1978.

[12]. D. Middleton, An Introduction to Statistical Communication Theory McGraw-Hill (New York), 1960.

[13]. D. Middleton, "Canonical Non-Gaussian Noise Models: Their Implications for Measurement and for Prediction of Receiver Performance", IEEE Trans. on Electromagnetic Compatibility, EMC-21, No. 3, August 1979, pp. 209-220.

[14]. _____, "Canonically Optimum Threshold Detection", IEEE Trans. on Information Theory, Vol. IT-12, No. 2, April, 1966, pp. 230-243.

[15]. _____, "The Statistical Theory of Detection, I", M.I.T. Lincoln Laboratory Report No. 35, Nov. 1953. See, also, highlights of this Report, published as "Statistical Theory of Detection", Symposium on Statistical Methods in Communication Engineering, IRE Trans. on Info. Theory, PGIT-3, p. 26, March 1954.

[16]. D. Middleton, Ref. [12], Sec. 19.4.

[17]. P. Rudnick, "Likelihood Detection of Small Signals in Stationary Noise", J. Appl. Phys. 32, p. 140, Feb., 1961.

[18]. J. Capon, "On the Asymptotic Efficiency of Locally Optimum Detectors", IRE Trans. on Info. Theory, Vol. IT-7, pp. 67-71, April, 1961.

[19]. D. Middleton and D. Van Meter, "Detection and Extraction of Signals in Noise from the Point of View of Statistical Decision Theory", J. Soc. Industrial and Applied Math., Vol. 3, pp. 192 (1955), Vol. 4, 86 (1956), esp.

[20]. D. Middleton, Topics in Communication Theory, McGraw-Hill (New York), 1965; and RAND Report RM-4687-PR, Nov., 1965. See also the Nirenberg-Middleton Letter to the Editor, IEEE Trans. Comm. Vol. COM-23, p. 1002, Sep't. 1975, for a brief listing of other references.

[21]. J.B. Thomas, "Nonparametric Detection", Proc. IEEE, 58, pp. 623-631, 1970.

[22]. J.H. Miller and J.B. Thomas, "Detectors for Discrete Time Signals in Non-gaussian Noise", IEEE Trans. Info. Theory, Vol. IT-18, pp. 241-250, 1972.

[23]. M. Kanefsky and J.B. Thomas, "On Polarity Detection Schemes with Nongaussian Inputs", J. Franklin Inst., pp. 120-138, 1965.

[24]. S.A. Kassam and J.B. Thomas, "A Class of Nonparametric Detectors for Dependent Input Data", IEEE Trans. Info. Theory, Vol. IT-21, pp. 431-437, 1975. See also Saleem A. Kassam, "A Bibliography on Nonparametric Detection", IEEE Trans. Info. Theory, Vol. IT-26, No. 5, Sept., 1980, for many additional related papers.

[25]. O.Y. Antonov, "Optimum Detection of Signals in Non-Gaussian Noise", Radio Eng. + Electronic Phys., Vol. 12, 541-548, 1967.

[26]. B.R. Levin and A.F. Kushnir, "Asymptotically Optimal Algorithms of Detection and Extraction of Signals from Noise", Radio Eng. and Electron. Phys. Vol. 14, No. 2, pp. 213-221, 1970 (1969 Russian Ed.).

[27]. B.R. Levin and Y.S. Shinakov, "Asymptotic Properties of Bayes Estimates of Parameters of a Signal Masked by Interference", Int'l. Symp. on Info. Theory, Noordwijk, The Netherlands, June 15-19, 1970.

[28]. B.R. Levin, A.F. Kushnir, add A.I. Pinskii, "Asymptotically Optimum Algorithms for Detection and Discrimination of Signals Immersed in Correlated Noise," Rad. Eng. and Electron. Phys., Vol. 14, No. 2, 784-793, 1970 (1969 Russian Ed.).

[29]. J.J. Sheehy, "Optimum Detection of Signals in Nongaussian Noise", J. Acous. Soc. Amer., 63 (1), Jan; 1978, pp. 81-90.

[30]. D. Middleton, "Performance of Telecommunications Systems in the Spectral-Use Environment: Part V: Land-Mobile and Similar Scenarios in Class A Interference". NTIA Contractor Report 79-4, June 1979, NTIA, U.S. Dep't. of Commerce, NTIS Acces. No. PB80-112097.
cf. Sec. 3.

[31]. D. Middleton and D.J. Cohen, "_____: Part VIII. Channel Occupancy Statistics for Land-Mobile and Other Scenarios in Class A Interference", in preparation.

[32]. D. Middleton, "_____; Part VII. Interference Scenarios and the Canonical and Quasi-Canonical (First-Order) Probability Models of Class A Interference," NTIA-CR-82-18, March, 1982 (see [9]).

[33]. A.D. Spaulding, "Optimum Threshold Signal Detection in Broad-Band Impulsive Noise Employing Both Time and Spatial Sampling", IEEE Trans. on Communications, Vol. COM-29, No. 2, February, 1981, pp. 147-152.

[34]. D. Middleton, "Threshold Signal Reception in Electromagnetic Interference Environments: Part II. Receiver Structures and Performance for Class A EMI Environments and Scenarios", NTIA Contractor Report 81-17, March, 1982, for ITS/NTIA, Boulder, Colo. 80303, NTIS Acces. No. PB82-226846.

[35]. R.S. Kennedy, Fading Dispursive Communication Channels, John Wiley (New York), 1969; esp. Chapters 2,3.

[36]. V.V. Ol'shevskii, Statistical Methods in Sonar, Plenum (New York-Consultant's Bureau), 1978, cf. Chapters 4,5.

[37]. D. Middleton, "Channel Characterization and Threshold Reception for Complex Underwater Media", EASCON Sept-Oct.'80, IEEE-0531-6863/80/0000 -171; pp. 171-180, and references.

[38]. _____, "The Underwater Medium as a Generalized Communication Channel", p. 589-612 of Underwater Acoustics and Signal Processing Ed, L. Bjørnø, NATO Advanced Study Institute, D. Reidel Pub. Co., Dordrecht, Holland, 1981.

[39]. B.R. Levin, Theoretical Principles of Statistical Radio Engineering, III, "Soviet Radio", Moscow, 1976, cf. Chapters 1 and 3 in particular

[40]. L. LeCam, "On the Asymptotic Theory of Estimation and Testing Hypotheses", Proc. 3rd Berkeley Symposium on Math. and Statistics, 1956.

[40a]. L. LeCam, "Locally Asymptotically Normal Families of Distributions, Univ. of Cal. Publications in Statistics," U. of Cal. Press, Berkeley, Vol. 3, pp. 37-98, 1960.

[41]. E.L. Ince, Ordinary Differential Equations, Dover, New York, 1944.

[42]. A.D. Spaulding, "Robustness of LOBD's for NonGaussian Noise", pp. 143-152, Proceedings 5th International Symposium on Electromagnetic Compatibility (EMC), Wroclaw, Poland, Sept. 17-19, 1980

[43]. J.E. Evans and A.S. Griffiths,"Design of a Sanguine Noise Processor Based upon World-Wide Extremely Low Frequency (ELF) Recordings", IEEE Trans. Comm. Vol. COM. 22, no. 4, April, 1974, pp. 528-539.

[44]. R.F. Ingram and R. Houle, "Performance of Optimum and Several Suboptimum Receivers for Threshold Detection of Known Signals in Additive White, Non Gaussian Noise", NUSC Tech. Rep't. 6339, Nov. 24, 1980, NUSC, New London, Conn.

[45]. A.D. Spaulding, "Locally Optimum and Suboptimum Detection Performance in Non-Gaussian Noise", Proceedings Int'l. Comm. Conference (ICC), Philadelphia, June, 1982.

[46]. J.H. Van Vleck and D. Middleton, "The Spectrum of Clipped Noise", Proc. IEEE, Vol. 54, No. 1, Jan. 1966, pp. 2-19.

[47]. D. Middleton, "Some Canonical Approaches to the Evaluation of Telecommunication System Performance", NTIA Contractor Report 81-11, June 1981. (U.S. Dept. of Commerce), NTIS Acces. No. PB81-249310.

[48]. D. Middleton and A.D. Spaulding, Correspondence - IEEE Trans. Information Theory, 1983.

[49]. D. Middleton, "Threshold Detection in Nongaussian Interference Environments: Exposition and Interpretation of New Results for EMC Applications," 5th International Symposium on Electromagnetic Compatibility, Zürich, Switzerland, March 8-10, 1983.

[50]. D. Middleton, G. Hagn, and A. D. Spaulding, "Statistical-Physical Models of Nongaussian Electromagnetic Interference Environments and their Predicted Effects on Telecommunications--a Review (tentative title), invited paper for Proc. IEEE, 1984.

[51]. D. Middleton, "Threshold Signal Reception in Electromagnetic Interference Environments: Part III, An Introduction to Canonical Threshold Signal and Parameter Estimation, NTIA Contractor Report 83-21, Jan. 1983, for NTIA/ITS, Boulder, CO 80303, (NTIS Acces. No. not yet available).

[52]. W. A. Gardner, "Structural Characterization of Locally Optimum Detectors in Terms of Locally Optimum Estimators and Correlators," IEEE Trans. on Inf. Theory, Vol. IT-28, No. 6, Nov. 1982, pp. 924-932.

[53]. H. V. Poor, "Signal Detection in the Presence of Weakly Dependent Noise--Part I: Optimum Detection," pp. 735-744; Part II: "Robust Detection," pp. 744-752, IEEE Trans. On Inf. Theory, Vol. IT-28, No. 5, Sept., 1982.

[54]. D. Middleton, "Multiple-Element Threshold Signal Detection of Underwater Acoustic Signals in Nongaussian Interference Environments," Tech. Rept. (NOSC), approximately May, 1983.

GLOSSARY OF PRINCIPAL SYMBOLS

ARE	Asymptotic Relative Efficiency
$A_{A,B}$	overlap indexes
$\hat{A}_{\alpha}$	Class B parameter
A_o	(peak) signal amplitude
a	fading amplitude
$\langle a_o^2 \rangle^*_{min}$, $\langle a_o^2 \rangle_{min}$	minimum detectable signals
a_0, $\overline{a_o}$, $\sqrt{\overline{a_o^2}}$	normalized signal amplitudes
α, α^*	(conditional) probability of false alarm; α, also, a Class B noise parameter, cf. (3.14c)
α_o	λ_o/λ_1 = ratio of radii
$B^{(*)}$	probability control = $(C,C^*)^2$
$B_n, \hat{B}^*_n, B^*_n$	biases
$b_{1\alpha}$	Class B noise parameter
β, β^*	(conditional) probability of false signal detection
${}_mC_n$	binomial coefficient
C, C^*	probability controls
ε	signal epoch
$F_n(\underset{\sim}{x}\|\Theta)$	pdf of (signal and) noise
F_i	detector characteristic

G_B	Class B noise parameter
$G_o(\phi)$	beam pattern
$g(\underset{\sim}{x}), g^*,$	detection algorithms
γ	propagation law (exponent)
Γ'	ratio of intensities of gauss to non-gauss components
H_1, H_0, H_{12}, H_{21}	hypothesis states
$h_M,$	weighting function of matched filter
$\hat{I}_{os}$	source signal intensity
$\overline{I}_N$	average noise intensity
$k, \mathcal{K}$	thresholds
$L^{(2)}, L^{(4)}, L^{(1,2)} L^{(6)}$	(1st-order) statistics of the noise
Λ	likelihood ratio
$l_n^{(*)}$	likelihood ratio
ℓ_i, ℓ_j	transfer characteristic, cf. (4.2a)
λ	distance
λ_0, λ_1	boundaries of source domain
m_{ij}	second-moment function of signal amplitudes
$\mu=p/q$	ratio of a priori problems; also, power law of source distribution, cf. Eq. (3.5).
$n, n_{1,2}, n^*$	number of (independent, time) samples

$\Omega_{2A,2B}$	intensity of nongaussian component (Class A,B) noise
$\Delta\omega_d$	doppler "source"
ω_d	doppler shift
P_D, p_D^*	probability of correct signal detection
P_e, P_e^*	error probabilities
Π, Π^*	processing gains
P	a priori probability
Φ_d^*	degradation factor
ψ	mean noise intensity
ϕ, ϕ_o	phases
$Q_n \hat{Q}_n, \hat{Q}_n^{(21)}$	signal structure factors
q	a priori probability
$\hat{r}_o$	normalizing distance
ρ_s	second-moment function of signals
ρ_{ij}	function of signals at (t_i, t_j)
σ_G^2	gauss intensity
$\sigma^{*2}, \sigma_o^2, \sigma_{on}^2, \hat{\sigma}_o, {}^2\sigma_{01}{}^{*2}$,	variances
sgn x	"sign of"
$S, \overline{S}, \overline{S'}$	normalized signal waveforms
T	data interval
$\textcircled{H}, \Theta$	error function
Θ^2	signal-to-noise ratio
Θ_i	normal signal waveform parameter

W_n	pdf of noise
$w_1(x)$	pdf of noise
x	normalized data sample
x_o^*	coherent bound
y_o^*	incoherent bound

APPENDICES

Part I Optimal Threshold Detectors

(David Middleton)

APPENDIX A-1

Optimum Threshold Structure and Bias Terms: The "On-Off" Cases:

Here we develop the general LOBD structure, including dependent samples, leading to Eq.(2.9) and its various coherent and incoherent special forms (2.11), (2.12). We focus our attention initially on the "on-off" (H_1 vs. H_0) cases, as the extension to the binary signal situation (H_2 vs. H_1) follows immediately from these results, cf. (2.13) et seq. We consider only the general, and usual, case of additive signals and noise, cf. Sec. A.3-4) ff. however, so that

$$\Lambda_n(\underset{\sim}{x}|\theta) \equiv \mu\langle w_n(\underset{\sim}{x}-\underset{\sim}{\theta})_N\rangle/w_n(x)_N \quad ; \; \mu \equiv p/q; \; \underset{\sim}{x} = [x_i] = [x_i/\sqrt{x_i}] \tag{A.1-1}$$

is the likelihood ratio to be expanded according to the threshold concept described in Sec. 2.2.

A1-1: The General LOBD:

We begin by expanding the numerator in appropriate powers of $\underset{\sim}{\theta} = [a_{oj}s_j]$, cf. (2.9a), through $O(\theta^4)$, to obtain

$$\Lambda_n = \mu\Bigg\{1 - \sum_i^n \langle\theta_i\rangle \frac{\partial w_n}{w_n \partial x_i} + \frac{1}{2!}\sum_{ij}^n \langle\theta_i\theta_j\rangle \frac{1}{w_n}\frac{\partial^2 w_n}{\partial x_i \partial x_j}$$

$$- \frac{1}{3!}\sum_{ijk}^n \langle\theta_i\theta_j\theta_k\rangle \frac{1}{w_n}\frac{\partial^3 w_n}{\partial x_i \partial x_j \partial x_k} + \frac{1}{4!}\sum_{ijk\ell}^n \langle\theta_i\theta_j\theta_k\theta_\ell\rangle \frac{1}{w_n}\frac{\partial^4 w_n}{\partial x_i \cdots \partial x} \cdots\Bigg\}, \tag{A.1-2}$$

where

$$y_i \equiv \frac{\partial}{\partial x_i} \log w_n = \frac{1}{w_n} \frac{\partial w_n}{\partial x_i} \equiv \frac{w_n^i}{w_n} \quad ;$$

$$\frac{\partial^2 w_n}{w_n \partial x_i \partial x_j} = \frac{w_n^{ij}}{w_n} = \frac{\partial^2 \log w_n}{\partial x_i \partial x_j} + \frac{w_n^i w_n^j}{w_n^2} \equiv z_{ij} + y_i y_j \ , \qquad \text{(A.1-2a)}$$

i.e.

$$z_{ij} \equiv \frac{\partial^2}{\partial x_i \partial x_j} \log w_n, \quad \text{with } \frac{1}{w_n} \frac{\partial^3 w_n}{\partial x_i \partial x_j \partial x_k} \equiv \frac{w_n^{ijk}}{w_n} \ , \text{ etc.,}$$

e.g.

$$\frac{\partial^m w_n}{\partial x_i \ldots \partial x_m} \equiv \frac{w_n^{1,2\ldots m}}{w_n} \quad , \text{ etc.} \qquad \text{(A.1-2b)}$$

Our next step is to expand $\log \Lambda_n$, using (A.1-2) and the relation $\log(1+x) = x - (x^2/2) + (x^3/3) - (x^4/4)\ldots$; $|x|<1$:

$$\log \Lambda_n = \log \mu + \log \left[1 - A^{(1)}_{(i)} + \frac{1}{2!} A^{(2)}_{(ij)} - \frac{1}{3!} A^{(3)}_{(ijk)} + \frac{1}{4!} A^{(4)}_{(ijk\ell)} \ldots\right] \qquad \text{(A.1-3a)}$$

$$= \log \mu + \left[-A^{(1)} + \frac{1}{2!} A^{(2)} - \frac{1}{3!} A^{(3)} + \frac{1}{4!} A^{(4)} \ldots\right]_{\leq O(\theta^4)}$$

$$- \frac{1}{2} \left[A^{(1)^2} + \frac{1}{2!^2} A^{(2)^2} + \ldots - \frac{2A^{(1)}A^{(2)}}{2!} + \frac{2}{3} A^{(1)}A^{(3)} + \ldots\right]_{\leq O(\theta^4)}$$

$$+ \frac{1}{3} \left[+A^{(1)^3} + \frac{3A^{(1)^2}A^{(2)}}{2!} + \ldots\right]_{\leq O(\theta^4)}$$

$$- \frac{1}{4} \left[A^{(1)^4} + \ldots\right]_{\leq O(\theta^4)} \qquad \text{(A.1-3b)}$$

$$\therefore \quad \log \Lambda_n = \log \mu - A^{(1)} + \frac{1}{2!}[A^{(2)} - A^{(1)^2}] - \frac{1}{3!}[A^{(3)} - \frac{3!}{2!} A^{(1)}A^{(2)} + \frac{3!A^{(1)^3}}{3}]$$

$$+ \frac{1}{4!}[A^{(4)} - \frac{4!}{2!^3} A^{(2)^2} - \frac{4!}{3!} A^{(1)}A^{(3)} + \frac{4!}{2!} A^{(1)^2}A^{(2)} - \frac{4!}{4} A^{(1)^4}] + \ldots, \tag{A.1-3c}$$

which becomes, more compactly

$$\therefore \log \Lambda_n = \log \mu - \sum_{i}^{n} \langle \theta_i \rangle y_i + \frac{1}{2!} \sum_{ij}^{n} \{\langle \theta_i \theta_j \rangle (y_i y_j + z_{ij}) - \langle \theta_i \rangle \langle \theta_j \rangle y_i y_j\}$$

$$+ \Theta_3 + \Theta_4 + O(\langle \theta^5 \rangle) \ , \tag{A.1-4}$$

where now, specifically

$$\Theta_3 \equiv - \frac{1}{3!} \sum_{ijk}^{n} \{\langle \theta_i \theta_j \theta_k \rangle \frac{w_n^{ijk}}{w_n} - 3\langle \theta_i \rangle \langle \theta_j \theta_k \rangle y_i (y_j y_k + z_{jk})$$

$$+ 2y_i y_j y_k \langle \theta_i \rangle \langle \theta_j \rangle \langle \theta_k \rangle\} \tag{A.1-4a}$$

$$\Theta_4 \equiv \frac{1}{4!} \sum_{ijk\ell}^{n} \{\langle \theta_i \theta_j \theta_k \theta_\ell \rangle \frac{w_n^{ijk\ell}}{w_n} - 3\langle \theta_i \theta_j \rangle \langle \theta_k \theta_\ell \rangle (z_{ij} + y_i y_j)(z_{k\ell} + y_k y_\ell)$$

$$- 4\langle \theta_i \rangle y_i \langle \theta_j \theta_k \theta_\ell \rangle \frac{w_n^{jk\ell}}{w_n} + 12\langle \theta_i \rangle \langle \theta_j \rangle y_i y_j \langle \theta_k \theta_\ell \rangle (z_{k\ell} + y_k y_\ell)$$

$$- 6\langle \theta_i \rangle \langle \theta_j \rangle \langle \theta_k \rangle \langle \theta_\ell \rangle y_i y_j y_k y_\ell\} \ . \tag{A.1-4b}$$

For coherent reception, as explained in Sec. 2.2 above, we retain only those terms in $(\underset{\sim}{x})$ which are $O(\langle \theta \rangle)$ and replace terms $O(\langle \theta^2 \rangle)$ by the resulting average (of $\underset{\sim}{x}$) over H_o, e.g. the LOBD here is now

$$g^*_{coh} = [\log \mu + \frac{1}{2!} \sum_{ij}^{n} \{\langle \theta_i \theta_j \rangle \langle y_i y_j + z_{ij} \rangle_{H_o} - \langle \theta_i \rangle \langle \theta_j \rangle \langle y_i y_j \rangle_{H_o}\}] - \sum_i \langle \theta_i \rangle y_i$$

(A.1-5a)

or

$$= [\log \mu + \frac{1}{2!} \sum_{ij} \{\langle y_i [\langle \theta_i \theta_j \rangle - \langle \theta_i \rangle \langle \theta_j \rangle] y_j \rangle_{H_o} + \langle \theta_i \theta_j \rangle \langle z_{ij} \rangle_{H_o}\}] - \sum_i \langle \theta_i \rangle y_i \ ,$$

(A.1-5b)

where the expressions in the square brackets are now the bias term, B^*_{n-c}.

Similarly, for purely incoherent reception, we require $\langle \theta_i \rangle = 0$ and $\langle \theta_i \theta_j \theta_k \rangle = 0$, at least,* for the LOBD, so that $\Theta_3 = 0$, and the LOBD now becomes

$$g^*_{inc} = [\log \mu + \frac{1}{4!} \left\langle \sum_{ijk\ell}^{n} \langle \theta_i \theta_j \theta_k \theta_\ell \rangle \frac{w_n^{(ijk\ell)}}{w_n} - 3[\sum_{ij} \langle \theta_i \theta_j \rangle (y_i y_j + z_{ij})]^2 \right\rangle_{H_o}]$$

$$+ \frac{1}{2!} \sum_{ij}^{n} \langle \theta_i \theta_j \rangle \{y_i y_j + z_{ij}\}, \qquad \text{(A.1-6)}$$

where the terms independent of the data ($\underset{\sim}{x}$) constitute the bias, B^*_{n-inc}, here.

To summarize, then, we have the LOBD's for coherent and incoherent detection, respectively

with

$$\boxed{g^*_c = B^*_{n-c} - \sum_i^n \langle \theta_i \rangle y_i = B^*_c - \langle \underset{\sim}{\tilde{\theta}} \rangle \underset{\sim}{y} \ , \qquad \text{(A.1-7)}}$$

with

$$\boxed{B^*_{n-c} = \log \mu + \frac{1}{2!} \langle \underset{\sim}{\tilde{y}} [\underset{\sim}{\rho}_\theta - \langle \underset{\sim}{\theta} \rangle \langle \underset{\sim}{\tilde{\theta}} \rangle] \underset{\sim}{y} + \langle \underset{\sim}{\tilde{\theta}} \underset{\sim}{z} \underset{\sim}{\theta} \rangle \rangle_{H_o}, \quad \underset{\sim}{\rho}_\theta \equiv \langle \underset{\sim}{\theta} \underset{\sim}{\tilde{\theta}} \rangle = \langle \theta_i \theta_j \rangle, \qquad \text{(A.1-7a)}}$$

---

* This second condition, $\langle \theta_i \theta_j \theta_k \rangle = 0$, is certainly satisfied for narrowband signals, $s_i = \sqrt{2} \cos[\omega_o (t_i - \epsilon) - \phi_i]$, when the first condition $\langle \theta_i \rangle = 0$ holds. For broad-band signals, however, we require that $\langle \theta_j \theta_k \theta_\ell \rangle = 0$, as well as $\langle \theta_i \rangle = 0$, for this so-called "purely" incoherent reception.

and

$$g^*_{inc} = B^*_{n\text{-}inc} + \frac{1}{2!}[\tilde{\underset{\sim}{y}}\, \underset{\sim}{\rho}_{\theta}\, \underset{\sim}{y} + \langle \tilde{\underset{\sim}{\theta}}\, \underset{\sim}{z}_{\theta} \rangle] \,, \tag{A.1-8}$$

where

$$B^*_{n\text{-}inc} = \log \mu + \frac{1}{4!} \Big\langle \sum_{ijk\ell} \langle \theta_i \theta_j \theta_k \theta_\ell \rangle \frac{w_n^{(ijk\ell)}}{w_n} - 3\Big[\sum_{ij} \langle \theta_i \theta_j \rangle (y_i y_j + z_{ij})\Big]^2 \Big\rangle_{H_o} \,, \tag{A.1-8a}$$

which are the results exhibited in Sec. 2.2 above. Here we have explicitly

$$\underset{\sim}{y} = [y_i] = \frac{\partial}{\partial x_i} \log w_n \;;\; \underset{\sim}{z} = [z_{ij}] = \Big[\frac{\partial^2 \log w_n}{\partial x_i \partial x_j}\Big] \;;$$

$$w_n^{(ijk\ell)} \equiv \frac{\partial^4 w_n}{\partial x_i \partial x_j \partial x_k \partial x_\ell} \,. \tag{A.1-9}$$

The results above hold for dependent or uncorrelated samples, e.g.

$$w_n(\underset{\sim}{x}) \left(\neq \atop =\right) \prod_i^n w(x_i),$$

generally.

A.1-2: Independent Sampling:

When the noise samples are independent(but not necessarily stationary)- the limiting situation of our present analysis- very considerable simplifications

in our general results (A.1-7), (A.1-8) above are possible. Now we have

$$w_n(\underset{\sim}{x})_N \equiv w_n(\underset{\sim}{x}|H_o) = \prod_{i=1}^{n} w_1(x_i|H_o) \tag{A.1-10}$$

so that

$$\left.\begin{aligned} y_i &= \frac{\partial}{\partial x_i}\log w_n \to \frac{\partial \log w_i}{\partial x_i} \equiv \ell_i \ ; \\ z_{ij} &= \frac{\partial^2}{\partial x_i \partial x_j}\log (w_i w_j) = [\frac{\partial^2}{\partial x_i^2}\log w_i]\delta_{ij} = \ell_i'\delta_{ij} \ ; \\ \therefore (\frac{w_1''}{w_1})_i &= \frac{\partial^2}{\partial x_i^2}\log w_{1i} + (\frac{w_1'}{w_1})_i^2 = \ell_i'\delta_{ij} + \ell_i^2 \ ; \\ \therefore \frac{w_1^{(ij)}}{w_{1i}w_{1j}} &= y_i y_j + z_{ij} = \ell_i\ell_j + \ell_i'\delta_{ij} \ . \end{aligned}\right\} \tag{A.1-11}$$

Accordingly, the LOBD's (A.1-7), (A.1-8) become now

$$\boxed{g_c^* = B_{n\text{-}c}^* - \sum_i^n \ell_i\langle\theta_i\rangle \ ; \ g_{inc}^* = B_{n\text{-}inc}^* + \frac{1}{2!}\sum_{ij}^n [\ell_i\ell_j + \ell_i'\delta_{ij}]\langle\theta_i\theta_j\rangle} \ , \tag{A.1-12}$$

cf. (4.1), (4.2), (4.4).

Our next task here is to obtain the biases (A.1-7a), (A.1-8a), for these independent samples. We begin with <u>the coherent case</u> (A.1-7a) and observe that

$$\sum_{ij} a_{ij}\langle y_i y_j\rangle_{H_o} = \sum_i a_{ii}\langle y_i^2\rangle_{H_o} + \sum_{ij}{}' a_{ij}\langle y_i\rangle_{H_o}\langle y_j\rangle_{H_o} , \tag{A.1-13a}$$

since x_i, x_j $(i \neq j)$ are independent, so that

$$\sum_{ij} a_{ij} \langle y_i y_j \rangle_{H_o} = \sum_i a_{ii} \langle y_i^2 \rangle_{H_o}$$

$$\langle y_i \rangle_{H_o} = \int_{-\infty}^{\infty} \ell_i w_{1i} dx_i = \int_{-\infty}^{\infty} w'_{1i} dx_i = w_{1i} \Big|_{-\infty}^{\infty} = 0 \ , \qquad \text{(A.1-13b)}$$

(<u>regardless of whether or not w_1 is symmetrical!</u>). This last follows from the necessary condition on the proper pdf w_{1i} that $w_1(\pm\infty)_i = 0$ always. Similarly, we have

$$\sum_{ij} b_{ij} \langle z_{ij} \rangle_{H_o} = \sum_{ij} \langle \theta_i \theta_j \rangle \langle \ell'_i \delta_{ij} \rangle_{H_o} = \sum_i \langle \theta_i^2 \rangle \int_{-\infty}^{\infty} \ell'_i w_{1i} dx_i$$

$$= \sum_i \langle \theta_i^2 \rangle \left(\int_{-\infty}^{\infty} \left[\frac{w''_1}{w_1} - \left(\frac{w'_1}{w_1} \right)^2 \right] w_1 dx \right)_i$$

$$= - \sum_i \langle \theta_i^2 \rangle \left(\int_{-\infty}^{\infty} \left(\frac{w'_1}{w_1} \right)^2 w_1 dx \right)_i \quad ; \quad \int_{-\infty}^{\infty} w''_1 dx_i = w'_1 \Big|_{-\infty}^{\infty} = 0, \qquad \text{(A.1-14)}$$

since $w'_1(\pm\infty) = 0$, also, for a proper pdf. Writing*

$$\boxed{L_i^{(2)} \equiv \int_{-\infty}^{\infty} \left(\frac{w'_1}{w_1} \right)_i^2 w_{1i} dx_i = \langle \ell_i^2 \rangle_{H_o}} = \langle y_i^2 \rangle_{H_o} \ , \qquad \text{(A.1-15)}$$

and observing that $a_{ii} = \rho_\theta|_{ii} - \langle \theta_i \rangle^2 = \langle \theta_i^2 \rangle - \langle \theta_i \rangle^2$; $b_{ii} = \langle \theta_i^2 \rangle$ in the above, we find that the bias (A.1-7a) becomes

---

*Incidentally, note that $L_i^{(2)}$ is equivalent to Fisher's Information I_i, at $\theta=0$, cf. Eq. (225),[12], i.e.,

$$I_i \Big|_{\theta-0} = \left\{ \left(\left[\frac{\partial / n \ w_1(x_i - \theta_i)}{\partial \theta_i} \right]^2 w_i(x_i | \theta_i) dx_i \right\}_{\theta=0} \right.$$

$$B^*_{n\text{-coh}} = \log \mu - \frac{1}{2}\sum_i^n \langle \theta_i \rangle^2 L_i^{(2)} = \log \mu + \hat{B}^*_{n\text{-coh}} \,. \qquad \text{(A.1-16)}$$

When the noise process $\{x\}$ is stationary, $w_{1i} = w_1$, all i and $\therefore\ \psi_i = \psi$, $L_i^{(2)} = L^{(2)}$, all i, etc., further considerable simplification occurs. We obtain for the coherent LOBD, g^*_{coh}, from (A.1-7), (A.1-16), $\ell_i = \ell_i(x_i) \to \ell(x_i)$ and

$$\therefore\quad g^*_{coh} = [\log \mu - L^{(2)} \sum_{i=1}^n \tfrac{1}{2}\langle a_{oi} s_i \rangle^2] - \sum_{i=1}^n \langle a_{oi} s_i \rangle \ell(x_i). \qquad \text{(A.1-17)}$$

Our next task is to evaluate the bias, (A.1-8a), for incoherent detection, now with independent sampling. Let us consider the first term of (A.1-8a), viz.

$$\left\langle \sum_{ijk\ell} \langle \theta_i \theta_j \theta_k \theta_\ell \rangle \frac{w_n^{(ijk\ell)}}{w_n} \right\rangle_{H_o} :$$

I. $(i \neq j \neq k \neq \ell)$:

$$\therefore \left\langle \frac{w_n^{(ijk\ell)}}{w_n} \right\rangle_{H_o} = \left\langle \frac{w_1^{(i)}}{w_{1i}} \cdot \frac{w_1^{(j)}}{w_{ij}} \cdot \frac{w_1^{(k)}}{w_{ik}} \cdot \frac{w_1^{(\ell)}}{w_i} \right\rangle_{H_o} = \langle \ell_i \rangle_o \langle \ell_j \rangle_o \langle \ell_k \rangle_o \langle \ell_\ell \rangle_o = 0,$$

cf. (A.1-13b) ; (A.1-18a)

II. $i=j(\neq k \neq \ell)$:

$$\left\langle \frac{w_n^{(ijk\ell)}}{w_n} \right\rangle_{H_o} = \left\langle \frac{w_1^{(ii)}}{w_{1i}} \cdot \frac{w_1^{(k)}}{w_{1k}} \cdot \frac{w_1^{(\ell)}}{w_1} \right\rangle_{H_o} = \left\langle \left(\frac{w_1''}{w_1}\right) \right\rangle_{H_o} \langle \ell_k \rangle_o \langle \ell_\ell \rangle_o = 0,$$

cf. (a.1-13b) ; (A.1-18b)

There are ${}_{N}C_{N-(E-1)}$ combinations of the above, where N = no. of indexes (= 4 here) and E no. of indexes that are equal, i.e. k=j, ∴ E = 2, so that ${}_{4}C_{4-1} = {}_{4}C_{3} = 4$ combinations of the above. (For I, E = 1 (identity), ∴ ${}_{4}C_{4-0} = 1$.)

III. i=j; k=ℓ (i≠k):

$$\left\langle \frac{w_n^{(ijk\ell)}}{w_n} \right\rangle_{H_o} = \left\langle \frac{w_1^{(ii)}}{w_{1i}} \right\rangle_o \left\langle \frac{w_1^{(kk)}}{w_{1k}} \right\rangle_o = \left\langle \left(\frac{w_1''}{w_1}\right)_i \right\rangle_o \left\langle \left(\frac{w_1''}{w_1}\right)_k \right\rangle_o = \left\langle \ell_i^2 \delta_{ij} + \ell_{ij}^2 \right\rangle_o \left\langle \ell_k^2 \delta_{k\ell} + \ell_{k\ell}^2 \right\rangle_o = 0$$

cf. (A.1-11), (A.1-14). (A.1-18c)

Similarly, we have

IV. i = j = k(≠ℓ):

$$\left\langle \frac{w_n^{(ijk\ell)}}{w_n} \right\rangle_{H_o} = \left\langle \frac{w_1^{(iii)}}{w_{1i}} \right\rangle_o \left\langle \frac{w_1^{(\ell)}}{w_{1\ell}} \right\rangle_o = 0, \text{ since } \left\langle \frac{w_1^{(\ell)}}{w_{1\ell}} \right\rangle_o = \left\langle \left(\frac{w_1'}{w_1}\right)_\ell \right\rangle_o = \langle \ell \rangle_{\ell,o} = 0$$

(A.1-18d)

V. (i=j=k=ℓ):

$$\left\langle \frac{w_n^{(ijk\ell)}}{w_n} \right\rangle_{H_o} = \left\langle \left(\frac{w_1^{(4)}}{w_1}\right)_i \right\rangle_o = 0, \text{ since } \left(\int_{-\infty}^{\infty} w_1^{(4)} dx\right)_i = w_{1i}^{(3)} \Big|_{-\infty}^{\infty} = 0. \quad \text{(A.1-18e)}$$

Accordingly, the first term of (A.1-8a), (apart from log μ) vanishes.

The second term, however, has a definite, nonzero contribution. We distinguish the following combinations of terms, on expanding:

$$-\frac{1}{8}\left\langle\left[\sum_i\langle\theta_i^2\rangle\frac{w_{1i}^{(")}}{w_{1i}}+\sum_{ij}^{(i\neq j)}\langle\theta_i\theta_j\rangle\ell_i\ell_j\right]\left[\sum_k\langle\theta_k^2\rangle\frac{w_{1k}^{(")}}{w_{1k}}+\sum_{k\ell}^{(k\neq\ell)}\langle\theta_k\theta_\ell\rangle\ell_k\ell_\ell\right]\right\rangle_{H_o}:$$

(A.1-19)

(1). <u>(i≠k):</u>

$$\left\langle w_{1i}^{(")}/w_{1k}\right\rangle_o=\left\langle\frac{w_{1i}^{(")}}{w_{1k}}\right\rangle_o\left\langle\frac{w_{1k}^{(")}}{w_{1k}}\right\rangle_o=0\ :\qquad\text{(A.1-19a)}$$

(2). <u>(i=k):</u>

$$\boxed{\left\langle\left(\frac{w_{1k}^{(")}}{w_{1i}}\right)^2\right\rangle_o=\left(\int_{-\infty}^{\infty}\left(\frac{w_1''}{w_1}\right)^2w_1\,dx\right)_i\equiv L_i^{(4)}\ (>0),\ =\left\langle(\ell_i'\delta_{ij}+\ell_i^2)^2\right\rangle_{H_o},}$$

cf. (A.1-18c); (A.1-19b)

<u>(3). (i≠j)≠(k≠ℓ):</u>

$$\left\langle\ell_i\ell_j\ell_k\ell_\ell\right\rangle_o=\langle\ell_i\rangle_o\langle\ell_j\rangle_o\langle\ell_k\rangle_o\langle\ell_\ell\rangle_o=0;\qquad\text{(A.1-19c)}$$

(4). <u>(i≠j); (k≠ℓ):</u>

(a). $\left.\begin{matrix}i=k\\(j\neq\ell)\end{matrix}\right\}:\ \langle\ell_i^2\ell_j\ell_\ell\rangle_o=0\ ;\qquad\text{(A.1-19d)}$

(b). $\left\{\begin{matrix}\underline{i=k;\ j=\ell}\\ \\ \underline{i=\ell;\ j=k}\end{matrix}\right\}^{(k\neq\ell)}_{(i\neq j)}\ ;\quad\begin{matrix}\langle\ell_i^2\ell_j^2\rangle_o=\langle\ell_i^2\rangle_o\langle\ell_j^2\rangle_o=L_i^{(2)}L_j^{(2)}\ ,\\ \langle\ell_i^2\ell_k^2\rangle_o=\langle\ell_i^2\rangle_o\langle\ell_k^2\rangle_o=L_i^{(2)}L_k^{(2)}\ .\end{matrix}\qquad\text{(A.19c)}$

Combining (A.1-19a-e) we get for (A.1-19), and in fact, for the entire bias term, finally,

$$B^*_{n\text{-inc}} = \log\mu - \frac{1}{8}\{\sum_i^n L_i^{(4)}\langle\theta_i^2\rangle^2 - 2L_i^{(2)^2}\langle\theta_i^2\rangle^2 + 2\sum_{ij} L_i^{(2)}L_j^{(2)}\langle\theta_i\theta_j\rangle^2\}$$

$$\equiv \log\mu + \hat{B}^*_{n\text{-inc}}\ , \qquad \text{(A.1-20a)}$$

and when the noise process is stationary, e.g. $L_i^{(4)} = L^{(4)}$, $L_i^{(2)} = L^{(2)}$, etc. the simpler result

$$\therefore\quad B^*_{n\text{-inc}} = \log\mu - \frac{1}{8}\sum_{ij}\langle\theta_i\theta_j\rangle^2\{(L^{(4)} - 2L^{(2)^2})\delta_{ij} + 2L^{(2)^2}\} \equiv \log\mu + \hat{B}^*_{n\text{-inc}}. \qquad \text{(A.1-20b)}$$

Accordingly, in the stationary cases the incoherent LOBD (A.1-8) now becomes explicitly

$$g^*_{inc} = [\log\mu - \frac{1}{8}\sum_{ij}\langle a_{oi}a_{oj}s_is_j\rangle^2\{(L^{(4)} - 2L^{(2)^2})\delta_{ij} + 2L^{(2)^2}\}]$$

$$+ \frac{1}{2!}\sum_{ij}(\ell_i\ell_j + \ell_i'\delta_{ij})\langle a_{oi}a_{oj}s_is_j\rangle\ , \qquad \text{(A.1-21)}$$

$$\ell_i = \ell(x_i) \qquad = \frac{d}{dx}\log w_1(x|H_o)\Big|_{x=x_i}\ , \text{ etc.,}$$

where the term $[\ ](=B^*_{n\text{-inc}})$ is the bias and $L^{(2)} = \langle\ell^2\rangle_o$; $L^{(4)} = \langle(\ell' + \ell^2)^2\rangle$. cf. (A.1-15), (A.1-19b).

A.1-3: Gauss Noise and Independent Sampling:

Our results (A.1-17), (A.1-21) for g* should reduce to the previously obtained forms when the noise is gaussian. Here we have (for independent noise samples)

$$w_1(x)_o \equiv w_1(x|H_o) = \frac{e^{-x^2/2}}{\sqrt{2\pi}} \; \therefore \; \ell = -x \; ; \; \ell' = -1;$$

$$L^{(2)} = \int_{-\infty}^{\infty} \frac{x^2 e^{-x^2/2}}{\sqrt{2\pi}}\, dx = \overline{x^2} = 1; \; L^{(4)} = \int_{-\infty}^{\infty} (x^2-1)^2 w_1(x)_o\, dx = \overline{x^4} - 2\overline{x^2} + 1 = 3-2+1 = 2. \tag{A.1-22}$$

Additional quantities needed later (cf. Appendixes 2, 4) are (for the gauss pdf (A.1-22))

gauss

$$\begin{cases} L^{(2,2)} = 2\langle \ell^4 \rangle_o = 2\int_{-\infty}^{\infty} x^4 w_1(x)\, dx = 2\overline{x^4}\Big|_{gauss} = 6\overline{x^2} = 6 \; , \; (\overline{x^2} = 1); \\ L^{(6)} = \left\langle \left(\frac{w_1''}{w_1}\right)^3 \right\rangle_o = \langle (x^2-1)^3 \rangle_o = \overline{x^6} - 3\overline{x^4} + 3\overline{x^2} - 1\Big|_{gauss} = 15-3\cdot 3+3-1 = 8. \end{cases} \tag{A.1-22a}$$

Consequently, we have

$$L^{(4)} - 2L^{(2)^2}\Big|_{gauss} = 2-2\cdot 1^2 = 0 \; , \tag{A.1-23}$$

so that (A.1-17) and (A.1-21) reduce now to

$$g^*_{coh}\Big|_{gauss} = [\log \mu - \sum_i^n \frac{\bar{\theta}_o^2}{2}] + \sum_i^n \bar{\theta}_i x_i \; ; \quad \theta_i = a_{oi} s_i \; ; \tag{A.1-24}$$

$$g^*_{inc}\Big|_{gauss} = [\log \mu - \frac{1}{2}\sum_i^n \langle \theta_i^2 \rangle - \frac{1}{4}\sum_{ij}^n \langle \theta_i \theta_j \rangle^2] + \frac{1}{2!}\sum_{ij}^n \langle \theta_i \theta_j \rangle x_i x_j \; . \tag{A.1-25}$$

These results demonstrate that the LOBD's for coherent and incoherent reception in gauss noise are, respectively, the cross-correlator $\sum_i^n \bar{\theta}_i x_i$, and the autocorrelator, $\sum_{ij}^n \langle \theta_i \theta_j \rangle x_i x_j$, specifically here for independent noise samples. (With correlated noise samples the corresponding structures are given in Sec. 2.3 above.) These results also agree precisely with the earlier developments (20.72), (20.81) or (20.11) of [12], when $\underset{\sim}{k}_N^{-1} = \delta_{ij}$ therein (independent noise samples). Note that these results apply for non-stationary as well as stationary noise processes: provided $w_1(x_i)$ is normalized to the mean intensity of the i^{th} sample, so that $L^{(2)}$, $L^{(4)}$ are then invariant of i. If a fixed normalization (over the observation period) is used, then $w_1 \to w_{1i}$, and we must explicitly account for the scale of the i^{th} sample. In the following analysis we shall, in the nonstationary cases, generally assume that the latter convention is chosen, so that the $L^{(2)}$, etc., must be indexed, e.g., $L_i^{(2)}$, etc., as distinct from the stationary cases.

APPENDIX A-2

Means and Variances of the Optimum Threshold Dectection Algorithm:

Here we calculate the first and second moments of the LOBD's g^*_{coh}, g^*_{inc}, in order to obtain the desired performance measures (P^*_D, P^*_e), as described generally in Section 2.4, for these threshold detection régimes. Again, independent noise samples are postulated, cf. Sec. A.1-2. We begin with the "on-off" cases (H_1 vs. H_0) in the coherent detection mode.

A.2-1: Coherent Detection

Let us consider the H_1-average, $\langle\ \rangle_{1,\theta}$ of g^*_{coh}, (A.1-17), for independent samples, viz:

$$\left\langle g^*_{coh}\right\rangle_{1,\theta} = \left\langle \int_{-\infty,(\underset{\sim}{x})}^{\infty} \prod_{i=1}^{n} w_1(x_i-\theta_i)_N g^*_{coh}(\underset{\sim}{x})d\underset{\sim}{x}\right\rangle_\theta$$

$$= B^*_{n-c} - \sum_{i=1}^{n}\langle\theta_i\rangle\left\langle\int_{-\infty}^{\infty}\ell(x_i)w_1(x_i-\theta_i)dx_i\right\rangle_\theta . \qquad \text{(A.2-1)}$$

Expanding w_1 about θ_i, we see that now for symmetrical pdf's, w_1,

$$\left\langle\int_{-\infty}^{\infty}\ell w_1 dx\right\rangle_\theta\Big|_i = \left(\left\langle\int_{-\infty}^{\infty}\frac{w_1'}{w_1}\left[w_1-\theta w_1'+\frac{\theta^2}{2!}w_1^{(")}-\frac{\theta^3}{3!}w_1^{("')}+\ldots\right]dx\right\rangle_\theta\right)_i \qquad \text{(A.2-2a)}$$

$$= 0-\langle\theta_i\rangle\left(\int_{-\infty}^{\infty}\left(\frac{w_1'}{w_1}\right)^2 w_1 dx\right)_i + 0-\frac{\langle\theta_i^3\rangle}{3!}\left(\int_{-\infty}^{\infty}\frac{w_1' w_1^{("')}}{w_1}dx\right)_i + O(\langle\theta_i^5\rangle), \qquad \text{(A.2-2b)}$$

since if w_1 is symmetric (about x=0), w_1', $w_1^{("')}$, etc. are anti-symmetric, while $w_1^{(")}$, $w_1^{(4)}$, etc. remain symmetric. We have for (A.2-1), accordingly

$$\langle g^*_{coh}\rangle_{1,\theta} = B^*_{n-c} + \sum_{i=1}^{n} \{\langle\theta_i\rangle^2 L_i^{(2)} + \frac{\langle\theta_i^3\rangle\langle\theta_i\rangle}{3!} L_i^{(1,3)} + O(\langle\theta_i^5\rangle)\}$$

$$\doteq \boxed{B^*_{n-c} + \sum_{i}^{n} \langle\theta_i\rangle^2 L_i^{(2)} + O(\overline{\theta^4}) \ ,} \qquad \text{(A.2-3)}$$

where

$$L^{(1,3)} \equiv \int_{-\infty}^{\infty} \frac{w_1'}{w_1} \cdot \frac{w_1^{(''')}}{w_1} w_1 dx \ (\neq 0), \text{ etc.}$$

The H_o-average, $\langle\ \rangle_{o,\theta=0}$, of (A.1-17 follows at once from (A.2-2a) on setting θ=0 therein (before $\langle\ \rangle_\theta$), e.g.

$$\boxed{\langle g^*_{coh}\rangle_o = B^*_{n-c}} \ , \quad (\text{all } \theta). \qquad \text{(A.2-4)}$$

We proceed in the same fashion for <u>the second moment:</u>

$$\langle (g^*_{coh})^2\rangle_{1,\theta} = \Big\langle B^{*2}_{n-c} - 2B^*_{n-c} \sum_i \langle\theta_i\rangle \ell(x_i) + \sum_{ij} \langle\theta_i\rangle\langle\theta_j\rangle \ell_i \ell_j \Big\rangle_{1,\theta}. \qquad \text{(A.2-5)}$$

Equation (A.2-2) gives us $\langle\ell\rangle_{1,\theta}$. For $\langle\ell_i\ell_j\rangle_{1,\theta}$ we have

<u>(i=j):</u>

$$\langle \ell_i^2\rangle_{1,\theta} = \Big\langle \int_{-\infty}^{\infty} (\frac{w_1'}{w_1})^2 [w_1 - \theta w_1' + \frac{\theta^2}{2!} w_1'' \ \ldots] dx \Big\rangle_\theta \Big|_i$$

$$= L_i^{(2)} + \frac{\langle\theta_i^2\rangle}{2} L_i^{(2,2)} + O(\langle\theta_i^4\rangle); \quad \boxed{L_i^{(2,2)} \equiv \int_{-\infty}^{\infty} (\frac{w_1'}{w_1})^2 (\frac{w_1''}{w_1}) w_1 dx)_i;}$$

(A.2-6)

$(i \neq j)$:

$$\langle \ell_i \ell_j \rangle_{1,\theta} = \left\langle \langle \ell_i \rangle_1 \langle \ell_j \rangle_1 \right\rangle_\theta = \left\langle (-\theta_i L_i^{(2)} - \frac{\theta_i^3}{3!} L_i^{(1,3)} \ldots)(-\theta_j L_j^{(2)} - \frac{\theta_j^3}{3!} L_j^{(1,3)} \ldots) \right\rangle_\theta \tag{A.2-7a}$$

$$\therefore \langle \ell_i \ell_j \rangle_{1,\theta} = \langle \theta_i \theta_j \rangle L_i^{(2)} L_j^{(2)} + \frac{1}{3!} \langle \theta_i^3 \theta_j \rangle L_i^{(1,2)} L_j^{(2)} + \frac{1}{3!} \langle \theta_i \theta_j^3 \rangle L_j^{(1,3)} L_i^{(2)} + \ldots; \quad (i \neq j) \ . \tag{A.2-7b}$$

The result for the last term of (A.2-5) is

$$\sum_{ij} \langle \theta_i \rangle \langle \theta_j \rangle \langle \ell_i \ell_j \rangle_{1,\theta} = \sum_i \langle \theta_i \rangle^2 [L_i^{(2)} + \frac{\langle \theta_i^2 \rangle}{2} L_i^{(2,2)} + \ldots]$$

$$+ \sum_{ij}{}' \langle \theta_i \rangle \langle \theta_j \rangle [\langle \theta_i \theta_j \rangle L_i^{(2)} L_j^{(2)} + \ldots]. \tag{A.2-8}$$

Since we ultimately want the variance, $\mathrm{var}_{1,\theta} g_c^*$, rather than the second moment alone, we can write

$$\boxed{\mathrm{var}_{1,\theta} g_c^* = \langle g_c^{*2} \rangle_{1,\theta} - \langle g_c^* \rangle_{1,\theta}^2 = \sum_{ij} \langle \theta_i \rangle \langle \theta_j \rangle [\langle \ell_i \ell_j \rangle_{1,\theta} - \langle \ell_i \rangle_{1,\theta} \langle \ell_j \rangle_{1,\theta}],} \tag{A.2-9}$$

a simpler result, independent of the bias B_{n-c}^*, as expected. Since from (A.2-2b)

$$\langle \ell_i \rangle_{1,\theta} = -\langle \theta_i \rangle L_i^{(2)} - \frac{\langle \theta_i^3 \rangle}{3!} L_i^{(1,3)} \ldots, \tag{A.2-10}$$

we obtain from (A.2-8), (A.2-10), in (A.2-9)

$$(\sigma_1^*)^2 \equiv \mathrm{var}_{1,\theta} g_c^* = \sum_i \langle\theta_i\rangle^2 (L_i^{(2)} + \frac{\langle\theta_i^2\rangle}{2} L_i^{(2,2)} + \ldots - L_i^{(2)^2} \langle\theta_i\rangle^2 \ldots)$$

$$+ \sum_{ij}{}' \langle\theta_i\rangle\langle\theta_j\rangle (\langle\theta_i\theta_j\rangle L_i^{(2)} L_j^{(2)} + 1 \ldots - \langle\theta_i\rangle\langle\theta_j\rangle L_i^{(2)} L_j^{(2)} \ldots).$$

(A.2-11a)

In a similar way we obtain

$$\boxed{\mathrm{var}_{o,o} g_c^* = \langle g_c^{*2}\rangle_{o,o} - \langle g_c^*\rangle_{o,o}^2 = \sum_{ij}^{n} \langle\theta_i\rangle\langle\theta_j\rangle [\langle\ell_i\ell_j\rangle_{o,o} - \langle\ell_i\rangle_{o,o}\langle\ell_j\rangle_{o,o}].}$$

(A.2-12)

From (A.2-2) $\langle\ell_i\rangle_{o,o} = 0$ and

$$\langle\ell_i\ell_j\rangle_{o,o} = \langle\ell_i^2\rangle_{o,o} = L_i^{(2)}\delta_{ij} \; ; = \langle\ell_i\rangle_o\langle\ell_j\rangle_o = 0, \; i \neq j \; , \qquad \text{(A.2-13)}$$

so that

$$\boxed{(\sigma_o^*)^2 \equiv \mathrm{var}_{o,o} g_c^* = \sum_i^n \langle\theta_i\rangle^2 L_i^{(2)} = -2\hat{B}_{n-c}^*, \text{ cf. (A.1-16)} \; ,} \qquad \text{(A.2-14)}$$

exactly.

From a comparison of (A.2-11) and (A.2-14) we see at once that because of the consistency condition on the threshold expansion by which the bias is determined [cf. Sec. (2.4)], which also requires that $\sigma_1^{*2} \doteq \sigma_o^{*2}$, we have specifically the requirement on input signal level $\langle\theta\rangle$, or $\langle\theta\rangle^2$, that

$\sigma^{*2}_{1c} \doteq \sigma^{*2}_{oc}$:

$$\left| \sum_i \langle\theta_i\rangle^2 \left[\langle\theta_i^2\rangle \frac{L_i^{(2,2)}}{2} - \langle\theta_i\rangle^2 L_i^{(2)^2} + \right.\right.$$

$$\left.\left. + \sum_{ij}{}' \langle\theta_i\rangle\langle\theta_j\rangle L_i^{(2)} L_j^{(2)} \left(\langle\theta_i\theta_j\rangle - \langle\theta_i\rangle\langle\theta_j\rangle\right)\right| << \sigma_o^{*2} = \sum_i \langle\theta_i\rangle^2 L_i^{(2)} \ . \qquad \text{(A.2-15a)}$$

This reduces in the stationary régimes [where now $\langle\theta_i\rangle = \overline{a_o}\ \overline{s_i} = \overline{a_o}$, since because of coherence $\overline{s_i} = s_{max} = \sqrt{2}$, etc.] to

$\sigma^{*2}_{1c} \doteq \sigma^{*2}_{oc}$:

$$\left| \{\overline{a_o^2}\, L^{(2,2)}/2L^{(2)} - \bar{a}_o^2 L^{(2)}\} + \frac{L^{(2)}}{n} \sum_{ij}{}' \left(\overline{a_{oi} a_{oj}} - \bar{a}_o^2\right)\right| << 1 \qquad \text{(A.2-15b)}$$

and clearly there is a dependence on sample size (n). For slow and rapid fading (A.2-15b) reduces further to

(i). slow fading and no fading:

$$\left| \overline{a_o^2}\, L^{(2,2)}/2L^{(2)} - \overline{a_o^2} L^{(2)}\right| << 1 \ ; \qquad \text{(A.2-15c)}$$

(ii). rapid fading:

$$\left|\{\overline{a_o^2}\, L^{(2,2)}/2L^{(2)} - \bar{a}_o^2 L^{(2)}\}\right| << 1 \quad ; \qquad \text{(A.2-15d)}$$

(iii). no fading:

$$\overline{a_o^2}\,|(L^{(2,2)}/2 - L^{(2)^2})/L^{(2)}| \ll 1, \tag{A.2-15e}$$

cf. (A.2-17a) ff.

In the strictly coherent régimes (no fading), we have $\langle\theta_i\theta_j\rangle = \langle\theta_i\rangle\langle\theta_j\rangle$ here. Moreover

$$L^{(2,2)} = \int_{-\infty}^{\infty} (\frac{w_1'}{w_1})^2 w_1'' dx = w_1'(\frac{w_1'}{w_1})^2\Big|_{-\infty}^{\infty} - \int_{-\infty}^{\infty} (\frac{2w_1''}{w_1^2} - 2\frac{w_1'^2 \cdot w_1'}{w_1^3})\, w_1' dx$$

$$= 2\int_{-\infty}^{\infty} (\frac{w_1'}{w_1})^4 w_1 dx = 2\langle \ell^4\rangle_o\ , \tag{A.2-16a}$$

$$\therefore\ \frac{L^{(2,2)}}{2} - L^{(2)^2} = \frac{2\langle\ell^4\rangle_o}{2} - \langle\ell^2\rangle_o = \mathrm{var}_o\ell^2\ ;\ \ L^{(2)} = \langle\ell^2\rangle_o = \mathrm{var}_o\ell. \tag{A.2-16b}$$

Accordingly, the condition on $\langle\theta_i\rangle$, (A.2-15a), becomes

$$\boxed{\sum_i^n \langle\theta_i\rangle^4 \mathrm{var}_o\ell_i^2 \Big/ \sum_i^n \langle\theta_i\rangle^2 \mathrm{var}_o\ell_i \ll 1. \quad ,} \tag{A.2-17}$$

for $\sigma_1^{*2} \doteq \sigma_o^{*2}$.

When stationarity obtains, in addition, $L_i^{(2)} = L^{(2)}$, etc., $\langle\theta_i\rangle = \bar{a}_o\bar{s}$, all i, so that (A.2-17) reduces further to

$$\boxed{\bar{a}_o^2\,\bar{s}^2\,(\frac{\mathrm{var}_o\ell^2}{\mathrm{var}_o\ell}) \ll 1} \quad ,\ \ \overline{a_o}\ ,\ \bar{s} > 0\ , \tag{A.2-17a}$$

which is independent of sample size (n), as is (A.2-17) essentially, if ℓ_i does not vary too much (i=1,...n).

A.2-2: Incoherent Detection:

Here we seek the mean and variance of g^*_{inc}, (A.1-21), when (A.1-20a) is the general bias in the non-stationary cases. We proceed as in Sec. A.2-1 and consider first the H_1-average of g^*_{inc}:

$$\langle g^*_{inc}\rangle_{1,\theta} = B^*_{n\text{-}inc} + \frac{1}{2}\sum_{ij}^{n} \langle\theta_i\theta_j\rangle\langle \ell_i\ell_j+\ell'_i\delta_{ij}\rangle_{1,\theta} \tag{A.2-18}$$

Specifically, we have (cf. A.1-11):

(i=j):

$$\langle \ell_i^2+\ell'_i\rangle_{1,\theta} = \left\langle \int_{-\infty}^{\infty} \left(\frac{w_1''}{w_1}\right)_i w_1(x_i-\theta_i)dx_i\right\rangle_{\theta_i} \tag{A.2-19a}$$

$$= \left\langle \int_{-\infty}^{\infty}\frac{w_1''}{w_1}\left[w_1-\theta w_1'+\frac{\theta^2}{2!}w_1''+\frac{-\theta^3}{3!}w_1^{(''')}+\ldots\right]dx\right\rangle_{\theta,i}$$

$$= 0 - 0 + \frac{\langle\theta_i^2\rangle}{2!}\left(\int_{-\infty}^{\infty}\left(\frac{w_1''}{w_1}\right)^2 w_1\,dx\right)_i - 0 + \frac{\langle\theta_i^4\rangle}{4!}\left(\int_{-\infty}^{\infty}\left(\frac{w_1^{(''')}}{w_1}\right)\left(\frac{w_1^{(4)}}{w_1}\right)w_1\,dx\right)_i \cdots$$

$$= \frac{\langle\theta_i^2\rangle}{2}L_i^{(4)} + \frac{\langle\theta_i^4\rangle}{4!}L_i^{(2,4)} + O(\overline{\theta^6}) \ , \tag{A.2-19b}$$

where

$$L_i^{(2,4)} \equiv \left(\int_{-\infty}^{\infty}\left(\frac{w_1''}{w_1}\right)\left(\frac{w_1^{(4)}}{w_1}\right)w_1\,dx\right)_i \ , \tag{A.2-19c}$$

and we have used the symmetry property of w_1, $w_1^{(''')}$, etc., and the antisymmetry of w_1', $w_1^{(3)}$, etc.

Similarly, we have

(i≠j):

$$\langle \ell_i \ell_j + \ell_i' \delta_{ij} \rangle_{1,\theta} = \langle \langle \ell_i \rangle_1 \langle \ell_j \rangle_1 \rangle_\theta = \langle \theta_i \theta_j \rangle L_i^{(2)} L_j^{(2)} + O(\bar{\theta}^4), \quad \text{Eq. (A.2-7b)}, \tag{A.2-20}$$

so that combining (A.2-19b) and (A.2-20) in (A.2-18) yields specifically

$$\langle g_{inc}^* \rangle_{1,\theta} = B_{n\text{-}inc}^* + \frac{1}{2} \left\{ \sum_{ij}{}' \langle \theta_i \theta_j \rangle^2 L_i^{(2)} L_j^{(2)} + \sum_i \frac{\langle \theta_i^2 \rangle^2}{2} L^{(4)} + O(\overline{\theta_i^6}) \right\} \tag{A.2-21a}$$

$$= B_{n\text{-}inc}^* + \frac{1}{4} \left\{ \sum_{ij} \langle \theta_i \theta_j \rangle^2 [(L_i^{(4)} - 2L_i^{(2)^2}) \delta_{ij} + 2L_i^{(2)} L_j^{(2)}] \right\}, \tag{A.2-21b}$$

which now combined with (A.1-20a) for the bias $B_{n\text{-}inc}^*$ gives directly

$$\langle g_{inc}^* \rangle_{1,\theta} = \log \mu + \frac{1}{8} \sum_{ij} \langle \theta_i \theta_j \rangle^2 [L_i^{(4)} - 2L_i^{(2)^2}) \delta_{ij} + 2L_i^{(2)} L_j^{(2)}] \tag{A.2-22a}$$

$$= \log \mu - \hat{B}_{n\text{-}inc}^* , \tag{A.2-22b}$$

cf. (A.1-20a).

The H_o-moment of g_{inc}^* is found at once to be

$$\langle g_{inc}^* \rangle_{o,o} = B_{n\text{-}inc}^* + \frac{1}{2} \sum_{ij} \langle \ell_i \ell_j + \ell_i' \delta_{ij} \rangle_{o,o} \langle \theta_i \theta_j \rangle, \tag{A.2-23}$$

where

$$\underline{(i=j):} \qquad \langle \ell_i^2+\ell_i' \rangle_{o,o} = \int_{-\infty}^{\infty} \frac{w_{1i}''}{w_{1i}} \, w_1(x_i)dx_i = w_{1i}' \Big|_{-\infty}^{\infty} = 0 \ , \tag{A.2-24a}$$

$$\underline{(i\neq j):} \qquad \langle \ell_i \rangle_o \langle \ell_j \rangle_o = 0 \ , \text{ (A.1-13b)}, \tag{A.2-24b}$$

so that

$$\boxed{\langle g^*_{inc} \rangle_{o,o} = B^*_{n\text{-}inc} = \text{Eq. (A.1-20a)} = \log \mu + \hat{B}^*_{inc}.} \tag{A.2-25}$$

We proceed similarly for $\text{var}_{1,\theta} g^*_{inc}$, cf. (A.2-9). From (A.1-21) specifically we write

$$\text{var}_{1,\theta} g^*_{inc} = \frac{1}{4} \sum_{ijk\ell}^{n} \{ \langle F(x_i,x_j|\theta_i,\theta_j)F(x_k,x_\ell|\theta_k,\theta_\ell) \rangle_{1,\theta}$$

$$- \langle F(x_i,x_j|\theta_i,\theta_j) \rangle_{1,\theta} \langle F(x_k,x_\ell|\theta_k,\theta_\ell) \rangle_{1,\theta} \ , \tag{A.2-26}$$

where

$$F(x_i,x_j|\theta_i,\theta_j) \equiv (\ell_i\ell_j+\ell_i'\delta_{ij}) \langle \theta_i\theta_j \rangle \ . \tag{A.2-26a}$$

Let us consider the first average in (A.2-26). We have

$$\sum_{ijk\ell} \langle F_{ij}F_{k\ell} \rangle_{1,\theta} = \Big\langle \Big[\sum_i \frac{w_{1i}^{(")}}{w_{1i}} \langle \theta_i^2 \rangle + \sum_{ij}^{(i\neq j)} \ell_i\ell_j \langle \theta_i\theta_j \rangle \Big]$$

$$\cdot \Big[\sum_k \frac{w_{1k}^{(")}}{w_{1k}} \langle \theta_k^2 \rangle + \sum_{k\ell}^{(k\neq \ell)} \ell_k\ell_\ell \langle \theta_k\theta_\ell \rangle \Big] \Big\rangle_{1,\theta} \ , \tag{A.2-27}$$

cf. (A.1-19). We proceed as for (A.1-19) et seq. and distinguish the following terms [through $O(\theta^6)$ in (A.2-27), or equivalently, through $O(\theta^2)$ in the

coefficients of $\langle\theta_i^2\rangle$, etc.]:

(1). $(i\neq k)$:

$$\left\langle\left\langle\frac{w_{1i}^{(")}}{w_{1i}}\right\rangle_1\left\langle\frac{w_{1k}^{(")}}{w_{1k}}\right\rangle_1\right\rangle_\theta = \left\langle\int_{-\infty}^{\infty}\frac{w_{1i}^{(")}}{w_{1i}}w_1(x_i-\theta_i)dx_i\int_{-\infty}^{\infty}\frac{w_{1k}^{(")}}{w_{1k}}w_1(x_k-\theta_k)dx_k\right\rangle_\theta \quad \text{(A.2-28a)}$$

$$= \left\langle\int_{-\infty}^{\infty}\frac{w_{1i}^{(")}}{w_{1i}}[w_{1i}-\theta_i w'_{1i}+\frac{\theta_i^2}{2}w''_{1i}\cdots]dx_i\right.$$

$$\left.\cdot\int_{-\infty}^{\infty}\frac{w_{1k}^{(")}}{w_{1k}}[w_{1k}-\theta_k w'_{1k}+\frac{\theta_k^2}{2}w''_{1k}\cdots]dx_k\right\rangle_\theta$$

$$= \left\langle[0-0+\frac{\theta_i^2}{2}\left\langle\left(\frac{w''_{1i}}{w_{1i}}\right)^2\right\rangle_o+..][0-0+\frac{\theta_k^2}{2}\left\langle\left(\frac{w''_{1k}}{w_{1k}}\right)^2\right\rangle_o+\ldots]\right\rangle_\theta$$

$$= \frac{\langle\theta_i^2\theta_k^2\rangle}{4}L_i^{(4)}L_k^{(4)}+O(\overline{\theta^6}) \ . \quad \text{(A.2-28b)}$$

(2). $(i=k)$:

$$\left\langle\left(\frac{w_{1i}^{(")}}{w_{1i}}\right)^2\right\rangle_{1,\theta} = L_i^{(4)}+\frac{\langle\theta_i^2\rangle}{2}\left\langle\left(\frac{w_{1i}^{(")}}{w_{1i}}\right)^3\right\rangle_o+.. = L_i^{(4)}+\frac{\langle\theta_i^2\rangle}{2}L_i^{(6)}+\ldots, \quad \text{(A.2-29a)}$$

where

$$\boxed{L_i^{(6)} \equiv \int_{-\infty}^{\infty}\left(\frac{w_{1i}^{(")}}{w_{1i}}\right)^3 w_{1i}dx_i \ .} \quad \text{(A.2-29b)}$$

Next, let us consider the product terms $J_4 \equiv \left\langle\sum_{ij}{}' a_{ij}\sum_{k\ell}{}' a_{k\ell}\right\rangle_{1,\theta}$ (where the prime, as before, indicates that terms j=i, etc., are omitted in the summations). Let us rewrite J_4 as

$$J_4 \equiv \sum_{ijk\ell} \left\langle (1-\delta_{ij})(1-\delta_{k\ell}) a_{ij} a_{k\ell} \right\rangle_{1,\theta} =$$

$$= \sum_{ijk\ell} \left\langle a_{ij} a_{k\ell} \right\rangle_{1-\theta} - 2 \sum_{ij\ell} \left\langle a_{ii} a_{j\ell} \right\rangle_{1-o} + \sum_{ij} \left\langle a_{ii} a_{jj} \right\rangle_{1-o} , \qquad \text{(A.2-30a)}$$

where $a_{ij} = \langle \theta_i \theta_j \rangle \ell_i \ell_j$, etc. Of fourth-order **product** averages $J_{4/4}$, we have from the leading term of (A.2-30a):

(3) $\underline{(i \neq j) \neq (k \neq \ell)}$:

$$\left\langle \ell_i \ell_j \ell_k \ell_\ell \right\rangle_{1,\theta} = \left\langle \int_{-\infty}^{\infty} \cdots \int \left(\frac{w'_{1i}}{w_{1i}}\right)\left(\frac{w'_{ij}}{w_{ij}}\right)\left(\frac{w'_{ik}}{w_{1k}}\right)\left(\frac{w'_{1\ell}}{w_{1\ell}}\right)\left[w_{1i} - \theta_i w'_{1i} + \frac{\theta_i^2}{2} w''_{1i} + \ldots\right] \right.$$

$$\left. \cdot \left[w_{ij} - \theta_j w'_{ij} + \ldots\right]\left[w_{1k} - \theta_k w'_{1k} + \ldots\right]\left[w_{1\ell} - \theta_\ell w'_{1\ell} + \ldots\right] dx_i \ldots dx_\ell \right\rangle_\theta$$

$$= 0 + \left\langle \theta_i \theta_j \theta_k \theta_\ell \right\rangle L_i^{(2)} L_j^{(2)} L_k^{(2)} L_\ell^{(2)} + O(\overline{\theta^8}) , \qquad \text{(A.2-30b)}$$

which accordingly do not contribute $O(\overline{\theta^2})$, i.e. $O(\overline{\theta^6})$ in J_4 when we include the $\langle \theta_i \theta_j \rangle \langle \theta_k \theta_\ell \rangle$ factors in a_{ij}, $a_{k\ell}$, etc. Of third-order products, $J_{4/3}$, we need to consider the first two terms of (A.2-30a), where now

(4). $\underline{(i \neq j);(k \neq \ell)}$: (a). and k=i, or ℓ=i, or k=j, or ℓ=j, $\therefore$ 4x(k=i) contributions

$$\therefore \quad J_{4/3} = 4 \sum_{ij\ell}^{i\neq j\neq \ell} \left\langle a_{ij} a_{i\ell} \right\rangle_{1,\theta} - 2 \sum_{ij\ell}^{i\neq j\neq \ell} \left\langle a_{ii} a_{j\ell} \right\rangle_{1,\theta} \qquad \text{(A.2-30c)}$$

$$= \sum_{ij\ell}^{i\neq j\neq \ell} \left\langle \left\langle \ell_i^2 \right\rangle_1 \left\langle \ell_j \right\rangle_1 \left\langle \ell_\ell \right\rangle_1 \right\rangle_\theta \left[4 \left\langle \theta_i \theta_j \right\rangle \left\langle \theta_\ell \theta_i \right\rangle - 2 \left\langle \theta_i^2 \right\rangle \left\langle \theta_\ell \theta_j \right\rangle\right]. \qquad \text{(A.2-30d)}$$

Now

$$\left\langle \langle \ell_i^2 \rangle_1 \langle \ell_j \rangle_1 \langle \ell_\ell \rangle_1 \right\rangle_\theta = \left\langle \int_{-\infty}^{\infty} \cdots \int \left(\frac{w'_{1i}}{w_{1i}}\right)^2 \left(\frac{w'_{ij}}{w_{ij}}\right)\left(\frac{w'_{1\ell}}{w_{1\ell}}\right)[w_{1i}-\theta_i w_{1i}+\ldots]\right.$$

$$\left. \cdot[w_{1j}-\theta_j w'_{1j}+..][w_{1\ell}-\theta_\ell w'_{1\ell}+..]dx_i dx_j dx_\ell \right\rangle_\theta$$

$$= 0+L_i^{(2)}\langle \theta_j \theta_\ell \rangle L_j^{(2)} L_\ell^{(2)}+O(\overline{\theta^4}) \ , \qquad \text{(A.2-31)}$$

so that $J_{4/3}$ becomes

$$J_{4/3} = \sum_{ij\ell}''' L_i^{(2)} L_j^{(2)} L_\ell^{(2)} [4\langle \theta_i \theta_j \rangle \langle \theta_j \theta_\ell \rangle \langle \theta_\ell \theta_i \rangle - 2\langle \theta_i^2 \rangle \langle \theta_j \theta_\ell \rangle^2]. \qquad \text{(A.2-31a)}$$

For second-order products $J_{4/2}$ we have directly from J_4 as a whole:

(b) $\left.\begin{array}{l} i=k;j=\ell: \\ \\ i=\ell;j=k: \ (i\neq j;k\neq \ell) \end{array}\right\} \langle \ell_i^2 \ell_j^2 \rangle_{1,\theta} x2 :$

$$\langle \ell_i^2 \ell_j^2 \rangle x2 = 2\left\langle \int_{-\infty}^{\infty} \cdots \int \left(\frac{w'_{1i}}{w_{1i}}\right)^2 \left(\frac{w'_{ij}}{w_{ij}}\right)^2 [w_{1i}-\theta_i w'_{1i}+\frac{\theta_i^2}{2} w''_{1i}+..]\right.$$

$$\left. \cdot[w_{1j}-\theta_j w'_{1j}+\frac{\theta_j^2}{2} w''_{1j}+..]dx_i dx_j \right\rangle_\theta$$

$$= 2L_i^{(2)} L_j^{(2)}+L_i^{(2)} L_j^{(2,2)} \langle \theta_j^2 \rangle + L_j^{(2)} L_i^{(2,2)} \langle \theta_i^2 \rangle + O(\overline{\theta^4}) \qquad \text{(A.2-32a)}$$

$$\therefore J_{4/2} = 2 \sum_{ij} L_i^{(2)} L_j^{(2)} \langle \theta_i \theta_j \rangle^2 + 2 \sum_{ij} \langle \theta_i \theta_j \rangle^2 \langle \theta_i^2 \rangle L_i^{(2,2)} L_j^{(2)} + O(\overline{\theta^8}) \ . \qquad \text{(A.2-32b)}$$

In addition to the sets of terms (1)-(4) in the product (A.2-27) there are also the following:

(5). $\left\langle \frac{w''_{1i}}{w_{1i}} \ell_k \ell_\ell \right\rangle_{1,\theta}$: $\underline{k \neq \ell}$: i=k, or i=ℓ; or i≠k≠ℓ:

[(x2): for (i≠j): k=i, or k=j, or k≠i≠j:] (A.2-33)

We have

(5a) $\underline{k \neq \ell}$: i=k:

$$\left\langle \frac{w''_{1i}}{w_{1i}} \ell_i \ell_\ell \right\rangle_{1,\theta} = \left\langle \int_{-\infty}^{\infty} \cdots \int \frac{w''_{1i}}{w_{1i}} \frac{w'_{1i}}{w_{1i}} \frac{w'_{1\ell}}{w_{1\ell}} [w_{1i} - \theta_i w'_{1i} + ..] \right.$$

$$\left. \cdot [w_{1\ell} - \theta_\ell w'_{1\ell} + ..] dx_1 .. dx_\ell \right\rangle_\theta \qquad \text{(A.2-34a)}$$

$$= 0 + \langle \theta_i \theta_\ell \rangle \int_{-\infty}^{\infty} \cdots \int \frac{w''_{1i}}{w_{1i}} \left(\frac{w'_{1i}}{w_{1i}}\right)^2 \left(\frac{w'_{1\ell}}{w_{1\ell}}\right)^2 w_{1i} \, w_{1\ell} dx_i dx_\ell + O(\overline{\theta^4})$$

$$= 0 + L_i^{(2,2)} L_\ell^{(2)} \langle \theta_i \theta_\ell \rangle + O(\overline{\theta^4}) \ . \qquad \text{(A.2-34b)}$$

(5b). $\underline{k \neq \ell}$: i=ℓ:

$$\left\langle \frac{w''_{1i}}{w_{1i}} \ell_i \ell_k \right\rangle_{1,\theta} = 0 + L_i^{(2,2)} L_k^{(2)} \langle \theta_i \theta_k \rangle + O(\overline{\theta^4}) \ , \text{ similarly.} \qquad \text{(A.2-35)}$$

(5c). $k\neq\ell$: $i\neq k(\neq\ell)$:

$$\left\langle \frac{w''_{1i}}{w_{1i}}\, \ell_k \ell_\ell \right\rangle_{1,\theta} = \left\langle \int_{-\infty}^{\infty}\cdots\int \frac{w''_{1i}}{w_{1i}} \frac{w'_{1\ell}}{w_{1\ell}} \frac{w'_{1k}}{w_{1k}} [w_{1i}-\theta_i w'_{1i}+ \frac{\theta_i^2}{2} w''_{1i}+\ldots] \right.$$

$$\left. \cdot[w_{1k}-\theta_k w'_{1k}+..][w_{1\ell}-\theta_\ell w'_{1\ell}+..]dx_i dx_k dx_\ell \right\rangle_\theta$$

$$= 0 + \frac{L_i^{(4)}}{2} \langle \theta_i^2 \theta_k \theta_\ell \rangle L_k^{(2)} L_\ell^{(2)} = 0+0(\overline{\theta^4}) \ . \qquad \text{(A.2-36)}$$

From (A.2-33) we repeat the above, equivalent to multiplying by a factor 2 in the relevant summations.

Combining the results of (1)-(5) for the average (A.2-27) then yields:

$$\sum_{ijk\ell} \left\langle F_{ij}F_{k\ell} \right\rangle_{1,\theta} = \sum_{ij} \langle \theta_i\theta_j \rangle^2 [(L_i^{(4)}-2L_i^{(2)^2})\delta_{ij}+2L_i^{(2)}L_j^{(2)}]$$

$$+ \sum_i \frac{\langle \theta_i^2 \rangle^3}{2} L_i^{(6)} + 6 \sum_{ij} \langle \theta_i^2 \rangle \langle \theta_i\theta_j \rangle^2 L_j^{(2)} L_i^{(2,2)}$$

$$+ \sum_{ijk}^{(i\neq j\neq k)} L_i^{(2)} L_j^{(2)} L_k^{(2)} [4\langle \theta_i\theta_j \rangle \langle \theta_j\theta_k \rangle \langle \theta_k\theta_i \rangle$$

$$- 2\langle \theta_i^2 \rangle \langle \theta_j\theta_k \rangle^2] + 0(\overline{\theta^8}) \ . \qquad \text{(A.2-37)}$$

From the above it is seen directly that

$$\sum_{ijk\ell} \left\langle F_{ij}F_{k\ell} \right\rangle_{o,o} = \sum_{ij} \langle \theta_i\theta_j \rangle^2 [(L_i^{(4)}-2L_i^{(2)^2})\delta_{ij}+2L_i^{(2)}L_j^{(2)}] = -8\hat{B}^*_{n\text{-inc}},$$

cf. (A.1-20a). (A.2-38)

From (A.2-19b), (A.2-20) we obtain

$$\sum_{ijk\ell} \langle F_{ij} \rangle_{1,\theta} \langle F_{k\ell} \rangle_{1,\theta}$$

$$= \sum_{ij} \left\{ \begin{array}{l} 0+\langle \theta_i \theta_j \rangle^2 L_i^{(2)} L_j^{(2)} (1-\delta_{ij}) \\ \\ 0+ \dfrac{\langle \theta_i^2 \rangle^2}{2} L_i^{(4)} \delta_{ij} \end{array} \right\} \cdot \sum_{k\ell} \left\{ \begin{array}{l} 0+\langle \theta_k \theta_\ell \rangle^2 L_k^{(2)} L_\ell^{(2)} (1-\delta_{k\ell}) \\ \\ 0+ \dfrac{\langle \theta_k^2 \rangle^2}{2} L_k^{(4)} \delta_{k\ell} \end{array} \right\} = 0+0(\overline{\theta^8}) , \qquad \text{(A.2-39)}$$

so that this average is always ignorable [$0(\overline{\theta^6})$] in (A.2-26).

Accordingly, applying (A.2-37) - (A.2-39) to (A.2-26) gives us

$$\sigma^{*2}_{1\text{-inc}} \equiv \text{var}_{1,\theta} g^*_{\text{inc}} \doteq -2\hat{B}^*_{n\text{-inc}}$$

$$= \frac{1}{4} \sum_{ij}^{n} \langle \theta_i \theta_j \rangle^2 [(L_i^{(4)} - 2L_i^{(2)2}) \delta_{ij} + 2L_i^{(2)} L_j^{(2)}] \quad (>0)$$

$$\therefore \sigma^{*2}_{1\text{-inc}} \doteq \sigma^{*2}_{0\text{-inc}} \quad [\equiv \text{var}_{0,0} g^*_{\text{inc}} \text{ , cf. (A.2-38)}] \ . \qquad \text{(A.2-40)}$$

This last relation, viz. $\sigma^{*2}_{1\text{-inc}} \doteq \sigma^{*2}_{0\text{-inc}}$, as required by the nature of the LOBD expansion [cf. Sec. 2.4], puts the necessary condition on the smallness of the input signal by demanding that terms $0(\theta^6)$ in $\text{var}_{1,\theta} g^*_{\text{inc}}$, viz., in (A.2-37) be small vis-à-vis $\sigma^{*2}_{0\text{-inc}}$. Specifically, this condition is

$[\sigma^{*2}_{i\text{-inc}} \doteq \sigma^{*2}_{o\text{-inc}}]$:

$$\left|\sum_{ij}\langle\theta_i^2\rangle\langle\theta_i\theta_j\rangle^2\left[\left(\frac{L_i^{(6)}}{2}\right.\right.\right.\delta_{ij}+6L_i^{(2)}L_j^{(2,2)}\Big]$$

$$+\sum_{ijk}^{(i\neq j\neq k)}L_i^{(2)}L_j^{(2)}L_k^{(2)}\left[4\langle\theta_i\theta_j\rangle\langle\theta_j\theta_k\rangle\langle\theta_k\theta_i\rangle-2\langle\theta_i^2\rangle\langle\theta_j\theta_k\rangle^2\right]$$

$$<<\sum_{ij}\langle\theta_i\theta_j\rangle^2\left[\left(L_i^{(4)}-2L_i^{(2)^2}\right)\delta_{ij}+2L_i^{(2)}L_j^{(2)}\right]. \qquad \text{(A.2-41)}$$

The condition (A.2-41) is considerably more complex than (A.2-17) for the coherent cases, as we might expect from the generally complex nature of the correlated signal samples $\langle\theta_i\theta_j\rangle$, etc. Writing

$$Q_n \equiv \frac{1}{n}\sum_{ij} m_{ij}^2\rho_{ij}^2 \ (\geq 1)\ ;$$

$$R_n \equiv \frac{1}{n}\sum_{ijk}''' \{4m_{ij}m_{jk}m_{ki}\rho_{ij}\rho_{jk}\rho_{ki}-2m_{jk}^2\rho_{jk}^2\}, \qquad \text{(A.2-41a)}$$

with

$$m_{ij} \equiv \overline{a_{oi}a_{oj}}/\overline{a_o^2}\ ;\ \rho_{ij} \equiv \langle s_i s_j\rangle \qquad \text{(A.2-41b)}$$

as before, cf. (6.25), (in the stationary noise cases, e.g. $L_i^{(2)}=L^{(2)}$, etc.), we get directly for (A.2-41)

$$\frac{\overline{a_o^2}\left|\frac{L^{(6)}}{2}+6L^{(2)}L^{(2,2)}Q_n+L^{(2)^3}R_n\right|}{L^{(4)}+2L^{(2)^2}(Q_n-1)} \ll 1\ , \quad (L^{(6)}\neq 0)\ , \tag{A.2-42}$$

Which is the (essentially) general condition on input signal $(\overline{a_o^2})$ that $\sigma_1^{*2} \doteq \sigma_o^{*2}$. Here we have, from A.1, A.2 above, in summary

$$\left.\begin{aligned}
L^{(2)} &\equiv \left\langle\left(\frac{w_1'}{w_1}\right)^2\right\rangle_o = \left\langle \ell^2\right\rangle_o \ (>0), && \text{Eq. (A.1-15);}\\
L^{(2,2)} &\equiv 2\left\langle\left(\frac{w_1'}{w_1}\right)^4\right\rangle_o = 2\left\langle \ell^4\right\rangle_o \ (>0)\ , && \text{Eq. (A.2-16);}\\
L^{(4)} &\equiv \left\langle\left(\frac{w_1''}{w_1}\right)^2\right\rangle_o = \left\langle(\ell'+\ell^2)^2\right\rangle_o \ (>0), && \text{Eq. (A.1-19b);}\\
L^{(6)} &\equiv \left\langle\left(\frac{w_1''}{w_1}\right)^3\right\rangle_o = \left\langle(\ell'+\ell^2)^3\right\rangle_o \ (\lessgtr 0), && \text{Eq. (A.2-29b)}\ .
\end{aligned}\right\} \tag{A.2-42a}$$

We remark that whereas $L^{(2)}$, $L^{(2,2)}$, $L^{(4)}$ are always positive, $L^{(6)}$ can be negative (and zero). [In this last instance, we may have to include an additional term $B\,\overline{a_o^2}$ in the numerator of (A.2-42), e.g. $(L^{(6)}/2) \to (L^{(6)}/2)+B\,\overline{a_o^2}$, when Q_n, R_n vanish.]

For purely incoherent signals, we have $\rho_{ij} = \delta_{ij}$; such signals can result from scatter mechanisms, heavy doppler "smear", and/or rapid fading, or combinations of all these mechanisms. Then, $Q_n = 1$, and $R_n = 0$, cf. (A.2-41a), so that (A.2-42) becomes

incoh.signals :
[Incoh.reception]

$$a_o^2\, F(L^{(2)},\ldots|Q_n,R_n)^{-1} = a_o^2 \cdot \frac{\left|\frac{L^{(6)}}{2} + 6L^{(2)}L^{(2,2)}\right|}{L^{(4)}} << 1. \qquad \text{(A.2-42b)}$$

At the other extreme of purely coherent signals, (e.g. sinusoidal wave trains), we have $\rho_{ij} = \cos\,\omega_o(t_i-t_j)$ etc., with $m_{ij}=1$, etc. Letting $T = n\Delta t$, $t_i = i\Delta t = x$, etc., we have (n large)

$$\left.\begin{aligned} I_1 &\equiv 4 \sum_{ijk}''' \rho_{ij}\rho_{jk}\rho_{ki} \doteq \left(\frac{n}{T}\right)^3 4 \iiint_o^T \cos\,\omega_o(x-y)\cos\,\omega_o(y-z)\cos\,\omega_o(z-x)\,dx\,dy\,dz \\ I_2 &\equiv 2 \sum_{ijk}''' \rho_{jk}^2 \doteq 2n\left(\frac{n}{T}\right)^2 \iint_o^T \cos^2\omega_o(y-z)\,dy\,dz \end{aligned}\right\}. \qquad \text{(A.2-42c)}$$

Expanding and integrating gives, after some algebra:

$$\left\{\begin{aligned} R_n &= \frac{1}{n}(I_1-I_2) = \frac{1}{n}\left(\left[n^3+2n^3\left\{\frac{1-\cos\,2n\omega_o\Delta t}{(2n\omega_o\Delta t)^2} + \frac{\sin\,2n\omega_o\Delta t}{2n\omega_o\Delta t}\right\}\right]_{I_1}\right. \\ &\qquad \left. -\left[n^3+2n^3\left\{\frac{1-\cos\,2n\omega_o\Delta t}{(2n\omega_o\Delta t)^2}\right\}\right]_{I_2}\right) \\ &= 2n\cdot\left(\frac{\sin\,2n\omega_o\Delta t}{2\omega_o\Delta t}\right)\ ; \qquad \text{(A.2-42d)} \\ Q_n &= \frac{n}{2}\left\{1+2\left(\frac{1-\cos\,2n\omega_o\Delta t}{(2n\omega_o\Delta t)^2}\right)\right\}. \qquad \text{(A.2-42e)} \end{aligned}\right.$$

Consequently, the condition (A.4-42) becomes here (n>>1):

Coh. signals
[Incoh.reception]:

$$\overline{a_o^2}\, F_n^{-1} = \overline{a_o^2}\left|\frac{3L^{(2,2)}}{L^{(2)}} + 2L^{(2)}\,\frac{\sin 2n\omega_o\Delta t}{2\omega_o\Delta t}\right| \ll 1,\ n \gg 1, \qquad \text{(A.2-42f)}$$

and we can drop the $|\ |$, since $L^{(2,2)}-2L^{(2)^2} = 2\,\mathrm{var}_o\ell^2(>0)$. As required (and expected), $F_{n\to\infty}$ is effectively independent of sample-size (n). Finally, both Q_n, R_n are $O(n^\lambda,\ 0 \le \lambda < 1)$ when the input signal structure is partially incoherent; $\lambda=0$ usually.

A.2-3: Binary Signal Detection: Optimum Coherent Detection:

Here we extend the analysis above for "on-off" operation [Secs. A.2-1,2] to the important cases of (optimum) binary signal detection, where the optimum algorithm is given generally by (2.15) and (A.1-7), viz:

$$g^{(21)}(\underset{\sim}{x})_c^* = \{\log \mu_{21} + \hat{B}_{nc}^{(21)*}\} + \tilde{\underset{\sim}{y}}\{\langle\underset{\sim}{\theta}^{(2)}\rangle - \langle\underset{\sim}{\theta}^{(1)}\rangle\}, \qquad \text{(A.2-43)}$$

where

$$\tilde{\underset{\sim}{y}}\{\overline{\underset{\sim}{\theta}^{(2)}} - \overline{\underset{\sim}{\theta}^{(1)}}\} = \sum_{i=1}^{n} \ell_i\{\langle a_{oi}^{(2)}s_i^{(2)}\rangle - \langle a_{oi}^{(1)}s_i^{(1)}\rangle\}\ ;\ \underset{\sim}{\theta}^{(1,2)} = \{a_{oi}s_i\}^{(1,2)} \qquad \text{(A.2-43a)}$$

$$\hat{B}_{nc}^{(21)*} = \frac{1}{2!}\Big\langle \tilde{\underset{\sim}{y}}\{\underset{\sim}{\rho}_\theta^{(2)} - \underset{\sim}{\rho}_\theta^{(1)} - (\langle\tilde{\underset{\sim}{\theta}}\rangle^{(2)}\langle\underset{\sim}{\theta}^{(2)}\rangle - \langle\tilde{\underset{\sim}{\theta}}^{(1)}\rangle\langle\underset{\sim}{\theta}^{(1)}\rangle)\underset{\sim}{y}$$

$$+ \langle\underset{\sim}{\theta}^{(2)}\underset{\sim}{z}_\theta^{(2)}\rangle - \langle\underset{\sim}{\theta}^{(1)}\underset{\sim}{z}_\theta^{(1)}\rangle\Big\rangle_{H_o}, \qquad \text{(A.2-43b)}$$

cf. (2.14), with $\underset{\sim}{\rho}_{\theta}^{(1,2)} \equiv \langle a_{oi} a_{oj} s_i s_j \rangle^{(1,2)}$, etc., and $\underset{\sim}{y}$, $\underset{\sim}{z}$ given by A.1-7, A.1-9 etc. Note that the bias is obtained once more by taking the average $\langle\ \rangle_{H_o}$ with respect to H_o: N alone, since these binary detectors are the <u>difference</u> of a pair of "on-off" detectors, cf. (2.14).

Specializing again to independent (noise) sampling, according to (A.1-10) et seq., we get directly [cf. (4.3)]

$$\boxed{g_c^{(21)*} = \log \mu_{21} + \hat{B}_{nc}^{(21)*} - \sum_i^n \ell_i [\langle \theta_i^{(2)} \rangle - \langle \theta_i^{(1)} \rangle]; \quad \overline{\Delta\theta}_i \equiv \langle \theta_i^{(2)} \rangle - \langle \theta_i^{(1)} \rangle .} \tag{A.2-44}$$

Our main problem now is to obtain the bias $\hat{B}_{nc}^{(21)*}$. Having already obtained the bias in the "on-off" cases, cf. (A.1-16) above, we invoke the fact that these binary algorithms are the difference of two "on-off" algorithms, cf. (A.2-43,44), and (2.13)-(2.17) to get directly

$$\boxed{\hat{B}_{nc}^{(21)*} = -\frac{1}{2} \{ \sum_{i=1}^n L_i^{(2)} [\langle \theta_i^{(2)} \rangle^2 - \langle \theta_i^{(1)} \rangle^2] \}.} \tag{A.2-45}$$

(This may also be obtained using (A.1-13)-(A.1-15) directly on (A.2-43b).) Thus, the LOBD for coherent reception in the binary cases (independent noise sampling) can be written explicitly

$$\boxed{\begin{aligned} g_c^{(21)*} = \log \mu_{21} - \frac{1}{2} \{ \sum_i^n L_i^{(2)} [\langle a_{oi}^{(2)} s_i^{(2)} \rangle^2 - \langle a_{oi}^{(1)} s_i^{(1)} \rangle^2] \} \\ - \sum_i^n \ell_i [\langle a_{oi}^{(2)} s_i^{(2)} \rangle - \langle a_{oi}^{(1)} s_i^{(1)} \rangle] . \end{aligned}} \tag{A.2-45a}$$

Note that with gauss noise (A.2-45a) reduces to, cf. (A.1-22):

$$g_c^{(21)*}\Big|_{\text{gauss}} = \{\log \mu_{21} - \frac{1}{2}\sum_i^n [\langle\theta_i^{(2)}\rangle^2 - \langle\theta_i^{(1)}\rangle^2]\} - \sum_i^n [\langle\theta_i^{(2)}\rangle - \langle\theta_i^{(1)}\rangle]x_i , \tag{A.2-46}$$

which shows, as expected, that the (cross-) correlator is now the LOBD once more, with a weighting and bias appropriately structured for these binary cases, cf. (A.1-24).

Our next problem is to obtain the means and variances of $g_c^{(21)*}$, now under (H_2, H_1) respectively, in place of (H_1, H_0) for the "on-off" situations. We take direct advantage of our preceding results in Sec. A.2-1 for the average H_1 and appropriately apply it $g_c^{(21)*}$, (A.2-45a), changing H_1 to H_2 as demanded. First, we see that (A.2-1) becomes now

$$\langle g_c^{(21)*}\rangle_{2,1:\theta} = \left\langle \int_{-\infty}^{\infty} \prod_i^n w_1(x_i - \theta_i^{(2),(1)})_N g_c^{(21)*}(\underset{\sim}{x})\underset{\sim}{dx} \right\rangle_{H_2,H_1:\theta} \tag{A.2-47}$$

$$= B_c^{(21)*} - \sum_i^n \langle\Delta\theta_i\rangle \left\langle \int_{-\infty}^{\infty} \ell(x_i) w_1(x_i - \theta_i^{(2),(1)})_N dx_i \right\rangle_{2,1:\theta}$$

for H_2, or H_1 averages (over $\theta^{(2)}$, $\theta^{(1)}$ respectively). Comparing (A.2-47), (A.2-1), and (A.2-3), we have at once

$$\boxed{\begin{aligned} \langle g_c^{(21)*}\rangle_{2,1:\theta} &\doteq B_c^{(21)*} + \sum_i^n \langle\Delta\theta_i\rangle\langle\theta_i^{(2),(1)}\rangle L_i^{(2)} + O(\overline{\theta^4}) \\ &= \log \mu_{21} \pm \frac{1}{2}\sum_{i=1}^n \langle\Delta\theta_i\rangle^2 L_i^{(2)} + O(\overline{\theta^4}) \ ; \end{aligned}} \tag{A.2-48}$$

where (+,-) refer respectively to the (H_2, H_1) averages, and we have used (A.2-45).

The second moment is obtained in the same way. We have

$$\left\langle (g_c^{(21)*})^2 \right\rangle_{2,1:\theta} = \left\langle (B_c^{(21)*\,2} - 2B_c^{(21)*} \sum_i^n \langle \Delta\theta_i \rangle \ell_i \right.$$

$$\left. + \sum_{ij}^n \langle \Delta\theta_i \rangle \langle \Delta\theta \rangle_j \, \ell_i \ell_j \right\rangle_{2,1:\theta} \qquad \text{(A.2-49)}$$

Here, as before, $\langle \ell_i \rangle_{2,1:\theta} = -\langle \theta_i^{(2),(1)} \rangle L_i^{(2)}$. For the moments $\langle \ell_i \ell_j \rangle_{2,1:\theta}$ we simply parallel the analysis of (A.2-6)-(A.2-11) to get finally

$$(\sigma_{oc-2,1}^{(21)*})^2 \equiv \mathrm{var}_{2,1:\theta}\, g_c^{(21)*}$$

$$= \sum_{ij}^n \langle \Delta\theta_i \rangle \langle \Delta\theta \rangle_j \{ \langle \ell_i \ell_j \rangle_{2,1:\theta} - \langle \ell_i \rangle_{2,1:\theta} \langle \ell_j \rangle_{2,1:\theta} \} \qquad \text{(A.2-50)}$$

$$= \sum_i^n \langle \Delta\theta_i \rangle^2 \{ L_i^{(2)} + \langle (\theta_i^{(2),(1)})^2 \rangle \tfrac{1}{2} \cdot L_i^{(2,2)} + \ldots - \langle \theta_i^{(2),(1)} \rangle^2 L_i^{(2)^2} \}$$

$$+ \sum_{ij}{}' \langle \Delta\theta_i \rangle \langle \Delta\theta_j \rangle \{ \langle \theta_i^{(2),(1)} \theta_j^{(2),(1)} \rangle L_i^{(2)} L_j^{(2)} + \ldots$$

$$- \langle \theta_i^{(2),(1)} \rangle \langle \theta_j^{(2),(1)} \rangle L_i^{(2)} L_j^{(2)} \} \, . \qquad \text{(A.2-50a)}$$

Note that the leading term of $(\sigma_{c-2,1}^{(21)*})^2$ is independent of the particular hypothesis state H_2, or H_1. More important, we see that

$$\boxed{\sigma_{oc-2,1}^{(21)*2} \doteq -2B_{ncoh}^{(21)*}} \qquad \text{(A.2-50b)}$$

as is evident from (A.2-45) and the leading term $O(\theta^2)$ in (A.2-50).

In the stationary cases where $a_o^{(1)} = a_o^{(2)} = a_o$, and $\bar{s}_i^{(1)} \neq \bar{s}_i^{(2)}$ because, of course, we must have <u>different</u> signals in order to convey information), we see that (A.2-50a) reduces to the conditions

<u>$(\sigma_{oc-2}^{(21)*})^2 \doteq (\sigma_{oc-1}^{(21)*})^2$:</u>

$$\left| \{\overline{a_o^2}\, L^{(2,2)}/2L^{(2)} - \bar{a}_o^2 L^{(2)}\} \sum_i^n (\bar{s}_i^{(2)} - \bar{s}_i^{(1)})^2 \bar{s}_i^{(2),(1)} \right.$$

$$\left. + L^{(2)} \sum_{ij}^{n'} (\bar{s}_i^{(2)} - s_i^{-(1)})(\bar{s}_j^{(2)} - \bar{s}_j^{(1)}) \bar{s}_i^{(2),(1)} \bar{s}_j^{(2),(1)} (\overline{a_{oi} a_{oj}} - \bar{a}_o^2) \right|$$

$$<< \sum_i^n (\bar{s}_i^{(2)} - \bar{s}_i^{(1)})^2 \,, \qquad \text{(A.2-50b)}$$

for $s^{(2)}, s^{(1)}$, respectively, which are to be compared with (A.2-15b) earlier. Clearly, there is dependence on sample size (n) and on the statistics of the signal amplitude (a_o). Thus, for slow, rapid, and no fading we get directly the following simplified conditions (for each $s^{(2)}$, $s^{(1)}$):

(i). <u>slow-fading:</u>

Equations (A.2-50b), with $\overline{a_{oi} a_{oj}} - \bar{a}_o^2 \to \overline{a_o^2} - \bar{a}_o^2 = \text{var } a_o$; (A.2-50c)

(ii). rapid fading: $\overline{a_{oi}a_{oj}} = \bar{a}_o^2(1-\delta_{ij})$:

$$\frac{\left|\{\overline{a_o^2}L^{(2,2)}/2L^{(2)} - \bar{a}_o^2 L^{(2)}\} \sum_i^n (\bar{s}_i^{(2)} - \bar{s}_i^{(1)})^2 \bar{s}_i^{(2),(1)}\right|}{\sum_i^n (\bar{s}_i^{(2)} - \bar{s}_i^{(1)})^2} << 1; \qquad \text{(A.2-50d)}$$

(iii). no fading: $\overline{a^2}_o = \bar{a}_o^2 = a_o^2$:

$$\frac{\left|a_o^2\{L^{(2,2)}/2L^{(2)} - L^{(2)}\} \sum_i^n (\bar{s}_i^{(2)} - \bar{s}_i^{(1)})^2 \bar{s}_i^{(2),(1)}\right|}{\sum_i^n (\bar{s}_i^{(2)} - \bar{s}_i^{(1)})^2} << 1\ , \qquad \text{(A.2-50e)}$$

which are to be compared with (A.2-15c-e).

The extension of the consistency condition here [cf. Sec. (2.4) and (A.2-15a) et seq.] to the bias associated with these threshold binary cases, which puts one condition on how large the input signals (θ_2,θ_1) can be [cf. Sec. 6.4 also], requires that $(\sigma_{c-2,1}^{(21)*})^2$ be invariant of the hypothesis states H_1, H_2. Accordingly, the higher-order terms in (A.2-50a) must be suitably small vis-à-vis the leading term. This gives a pair of joint conditions on $\langle\theta_i^{(2),(1)}\rangle$ now, viz.

$$\left|\sum_i^n \langle\Delta\theta_i\rangle^2 \{\langle(\theta_i^{(2),(1)})^2\rangle \frac{L_i^{(2,2)}}{2} - \langle\theta_i^{(2),(1)}\rangle^2 L_i^{(2)^2}\}\right| << (\sigma_{oc}^*)^2$$

$$\equiv \sum_i^n \langle\Delta\theta_i\rangle^2 L_i^{(2)}, \qquad \text{(A.2-51)}$$

where we have used the strict (no fading) coherence condition of reception $\langle\theta_i\theta_j\rangle = \langle\theta_i\rangle\langle\theta_j\rangle$, which eliminates the Σ_{ij}' terms in (A.2-50a). Similarly, $\langle\theta_i^2\rangle = \langle\theta_i\rangle^2$, and so (A.2-51) is modified with the help of (A.2-16) to the condition

$(\sigma_{c-2,1}^{(21)*})^2 \doteq (\sigma_{oc}^{*})^2$:

$$\sum_i^n \langle \Delta\theta_i \rangle^2 \langle \theta_i^{(2),(1)} \rangle^2 \mathrm{var}_o \ell_i^2 / \sum_i^n \langle \Delta\theta_i \rangle^2 \mathrm{var}_o \ell_i << 1 \quad (1,2). \tag{A.2-51a}$$

With stationary regimes, $L_i^{(2)} = L^{(2)}$, etc., $\langle \theta_i \rangle^{(1,2)} = (\bar{a}_o\ \bar{s})^{(1,2)}$ all i, so that (A.2-51a) reduces further to

$$(\bar{a}_o^{(2),(1)} \bar{s}^{(2),(1)})^2 [\mathrm{var}_o \ell^2 / \mathrm{var}_o \ell] << 1, \quad \bar{a}_o, \bar{s} > 0, \tag{A.2-51b}$$

which not too surprisingly is just our earlier condition (A.2-17a), now for each input signal separately. Equation (A.2-51b) is independent of sample size (n).

A.2-4: Binary Signal Detection: Optimum Incoherent Detection:

We may proceed as above, now for optimum incoherent threshold detection of binary signals. The optimum algorithm is given by (4.5), where now the bias is found most simply by again observing that detector structure here is the difference of two "on-off" types of incoherent algorithm. Accordingly, the binary LOBD is now (for independent noise samples)

$$g_{inc}^{(21)*} = \log \mu_{21} + \hat{B}_{inc}^{(21)*} + \frac{1}{2!} \sum_{ij}^n \Delta\rho_{ij}^{(21)} (\ell_i \ell_j + \ell_i^! \delta_{ij}) , \tag{A.2-52}$$

[cf. (2.16) for dependent samples], where specifically

$$\Delta\rho_{ij}^{(21)} \equiv \langle a_{oi}^{(2)} a_{oj}^{(2)} s_i^{(2)} s_j^{(2)} \rangle - \langle a_{oi}^{(1)} a_{oj}^{(1)} s_i^{(1)} s_j^{(1)} \rangle$$

$$= \langle a_o^{(2)2} \rangle m_{ij}^{(2)} \rho_{ij}^{(2)} - \langle a_o^{(1)2} \rangle m_{ij}^{(1)} \rho_{ij}^{(1)} \quad ; \tag{A.2-52a}$$

$$\therefore \hat{B}_{inc}^{(21)*} = -\frac{1}{8} \{ \sum_{ij}^{n} [(L_i^{(4)} - 2L_i^{(2)2}) \delta_{ij} + 2L_i^{(2)} L_j^{(2)}] \}$$

$$\cdot [\langle a_o^{(2)2} \rangle m_{ij}^{(2)} \rho_{ij}^{(2)} - \langle a_o^{(1)2} \rangle m_{ij}^{(1)} \rho_{ij}^{(1)}] \quad . \tag{A.2-52b}$$

The reduction of the LOBD (A.2-52) when the noise is gaussian is immediate: $\ell_i = -x_i$, $\ell_i' = -1$ and $L_i^{(2)} = 1$; $L_i^{(4)} = 2$, cf. Sec. A.1-3. We get

$$g_{inc}^{(21)*}\Big|_{gauss} = [\log \mu_{21} - \frac{1}{2} \sum_{i}^{n} \{ \langle \theta_i^{(2)2} \rangle - \langle \theta_i^{(1)2} \rangle \} - \frac{1}{4} \sum_{ij} \{ \langle \theta_i^{(2)} \theta_j^{(2)} \rangle^2$$

$$- \langle \theta_i^{(1)} \theta_j^{(1)} \rangle^2 \}] + \frac{1}{2!} \sum_{ij}^{n} x_i x_j \Delta\theta_{ij}^{(21)} \quad , \tag{A.2-53}$$

cf. (4.11), (4.12), as required.

We make the same kind of modifications of the results of Sec. A.2-2 here, for the incoherent binary cases, as we did above in the coherent cases. We find directly that the means (under H_2, H_1) become

$$\left\langle g_{inc}^{(21)*}\right\rangle_{2,1:\theta} = \log \mu_{21} + \hat{B}_{inc}^{(21)*} + \frac{1}{4}\sum_{ij}^{n} \Delta\rho_{ij}^{(21)} \left\langle \theta_i^{(2),(1)} \theta_j^{(2),(1)} \right\rangle$$

$$\cdot[(L_i^{(4)} - 2L_i^{(2)^2})\delta_{ij} + 2L_i^{(2)}L_j^{(2)}] + O(\overline{\theta^6}) \ , \qquad \text{(A.2-54a)}$$

i.e.

$$\left\langle g_{inc}^{(21)*}\right\rangle_{2,1:\theta} = \log \mu_{21} \pm \frac{1}{8}\sum_{ij}^{n} (\Delta\rho_{ij}^{(21)})^2$$

$$\cdot[L_i^{(4)} - 2L_i^{(2)^2})\delta_{ij} + 2L_i^{(2)}L_j^{(2)}] + O(\overline{\theta^6}) \ , \qquad \text{(A.2-54b)}$$

where (+) refers to the H_2 and (-) to the H_1 averages.

We proceed similarly for $\text{var}_{2,1:\theta} g_{inc}^{(21)*}$. Using (A.2-52) we see that Equation (A.2-26) is now modified to

$$\text{var}_{2,1:\theta} g_{inc}^{(21)*} = \frac{1}{4}\sum_{ijk\ell}^{n} \{\left\langle F_{ij}^{(21)} F_{k\ell}^{(21)}\right\rangle_{2,1:\theta} - \left\langle F_{ij}^{(21)}\right\rangle_{2,1:\theta} \left\langle F_{k\ell}^{(21)}\right\rangle_{2,1:\theta}\} \ , \qquad \text{(A.2-55)}$$

where

$$F_{ij}^{(21)} \equiv F(x_i, x_j | \Delta\rho_{ij}^{(21)}) \equiv (\ell_i \ell_j + \ell_i' \delta_{ij})\Delta\rho_{ij}^{(21)} \ . \qquad \text{(A.2-55a)}$$

By inspection, from (A.2-27)-(A.2-29) we get

$$(\sigma_{inc-2,1}^{(21)*})^2 \equiv \text{var}_{2,1:\theta} g_{inc}^{(21)*} \doteq \frac{1}{4}\sum_{ij}^{n} (\Delta\rho_{ij}^{(21)})^2$$

$$\cdot[(L_i^{(4)} - 2L_i^{(2)^2})\delta_{ij} + 2L_i^{(2)}L_j^{(2)}] \equiv \sigma_{o-inc}^{(21)*} = -2\hat{B}_{inc}^{(21)*} . \qquad \text{(A.2-56)}$$

The condition on the smallness of $\theta^{(2)}$, $\theta^{(1)}$, i.e., the "consistency condition" on the bias, here becomes from the appropriate extension of (A.2-41), (A.2-42):

$$\underline{\sigma^{(21)*2}_{\text{inc-2}} \doteq \sigma^{(21)*2}_{\text{inc-1}}}:$$

$$\left| \sum_{ij}^{n} \Delta\rho_{ij}^{(21)2} \left\langle \theta_i^{(2),(1)} \theta_j^{(2),(1)} \right\rangle \{ \left(\frac{L_i^{(6)}}{2}\right) \delta_{ij} + 6 L_i^{(2)} L_j^{(2,2)} \} \right.$$

$$+ \sum_{ijk}^{(i\neq j\neq k)} [4 \Delta\rho_{ij}^{(21)} \Delta\rho_{jk}^{(21)} \left\langle \theta_k^{(2),(1)} \theta_i^{(2),(1)} \right\rangle$$

$$\left. -2 \Delta\rho_{ii}^{(21)} \Delta\rho_{jk}^{(21)} \left\langle \theta_k^{(2),(1)} \theta_i^{(2),(1)} \right\rangle] L_i^{(2)} L_j^{(2)} L_k^{(2)} \right|$$

$$<< \sum_{ij}^{n} \Delta\rho_{ij}^{(21)2} [(L_i^{(4)} - 2 L_i^{(2)2}) \delta_{ij} + 2 L_i^{(2)} L_j^{(2)}] \, . \qquad \text{(A.2-57)}$$

This is to be compared with (A.2-50), (A.2-51) for the coherent cases; it is considerably more complex, which is not unexpected in view of the considerably greater complexity of the incoherent detection algorithm (A.2-50) vis-à-vis the coherent algorithm (A.2-45a).

In the case of narrowband signals, with slow fading (i.e. $m_{ij}=1$, etc.) and stationary noise, cf. (A.2-41a), we find that the condition (A.2-57) now reduces to

$$\left\{ \begin{matrix} \langle a_o^{(2)2} \rangle \\ \langle a_o^{(1)2} \rangle \end{matrix} \right\} F_n^{(21)}(L^{(2)},.. \; Q_n^{(21)}, R_n^{(21)})^{-1} << 1 \quad : \qquad \text{(A.2-58)}$$

$$\sigma_{inc-2}^{(21)*2} \doteq \sigma_{inc-1}^{(21)*2} \equiv (\sigma_{o-inc}^{(21)*})^2 \ ,$$

where specifically

$$F_n^{(21)} \equiv \frac{L^{(4)} + 2L^{(2)2}(Q_n^{(21)} - 1)}{\left| \frac{L^{(6)}}{2} + 6L^{(2)}L^{(2,2)}Q_n^{(21)} + L^{(2)3}R_n^{(21)} \right|} \ , \qquad \text{(A.2-59)}$$

in which

$$Q_n^{(21)} - 1 \equiv \frac{1}{n} \sum_{ij}^{n'} \frac{\{\langle a_o^{(2)2} \rangle \rho_{ij}^{(2)} - \langle a_o^{(1)2} \rangle \rho_{ij}^{(1)}\}^2}{\{\langle a_o^{(2)2} \rangle - \langle a_o^{(1)2} \rangle\}^2} \quad (\geq 0), \qquad \text{(A.2-60a)}$$

$$R_n^{(21)} \equiv \frac{1}{n} \sum_{ijk}^{'''} \frac{\{4\Delta\rho_{ij}^{(21)}\Delta\rho_{jk}^{(21)}\rho_{ki}^{(2) \text{ or } (1)} - 2\Delta\rho_{ii}^{(21)}\Delta\rho_{jk}^{(21)}\rho_{ki}^{(2)\text{or}(1)}\}}{\{\langle a_o^{(2)2} \rangle - \langle a_o^{(1)2} \rangle\}^2} \ , \qquad \text{(A.2-60b)}$$

where

$$\Delta\rho_{ij}^{(21)} \equiv \langle a_o^{(2)2} \rangle \rho_{ij}^{(2)} - \langle a_o^{(1)2} \rangle \rho_{ij}^{(1)} \ , \text{ cf. (A.2-52a).} \qquad \text{(A.2-60)}$$

[In the most general cases, $m_{ij} \neq 1$, $L^{(2)} \to L_i^{(2)}$, etc., we use (A.2-57) directly, remembering that $\Delta\rho_{ij}^{(21)}$ is given by (A.2-52a).]

In the important special cases of symmetric channels, where $\mu=1$ and where $a_o^{(2)} = a_o^{(1)} = a_o$, (A.2-58)-(A.2-60) are modified to

$$\boxed{\langle a_o^2\rangle F_n^{(21)^{-1}} \ll 1} : \begin{cases} Q_n^{(21)}-1 = \frac{1}{n}\sum_{ij}^{n'} \{\rho_{ij}^{(2)}-\rho_{ij}^{(1)}\}^2 \cong n(\gg 1) \ ; \quad \text{cf. (A.6-5c).} & \text{(A.2-61a)} \\ R_n^{(21)} = \frac{1}{n}\sum_{ijk}^{'''} [4(\rho_{ij}^{(2)}-\rho_{ij}^{(1)})(\rho_{jk}^{(2)}-\rho_{jk}^{(1)})\rho_{ki}^{(2)\text{or}(1)} \doteq 0, & \text{(A.2-61b)} \end{cases}$$

since $\rho_{ij}^{(2)} \doteq \rho_{ij}^{(1)}$, over the sums with proper choice of Δt, viz. $\Delta\pi k\Delta t' = \omega_{o2}-\omega_{o1}$. For example, for signals with an entirely coherent structure, e.g. $\rho_{ij}^{(2)} = \cos \omega_{o2}(t_i-t_j)$, etc., and the proper choice of Δt, in $[t_i=i\Delta t]$, etc., $Q_n^{(21)} \doteq 1$, $R_n^{(2)} = 0$, and $F_n^{(21)}$, (A.2-59), becomes

$$\left.\begin{array}{l}\underline{\text{coh. signals:}} \\ \underline{\text{incoh.signals:}}\end{array}\right\} F_n^{(21)} \doteq \frac{L^4}{\left|\frac{L^{(6)}}{2} + 6L^{(2)}L^{(2,2)}\right|} \ , \qquad \text{(A.2-62)}$$

cf. (A.2-42b). For other choices of Δt (vis-à-vis $\omega_{o2}-\omega_{o1}$) we have $Q_n^{(21)} = O(n^o)$, $R_n^{(21)} = O(n^o)$, so that the complete relation (A.2-59) is required for $F_n^{(21)}$. Equation (A.2-62) also applies for signals with an entirely incoherent structure, e.g. $\rho_{ij}^{(1),(2)} = \delta_{ij}$, regardless of the symmetry of the channel, as we can see directly from (A.2-60a,b) in (A.2-59).

APPENDIX A-3

The Optimal Character of the LOBD:

In this Appendix we demonstrate that the canonical LOBD's derived in this study [cf. Sec. 2.2] and by Middleton earlier, in 1966 [14], and recently [34], cf. also [1], [1a], are indeed optimum for small (but nonzero input signals) and all sample sizes (particularly for large samples, $n \gg 1$, and in the limit $n \to \infty$). This is in contrast to the conventionally defined locally optimum detectors, whose optimal character is limited to small-sample conditions. The practical as well as analytic superiority of these LOBD algorithms stems from the addition of a suitable "bias" term and the associated condition, consistent with the way the bias term is derived, that the variances of the test statistic (g^*) under (H_0, H_1) be the same (and similarly under (H_1, H_2) for binary signal reception). This equality of variances, in turn, insures that the input signal be suitably small but nonvanishing, essentially independent of sample-size as $n \to \infty$, under conditions readily achieved in practice.

The LOBD is not unique: there may be other algorithms which give the same optimal performance [cf. Sec. A.3-4], but most such are structurally (i.e. operationally) more complex, or converge more slowly to the limiting "global" optimum, or both. The LOBD is canonical (i.e. exhibits an invariant <u>form</u>) vis-à-vis <u>both</u> signal and noise statistics and structures. In fact, the LOBD is determined by the appropriate pdf of the interference and by the lower-order moments of the input signal, and in this fashion is different in some important respects from the Asymptotically Optimum Detectors (AOD's) developed recently (1976) by Levin [39] and his colleagues (1967-), [25]-[28], as we shall see below.

A.3-1. Introductory Remarks:

Conventional locally optimum detectors (LOD's) are defined by the term linear in the signal parameter (θ), in the expansion of the [globally optimum] likelihood ratio $\Lambda_n(\underset{\sim}{x};\theta)$ ($\equiv \mu\langle F_n(\underset{\sim}{x}|\theta)\rangle_\theta / F_n(\underset{\sim}{x}|0)$), or its

logarithm $\log \Lambda_n(\underset{\sim}{x};\theta)$, about the null signal state $\theta = 0$, viz:

$$\log \Lambda_n^{(\ell_o)} \equiv \frac{\partial}{\partial\theta} \log \Lambda_n(\underset{\sim}{x};\theta)\Big|_{\theta=0} , \tag{A.3-1}$$

where the decision that a signal is present, (H_1) vs. noise alone (H_o), is made when

$$H_1: \log \Lambda_n^{(\ell_o)} \geq K \quad ; \quad H_o: \log \Lambda_n^{(\ell_o)} < K , \tag{A.3-2}$$

with K some appropriately chosen threshold. This threshold is usually determined by the false alarm probability α_F, e.g.

$$P_1(\log \Lambda_n^{(\ell_o)} \geq K|H_o) = \alpha_F. \tag{A.3-3}$$

The detection algorithm based on (A.3-1) is called <u>locally optimum</u> (or "e-optimum") if it gives the <u>minimum</u> missed-signal probability $\beta_n^{(\ell_o)}(\theta)$ for all values of θ in some finite range ($0 < \theta \ll \epsilon$) for specified $\alpha = \alpha_F$. In the usual cases ϵ is taken to be small, so that local optimality applies to those cases where the input signal is small and sample-size (n) is finite. In this situation (i.e. local optimality) it is required that

$$\frac{\partial\beta_n^*(\delta_n^*)}{\partial\theta}\Big|_{\theta=0} = \frac{\partial\beta_n^{(\ell_o)}(\delta_n^{(\ell_o)})}{\partial\theta}\Big|_{\theta=0} \tag{A.3-4}$$

where δ_n^*, $\delta_n^{(\ell_o)}$ are respectively the decision rules for the strictly (or "globally" i.e. all signal levels) optimum and locally optimum algorithms.

Similarly, the locally optimum approach is extended to the more general Bayes decision formulation by replacing log $\Lambda_n^{(\ell_o)}$ by the conditional risk $r(\theta,\delta_n)$, so that if δ_n^* is a Bayes rule (i.e. one minimizing the conditional risk), then the locally optimum Bayes rule $(\sigma_n^{(\ell_o)})$ is determined from the conditions (obtained on expanding $r(\theta,\delta_n)$ about $\theta=0$):

$$r^{(\ell_o)}(0,\delta_n^{(\ell_o)}) = r^*(0,\delta_n^*) \; ; \quad \left.\frac{\partial r^{(\ell_o)}(\theta,\delta_n^{(\ell_o)})}{\partial\theta}\right|_{\theta=0} = \left.\frac{\partial r^*(\theta,\delta_n^*)}{\partial\theta}\right|_{\theta=0}, \tag{A.3-5}$$

where the decision that a signal is present is again made on the basis of the inequality (A.3-2), where now K depends on the various cost assignments. A more general Bayes formulation, based on the minimization of average risk, employs the same approach, with r^*, $r^{(\ell_o)}$ replaced by the average risks R^*, $R^{(\ell_o)}$ in (A.3-5), and K dependent not only on the cost assignments but also on the a priori probabilities associated with the signal and its presence or absence (p,q) in the data sample. See, for example, Sec. II of [14].

A critical problem with the conventional LOD's is that higher order terms in the expansion of log $\Lambda_n(\underset{\sim}{x};\theta)$ about $\theta=0$ can be discarded for weak input signals only if the sample size (n) is small. This is easily seen from the following argument: for the m^{th}-order term in the expansion, one has a contribution $(\theta^m/m!)O(n^m) = O([\theta n]^m/m!)$. Thus, for terms $m\geq 2$ to be discarded vis-à-vis m=1, for instance, one requires $\theta n >> (\theta n)^2/2!$, or $\theta n << 1$ essentially. Even for small input signals [$\theta=O(10^{-3}$ or less], n must also be comparatively small, say n=20, to satisfy the inequality $\theta n << 1$. [Clearly, if the m^{th}-order inequality is satisfied, so also will all m+1, etc.] But for this situation the correct-signal detection probability, $p_D^{(\ell_o)}=1-\beta^{(\ell_o)}$, is the same order as $\alpha^{(\ell_o)} = \alpha_F$. Then, in order to achieve a correct detection probability $p_D^{(\ell_o)}$ which is close to unity for weak signals, it is necessary to increase the sample size (n) by a

suitable amount. This inevitably brings in higher order terms (beyond the linear one in θ), which now cannot be ignored if optimal performance is to be maintained. These more complex algorithms are no longer close to the LOD's, either in structure or performance, nor can they be made so generally.

Accordingly, we must seek an appropriate modification, and extension, of the locally optimal (i.e., weak-signal) detection concept, which preserves the comparatively simple structure embodied in (A.3-1) and which at the same time permits the use of large (and ultimately very large ($n\to\infty$)) samples, which are required in practice for detecting weak signals. This must be done without destroying the optimal nature of the algorithm itself. As we shall see below subsequently, the canonical LOBD algorithms derived by Middleton [14] in 1966 for optimum threshold signal detection, under some simple conditions, do indeed provide such desired extensions and generalization. We emphasize that we are considering here fully canonical developments, whose general form [cf. (2.9),(2.11), (2.12)] is invariant of the particular waveform and statistical structures of both the signal and noise.

A.3-2 Asymptotically Optimum Signal Detection Algorithms (AODA's): General Remarks:

To develop the desired LOBD algorithms, which are to remain locally optimum for all sample sizes, with suitably small but nonzero input signals, we shall parallel the recent approach of Levin [39] and his colleagues [25]-[28] and employ the concept of an Asymptotically Optimum Detection Algorithm (AODA). This, however, unlike the AODA's used by Levin [39], is modified to admit nonvanishing input signals (as $n \to \infty$) and hence to provide consistency, (i.e. $\beta_n^* \to 0, n \to \infty$) of the LOBD algorithm, as well.

One class of asymptotically optimum detection algorithm (AODA) for signals in a general noise background is one for which structure and performance approach that of the appropriate (strictly) optimum algorithm for fixed (non-zero) error probabilities $[\alpha^{(\ell_0)}, \beta^{(\ell_0)}]$, as sample size

(n) becomes infinitely large and the input signal-to-noise ratio approaches zero. This is the class considered by Levin [39]. Another, related class of AODA is that for which structure and performance again approach that of the corresponding (strictly) optimum algorithm, but now for error probabilities [β^*, or $q\alpha^*+p\beta^*$, etc.] which vanish as sample-size becomes infinitely great and at the same time the input signal-to-noise ratio remains non-zero, although necessarily small. It is this latter class of AODA which we consider here, and to which the LOBD belongs, as we shall demonstrate.

The principal idea on which the theory of asymptotically optimum detection algorithms is based is to find an asymptotically sufficient statistic in the sense that its distribution converges in probability to a normal distribution when the sample size (n) increases without limit and the input signal amplitude ($\sim a_o$) is suitably small. For the class of AODA's considered by Levin [39] the signal amplitude $\lambda_n a_o s(t) \to 0$, $\lambda_n \to 0$. For the class of AODA's examined here, $0 < a_o^2 << 1$: the input signal is small but never vanishingly so. In any case, the reasonable assumption is that if such asymptotically sufficient statistics are substituted for the known optimum decision rule, or are otherwise shown to be equivalent to it, for normal distributions, the result is an AODA which, as $n \to \infty$, becomes strictly optimum. The canonical character of the resulting AODA then stems from the generic form of the noise distribution alone, as expressed formally by an appropriate expansion of the (always optimum) likelihood ratio about the null-signal (H_o) condition. The explicit form of the expansion, however, is not unique, and therefore it is desireable to choose those expansions which: (i), converge rapidly to the (strict) optimum (as $n \to \infty$); and (ii), which are not excessively complex in structure.

In more precise fashion let us give a definition of the notion of "asymptotic optimality", for the class, $0 < a_o^2 << 1$. As an example, let us consider a detection algorithm, $\hat{\delta}_n = \delta_n^{(0)}$, to be the strictly optimum algorithm, which for fixed false-alarm probability α_n and fixed sample size (n) minimizes the missed-signal probability $\hat{\beta}_n(\delta_n; a_o(t))$, that

signal $a_o s(t)$ will not be detected (the Neyman-Pearson Observer). Then, for some sequence of algorithms $\{\delta_n\}$ we denote the corresponding missed-signal probability by $\beta_n(\delta_n;a_o s)$. We next call the sequence of algorithms $\{\delta_n^{(a_o)}\}$ <u>asymptotically optimal</u> if for any other sequence of algorithms $\{\delta_n\}$ the relation

$$\lim_{n\to\infty} [\beta_n(\delta_n;a_o s)-\beta_n(\delta_n^{(ao)},a_o s)] \geq 0, \text{ when } \lim n\to\infty(\delta_n^{(ao)}\to\delta_n^{(0)}\to\delta_\infty^{(0)}), \tag{A.3-6}$$

is valid for fixed false alarm level $\alpha_\infty=\alpha$, where $\alpha_\infty = \lim_{n\to\infty} \alpha_n(\delta_n;0)\equiv\alpha$. In the case of the Ideal Observer, the corresponding relation is

$$\lim_{n\to\infty}\{q\alpha_n(\delta_n;a_o s)+p\beta_n(\delta_n;a_o s)-q\alpha_n(\delta_n^{(ao)},a_o s)-p\beta_n(\delta_o^{(ao)},a_o s)\} \geq 0. \tag{A.3-6a}$$

Of course, for our class of AODA's being examined here, $\beta_n(\delta_n^{(ao)},a_o s) \to 0$ as $n \to \infty$, $(a_o s>0)$, to insure the required consistency of the AODA: a necessary condition for a properly chosen sequence of algorithms $\{\delta_n^{(ao)}\}$ is that they provide a consistent test of the hypotheses states H_o (noise alone) and H_1 (signal and noise), with $\beta_n < 1 - \alpha_n$, all n.

<u>A.3-3 The LOBD as an Asymptotically Optimum Detection Algorithm - AODA:</u>

Here we shall show that the LOBD is an AODA, as well as being locally optimum for all sample sizes, n. [In fact, the latter follows at once from the former here, because of the convergence of the LOBD with finite n to the limiting AODA, as $n \to \infty$.]

Remembering that the (generalized) likelihood ratio $(\Lambda_n^{(1)})$, cf..(2.1), or any monotonic function of it, e.g. $\log \Lambda_n^{(1)}$ for instance, is always (strictly) optimum, for all n, <u>including n→∞,</u> we see that (cf. 2.2, [14]) it is entirely reasonable to seek acceptable candidates for an AODA by an approprate expansion of the (logarithm) of the likelihood ratio about the null

signal ($\theta=0$). The LOBD, g_n^*, (2.9), here for additive signal and noise,* and specifically for coherent and incoherent reception, as described by (2.11), (2.12), is one such class of expansions. Thus, we write

$$\log \ell_n^{(1)}(\underset{\sim}{x};\theta) = g_n^*(\underset{\sim}{x};\theta)+t_n(\underset{\sim}{x},\theta), \text{ with } \log \Lambda_n^{(1)}=\log \mu+\log \ell_n^{(1)}(\underset{\sim}{x};\theta), \tag{A.3-7}$$

cf. (2.1), where

$$\ell_n^{(1)}(\underset{\sim}{x};\theta) \equiv \left\langle F_n(\underset{\sim}{x}|\theta)\right\rangle_\theta / F_n(\underset{\sim}{x}|\theta) \tag{A.3-7a}$$

is also a generalized likelihood ratio, and $\hat{g}_n^*$ is the LOBD $\hat{g}_n^*=g_n^*-\log \mu$, without the a priori "bias term", $\log \mu$. Here the necessary and sufficient condition that the LOBD, $\hat{g}_n^*$ (and hence g_n^* $(=\hat{g}_n+\log \mu)$ itself) is an AODA (as $n\to\infty$), is that the "remainder", t_n, coverge to zero with respect to the sequence (n) of pdf's governing the null $(H_o|N)$ and alternative $(H_1|S+N)$ hypotheses, viz., with respect to H_1: $F_n(\underset{\sim}{x};\theta)\equiv\left\langle F_n(\underset{\sim}{x}|\theta)\right\rangle_\theta$, and H_o: $F_n(\underset{\sim}{x};0)$, as $n\to\infty$. The general problem is to find suitable expansions for which the above is true. Our particular problem here is to show that the LOBD, $\hat{g}_n^*$, is an AODA. It is clear that the LOBD $\hat{g}_n^*$ here is not a unique locally optimum or asymptotically optimum algorithm. Other, more complex structures can give equivalent results, but they can not be any better than the LOBD and its AODA form, and they suffer from the operational defect of complexity and possibly slower convergence (as $n\to\infty$) to the limiting AODA here.

Our next step is to establish specific conditions for which the "remainder" term t_n vanishes as $n\to\infty$, on H_o, H_1. For this we shall use (a limiting form of) Le Cam's theorem and his concept of the asymptotic equivalence of sequences of distributions [40],[40a]. Here, two sequences of pdf's

---

* The general approach of Sec. A.3-3 is not necessarily limited to purely additive cases. The results for nonadditive cases are reserved to a later study.

$\{F_n(\underset{\sim}{x};\theta)\}$ and $\{F_n(\underset{\sim}{x};0)\}$ are termed asymptotically equivalent (AE) if the convergence in probability of any statistic (say, t_n above) to zero, i.e. $\lim_{n\to\infty} t_n \to 0$ (in prob.), for one sequence of pdf's, e.g. $\{F_n(\underset{\sim}{x};0),\ n\to\infty\}$ here, entails the convergence in probability of that statistic (t_n) to zero, for the other sequence, $\{F_n(\underset{\sim}{x};\theta),\ n\to\infty\}$. As Le Cam has shown [40a], the necessary and sufficient condition for the asymptotic equivalence (AE) of two sequences of distributions (pdf's) is

$$AE_0 \equiv \int_{-\infty}^{\infty} e^z\, w_1(z|H_0)_\infty dz = 1 \qquad \text{(A.3-8)}$$

where $w_1(z|H_0)_\infty$ is thus the limiting pdf (as $n\to\infty$) for $z = \lim_{n\to\infty} \log \ell_n^{(1)}$ under hypothesis $H_0(N)$, e.g. $\theta=0$. [Note here that the sample values $\{x_i\}$ in ℓ_n need not be independent!]

For the two pdf's $F_n(\underset{\sim}{x};\theta)$ and $F_n(\underset{\sim}{x};0)$ to be asymptotically equivalent, it is sufficient that the logarithm of the likelihood ratio $\ell_n^{(1)}(\underset{\sim}{x};\theta)$, cf. (A.3-7a), be asymptotically normal (G) under hypothesis H_0, with the parameters $G_0((-\sigma_0^{*2}/2),\sigma_0^{*2})$ with $\sigma_0^{*2} = \lim_{n\to\infty} \sigma_{on}^{*2}$, where $\sigma_{on}^{*2}[=\mathrm{var}_0 \hat{g}_n^* = \langle \hat{g}_n^{*2}\rangle_0 - \langle \hat{g}_n^*\rangle_0^2]$ is the variance of $\hat{g}_n^*$ under H_0. Furthermore, from Le Cam's theorem it follows that if the pdf of $\log \ell_n^{(1)}$ under H_0 is asymptotically normal with $G_0(-\sigma_0^{*2}/2,\ \sigma_0^{*2})$, then the pdf of $\ell_n^{(1)}$ is also asymptotically normal, for the "close alternative", with the parameters $G_1(+\sigma_0^{*2}/2,\sigma_0^{*2})$. Then, if the above (sufficient) conditions on $\log \ell_n^{(1)} = \hat{g}_n^* + t_n$ are satisfied and $\hat{g}_n^*$ is the asymptotically normal form of $\log \ell_n^{(1)}$, it is at once evident that $t_n \to 0$ under H_0, H_1 and that $\hat{g}_n^*$ is an AODA. That the condition (A.3-8) is satisfied here is easily shown: if $\lim_{n\to\infty} \hat{g}_n^* \equiv z$ is $G_0(-\sigma_0^{*2}/2,\sigma_0^{*2})$, then (A.3-8) becomes

$$AE|H_0 = \int_{-\infty}^{\infty} e^z \cdot e^{-(z+\sigma_0^{*2}/2)^2/2\sigma_0^{*2}} \frac{dz}{\sqrt{2\pi\sigma_0^{*2}}} = \int_{-\infty}^{\infty} e^{-(z-\sigma_0^{*2}/2)^2/2\sigma_0^{*2}} \frac{dz}{\sqrt{2\pi\sigma_0^{*2}}}$$

$$= \int_{-\infty}^{\infty} e^{-(y-\sigma_0^{*}/2)^2/2} \frac{dy}{\sqrt{2\pi}} = 1\ . \qquad \text{(A.3-9)}$$

[Similarly, for z to be $G_1(\sigma_o^{*2}/2,\sigma_o^{*2})$, (A.3-8) becomes under H_1, [40a]

$$AE|H_1 = \int_{-\infty}^{\infty} e^{-z}.e^{-(z-\sigma_o^{*2}/2)^2/2\sigma_o^{*2}} \frac{dz}{\sqrt{2\pi\sigma_o^{*2}}} = \int_{-\infty}^{\infty} e^{-(z+\sigma_o^{*2}/2)^2/2\sigma_o^{*2}} \frac{dz}{\sqrt{2\pi\sigma_o^{*2}}}$$

$$= \int_{-\infty}^{\infty} e^{-(y+\sigma_o^{*}/2)^2/2} \frac{dy}{\sqrt{2\pi}} = 1 \ .] \qquad \text{(A.3-9a)}$$

The "distance" between $\langle \hat{g}_n^* \rangle_{H_o}, \langle \hat{g}_n^* \rangle_{H_1}$ in the "close alternatives" (H_o,H_1) here is given asymptotically by

$$\lim_{n\to\infty}(\langle \hat{g}_n^* \rangle_1 - \langle \hat{g}_n^* \rangle_o) = \sigma_o^{*2}/2 - (-\sigma_o^{*2}/2) = \sigma_o^{*2} \ , \qquad \text{(A.3-10)}$$

with the normalized "distance"

$$\lim_{n\to\infty}\left\{\frac{\langle \hat{g}_n^* \rangle_1 - \langle \hat{g}_n^* \rangle_o}{\sigma_o^*}\right\} = \sigma_o^* \ . \qquad \text{(A.3-10a)}$$

We emphasize that the above results [(A.3-8) et seq.] apply for correlated samples, as well as for the independent samples $\{x_i\}$ of our detailed analysis here.

In the above we have assumed that $\sigma_o^{*2} < \infty$. The above conditions and results still apply when $\lim_{n\to\infty} \sigma_{on}^{*2} \equiv \sigma_o^{*2} \to \infty$, provided we replace the limits $(-\infty,\infty)$ in (A.3-9,9a) by $(-\infty-,\infty+)$ where $(-\infty-)$ and $(\infty+)$ are such that $\lim_{n\to\infty}(-\infty-) - a_n \leq 0-$ and $\lim_{n\to\infty}[(\infty+)-a_n] \geq 0+$, $\lim a_n \to \sigma_o^{*2}/2(\to\infty)$. Thus, letting $z - \sigma_o^{*2}/2 = x$, we have (cf.(A.3-8) and (A.3-9))

$$AE|H_o = \int_{(-\infty-)}^{\infty+} \lim_{n\to\infty} \frac{e^{-(z-\sigma^{*2}_{on}/2)^2/2\sigma^{*2}_{on}}}{(2\pi\sigma^{*2}_{on})^{1/2}}\, dz$$

$$= \int_{(-\infty-)}^{\underline{>}0+} \lim_{n\to\infty} \frac{e^{-x^2/2\sigma^{*2}_{on}}}{\sqrt{2\pi\sigma^{*2}_{on}}}\, dx = \int_{-\infty}^{\underline{>}0+} \delta(x-o)dx = 1, \qquad \text{(A.3-11)}$$

and similarly,

$$AE|H_1 = \int_{(-\infty-)}^{\infty+} \lim_{n\to\infty} \frac{e^{-(z+\sigma^{*2}_{on}/2)^2/2\sigma^{*2}_{on}}}{\sqrt{2\pi\sigma^{*2}_{on}}}\, dz$$

$$= \int_{\underline{<}0-}^{\infty+} \lim_{n\to\infty} \frac{e^{-x^2/2\sigma^{*2}_{on}}}{\sqrt{2\pi\sigma^{*2}_{on}}}\, dx = \int_{\underline{<}0-}^{\infty} \delta(x-o)dx = 1. \qquad \text{(A.3-11a)}$$

(For finite σ^{*2}_o these limits clearly reduce to those of (A.3-9,9a), as required.) This extension of the limits $(-\infty,\infty)$ insures that the integrand always remains within the suitably (infinite) domain of integration $(-\infty-,\infty+)$. Thus, a sufficient condition that the LOBD $\hat{g}^*_n$, when $\lim_{n\to\infty} \sigma^{*2}_{on} \to \sigma^{*2}_o \to \infty$, be an AODA is that $\hat{g}^*_n$ be asymptotically normal, with $\lim_{n\to\infty}$ (mean/variance = $-1/2{:}H_o$, $=+1/2{:}H_1$). The "distances" (A.3-10), (A.3-10a), of course, are infinite $O(\sigma^{*2}_o$ or $\sigma^*_o)$: (A.3-10a) with $\sigma^*_o \to \infty$ expresses the fact that the means under H_o, H_1 become infinitely separated, while the spread of each pdf increases less rapidly as $n\to\infty$, cf. Figure A.3-1. That the "distances" $[\sigma^{*2}_o$, or $\sigma^*_o]$ are greater than zero (and greater than the spread $(\sim\sigma^*_o)$ of each pdf) reflects the fact that $0 < \beta_h < 1-\alpha_n$, all $n\to\infty$, and when $\alpha^*_o \to \infty$, then $\beta_n \to \beta_\infty \to 0$: the test of H_1 is <u>consistent</u> as well as asymptotically optimum.

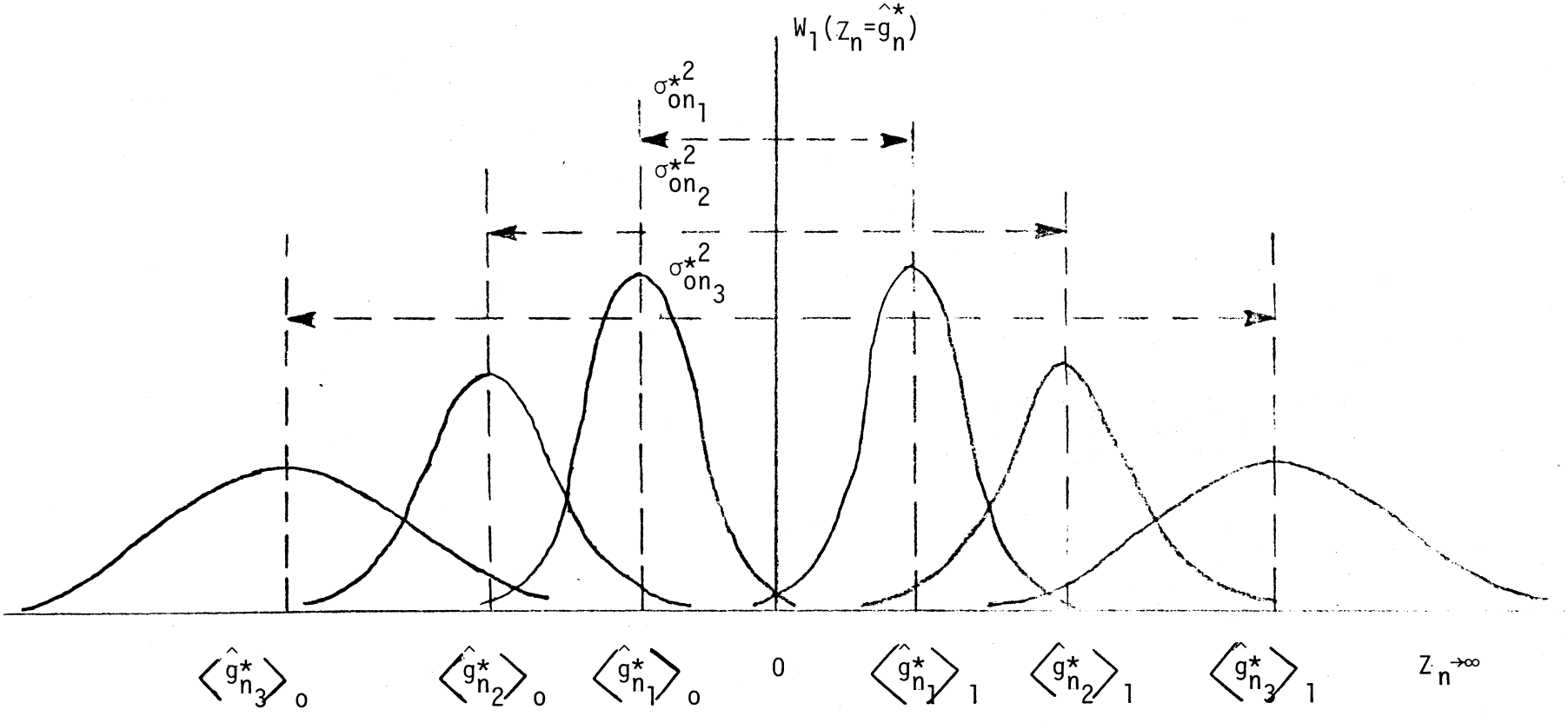

Figure A.3-1. The asymptotically normal pdf of the test statistic, $\hat{g}_n^* = Z_n$, as $n_1 < n_2 < n_3 \to \infty$.

The LOBD's here as derived by Middleton (for additive signal and noise) [14], cf. Sec. 2.2 and Appendix A.1, are clearly AODA's, as well as locally optimum (all n), when we note the results of Appendix 2 and Sec. 6. Specifically, we have $\hat{g}_n^*$ asymptotically normal $G_0(-\sigma_0^{*2}/2,\sigma_0^{*2})$, $G_1(+\sigma_0^{*2}/2,\sigma_0^{*2})$, for both coherent (2.11) and incoherent threshold reception (2.12), cf. Eqs. A.2-3,4 for the coherent means and Eqs. (A.2-14) for the coherent variances, and correspondingly, Eqs. (A.2-22b,25) for the incoherent means and Eq. (A.2-40) for the incoherent variances. [These results are summarized in Table 6.1, Sec. 6.] The full LOBD's, $g_n^* = \hat{g}_n^* + \log \mu$, are of course, AODA's also, with all the properties of $\hat{g}_n^*$: the various means under H_0, H_1 now have an added term, $\log \mu$, e.g., $G_0(-\sigma_0^{*2}/2,\sigma_0^{*2}) \rightarrow G_0(\log \mu - \sigma_0^{*}/2,\sigma_0^{*2})$, and $G_1(\sigma_0^{*2}/2,\sigma_0^{*2}) \rightarrow G_1(\log \mu + \sigma_0^{*2}/2,\sigma_0^{*2})$; the "distance" (A.3-10) etc. remains unchanged. The condition $\sigma_1^{*2} \doteq \sigma_0^{*2}$, cf. (2.29), (A.2-15), (A.2-41), etc. required for the AODA's here, in turn postulates a nonzero input signal-to-noise ratio, a_0^2 (>0), which is always suitably small, e.g. $a_0^2 \ll 1$. These LOBD's are not uniquely optimum, since it is possible that other expansions of $\log \ell_n^{(1)}$, cf. (A.1-7), may possess the desired properties, $G_{0,1}(\mp\sigma_0^{*2}/2,\sigma_0^{*2})$, in the limit. However, such other expansions usually include higher order terms (in θ) and are therefore much more complex in structure than the present LOBD's. In any case, there are no LO algorithms which are better than these LOBD's.

A.3-4 Remarks on A Comparison of Middleton's LOBD's [14] and Levin's AODA's, [39]:

There are certain distinct differences between Levin's approach [39] to the optimum threshold detection and that of Middleton [14]. The principal one is that the former is concerned with the asymptotic optimization of one type of expansion of the conditional likelihood ratio $\ell_n^{(1)}(\underset{\sim}{x}|\theta) \equiv F_n(\underset{\sim}{x}|\theta)/F_n(\underset{\sim}{x}|o)$, while the latter (Middleton) is concerned with the asymptotic optimization of the unconditional likelihood ratio $\ell_n^{(1)}(\underset{\sim}{x};\theta) \equiv \langle F_n(\underset{\sim}{x}|\theta)\rangle_\theta / F_n(\underset{\sim}{x}|o)$, cf. (A.3-7a), (2.9) etc. This may be summarized by

Levin (p. 128, [39]): log av. asymptot. expan. of conditional likelihood ratio

$$= \log\left\langle \exp\, \ell^{(1)}_{asymp}(\underset{\sim}{x}|\theta)\right\rangle_\theta$$

Middleton (Sec. 2.2) : asymp expan. of log av. condit.
(Sec. A.3-3) likelihood ratio

$$= \text{asymp. exp log } \left\langle \ell^{(1)}_n(\underset{\sim}{x}|\theta)\right\rangle_\theta . \tag{A.3-12}$$

In the approach of Levin et al., [39], the input signal samples $a_{oi}s_i$ are replaced by a decreasing set of signal samples, $\gamma\, a_{oi}s_i/\sqrt{n}$, $(\gamma>0)$, so that the input signal vanishes in the asymptotic limit $(n\to\infty)$, and the error probabilities remain preset and nonvanishing, e.g. $0 < \beta_{n\to\infty} = \beta$; $0 < \alpha_n = \alpha$, etc., with $\beta < 1-\alpha$. This leads to finite values of σ^{*2}_o in the limit.

On the other hand, in Middleton's development (2.9) etc., which includes a proper selection of bias term, $\hat{B}^*_n(=B^*_n-\log\mu)$, the input signal-to-noise ratio always remains nonvanishing, so that $\lim_{n\to\infty} \beta^*_n \to 0$, for $\alpha^*>0$, etc. (and $\lim_{n\to\infty} q\alpha^*_n + p\beta^*_n \to 0$ in the communication examples where the Ideal Observer is appropriate). To assure the AO character of this LOBD it is required that $\sigma^{*2}_1 \doteq \sigma^{*2}_o$, i.e. the variances of the LOBD under H_1 and H_o be essentially the same, which means, in turn, that $(a^2_o)_{in} << 1$, suitably, cf. (A.2-15), (A.2-41). In addition, the variance $\lim_{n\to\infty} \sigma^{*2}_{on} \to \sigma^{*2}_o \to \infty$, cf. A.3-3 above.

The two approaches above give equivalent results if we set $\beta^*_n = \beta^{(ao)}$, (>0) of Levin (in the Neyman Pearson cases, α fixed, for instance). This determines the unspecified constant, γ, and relates the various limiting parameters of Levin's approach to those in the LOBD's of Middleton. In particular, one can equate the missed-signal probabilities of detection of Sections 3.1.3-3.1.10, [39], to the corresponding results here (i.e., coherent, incoherent reception, post-detection optmization, "mismatch", etc.), and determine the corresponding values of γ.

It should be pointed out that Levin's approach is not restricted to additive signal and noise situations, only to those where the noise does not vanish when the signal does. Our present analysis can be extended to include such more general cases. Moreover, the present LOBD approach provides a natural distinction between various modes of reception (coherent, incoherent, mixed), and since $(a_o^2)_{in} > 0$ here, the useful notions of processing gain (Π^*), cf. Sec. 6. , and associated minimum detectable signal ($\langle a_o^2 \rangle^*_{min}$), likewise appear naturally. Both approaches provide a processing structure, but the LOBD structures of the present analysis appear to be the more appropriate in actual applications. [These points will be discussed in more detail in a later study.]

A.3-5. Extensions of the AODA to Binary Signals:

We may readily extend the earlier results of Sec. (A.3-3) on the AODA's for "on-off" cases to binary signal reception. Analogous to (A.3-7) we now write

$$\log \ell_n^{(21)}(\underset{\sim}{x};\theta) = \hat{g}_n^{(21)*}(\underset{\sim}{x};\theta)+t_n^{(21)}(\underset{\sim}{x},\theta), \text{ with } \log \Lambda_n^{(21)}=\log \mu_{21}+\log \ell_n^{(21)} , \tag{A.3-13}$$

where

$$\log \ell_n^{(21)} = \log\{\langle F_n(\underset{\sim}{x}|\theta_2)\rangle_2/\langle F_n(\underset{\sim}{x}|\theta_1)\rangle_1\} \equiv \log\{F_n(\underset{\sim}{x};\theta_2)/F_n(\underset{\sim}{x};\theta_1)\} \tag{A.3-13a}$$

and now $\hat{g}_n^{(21)*}$ is the LOBD for binary signal reception (coherent or incoherent) $= g_c^{(21)*} - \log \mu_{21}$.

The extension of Le Cam's theorem for asymptotic equivalence, [40a], now under H_1, H_2 (i.e. $AE_{1,2}$), of the two sequences of distributions $\{F_n(\underset{\sim}{x};\theta_2)$ $(\equiv\langle F_n(\underset{\sim}{x}|\theta_2)\rangle_2)\}, \{F_n(\underset{\sim}{x};\theta_1)(\equiv\langle F_n(\underset{\sim}{x}|\theta_1)\rangle_1)\}$ as $n\to\infty$, i.e. $\lim_{n\to\infty} t_n^{(21)} \to 0$ (in prob.) under H_1 and H_2 is immediate. The necessary and sufficient

conditions for $AE_{1,2}$ here are

$$AE_1 \equiv \int_{-\infty}^{\infty} e^{z} w_1(z|H_1)_\infty dz = 1 \leftrightarrow AE_2 \equiv \int_{-\infty}^{\infty} e^{-z} w_1(z|H_2) dz \ , \tag{A.3-14}$$

(i.e. AE_1 implies AE_2 and vice-versa), where $w_1(z|H_{1,2})_\infty$ are the limiting pdf's for $z(= \lim_{n\to\infty} \log \ell_n^{(21)})$ under H_1 and H_2.

For $F_n(\underset{\sim}{x};\theta_1)$, $F_n(\underset{\sim}{x};\theta_2)$ to be asymptotically equivalent, i.e. to have the "remainder term", $t_n^{(21)}$ vanish under H_1, H_2 as $n\to\infty$, it is again sufficient that: (i), $z = \lim_{n\to\infty} \ell_n^{(21)}(\underset{\sim}{x};\theta)$ be asymptotically normal under H_1, with parameters

$$G[-\frac{(\sigma_o^{(21)*})^2}{2} \ , \ (\sigma_o^{(21)*})^2] \ , \ (\sigma_o^{(21)*} = \lim_{n\to\infty} \sigma_{on}^{(21)*}) \ .$$

This also insures that (ii), $\ell_n^{(21)}(\underset{\sim}{x};\theta)$ is asymptotically normal under H_2, with parameters

$$G(+\frac{(\sigma_o^{(21)*})^2}{2} \ , (\sigma_o^{(21)*})^2).$$

Now, from Section A.2-3,4 preceding we see that, indeed (for any sample size n)

$$\left\langle \hat{g}_{c,inc}^{(21)*} \right\rangle_{\substack{2:\theta \\ 1}} = \pm \frac{1}{2} (\sigma_o^{(21)*})^2 \Big|_{C,inc} \ , \quad \begin{matrix} \text{Eqs. (A.2-48), with (A.2-50a)} \\ \text{Eqs. (A.2-54b), with (A.2-56)} \end{matrix} \Bigg\} \tag{A.3-15}$$

as required, where $(\sigma_o^{(21)*})^2$ is the appropriate variance (as $n \to \infty$) of $\hat{g}_{c,inc}^{(21)*}$. Applying the above to (A.3-14) along the lines of (A.3-11),

(A.3-11a) at once shows the desired sufficiency. Thus, not unexpectedly, the LOBD's $g_{c,inc}^{(21)*}$ are AODA's here, in the binary signal cases, as well as in the "on-off" detection situations examined initially. [Again, see the remarks following Eqs. (A.3-10,11).] The comments in Section A.3-4 also apply here, as well.

A.3-6 Rôle of the Bias in the AODA's: The Composite LOBD:

In the preceeding sections of Appendix A.1-A.3 we have seen that the bias, $\hat{B}_n^*$, must have the proper structure in order that the LOBD in question be an AODA as $n\to\infty$. In fact, from the sufficient conditions that the "on-off" LOBD, g_n^* ($\equiv \hat{g}_n^*+\log\mu$), be asymptotically gaussian, i.e. $\lim_{n\to\infty} G(\log\mu\mp\sigma_{on}^{*2}/2,\sigma_{on}^{*2})$, where $\sigma_{on}^{*2} = \mathrm{var}_o g_n^*$, ($\mp$: H_o,H_1) in H_o, H_1 respectively, we can at once obtain the conditions on the bias that the resulting LOBD is an AODA.

Thus, from $G(\log\mu\mp\sigma_{on}^{*2}/2,\ \sigma_{on}^{*2})$ for g_n^* [or $G(\mp\sigma_{on}^{*2}/2,\sigma_{on}^{*2})$ for $\hat{g}_n^*$] we have directly

$$\underline{H_o}:\ \langle\hat{g}^*\rangle_{o,o} = \hat{B}_n^*+\langle H_n(\underset{\sim}{x})^*\rangle_{o,o} = \frac{-\sigma_{on}^{*2}}{2}\ ;$$

$$\underline{H_1}:\ \langle\hat{g}^*\rangle_{1,\theta} = \hat{B}_n^*+\langle H_n(\underset{\sim}{x})^*\rangle_{1,\theta} = \frac{\sigma_{on}^{*2}}{2}+O(\overline{\theta^4}\ \text{or}\ \overline{\theta^6}), \qquad \text{(A.3-16)}$$

where the terms $O(\overline{\theta^4}$ or $\overline{\theta^6})$ are negligible vis-à-vis $\sigma_{on}^{*2}/2$ (as a result of the "small-signal" condition that $\sigma_{on}^{*2} \doteq \sigma_{on}^{*2}$, cf. (2.29)). Here specifically

$$H_n(\underset{\sim}{x})^* = \sum_i^n h_i^{(1)}(x_i)+\frac{1}{2}\sum_{ij}^n h_{ij}^{(2)}(x_i,x_j) \qquad \text{(A.3-17a)}$$

$$= \sum_i -\langle\theta_i\rangle\ell_i+\frac{1}{2}\sum_{ij}\{\langle\theta_i\theta_j\rangle(\ell_i\ell_j+\ell_i'\delta_{ij})-\langle\theta_i\rangle\langle\theta_j\rangle\ell_i\ell_j\}:$$

$$\underbrace{\text{"composite" LOBD}}_{\text{Eq. (2.9)}},\ \langle\theta\rangle > 0 \quad ; \qquad \text{(A.3-17b)}$$

$$H_n(x)^* = \sum_i -\langle\theta_i\rangle \ell_i \quad : \qquad \underset{\text{Eq. (2.11)}}{\text{coherent LOBD}}, \ \langle\theta\rangle > 0; \tag{A.3-17c}$$

$$= \sum_{ij} \{\langle\theta_i\theta_j\rangle(\ell_i\ell_j + \ell_i' \delta_{ij})\}: \qquad \underset{\text{Eq. (2.12)}}{\text{incoherent LOBD}}, \ \langle\theta\rangle = 0. \tag{A.2-17d}$$

Applying (A.3-17) to (A.3-16), we see that <u>two conditions</u> jointly involving the bias and the AO character of $\hat{g}_n^*$ must be satisfied simultaneously. These are

$$\text{I.} \quad \langle\hat{g}^*\rangle_{1,\theta} - \langle\hat{g}^*\rangle_{o,o} \doteq \sigma_{on}^{*2} \left(= \text{var}_o \hat{g}_n^*\right) \ ;$$

$$\text{II.} \quad \hat{B}_n^* = -\frac{1}{2}\left(\langle\hat{g}^*\rangle_{1,\theta} + \langle\hat{g}^*\rangle_{o,o}\right) \doteq -\sigma_{on}^{*2}/2 \ . \tag{A.3-18}$$

For both purely coherent and incoherent detection, cf. (A.3-17c,d), we have already shown that I and II, (A.3-18), are satisfied, subject to the "small-signal" condition $\sigma_{on}^{*2} >> |F_n^*(\langle\theta_o\rangle, \text{or} \langle\theta^2\rangle)|$, cf. (2.29), which insures that $\sigma_{1n}^{*2} \doteq \sigma_{on}^{*2}$. [See, specifically (A.2-14), (A.2-40), and (A.2-50b), (A.2-5b) in the binary signal cases.] However, as a preliminary to examining the composite LOBD, (A.3-17b), in regard to satisfying conditions I,II, (A.3-18), let us briefly outline the evaluations. We have

<u>Coherent Reception:</u>

$$\underline{\text{I.}} \quad -\sum_i \langle\theta_i\rangle\langle\ell_i\rangle_{1,\theta} + \sum_i \langle\theta_i\rangle\langle\ell_i\rangle_{o,o} = \sum_i \langle\theta_i\rangle^2 L_i^{(2)} + \sum_i \langle\theta_i^2\rangle\langle\theta_i\rangle^2 L_i^{(2,2)} + 0$$

$$\doteq \text{var}_o \hat{g}_{coh}^* = \sigma_{on\text{-}coh}^{*2} \ ; \tag{A.3-19a}$$

$$\text{II.}\quad \hat{B}_n^* = -\frac{1}{2}\left(\sum_i \langle\theta_i\rangle^2 L_i^{(2)} + O(\overline{\theta^4}) + 0\right) \doteq -\frac{1}{2}\,\sigma^{*2}_{\text{on-coh}}\,, \tag{A.3-19b}$$

which establishes (A.3-18) for the coherent LOBD, as expected. Similarly, for $(\text{LOBD})_{\text{inc}}$, (A.3-17d), we get

Incoherent Reception:

$$\text{I.}\quad \sum_{ij}\langle\theta_i\theta_j\rangle\left[\langle \ell_i\ell_j + \ell_i'\delta_{ij}\rangle_{1,\theta} - \langle \ell_i\ell_j + \ell_i'\delta_{ij}\rangle_{0,o}\right]$$

$$= 0 + \frac{1}{4}\sum_{ij}\langle\theta_i\theta_j\rangle^2\{(L_i^{(4)} - 2L_i^{(2)^2})\delta_{ij} + 2L_i^{(2)}L_j^{(2)}\} - 0 \qquad \text{Eq. (A.2-21)}; \tag{A.3-20a}$$

$$\sigma^{*2}_{\text{on-inc}} = \frac{1}{4}\sum_{ij}\langle\theta_i\theta_j\rangle^2\{(L_i^{(4)} - 2L_i^{(2)^2})\delta_{ij} + 2L_i^{(2)}L_j^{(2)}\},\ \text{Eq. (A.2-40)}, \tag{A.3-20b}$$

so that I, (A.3-18), is clearly obeyed. We have also directly

$$\text{II.}\quad \hat{B}_n^* = -\frac{1}{2}\cdot\left(\frac{1}{4}\sum_{ij}\langle\theta_i\theta_j\rangle^2\{(L_i^{(4)} - 2L_i^{(2)}L_j^{(2)})\delta_{ij} + 2L_i^{(2)}L_j^{(2)}\} + 0\right) = \frac{-\sigma^{*2}_{\text{on-inc}}}{2}\,, \tag{A.3-20c}$$

which again establishes the desired conditions (A.3-18) for the purely incoherent LOBD, (A.3-17d). Moreover, the proper bias, $\hat{B}_n^*$, in these cases is also equivalent to the average under H_0 of the next nonvanishing term after $H_n(\underset{\sim}{x})^*$, cf. (A.3-17) in the expansion of the original likelihood ratio (here $\log \Lambda_n$), as demonstrated in detail in Appendix A.1 above. In fact, this choice of bias was originally taken [14] to ensure consistency of the test (H_1 vs. H_0) as $n\to\infty$. We have shown above (and in Appendixes A.1, A.2)) that, with the appropriate "small-signal" condition on the input signal ($\bar{a}_0 > 0$) these biases are also the proper biases to insure the AO character of such LOBD's!

I. Detection of the Completely Coherent Signal (Case I):

We must distinguish two general cases of "composite" reception: Case I represents the situation where the signal to be detected is completely deterministic, i.e., entirely specified at the receiver; the only thing unknown to the detector is whether or not the signal is present in the accompanying noise. This means that $\langle\theta_i\rangle = \theta_i$; $\langle\theta_i^2\rangle = \langle\theta_i\rangle^2 = \theta_i^2$, etc., viz., $\langle\theta_i\theta_j\rangle = \langle\theta_i\rangle\langle\theta_j\rangle = \theta_i\theta_j$, etc. Reception is then fully coherent. Case II is the usual practical situation where the signal has random features vis-à-vis the detector, e.g., random fading amplitude, partial phase uncertainties, doppler, etc., so that $\langle\theta_i^2\rangle \neq \langle\theta_i\rangle^2 \neq \theta_i^2$, $\langle\theta_i\theta_j\rangle \neq \langle\theta_i\rangle\langle\theta_j\rangle$, etc. In the coherent detection cases signal epoch is still fully, or at least partially, known, but now the signal itself is only partially deterministic as seen at the detector.

Case I is rare in practice, while Case II represent essentially all practical applications. Nevertheless, before we can proceed to establish the LOB and AO conditions for the "composite" algorithms consisting of a suitable combination of purely coherent and incoherent LOBD's [cf. III, below), we must examine Case I for the two subcases (i), general nongauss noise, (ii), gauss noise.

For this purpose, let us use (A.1-4), (A.1-4a,b) modified, as usual, for independent (noise) samples (cf. Sec. A.1-2), to write first the general expansion of the optimum algorithm (A.1-4) (cf. (2.9) et seq., also)

$$\log \Lambda_n = \log \mu - \sum_i^n \ell_i\langle\theta_i\rangle + \frac{1}{2}\sum_{ij}^n [\langle\theta_i\theta_j\rangle - (\ell_i\ell_j + \ell_i'\delta_{ij}) - \langle\theta_i\rangle\langle\theta_j\rangle\ell_i\ell_j]$$

$$+\Theta_3+\Theta_4+t_n, \qquad \text{(A.3-21)}$$

where explicitly,

$$\Theta_3 = -\frac{1}{3!}\Big\{\Big[\sum_i^n \langle\theta_i^3\rangle\Big(\frac{w_{1i}^{(''')}}{w_{1i}}\Big) + 3\sum_{ij}^{n'} \langle\theta_i\theta_j^2\rangle \ell_i(\ell_j^2+\ell_j') + \sum_{ijk}^{n(")=(i\neq j\neq k)} \langle\theta_i\theta_j\theta_k\rangle \ell_i\ell_j\ell_k\Big]$$

$$- \sum_{ijk}^{n} \langle\theta_i\rangle\langle\theta_j\theta_k\rangle \ell_i(\ell_j\ell_k+\ell_j'\delta_{jk}) + 2\sum_{ijk}^{n} \langle\theta_i\rangle\langle\theta_j\rangle\langle\theta_k\rangle \ell_i\ell_j\ell_k \; ; \qquad \text{(A.3-21a)}$$

$$\Theta_4\Big|_{\text{indep}} = \text{Eq. (A.1-4b), Independent samples;} \qquad \text{(A.3-21b)}$$

and t_n is a remainder term.

Now, in the fully coherent (deterministic) Case I described above we may drop all the averages $\langle\ \rangle$ on θ_i, etc., in (A.3-21)-(A.3-21b). Clearly, Θ_3, Θ_4 do not vanish identically when the noise is nongaussian, i.e. $\ell_i \neq -x_i$, $\ell_i' = -1$. Consequently, for nongaussian noise the expansion (A.3-21) does not terminate (t_n being a series itself). Next, we use as our algorithm the first two terms of (A.3-21), ($\langle\theta_i\theta_j\rangle = \theta_i\theta_j$, etc.) with the bias B_n^* chosen as before (cf. Sec. A.1-3)

$$g^*_{n\text{-comp}}\Big|_{\text{Case I}} \equiv \log\mu - \sum_i^n \ell_i\theta_i + \frac{1}{2}\sum_{ij}^n \theta_i^2\ell_i' + [\langle\Theta_3\rangle_0 \text{ or } \langle\Theta_4\rangle_0]_{\text{Case I}}, \qquad \text{(A.3-22)}$$

where the bias is established as the first non-vanishing term in the expansion of $\log\Lambda_n$ after the term $O(\langle\theta^2\rangle)$ when the average (over the data $\{x_i\}$) is taken with respect to the null hypothesis (H_0).

Let us evaluate $\langle\Theta_3\rangle_0$, (A.3-21a) here, without invoking the strictly deterministic conditions of Case I. Since $\langle\ell_i\rangle_0 = 0$, $\langle\ell_i^2+\ell_i'\rangle_0 = \langle w_1''/w_1\rangle_0 = 0$; $\langle\ell_i^3\rangle_0 = 0$, we see at once that each term of $\langle\Theta_3\rangle_0$, (A.3-21a), vanishes, so that $\langle\Theta_3\rangle_0 = 0$, without recourse to the condition $\langle\theta_i\theta_j\theta_k\rangle = 0$, cf. (A.1-6) and footnote. Accordingly, the bias term is always $\langle\Theta_4\rangle_0$ ($\neq 0$), here, cf. Sec. A.1-3, Eqs. (A.1-20a,b). For Case I (non-gauss) here we get accordingly

$$g^*_{n\text{-comp}}\Big|_{\text{Case I}} = \log\mu + \{-\frac{1}{8}\sum_{ij}\theta_i^2\theta_j^2[(L_i^{(4)}-2L_i^{(2)^2})\delta_{ij}+2L_i^{(2)}L_j^{(2)}]\}$$

$$-\sum_i\theta_i\ell_i+\frac{1}{2}\sum_i\theta_i^2\ell_i' \ . \qquad \text{(A.3-23)}$$

Our next step is to show that (A.3-23) does <u>not</u> satisfy the conditions (A.3-18) for LOBD and AODA's. To demonstrate this we evaluate $\langle g^*_{n\text{-Case I}}\rangle_{1,o}$ and $\text{var}_o g^*_{n\text{-Case I}}$. Accordingly, we have

$$\langle g^*_{n\text{-I}}\rangle_{1,\theta} = \log\mu+B^*_{N\text{-I}}-\sum_i\theta_i\langle\ell_i\rangle_{1,\theta}+\frac{1}{2}\sum_i\theta_i^2\langle\ell_i'\rangle_{1,\theta} \ , \qquad \text{(A.3-24)}$$

where

$$\left\{\begin{array}{l} \langle\ell_i\rangle_{1,\theta} = -\theta_iL_i^{(2)}-\theta_i^3L_i^{(2,2)};\ \langle\ell_i'\rangle_{1,\theta} = \int_{-\infty}^{\infty}(\frac{w''_{1i}}{w_{1i}}-\ell_i^2)w_{1i}(x_i-\theta_i)dx_i \\ \langle\ell_i\rangle_o = 0;\ \ \langle\ell_i'\rangle_o = -L_i^{(2)}\ ; \qquad\qquad = \int_{-\infty}^{\infty}(\frac{w''_{1i}}{w_{1i}}-\ell_i^2)[w_{1i}-\theta_iw'_{1i}+\frac{\theta_i^2}{2}w''_{1i}+..]dx_i \\ \qquad\qquad\qquad\qquad = \frac{\theta_i^2}{2}L_i^{(4)}-L_i^{(2)}-\frac{\theta_i^2}{2}L_i^{(2,2)}+.. \end{array}\right\} \qquad \text{(A.3-24a)}$$

$$\therefore\ \langle g^*_{n\text{-I}}\rangle_{1,\theta} \doteq \log\mu+B^*_{n\text{-I}}+\sum_i^n\left\{\frac{\theta_i^2L_i^{(2)}}{2}+\frac{\theta_i^4}{4}[L_i^{(4)}+3L_i^{(2,2)}]+...\right\}\ ; \text{ and} \qquad \text{(A.3-25a)}$$

$$\langle g^*_{n\text{-I}}\rangle_{o,o} = \log\mu+B^*_{n\text{-I}}-\sum_i\frac{\theta_i^2}{2}L_i^{(2)} \ . \qquad \text{(A.3-25b)}$$

Accordingly, Condition I., (A.3-18), becomes here

$$\langle g^* \rangle_{1,\theta} - \langle g^* \rangle_{o,o} = \sum_i \theta_i^2 L_i^{(2)} + \sum_i \frac{\theta_i^4}{4} (L_i^{(4)} + 3L_i^{(2,2)}) + O(\theta^6). \qquad \text{(A.3-26)}$$

Next, we evaluate

$$\mathrm{var}_o g^*_{n-I} = \left\langle \left[\sum_i^n \left\langle (-\ell_i \theta_i + \frac{1}{2} \ell_i' \theta_i^2) \right]^2 \right\rangle_o - \left\langle \sum_i (-\ell_i \theta_i + \frac{1}{2} \ell_i' \theta_i^2) \right\rangle_o^2 \qquad \text{(A.3-27)}$$

$$= \sum_{ij}^n \left\langle (\ell_i \ell_j \theta_i \theta_j - \ell_i \ell_j' \theta_i \theta_j^2 + \frac{1}{4} \ell_i' \ell_j' \theta_i^2 \theta_j^2) \right\rangle_o - \frac{1}{4} \left(\sum_i -\theta_i^2 L_i^{(2)} \right)^2. \qquad \text{(A.3-27a)}$$

We observe that

$$\langle \ell_i \ell_j \rangle_o = L_i^{(2)} \delta_{ij} \; ; \; \langle \ell_i \ell_j' \rangle_o = 0 \; ; \; \langle \ell_i' \ell_j' \rangle_o = L_i^{(2)} L_j^{(2)} (1 - \delta_{ij}) \; ; \text{ or}$$

$$= \langle \ell_i'^2 \rangle_o = \int_{-\infty}^{\infty} (\frac{w_1''}{w_1} - \ell^2)^2 w_1 \, dx$$

$$[\langle \ell^4 \rangle_o = \frac{L^{(2,2)}}{2} \text{, cf. (A.2-16a)}]: \qquad = L_i^{(4)} - 2L_i^{(2,2)} + \langle \ell_i^4 \rangle_o,$$

$$= L_i^{(4)} - \frac{3}{2} L_i^{(2,2)}, \qquad \text{(A.3-28)}$$

so that

$$\mathrm{var}_o g^*_{n-I} = \sum_i^n \theta_i^2 L_i^{(2)} + \left\{ \frac{1}{4} \sum_i^n \theta_i^4 [L_i^{(4)} - \frac{3}{2} L_i^{(2,2)} - L_i^{(2)^2}] = \sigma^{*2}_{on-I} \right. . \qquad \text{(A.3-29)}$$

Comparing (A.3-29) and (A.3-26), $O(\theta^4)$, shows indeed that $\langle g^* \rangle_{1,\theta} - \langle g^* \rangle_{o,o} \neq \sigma^{*2}_{on-I}$, so that Condition I, (A.3-18), is violated. Moreover, Condition II

(A.3-18), is also clearly not obeyed, since from (A.3-25a,b) on removing $\log \mu(g^* \to \hat{g}^*)$ we get

$$-\frac{1}{2}\{\langle \hat{g}^*_{n-I}\rangle_{1,\theta}+\langle \hat{g}^*_{n-I}\rangle_{o}\} = -\frac{1}{2}\{2\hat{B}^*_{n-I}+\frac{1}{4}\sum_i^n \theta_i^4(L_i^{(4)}+3L_i^{(2,2)})\} \neq -\sigma^{*2}_{on-I}/2 \ , \tag{A.3-30}$$

where $\hat{B}^*_{n-I}$ is the bias term of (A.3-23), without log μ.

The upshot of the above is that for nongauss noise, under Case I (entirely coherent signal) conditions, we must follow the schema for the Composite LOBD's (III ff.): the proper composite form to use here is the sum of the (purely) coherent LOBD and a completely incoherent LOBD form, as for case II in practical situations.

On the other hand, when the noise is gaussian, the general expansion (A.3-21) terminates, e.g. $\Theta_3 = \Theta_4 \ldots, t_n = 0$, and, since $\ell_i = -x_i$, $\ell_i' = -1$ here, we get

$$\log \Lambda_n\Big|_{\text{det-Case I}} = \{\log \mu - \frac{1}{2}\sum_i^n \theta_i^2\} + \sum_i^n \theta_i x_i \ , \tag{A.3-31}$$

which is the well-known, exact result in this very special, limiting situation. The reason that we get different results in the two different noise situations (same completely specified signal) is that the signal and noise interact in a more complex fashion in the nongauss cases, so that adding the "incoherent" term (properly) increases the information at the detector relevant to the interaction and hence improves detection.

II. The General Composite ("On-off") LOBD: (Case II)

Our next step is to determine whether or not the composite, or "mixed" LOBD, (A.3-17b), also obeys the fundamental AO conditions (A.3-18), or (A.3-16). Here for this LOBD there is enough phase coherence at the receiver to obtain a coherent ($\langle\theta\rangle > 0$) as well as an incoherent contribution.

Let us begin with Condition I., (A.3-18), writing

$$\boxed{H^*_{comp} = \gamma^*_{coh}+\gamma^*_{inc}-\frac{\gamma^{*2}_{inc}}{2}} \tag{A.3-32}$$

$$\gamma^*_{coh} = \sum_i -\langle\theta_i\rangle \ell_i \; ; \; \gamma^*_{inc} = \frac{1}{2}\sum_{ij}\langle\theta_i\theta_j\rangle(\ell_i\ell_j+\ell_i'\delta_{ij}) \; ; \tag{A.3-32a}$$

$$\therefore \; \hat{g}^*_{comp} = \hat{B}^*_n + H^*_{comp} = \hat{B}^*_n+(\gamma^*_{coh}+[\gamma^*_{inc}-\gamma^{*2}_{inc}/2]) \; ; \tag{A.3-33}$$

$$\therefore \; var_{o,o}\hat{g}^*_{comp} = \langle H^{*2}_{comp}\rangle_{o,o}-\langle H^*_{comp}\rangle^2_{o,o} \; . \tag{A.3-34}$$

Expanding (A.3-34) gives

$$var_{o,o}\hat{g}^*_{comp} = var_o\gamma^*_{coh}+var_o\gamma^*_{inc}+\{\frac{1}{4}\underset{①}{var_o\gamma^{*2}_{coh}}+2(\langle\gamma^*_{coh}\gamma^*_{inc}\rangle_o-\langle\gamma^*_{coh}\rangle_o\langle\gamma^*_{inc}\rangle_o)$$

$$-(\langle\gamma^{*3}_{coh}\rangle_o-\langle\gamma_{coh}\rangle_o\langle\gamma^{*2}_{coh}\rangle_o)$$

$$-(\underset{②}{\langle\gamma^*_{inc}\gamma^{*2}_{coh}\rangle}-\langle\gamma^*_{inc}\rangle_o\langle\gamma^{*2}_{coh}\rangle_o)\}. \tag{A.3-35}$$

Proceeding, we have

$$\langle\gamma^*_{coh}\rangle_o = 0; \; \langle\gamma^{*2}_{coh}\rangle_o = \sum_i\langle\theta_i\rangle^2 L_i^{(2)} [= var\,\hat{g}^*_{coh}, \text{ cf. (A.3-19a)}]; \tag{A.3-36}$$

$$\langle \gamma^{*3}_{coh} \rangle_o = - \sum_{ijk}^{n} \langle \theta_i \rangle \langle \theta_j \rangle \langle \theta_k \rangle \langle \ell_i \ell_j \ell_k \rangle_o = 0 \begin{cases} i \neq j \neq k \\ i=j(\neq k) \\ i=j=k: \text{ odd} \end{cases} \qquad \text{(A.3-36b)}$$

$$\langle \gamma^{*4}_{coh} \rangle_o = \sum_{ijk\ell}^{n} \langle \theta_i \rangle \langle \theta_j \rangle \langle \theta_k \rangle \langle \theta_\ell \rangle \langle \ell_i \ell_j \ell_k \ell_\ell \rangle_o = 0 \text{ unless } i=j=k=\ell;$$

" $(i=j) \neq (k=\ell)$ in various combinations.

i.e. $\begin{cases} 2\times(i=j) \neq (k=\ell): \ (i=j, j=i) \equiv 2\times(i=j) \text{ etc.} \\ 2\times(i=k) \neq (j=\ell) \\ 2\times(i=\ell) \neq (j=k) \end{cases}$

$$= \sum_{i}^{n} \langle \theta_i \rangle^4 \langle \ell_i^4 \rangle_o + 6 \sum_{ij}^{n'} \langle \theta_i \rangle^2 \langle \theta_j \rangle^2 L_i^{(2)} L_j^{(2)} \ ; \begin{cases} \langle \ell_i^4 \rangle_o = \frac{1}{2} L_i^{(2,2)} \ , \\ \text{cf. (A.2-16a)} \end{cases} \qquad \text{(A.3-36c)}$$

$$\therefore \text{var } \gamma^*_{coh} = \sum_{i} \langle \theta_i \rangle^2 L_i^{(2)} = \text{var } \hat{g}^*_{coh} \ . \qquad \text{(A.3-36d)}$$

① $\therefore \text{var } \gamma^{*2}_{coh} = \langle \gamma^{*4}_{coh} \rangle_o - \langle \gamma^{*2}_{coh} \rangle_o^2$

$$= \sum_{i}^{n} \langle \theta_i \rangle^4 \frac{L_i^{(2,2)}}{2} + 6 \sum_{ij}^{n'} \langle \theta_i \rangle^2 \langle \theta_j^2 \rangle L_i^{(2)} L_j^{(2)} - \sum_{ij} \langle \theta_i \rangle^2 \langle \theta_j \rangle^2 L_i^{(2)} L_j^{(2)}$$

$$= \sum_{i}^{n} \langle \theta_i \rangle^4 \begin{cases} \left(\frac{L_i^{(2,2)}}{2} - L_i^{(2)^2} \right) \\ = \text{var}_o \ell^2 \end{cases} + 5 \sum_{ij}^{n'} \langle \theta_i \rangle^2 \langle \theta_j^2 \rangle L_i^{(2)} L_j^{(2)} . \qquad \text{(A.3-36e)}$$

Also, we see that

② $\left\langle \gamma^*_{inc}\gamma^{*2}_{coh}\right\rangle_o = \sum_{ijk\ell}\left\langle\theta_i\theta_j\right\rangle\left\langle(\ell_i\ell_j+\ell_i!\delta_{ij})\left\langle\theta_k\right\rangle\left\langle\theta_\ell\right\rangle\ell_k\ell_\ell\right\rangle_o = 0$

$$\left.\begin{array}{l} i\neq j\neq k\neq \ell \\ i=j\ (\neq k\neq \ell) \\ (i=j)\neq(k=\ell) \end{array}\right\}$$

$$= 4\sum_{ij}{}' \left\langle\theta_i\theta_j\right\rangle\left\langle\theta_i\right\rangle\left\langle\theta_j\right\rangle L_i^{(2)}L_j^{(2)} \neq 0;$$

$$\left.\begin{array}{l} (i=k)\neq(j=\ell)x2 \\ (i=\ell)\neq(j=k)x2 \end{array}\right\} \qquad \text{(A.3-37a)}$$

and

$$\left\langle \gamma^*_{inc}\gamma^*_{coh}\right\rangle_o = -\sum_{ijk}\left\langle\theta_i\theta_j\right\rangle\left\langle(\ell_i\ell_j+\ell_i!\delta_{ij})\left\langle\theta_k\right\rangle\ell_k\right\rangle_o = 0; \qquad \text{(A.3-37b)}$$

$$\left\langle \gamma^*_{inc}\right\rangle_o = 0. \qquad \text{(A.3-37c)}$$

Consequently, (A.3-35) reduces to

$$\mathrm{var}_o\hat{g}^*_{comp} = \mathrm{var}_o\hat{g}^*_{coh}+\mathrm{var}\ \hat{g}^*_{inc} +\{\frac{1}{4}\sum_i^n\left\langle\theta_i\right\rangle^4\mathrm{var}_o\ell^2$$

$$+\frac{5}{4}\sum_{ij}^{n}{}'\left\langle\theta_i\right\rangle^2\left\langle\theta_j\right\rangle^2L_i^{(2)}L_j^{(2)}-4\sum_{ij}^{n}{}'\left\langle\theta_i\right\rangle\left\langle\theta_j\right\rangle\left\langle\theta_i\theta_j\right\rangle L_i^{(2)}L_j^{(2)}\}. \qquad \text{(A.3-38)}$$

Next, we have

$$(\langle\hat{g}^*\rangle_{1,\theta}-\langle\hat{g}^*\rangle_{o,o\ comb} = \langle\gamma^*_{coh}+\gamma^*_{inc}-\gamma^{*2}_{coh}/2\rangle_{1,\theta}-\langle\gamma^*_{coh}+\gamma^*_{inc}-\gamma^{*2}_{coh}/2\rangle_{o,o} \tag{A.3-39a}$$

$$= \mathrm{var}_o\hat{g}^*_{coh} + \mathrm{var}_o\hat{g}^*_{inc} - \langle\gamma^{*2}_{coh}/2\rangle_{1,\theta}-0-0+\frac{1}{2}\,\mathrm{var}_o\hat{g}^*_{coh}. \tag{A.3-39b}$$

Eq.(A.3-19a) Eqs.(A.3-20a,b)

Also, we obtain

$$\langle\gamma^{*2}_{coh}\rangle_{1,\theta} = \sum_{ij}^{n}\langle\theta_i\rangle\langle\theta_j\rangle\langle\ell_i\ell_j\rangle_{1,\theta} = \sum_{i}^{n}\langle\theta_i\rangle^2\{L_i^{(2)}+\frac{\langle\theta_i^2\rangle}{2}L_i^{(2,2)}+\ldots\}$$

$$+\sum_{ij}^{n'}\langle\theta_i\rangle\langle\theta\rangle_j\langle\theta_i\theta_j\rangle L_i^{(2)}L_j^{(2)}+\ldots, \tag{A.3-39c}$$

(from (A.2-8).

Inserting this into (A.3-39b) and using (A.3-36d), we get finally

$$(\langle\hat{g}^*\rangle_{1,\theta}-\langle\hat{g}^*\rangle_{o,o})_{comb} = \mathrm{var}_o\hat{g}^*_{coh}+\mathrm{var}_o\hat{g}^*_{inc}$$

$$-\sum_{i}^{n}\frac{\langle\theta_i\rangle^2\langle\theta_i^2\rangle}{4e}L_i^{(2,2)}-\frac{1}{2}\sum_{ij}^{n'}\langle\theta_i\rangle\langle\theta_j\rangle\langle\theta_i\theta_j\rangle L_i^{(2)}L_j^{(2)}$$

$$= \mathrm{var}_o\hat{g}_{coh}+\mathrm{var}\,\hat{g}^*_{inc}$$

$$-\frac{1}{2}\{\sum_{i}^{n}\langle\theta_i\rangle^4\mathrm{var}_o\ell^2+\sum_{ij}^{n}\langle\theta_i\rangle\langle\theta_j\rangle\langle\theta_i\theta_j\rangle L_i^{(2)}L_j^{(2)}\}. \tag{A.3-40}$$

Clearly, comparing (A.3-38) and (A.3-40) shows at once that condition I, (A.3-18), is not obeyed here for the composite LOBD, (A.3-17b).

Moreover, Condition II, (A.3-18), is seen from (A.3-39a)-(A.3-39c) to be

$$\hat{B}^*_n = -\frac{1}{2}\left[\mathrm{var}_o \hat{g}^*_{coh} + \mathrm{var}_o \hat{g}^*_{inc} + -\sum_i^n \langle\theta_i\rangle^2 L_i^{(2)}\right.$$

$$\left. -\frac{1}{2}\left[\sum_i^n \langle\theta_i\rangle^4 \,\mathrm{var}_o \ell^2 + \sum_{ij}^n \langle\theta_i\rangle\langle\theta_j\rangle\langle\theta_i\theta_j\rangle L_i^{(2)} L_j^{(2)}\right]\right], \qquad \text{(A.3-41)}$$

which is also not equal to $-\sigma^{*2}_{on}/2$ $\left(= -\frac{\mathrm{var}_o}{2}\hat{g}^*_{comp}\right)$, Eq. (A.3-27), unless $\bar{\theta}_i = 0$, (whereupon $\hat{g}_{coh} = 0$, of course).

Thus, we reach the important conclusion that when $\bar{\theta} > 0$ the general composite LOBD = $\hat{g}^*_{comp}$, (A.3-33), which includes the component $(-\gamma^{*2}_{inc}/2)$ in the incoherent position, is not an AODA as $n\to\infty$, Hence when $(\bar{\theta}_i > 0)$ it is always alternatively better to use the coherent LOBD alone, [without the full coherent term, $(\gamma^*_{inc} - \gamma^{*2}_{coh}/2)$ for small input signals, and hence large $n(>>1)$, for acceptably small error probabilities. However, as we note in III below, it is possible to find a composite LOBD which is better than either the LOBD_{inc} or LOBD_{coh} and the above general composite form (A.3-33):

III. The Composite ("On-off") LOBD: Case II

Although the general composite LOBD = g^*_{comp}, (A.3-33), which includes the term $(-\gamma^{*2}_{coh}/2)$ in the incoherent component, cf. (2.9), is not an AODA as we have shown above (I), we can easily find a composite LOBD which has the desired AO qualities and is better than either the coherent or incoherent LOBD's. This is accomplished immediately by setting $\langle\theta_i\rangle = 0$ in the incoherent portion of the algorithm, viz.

$$\hat{g}^*_{comp} = \hat{B}^*_{comp} + \cdot\,\gamma^*_{coh} + \gamma^*_{inc}\,, \qquad \text{(A.3-42)}$$

cf. (A.3-32,33). We call this composite LOBD a composite LOBD, or simply a composite or "mixed" LOBD, as distinct from the "general composite" LOBD discussed in I preceding. Accordingly, from (A.3-38) and (A.3-40), (A.3-41), we see that with $\langle\theta_i\rangle = 0$ in the $\gamma^{*2}_{coh}/2$ term (which then vanishes) that

$$\text{var}_o \hat{g}^*_{comp} = \text{var}_o \hat{g}^*_{coh} + \text{var}_o \hat{g}^*_{inc} = (\langle \hat{g}^* \rangle_{1,\theta} - \langle \hat{g}^* \rangle_{o,o})_{comp}$$

$$= -2\hat{B}^*_{n\text{-}comp} = -2(\hat{B}^*_{n\text{-}coh} + \hat{B}^*_{n\text{-}inc}) \ . \qquad \text{(A.3-43)}$$

Thus, conditions I and II, (A.3-16), or (A.3-18) are fulfilled, and consequently $\hat{g}^*_{comp}$ is LOBD and AODA. Accordingly, this composite or mixed LOBD is simply the sum of the separate strictly coherent and strictly incoherent ($\bar{\theta}_1 = 0$) LOBD's of our principal analysis, with a composite bias which is the sum of the separate biases. Thus, this composite or "mixed" LOBD is specifically (in these "on-off" cases)

$$g^*_{n\text{-}comp} = \log \mu + [-\frac{1}{2}\sum_i^n \langle\theta_i\rangle^2 L_i^{(2)} - \frac{1}{8}\sum_{ij}^n \langle\theta_i\theta_j\rangle^2 \{(L_i^{(4)} - 2L_i^{(2)^2})\delta_{ij}$$

$$+ 2L_i^{(2)}L_j^{(2)}\}] - \sum_i^n \langle\theta_i\rangle \ell_i + \frac{1}{2}\sum_{ij}^n \langle\theta_i\theta_j\rangle[\ell_i\ell_j + \ell_i'\delta_{ij}] \ , \qquad \text{(A.3-44)}$$

$$= \log \mu + \hat{B}^*_{n\text{-}coh} + \hat{B}^*_{n\text{-}inc} + \sum_i^n -\ell_i\langle\theta_i\rangle + \frac{1}{2}\sum_{ij}^n [\ell_i\ell_j + \ell_i'\delta_{ij}]\langle\theta_i\theta_j\rangle \qquad \text{(A.3-44a)}$$

$$= \log \mu + \text{LOBD}_{coh.} + \text{LOBD}_{inc.} = \log \mu + \text{LOBD}_{comp} \ . \qquad \text{(A.3-44b)}$$

These are the optimum canonical forms for the mixed threshold cases, for general signals and interference, which become AODA's as sample-size $n \to \infty$.

Several remarks are in order: (i), the "small-signal" condition here is essentially that which applies to the essential equality of the H_1 and H_0 variances; there is now no purely coherent or incoherent algorithm, cf. remarks ff. (6.79c); (ii), we can obtain the various (optimum) performance (i.e. error probability) measures [Sec. 6.1] directly, by appropriate use of the variance σ^{*2}_{on} ; (iii), extension to the binary signal cases is direct, cf. (6.12), (6.28), for $\sigma^{(21)*2}_{coh}$, $\sigma^{(21)*2}_{inc}$ used in (A.3-44). However the notions of processing gain and minimum detectable signal [Sec. 6.2] need to be redefined, a task we have briefly outlined in Sec. 6.5; (iv), for suboptimum systems, the conditions (A.3-16,18) are not obeyed, and these algorithms are neither LOBD's or AODA's, since $f_1^2 = f_1^*$, $f_2 \neq f_2^*$, cf. (A.3-38), i.e. they are not derived from the expansion of a likelihood ratio.

We note, also, that the composite results (A.3-44) apply, as well, for completely deterministic signals [with $\langle \theta_i \rangle = \theta_i$, $\langle \theta_i \theta_j \rangle = \theta_i \theta_j$, etc.] Case I, cf. I above, as long as the noise is nongaussian (which means that g_n^* is not the full expansion of $\log \Lambda_n$). In the gaussian situation (Case I), $\log \Lambda_n = g_n^*\big|_{gauss}$ terminates after the term $O(\theta^2)$ in the expansion, as required, cf. (A.3-31). The improvement gained in the Case I situations (when the noise is nongaussian) arises from the additional information relevant to signal and noise interaction in the composite LOBD form vis-à-vis the purely coherent LOBD form. For example, let us suppose that the noise is "Laplace" noise (A.4-50b); then for these Case I situations we have explicitly

$$\log \Lambda_n = \log \exp \{ \sqrt{2} \sum_i (|x_i| - |x_i - \theta_i|) \doteq g^*_{n\text{-comp}} , \qquad \text{(A.3-44c)}$$

and clearly the signal-noise "interaction" embodied in $|x_i - \theta_i|$, is not at all simple, resulting in a non-terminating series of the form (A.3-21).

Finally, we note that $g^*_{n\text{-comp}}$ is never less effective (in performance) than $g^*_{n\text{-inc}}$ and is always better than $g^*_{n\text{-coh}}$ when coherent reception is possible at the receiver. This follows at once from the fact that, cf. (A.3-32):

$$\sigma^{*2}_{o\text{-comp}} = \sigma^{*2}_{o\text{-coh}} + \sigma^{*2}_{o\text{-inc}} \geq \sigma^{*2}_{o\text{-coh}} \text{ or } \sigma^{*2}_{o\text{-inc}} , \tag{A.3-33}$$

where explicitly

("on-off"):

$$\boxed{\sigma^{*2}_{o\text{-comp}} = \sum_i^n \langle\theta_i\rangle^2 L_i^{(2)} + \frac{1}{4}\sum_{ij}^n \langle\theta_i\theta_j\rangle^2 \{(L_i^{(4)} - 2L_i^{(2)^2})\delta_{ij} + 2L_i^{(2)}L_j^{(2)}\},}$$

(A.3-34a)

with bias

$$\hat{B}^*_{n\text{-comp}} = -\frac{1}{2}(\sigma^{*2}_{o\text{-coh}} + \sigma^{*2}_{o\text{-inc}}) = -\frac{1}{2}\sigma^{*2}_{o\text{-mixed}} = -\frac{1}{2}\cdot\text{Eq. (A.3-34a)}. \tag{A.3-34b}$$

Using (A.3-33), (A.3-34a) in (6.2), (6.5), (and (6.5a), (6.5e) for binary signals), at once establishes the above statements.

IV. Binary Signals:

In the case of binary signals, we have at once from (6.12), (6.28), generally

(binary):

$$(\sigma^{(21)*}_{o\text{-}comp})^2 = (\sigma^{(21)*}_{o\text{-}coh})^2+(\sigma^{(21)*}_{o\text{-}inc})^2 = \sum_i^n L_i^{(2)}\{\langle a_{oi}^{(2)}s_i^{(2)}\rangle-\langle a_{oi}^{(1)}s_i^{(1)}\rangle\}^2$$

$$+ \frac{1}{4}\sum_{ij}^n(\{L_i^{(4)}-2L_i^{(2)^2}\}\delta_{ij}+2L_i^{(2)}L_j^{(2)})$$

$$\cdot(\langle a_{oi}^{(2)}a_{oj}^{(2)}s_i^{(2)}s_j^{(2)}\rangle - \langle a_{oi}^{(1)}a_{oj}^{(1)}s_i^{(1)}s_j^{(1)}\rangle)^2 \quad . \tag{A.3-35}$$

However, bias is now from (4.3a), (4.5a)

(binary):

$$\hat{B}^{(21)*}_{n\text{-}comp} = \hat{B}^*_{n\text{-}coh}+\hat{B}^*_{n\text{-}inc} = -\frac{1}{2}\sum_i^n L_i^{(2)}\{\langle a_{oi}^{(2)}s_i^{(2)}\rangle^2=\langle a_{oi}^{(1)}s_i^{(1)}\rangle^2\}$$

$$-\frac{1}{8}\sum_{ij}^n[(L_i^{(4)}-2L_i^{(2)^2})\delta_{ij}+2L_i^{(2)}L_j^{(2)}]$$

$$\cdot[\langle a_{oi}^{(2)}a_{oj}^{(2)}s_i^{(2)}s_j^{(2)}\rangle^2 - \langle a_{oi}^{(1)}a_{oj}^{(1)}s_i^{(1)}s_j^{(1)}\rangle^2] \quad , \tag{A.3-36}$$

which with the appropriate averages [$\langle\rangle_{1,\theta}$, etc.] over $\gamma^{(21)*}_{coh}$, $\gamma^{(21)*}_{inc}$, cf. (A.3-17), is required to give the correct variance (A.3-35) to this level of "small-signal" approximation, which insures that $\sigma^{(21)*}_{o\text{-}comp} \doteq \sigma^{(21)*}_{o\text{-}comp}$. The actual "small-signal" conditions are given by (A.2-15a), (A.2-42). However, we note again that the only condition here is that of equal variances; cf. remarks after (A.3-44). The LOBD (and AODA) in these binary cases is, of

course, like (A.3-27) in the "on-off" situation,

$$g^{(21)*}_{n\text{-comp}} = \log \mu + \mathrm{LOBD}^{(21)}_{coh} + \mathrm{LOBD}^{(21)}_{inc}$$

$$= \log \mu + \hat{B}^{(21)*}_{n\text{-comp}} - \sum_{i}^{n} \ell_i \left(\langle a^{(2)}_{oi} s^{(2)}_i \rangle - \langle a^{(1)}_{oi} s^{(1)}_i \rangle \right)$$

$$+ \frac{1}{2} \sum_{ij}^{n} (\ell_i \ell_j + \ell'_i \delta_{ij}) \left[\langle a^{(2)}_{oi} a^{(2)}_{oj} s^{(2)}_i s^{(2)}_j \rangle - \langle a^{(1)}_{oi} a^{(1)}_{oj} s^{(1)}_i s^{(1)}_j \rangle \right]. \quad \text{(A.3-37)}$$

cf. (4.3),(4.5). (Optimum) performance, again, is obtained from (A.3-35) in (6.5a, 6.5e) directly. [For an example, see Part II, Section II, C of [1], and Figure 2 therein, in the specific binary case of narrow band signals with partially known RF phases.]

APPENDICES (cont'd):

Part II. Suboptimum Threshold Detectors

(David Middleton)

APPENDIX A-4

Canonical Formulations:

In this Appendix we shall derive both general and particular forms of suboptimum threshold signal detection algorithms, and their associated means and variances under (H_0,H_1), [or H_1,H_2) in the binary signal cases]. Again, we postulate independent noise samples, although our canonical approach is not in principle affected by this (not serious) constraint. In the following we first consider the canonical treatment of suboptimum receivers and then specialize the results to two particular limiting cases of suboptimum detectors, namely, clipper-correlators, using "super-clippers", and simple correlation detectors (i.e., without clipping). In these suboptimum cases we cannot, of course, expect the algorithms to be AODA's, [cf. Sec. A.3-3)], nor are they LOB optimum for any finite sample size ($n>\infty$). However, an exception to this arises when this particular class [cf. (A.4-1,2) ff.] of detectors is employed in the interference for which they are optimum, as we shall see in what follows, cf. Sec. A.4-1 ff.

A.4-1. A Class of Canonical Suboptimum Threshold Detection Algorithms:

Guided by the optimum canonical forms above [cf. (2.9) et seq., and in particular, (4.1) and (4.4)], we can specify a broad general class of generally suboptimum detection algorithms, defined essentially by their similar dependence on input signal structure [through $\langle\theta_i\rangle$, $\langle\theta_i\theta_j\rangle$], viz:

I. Coherent Detection:

$$g(\underset{\omega}{x})_{coh} = \log \mu + \hat{B}'_{coh} - \sum_{i}^{n} \langle\theta_i\rangle F(x_i) \; ; \qquad (A.4\text{-}1)$$

II. Incoherent Detection:

$$g(\underset{\sim}{x})_{inc} = \log \mu + \hat{B}'_{inc} + \frac{1}{2!}\sum_{ij}^{n} \langle \theta_i \theta_j \rangle H(x_i, x_j) \ , \qquad \text{(A.4-2)}$$

where F, H are (real) functions of the data elements $\{x_i, x_j\}$, subject to appropriate constraints (to be discussed presently, cf. A.4-1,D) to insure that these algorithms do not produce singular results on finite sample sizes ($n<\infty$).

For the moment, the biases, $\hat{B}'_{(\ )}$, are arbitrary, while it is assumed that F and H are specified. It is desireable, however, that under appropriate circumstances these algorithms become LOBD's. This means, then, at once by direct comparison with the canonical LOBD forms (4.1), (4.4), that

$$\ell_{F_i} = F_i \ ; \text{ i.e., } \ell_i \text{ generally} \to F_i \ ; \therefore \ell'_i \to F'_{(\ )}, \text{ etc.,} \qquad \text{(A.4-3a)}$$

$$H(x_i, x_j) \to \ell_{Fi}\ell_{Fj} + \ell'_{Fi}\delta_{ij} \to F_i F_j + F'_i \delta_{ij}. \qquad \text{(A.4-3b)}$$

[A sometimes useful extension of this is $F_i \to F_{ij}\delta_{ij}$, cf. Sec. A.4-3 for an example. One simply replaces F_i by $F_{ij}\delta_{ij}$, etc. in the results below.] The bias is unspecified, and the algorithms contain no higher order terms in θ_i, so that we cannot apply the usual technique of the optimal cases of determining the biases by H_0-averaging of the next higher-order terms in θ.

However, our requirement that $g(\underset{\sim}{x})$ be optimal (all n) when the background noise has the pdf w_{1F} such that $F = \ell_F [\equiv (d/dx)\log w_{1F}(x)]$, i.e. derived from an appropriate $\log \Lambda_n$, suggests how to determine a bias, such that $g_F \to g_F^*$ is LOBD and AODA, cf. Sec. A.3-3. This is the observation that for symmetric channels ($\mu=1, K=1$)

$$\left\langle g^{(*)} \right\rangle_{1,\mu=1} = -\left\langle g^{(*)} \right\rangle_{0,\mu=1} \ , \qquad \text{(A.4-4)}$$

and hence in the optimum cases P_e^* reduces to the canonical form (6.5). [We retain here only the leading terms in θ, of course.] Also, when $g_F \to g_F^*$, then $\hat{\sigma}_F^2 \to \sigma_F^{*2}$, i.e. for the noise pdf w_{1F}, these are now the optimum variances and biases. When the actual noise obeys $w_{1E} \neq w_{1F}$, the algorithms are suboptimum, including the biases. Consequently, to obtain $\hat{\sigma}_F^2$, and $\hat{B}'_{(\ )}$, we must use (A.4-3) in our previous calculations of the means and variances of g*, Appendix A.2 above, to obtain the new means and variances (which take the optimum canonical forms of the text (4.1), (4.4), etc.). We then use (A.4-4) to obtain a bias with the desired limiting optimal properties.

A. Coherent Detection:

Accordingly let us start with Sec. A.2-1, replacing $\ell(x)$ by $F(x)$ in (A.2-1)-(A.2-4). We get

$$\langle g_{coh} \rangle_{1,\theta} = B'_{coh} - \sum_i^n \langle \theta_i \rangle \{ \bar{F}_i - \langle \theta_i \rangle \int_{-\infty}^{\infty} F_i w'_{1i} dx_i + O(\overline{\theta^2}) \}. \tag{A.4-5a}$$

At this point and subsequently we restrict F to be antisymmetrical, e.g. $F(-x) = -F(x)$, and w_{1E} to be symmetrical. This is no real restriction, since we are using both positive and negative values of the amplitude data ($-\infty \leq x \leq \infty$). Then, (A.4-5a) becomes

$$\left.\begin{aligned} &\langle g_{coh} \rangle_{1,\theta} = B'_{coh} - \sum_i^n \langle \theta_i \rangle^2 \langle F'_i \rangle_o + O(\langle \theta^4 \rangle) \\ &\langle g_{coh} \rangle_{1,0} = B'_{coh}, \ (\text{all } \theta). \end{aligned}\right\} \quad B'_{coh} \equiv B'_{coh} + \log \mu; \tag{A.4-5b}$$

with (A.4-6)

Similarly, we obtain the variances from (A.2-5)-(A.2-12). Since

$$\langle F_i \rangle_{1,\theta} = \langle \theta_i \rangle \langle F_i' \rangle_o + O(\overline{\theta_i^3}) \; ; \; \langle F_i F_j \rangle_{1,\theta} \big| i \neq j = \langle \theta_i \theta_j \rangle \langle F_i' \rangle_o \langle F_j' \rangle_o + \; O(\overline{\theta^4}) \; ; \tag{A.4-7a}$$

$$\langle F_i^2 \rangle_{1,\theta} = \langle F_i^2 \rangle_o + \langle \theta_i^2 \rangle \langle (F_i'^2 + F_i F_i'') \rangle_o + O(\overline{\theta_i^4}) \; ; \; \langle F_i \rangle_o = 0 \text{ by antisymmetry;} \tag{A.4-7b}$$

and setting

$$\therefore \; \langle F_i \rangle_o \equiv -L_{iF:E}^{(2)} \; ; \; \langle F_i'^2 + F_i F_i'' \rangle_o \equiv \frac{1}{2} L_{iF:E}^{(2,2)} \; ; \; \langle F_i^2 \rangle_o \equiv \hat{L}_{iF:E}^{(2)} \; ; \tag{A.4-7c}$$

we obtain the following suboptimum forms for (A.2-11),(A.2-12):

$$\hat{\sigma}_1^2 = \sum_i \langle \theta_i \rangle^2 \{ \langle F_1^2 \rangle_o + \frac{\langle \theta_i^2 \rangle}{2} L_{iF:E}^{(2,2)} - \langle \theta_i \rangle^2 \langle F_i' \rangle_o^2 + \ldots \}$$

$$+ \sum_{ij}{}' \langle \theta_i \rangle \langle \theta_j \rangle \{ \langle \theta_i \theta_j \rangle - \langle \theta_i \rangle \langle \theta_j \rangle \langle F_i \rangle_o \langle F_i' \rangle_o \} + \ldots \tag{A.4-8}$$

$$\therefore \; \boxed{\hat{\sigma}_{o,(coh)}^2 = \sum_i \langle \theta_i \rangle^2 \hat{L}_{iF:E}^{(2)} \; .} \tag{A.4-9}$$

The condition that $\hat{\sigma}_1^2 \doteq \hat{\sigma}_o^2$, i.e. "closeness" condition on the maximum size of the input signal (a_o) is

$$\boxed{\left| \sum_i \langle \theta_i \rangle^2 \left\{ \frac{\langle \theta_i^2 \rangle}{2} L_{if:E}^{(2,2)} - \langle \theta_i \rangle^2 L_{F:E}^{(2)^2} \right\} + \sum_{ij}{}' \langle \theta_i \rangle \langle \theta_j \rangle (\langle \theta_i \theta_j \rangle - \langle \theta_i \rangle \langle \theta_j \rangle) \langle L_{iF:E}^{(2)} \rangle_o \langle L_{jF:E}^{(2)} \rangle_o \right| \ll \sum_i \langle \theta_i \rangle^2 L_{iF:E}^{(2)} \; .} \tag{A.4-10}$$

cf. (A.2-15a), and (A.2-51),

From (A.4-5b), (A.4-6) we can write directly

$$\langle g_{coh}\rangle_1 - \langle g_{coh}\rangle_o \doteq -\sum_i \langle\theta_i\rangle^2 \langle F_i'\rangle_o \; (= \sum_i \langle\theta_i\rangle^2 L_{iF:E}^{(2)}) \; , \tag{A.4-11a}$$

and from A.4-4 now specify the bias (μ=1):

$$\boxed{\hat{B}'_{coh} = -\frac{1}{2}\sum_i \{\langle\theta_i\rangle^2 L_{F:E}^{(2)}\} \; ,} \tag{A.4-11b}$$

where terms $O(\langle\theta^4\rangle)$ are omitted. Note that when $F'\to\ell'$, $\langle F_i'\rangle_o = -L_{F:E}^{(2)} = -L^{(2)}$, since

$$\int_{-\infty}^{\infty} \ell' w_{1E} dx = -\int_{-\infty}^{\infty} \ell w_1' dx = -\int_{-\infty}^{\infty} \ell^2 w_1 dx = -L^{(2)} \; ,$$

cf. (A.1-15) and $\hat{B}'_{coh}\to\hat{B}^*_{coh} = -\frac{1}{2}\sum_i \langle\theta_i\rangle^2 L^{(2)} = -\sigma_o^{*2}/2$, as required, cf. Sec. A.3-3. The "distance" (A.4-10) becomes σ_o^{*2}, also as required, cf. (A.3-10). We observe, that although the bias ($\hat{B}'_{coh}$) does not appear in the "distance", it does show up implicitly when one sets the false-alarm probability $\alpha_F^{(*)}$, via (2.25).

Finally, let us observe that the resulting arguments of the eror functions in the probability measures of performance (2.31),(2.32) in this (coherent) suboptimum class, are here from (A.4-8), A.4-10)

$$\boxed{\frac{\langle g_{coh}\rangle_1 - \langle g_{coh}\rangle_o}{\sqrt{2}\,\hat{\sigma}_{o\text{-}coh}} \doteq \frac{\sum_i^n \langle\theta_i\rangle^2 L_{iF:E}^{(2)}}{\sqrt{2}\,(\sum_{i=1}^n \langle\theta_i\rangle^2 \hat{L}_{iF:E}^{(2)})^{1/2}} \equiv \frac{\sigma_{o\text{-}coh(F)}}{\sqrt{2}} \; ;} \tag{A.4-12a}$$

$$\frac{\langle g_{coh}\rangle_1}{\sqrt{2}\hat{\sigma}_{coh}} \doteq \frac{-\langle g_{coh}\rangle_o}{\sqrt{2}\,\hat{\sigma}_{coh}} \doteq \frac{\sum_{i=1}^{n}\langle\theta_i\rangle^2}{2\sqrt{2}\,(\sum_{i=1}^{n}\langle\theta_i\rangle^2 L_{1F:E}^{(2)})^{1/2}} \equiv \frac{\sigma_{o\text{-}coh(F)}}{2\sqrt{2}} \,. \qquad \text{(A.4-12b)}$$

[Clearly, when $F\to\ell_F$, these reduce to $(L_i^{(2)}\langle\theta_i\rangle^2)^{1/2}/\sqrt{2} = \sigma_o^*/\sqrt{2}$, and $\sigma_o^*/2\sqrt{2}$, respectively, cf. (6.2), (6.5), as required, i.e. $\sigma_{o\text{-}coh} \to \sigma^*_{o\text{-}coh}$, cf. (A.2-14); generally, $\sigma_{o\text{-}coh} \neq \hat{\sigma}_{o\text{-}coh}$, (A.4-9).]

B. Incoherent Detection:

We proceed as above, according to (A.4-3) applied to Section A.2-2. Thus (A.2-19) becomes now

(i=j):

$$\left\langle F_i^2+F_i'\right\rangle_{1,\theta} = \left\langle \int_{-\infty}^{\infty}(F_i^2+F_i')w_{1E}(x_i-\theta_i)dx_i\right\rangle_\theta \qquad \text{(A.4-13a)}$$

$$= \int_{-\infty}^{\infty}(F_i^2+F_i')[w_{1e}-\langle\theta_i\rangle w_{1E}'+\frac{\langle\theta_i^2\rangle}{2}w_{1E}''\ldots]dx_i;\ \langle\theta_i\rangle=0,\ \langle\theta_i^3\rangle=0,\ \text{etc.},$$

$$\left.\begin{aligned} &= \left\langle F_i^2+F_i'\right\rangle_o + \frac{\langle\theta_i^2\rangle}{2}\left\langle(F_i^2+F_i')''\right\rangle_o + O(\overline{\theta_i^4}) \qquad \text{(A.4-13b)}\\ &= \left\langle F_i^2+F_i'\right\rangle_o + \frac{\langle\theta_i^2\rangle}{2}\int_{-\infty}^{\infty}(F_i^2+F_i')w_{1E}''(x_i)dx_i \end{aligned}\right\}, \qquad \text{(A.4-13c)}$$

whichever is defined (e.g., $(F_i^2+F_i')''$ or w_{1E}''); w_{1E}'' is usually defined, $|<\infty|$.

Similarly, we have for (A.2-20) the general result

$(i \neq j)$:

$$\langle F_i F_j + F_i' \delta_{ij} \rangle_{1,\theta} = \langle F_i F_j \rangle_{1,\theta} = \langle \langle F_i \rangle_1 \langle F_j \rangle_1 \rangle_\theta = \langle \theta_i \theta_j \rangle \langle F_i' \rangle_o \langle F_j' \rangle_o + O(\overline{\theta^4}) \ , \tag{A.4-14}$$

so that combined with (A.4-13) in (A.4-15):

$$\langle g_{inc} \rangle_{1,\theta} = B_{inc}' + \frac{1}{2} \sum_{ij}^{n} \langle \theta_i \theta_j \rangle \langle F_i F_j + F_i' \delta_{ij} \rangle_{1,\theta}, \tag{A.4-15}$$

cf. (A.4-36) in (A.4-2). We get directly

$$\boxed{\begin{aligned} \langle g_{inc} \rangle_{1,\theta} = B_{inc}' + \frac{1}{2} \sum_{ij}^{n} \langle \theta_i \theta_j \rangle \{ & L_{iE:F}^{(1)} \delta_{ij} + \langle \theta_i \theta_j \rangle \left(\frac{L_{iF:E}^{(4)}}{2} - \langle F_i' \rangle_o^2 \right) \delta_{ij} \\ & + \langle \theta_i \theta_j \rangle \langle F_i' \rangle_o \langle F_j' \rangle + O(\overline{\theta^4}) \} \ , \end{aligned}} \tag{A.4-16}$$

where

$$\hat{L}_{iF:E}^{(4)} \equiv \langle (F_i^2 + F_i')'' \rangle_o = \int_{-\infty}^{\infty} (F_i^2 + F_i') w_{1E}'' dx_i \ ; \ L_{1F:E}^{(1)} \equiv \langle F_i^2 + F_i' \rangle_o ; \tag{A.4-16b}$$

and $\hat{L}_{iE|E}^{(4)} = L_i^{(4)} = \langle w_{1E}''/w_{1E})^2 \rangle_o$ = (A.1-19b) in the optimum cases (F→E). Moreover, also, we have

$$\langle F_i^2 + F_i' \rangle_o \rightarrow \langle \ell_{Ei}^2 + \ell_{Ei}' \rangle_o = \int_{-\infty}^{\infty} w_{1E}'' dx_i = 0$$

here, with $\langle F_i^1 \rangle_o = -L_{1E:E}^{(2)} = -L_i^{(2)}$, cf. (A.4-11) et seq.

In the H_o-case, (A.4-16) from (A.4-13) reduces at once to

$$\langle g_{inc}\rangle_o = B'_{inc} + \frac{1}{2!}\sum_{ij}^{n}\langle\theta_i\theta_j\rangle L^{(1)}_{iF:E}\,\delta_{ij}\ . \tag{A.4-17}$$

The bias is now chosen according to (A.4-4), (μ=1), which from (A.4-16), (A.4-17) becomes directly, with terms $O(\langle\theta^6\rangle)$ omitted:

$$\hat{B}'_{inc} = -\frac{1}{2}\sum_{i}^{n}\langle\theta_i^2\rangle L^{(1)}_{iF:E} - \frac{1}{8}\sum_{ij}^{n}\langle\theta_i\theta_j\rangle^2 \cdot[\{\hat{L}^{(4)}_{iF:E} - 2L^{(2)^2}_{iF:E}\}\delta_{ij} + 2\,L^{(2)}_{iF:E}\,L^{(2)}_{jF:E}\,]. \tag{A.4-18}$$

From the optimal forms [cf. (A.4-16b) ff.] we see that (A.4-16) reduces at once to (A.1-20b), which is now exact since $B^{*'}_{inc}$ is calculated under H_o. The same observation holds for the coherent cases (A.4-11) under optimality ($F \to E$).

Our next step is to obtain the variances $\hat{\sigma}^2_{o,1}$, by appropriate modification of the results of Sec. A.2-2, according to the substitution (A.4-3) in (A.2-26)-(A.2-41). We indicate the results of (1)-(5) therein:

(1). ($i \neq k$):

$$\left\langle\left\langle(F_i^2+F_i')\right\rangle_1\left\langle(F_k^2+F_k')\right\rangle_1\right\rangle_\theta = \langle F_i^2+F_i'\rangle_o\langle F_k^2+F_k'\rangle_o + O(\langle\theta^4\rangle) \tag{A.4-19a}$$

(2). ($i=k$):

$$\left.\begin{aligned}\left\langle(F_i^2+F_i')^2\right\rangle_{1,\theta} &= \left\langle(F_i^2+F_i')^2\right\rangle_o + \frac{\langle\theta_i^2\rangle}{2}\int_{-\infty}^{\infty}(F_i^2+F_i')^2 w''_{1E}\,dx_i + O(\overline{\theta^4}) \\ &= \left\langle(F_i^2+F_i')^2\right\rangle_o + \frac{\langle\theta_i^2\rangle}{2}L^{(6)}_{F:E} + O(\overline{\theta^4})\ ,\end{aligned}\right\} \tag{A.9-19b}$$

where

$$L^{(4)}_{F:E} \equiv \left\langle (F^2+F')^2 \right\rangle_o \; ; \; L^{(6)}_{F:E} \equiv \int_{-\infty}^{\infty} (F^2+F')^2 w''_{1E} dx \; ; \tag{A.4-19c}$$

(3). $(i\neq j)\neq(k\neq \ell)$:

$$\left\langle F_i F_j F_k F_\ell \right\rangle_{1,\theta} = O(\overline{\theta^4}) \left\langle F'_i \right\rangle_o \left\langle F'_j \right\rangle_o \left\langle F'_k \right\rangle_o \left\langle F'_\ell \right\rangle_o . \tag{A.4-19d}$$

(4). $(i\neq j)$; $(k\neq \ell)$:

$$\text{(a)}. \quad \left\langle F_i^2 F_j F_\ell \right\rangle_{1,\theta} = \hat{L}^{(2)}_{iF:E} \left\langle \theta_j \theta_\ell \right\rangle L^{(2)}_{jF:E} \; L^{(2)}_{\ell F:E} + O(\overline{\theta^4}) \; ; \tag{A.4-20a}$$

$$\text{(b)}. \quad \left\langle F_i^2 F_j^2 \right\rangle_{1,\theta} = \hat{L}^{(2)}_{iF:E} \; \hat{L}^{(2)}_{jF:E} + O(\overline{\theta^4}) \; , \tag{A.4-20b}$$

where the number of terms is as indicated in (A.2-31), (A.2-32) above. We continue with (A.2-33)-(A.2-36):

(5a).

$$\left.\begin{aligned} \left\langle (F_i^2+F'_i) F_k F_\ell \right\rangle_{1,\theta} : \underline{k\neq\ell : i=k :} &= \left\langle \theta_i \theta_\ell \right\rangle \int_{-\infty}^{\infty} (F_i^2+F'_i) F_i w'_{1i} dx_i \int_{-\infty}^{\infty} F_\ell w'_{1\ell} dx_\ell + O(\overline{\theta^4}) \\ &= \left\langle \theta_i \theta_\ell \right\rangle L^{(2)}_{\ell F:E} \; \hat{L}^{(2,2)}_{iF:E} + O(\overline{\theta^4}) \; , \end{aligned}\right\} \tag{A.4-21}$$

where

$$\hat{L}^{(2,2)}_{iF:E} \equiv -\left\langle (F^3+F'F')' \right\rangle_o = -\left\langle 3F^2F' + F'^2 + FF'' \right\rangle_o = \int_{-\infty}^{\infty} (F_i^2+F'_i) F_i w'_{1i} dx_i . \tag{A.4-21a}$$

(5b). $k\neq\ell$: $i=\ell$:

$$\left\langle (F_i^2+F_i')F_iF_k\right\rangle_{1,\theta} = \left\langle \theta_i\theta_k\right\rangle L_k^{(2)}\hat{L}_{iF:E}^{(2,2)}+O(\overline{\theta^4}) \ . \tag{A.4-22}$$

(5c). $k\neq\ell$: $i\neq k\ (\neq\ell)$:

$$\left\langle (F_i^2+F_i')F_kF_\ell\right\rangle_{1,\theta} = \left\langle F_i^2L_{iF:E}^{(1)}+F_i'\right\rangle_0 \left\langle \theta_k\theta_\ell\right\rangle L_{k:F:E}^{(2)}L_{F:E}^{(2)} \ , \ [\ \overline{\theta} = \overline{\theta^3} = 0]$$

$$+ \frac{\left\langle \theta_i^2\theta_k\theta_\ell\right\rangle}{2}\hat{L}_{iF:E}^{(4)}L_{k:F:E}^{(2)}L_{F:E}^{(2)} \ . \tag{A.4-23}$$

Now we combine (A.4-19a)-(A.4-23) according to the above and the "counting" of (A.2-28)-(A.2-36):

$$\begin{aligned}\sum_{ijk\ell}^{n}\left\langle F_{ij}F_{k\ell}\right\rangle_{1,\theta} &= \sum_{ij}^{n}\left\langle \theta_i\right\rangle^2\left\langle \theta_j\right\rangle^2L_{iF:E}^{(1)}L_{jF:E}^{(1)} + \\ &+ \sum_{ij}^{n}\left\langle \theta_i\theta_j\right\rangle^2\{(L_{iF:E}^{(4)}-2\hat{L}_{iF:E}^{(2)^2})\delta_{ij}+2\hat{L}_{iF:E}^{(2)}\hat{L}_{jF:E}^{(2)}\} \\ &+ \sum_i\left\langle \theta_i^2\right\rangle^3\frac{L_{iF:E}^{(6)}}{2}+6\sum_{ij}\left\langle \theta_i^2\right\rangle\left\langle \theta_i\theta_j\right\rangle(L_i^{(2)}\hat{L}_j^{(2,2)})_{F:E} \\ &+ \sum_{ijk}^{i\neq j\neq k}[4\left\langle \theta_i\theta_j\right\rangle\left\langle \theta_j\theta_k\right\rangle\left\langle \theta_k\theta_i\right\rangle-2\left\langle \theta_i^2\right\rangle\left\langle \theta_j\theta_k\right\rangle^2] \\ &\cdot(\hat{L}_i^{(2)}L_j^{(2)}L_k^{(2)})_{F:E}+2\sum_{ik\ell}^{i\neq k\neq\ell}\left\langle \theta_i^2\right\rangle\left\langle \theta_k\theta_\ell\right\rangle^2 \\ &\cdot(L_i^{(1)}L_k^{(2)}L_\ell^{(2)})_{F:E}+O(\overline{\theta^8}) \ .\end{aligned} \tag{A.4-24}$$

Similarly, we have

$$\sum_{ijk\ell}^{n} \langle F_{ij} \rangle_{1,\theta} \langle F_{k\ell} \rangle_{1,\theta} = \sum_{ij}^{n} \left\{ \begin{array}{l} \langle \theta_i \theta_j \rangle^2 L^{(2)}_{iF:E} L^{(2)}_{jF:E} (1-\delta_{ij}) \\ \langle \theta_i^2 \rangle L^{(1)}_{iF:E} + \langle \theta_i^2 \rangle^2 L^{(4)}_{iF:E} \delta_{ij} \end{array} \right\}$$

$$\cdot \sum_{k\ell}^{n} \left\{ \begin{array}{l} \langle \theta_k \theta_\ell \rangle^2 L^{(2)}_k L^{(2)}_\ell)_{F:E} (1-\delta_{k\ell}) \\ \langle \theta_k \rangle^2 L^{(1)}_k + \langle \theta_k^2 \rangle^2 \hat{L}^{(4)}_{iF:E} \delta_{k\ell} \end{array} \right\} + O(\overline{\theta^6}) \ . \tag{A.4-25}$$

cf. (A.2-29). We need to investigate (A.4-13) for terms $O(\overline{\theta^4})$, in order to obtain terms $O(\theta^6)$ in (A.4-25). We have

$$\underline{O(\overline{\theta^4}):} \quad \frac{\langle \theta_i^4 \rangle}{4!} \int_{-\infty}^{\infty} (F_i^2 + F_i') w^{(")}_{1E}(x_i) dx_i \equiv \frac{\langle \theta_i^4 \rangle}{4!} \hat{L}^{(6)}_{iFiE} \ , \tag{A.4-26}$$

so that the contributions of (A.4-25) become

$$\sum_{ijk\ell}^{n} \langle F_{ij} \rangle_{1,\theta} \langle F_{k\ell} \rangle_{1,\theta} = \sum_{ik}^{n} \langle \theta_i^2 \rangle \langle \theta_k^2 \{ L^{(1)}_i L^{(1)}_k + 2 \langle \theta_i^2 \rangle \hat{L}^{(4)}_i L^{(1)}_k + O(\overline{\theta^4}) \}$$

$$+ O(\overline{\theta^8})_{i \neq j, k \neq \ell} \ . \tag{A.4-27}$$

Accordingly, since

$$\mathrm{var}_{1,\theta} g_{inc} = (\hat{\sigma}^2_{1\text{-}inc}) = \frac{1}{4} \sum_{ijk\ell}^{n} \{ \langle F_{ij} F_{k\ell} \rangle_{1,\theta} - \langle F_{ij} \rangle_{1,\theta} \langle F_{k\ell} \rangle_{1,\theta} \}, \text{ cf. (A.2-26)}, \tag{A.4-28a}$$

$$\hat{\sigma}^2_{1\text{-inc}} \doteq \frac{1}{4}\sum_{ij}^{n} \langle\theta_i\theta_j\rangle^2\{(L_i^{(4)}-2\hat{L}_i^{(2)^2})\delta_{ij}+2\hat{L}_i^{(2)}\hat{L}_j^{(2)}\}_{F:E}$$

$$+O(\overline{\theta^6}) \ , \qquad \text{(A.4-28b)}$$

and

$$\therefore\ \hat{\sigma}^2_{o\text{-inc}} = \frac{1}{4}\sum_{ij}^{n} \langle\theta_i\theta_j\rangle^2\{(L_i^{(4)}-2\hat{L}_i^{(2)^2})\delta_{ij}+2\hat{L}_i^{(2)}\hat{L}_j^{(2)}\}_{F:E}, \qquad \text{(A.4-29)}$$

exactly.

The "smallness" condition on the input signal (a_0) is determined by $\hat{\sigma}^2_{o\text{-inc}} \doteq \hat{\sigma}^2_{o\text{-inc}}$, which requires accordingly that terms $O(\overline{\theta^6})$ in $\hat{\sigma}^2_{1\text{-inc}}$ be much less than $\hat{\sigma}^2_{o\text{-inc}}$, as before, cf. (A.2-41). From (A.4-24), (A.4-27) we obtain specifically

$\hat{\sigma}^2_{1\text{-inc}} \doteq \hat{\sigma}^2_{o\text{-inc}}$:

$$\Big|\{\sum_{ij}\langle\theta_i^2\rangle\langle\theta_i\theta_j\rangle^2(\{\frac{L_i^{(6)}}{2}\}\delta_{ij}+6L_i^{(2)}\hat{L}_j^{(2,2)})+\sum_{ijk}^{i\neq j\neq k}[4\langle\theta_i\theta_j\rangle\langle\theta_j\theta_k\rangle\langle\theta_k\theta_i\rangle$$

$$-2\langle\theta_i^2\rangle\langle\theta_j\theta_k\rangle^2]L_i^{(2)}L_j^{(2)}L_k^{(2)}\}_{F:E}+2\sum_{ijk}^{i\neq j\neq k}\{\langle\theta_j\theta_k\rangle^2\langle\theta_i^2\rangle$$

$$\cdot L_j^{(2)}L_k^{(2)}L_{ik}^{(1)}-\langle\theta_i^2\rangle\langle\theta_j^2\rangle\langle\theta_k^2\rangle\hat{L}_k^{(4)}L_i^{(1)}\delta_{jk}\}_{F:E}\Big|$$

$$<<\sum_{ij}\langle\theta_i\theta_j\rangle^2[\{L_i^{(4)}-2\hat{L}_i^{(2)^2}\}\delta_{ij}+2\hat{L}_i^{(2)}\hat{L}_j^{(2)}]_{F:E}\ .$$

(A.4-30)

We can now parallel the coherent cases (A.4-12) and write

$$\frac{\langle g_{inc}\rangle_1 - \langle g_{inc}\rangle_o}{\sqrt{2}\,\hat{\sigma}_{o\text{-}inc}} \doteq \frac{(\frac{1}{4})\sum_{ij}^{n}\langle\theta_i\theta_j\rangle^2(\{\hat{L}_i^{(4)}-2L_i^{(2)^2}\}\delta_{ij}+2L_i^{(2)})_{F:E}}{\sqrt{2}\,[(\frac{1}{4})\sum_{ij}^{n}\langle\theta_i\theta_j\rangle^2(\{L_i^{(4)}-2\hat{L}_i^{(2)^2}\}\delta_{ij}+2\hat{L}_i^{(2)}\hat{L}_j^{(2)}]^{1/2}_{F:E}}$$

$$\equiv \frac{\sigma_{o\text{-}inc(F)}}{\sqrt{2}} \,. \qquad \text{(A.4-31a)}$$

(μ=1):

$$\frac{\langle g_{inc}\rangle_1}{\sqrt{2}\,\hat{\sigma}_{o\text{-}inc}} = \frac{-\langle g_{inc}\rangle_o}{\sqrt{2}\,\hat{\sigma}_{o\text{-}inc}}$$

$$\doteq \frac{(\frac{1}{8})\sum_{ij}^{n}\langle\theta_i\theta_j\rangle^2(\{\hat{L}_i^{(4)}-2L_i^{(2)^2}\}\delta_{ij}+2L_i^{(2)}L_j^{(2)})_{F:E}}{\sqrt{2}\,[(\frac{1}{4})\sum_{ij}^{n}\langle\theta_i\theta_j\rangle^2(\{L_i^{(4)}-2\hat{L}_i^{(2)^2}\}\delta_{ij}+2\hat{L}_i^{(2)}\hat{L}_j^{(2)})_{F:E}]^{1/2}}$$

$$\equiv \frac{\sigma_{o\text{-}inc(F)}}{2\sqrt{2}} \,, \qquad \text{(A.4-31b)}$$

which defines $\sigma_{o\text{-}inc}$ now. When (F→E), i.e. F→ℓ_E: the system is optimum, we have $\hat{L}_i^{(2)} = L_i^{(2)} = \langle \ell_o^2\rangle_o$; $\hat{L}^{(4)} = L_i^{(4)} = \langle(\ell_i^2+\ell_i')^2\rangle_o$; (also, $L_{E:E}^{(1)} = 0$), and $\sigma_{o\text{-}inc} \to \sigma^*_{o\text{-}inc}$, Eq. (A.2-40), cf. (A.4-39)-(A.4-36). Since $\hat{L}^{(2)}, \hat{L}^{(4)} \neq L^{(2)}, L^{(4)}$, etc., generally in the suboptimum cases, we have the more complicated but symmetrical forms above for $\sigma_{o\text{-}inc}$ ($\neq \hat{\sigma}_{o\text{-}inc}$). For the usual stationary régimes we simply drop the (i,j) subscripts on

the various L's, as before.

C. The Canonical Parameters $L^{(2)}, \hat{L}^{(2)}$, etc.: Robustness Formulations:

Our results above are quite general for these broad classes (A.4-1), (A.4-2) of suboptimum (threshold) detectors. They not only permit an examination of various linear and nonlinear detector elements. They also allow us to study the robustness [see, for example, [42]-[45]] of one type of detection algorithm, optimum in one class of interference, when employed against another, as noted earlier in Sec. 4.3 above.

Here we summarize the canonical parameters ($\hat{L}^{(2)}_{F:E}$, $L^{(4)}_{F:E}$, etc.) employed in both the structure of these algorithms and in the parameters of their performance measures, with an appropriate expansion of the notation to indicate the specific character of the suboptimum state involved. Thus, we write (for a particular $i^{\underline{th}}$ sample):

$L^{(\ )}_{F:D|E}$, etc: F refers to the basic detector data processing element, F(x), cf. (A.4-1,2); D|E denotes the D-class of noise parameters used in an E-class noise pdf. The E-class pdf represents the actual noise in which detection is taking place [cf. Sec. 4.3].

From A and B above we can write, remembering that F(x) = -F(-x):

(Eq. (A.4-16b):

$$L^{(1)}_{F:D|E} \equiv \langle F^2+F' \rangle_o = \int_{-\infty}^{\infty} [F(x)^2+F'(x)] w_{1E}(x|D)_o \, dx \; ; \tag{A.4-32}$$

Eq. (A.4-7e):

$$L^{(2)}_{F:D|E} \equiv -\langle F' \rangle_o = -\int_{-\infty}^{\infty} F(x)' w_{1E}(x|D)_o dx \tag{A.4-33a}$$

$$\hat{L}^{(2)}_{F:D|E} \equiv \langle F^2 \rangle_o = \int_{-\infty}^{\infty} F(x)^2 w_{1E}(x|D)_o \, dx \; ; \tag{A.4-33b}$$

Eq. (A.4-19c):

$$L^{(4)}_{F:D|E} \equiv \left\langle (F^2+F')^2 \right\rangle_o = \int_{-\infty}^{\infty} [F(x)^2+F'(x)]^2 w_{1E}(x|D)_o dx \; ; \qquad \text{(A.4-34a)}$$

Eq. (A.4-16b):

$$\hat{L}^{(4)}_{F:D|E} \equiv \left\langle (F^2+F')'' \right\rangle_o = \left.\begin{aligned} &\int_{-\infty}^{\infty} [F^2(x)+F'(x)] w''_{1E}(x|D)_o dx \; , \\ &= \int_{-\infty}^{\infty} (F^2+F')'' w_{1E}(x|D)_o \, dx \end{aligned}\right\} ; \qquad \text{(A.4-34b)}$$

Eq. (A.4-7c):

$$L^{(2,2)}_{F:D|E} \equiv 2\left\langle F'^2+FF'' \right\rangle_o = \int_{-\infty}^{\infty} F^2(x) w''_{1E}(x|D)_o dx \; ; \qquad \text{(A.4-35a)}$$

Eq. (A.4-21a):

$$\hat{L}^{(2,2)}_{F:D|E} \equiv -\left\langle (F^3+FF')' \right\rangle_o = \begin{pmatrix} -\int_{-\infty}^{\infty} [F(x)^3+F(x)F'(x)]' w_{1E}(x|D)_o dx \\ \int_{-\infty}^{\infty} (F^2+F')F w'_{1E} dx \end{pmatrix} ; \qquad \text{(A.4-35b)}$$

Eq. (A.4-19c):

$$L^{(6)}_{F:D|E} \equiv \left\langle (F^2+F')^{2''} \right\rangle_o = \int_{-\infty}^{\infty} [F^2(x)+F'(x)]^2 w''_{1E}(x|D)_o dx \; . \qquad \text{(A.4-36)}$$

To examine the "robustness" question, say, of using a detector algorithm which is optimum in Class A noise, when actually the interference is Class B and the Class A, B parameters are exact, for example, we have $F \to \ell_A(x)$, $E{:}w_{1B}$, etc., so that from (A.4-32), (A.4-33), etc.:

$$L^{(1)}_{F:D|E} \to L^{(1)}_{A:B} = \int_{-\infty}^{\infty} [\ell_A(x)^2+\ell'_A(x)] w_{1B}(x|B)_o dx \; ; \qquad \text{(A.4-37a)}$$

$$L^{(2)}_{F:D|E} \to L^{(2)}_{A:B} = \int_{-\infty}^{\infty} \ell'_A(x) w_{1B}(x|B)_o \, dx, \text{ etc.} \tag{A.4-37b}$$

Another robustness problem of interest arises when the correct operator is used, say a Class A operator (in Class A noise), but only necessarily inaccurate estimates (A') of the true Class A parameters are employed. Then, we have $F \to A'|A$: $F(x) \to \ell_A(x|A')$, and $w_{1E} \to w_{1A}(x|A)_o$:

$$\therefore L^{(1)}_{A'|A:A|A} = L^{(1)}_{A'|A:A} = \int_{-\infty}^{\infty} [\ell_A(x|A')^2 + \ell'_A(x|A')] w_{1A}(x|A)_o dx \text{ , etc.} \tag{A.4-38}$$

Still other possibilities can be constructed: Class A noise, with parameter estimates (A'), in Class B noise, with Class B parameter estimates (B'), e.g. $L^{(1)} \to L^{(1)}_{A'|A:B'|B}$, $F(x) \to \ell_A(x|A')$, $w_{1E} \to w_{1B}(x|B')_o$, etc. [Usually, however, we wish to refer the various suboptimum situations to the "true" or limiting population statistics, where the estimates A', B' become (some) "true" or limiting values.]

Finally, it is clear that when $F \to E$, i.e. $F(x) \to +\ell_E(x|E)$, for $w_{1E}(x|E)_o$, the above canonical parameters must reduce to the optimum (or LOBD) values. Thus, from (A.4-32)-(A.4-36) we get

$$L^{(1)}_{F:D\ E} \to L^{(1)}_{E:E} \equiv L^{(1)}_E = \int_{-\infty}^{\infty} [\ell_E(x)^2 + \ell'_E(x)] w_{1E} dx = \int_{-\infty}^{\infty} w''_{1E} dx = w'_{1E}\Big|_{-\infty}^{\infty} = 0 \tag{A.4-39}$$

$$\left\{ \begin{aligned} L^{(2)}_{F:D\ E} \to L^{(2)}_{E:E} &= -\int_{-\infty}^{\infty} \ell'_E(x) w_{1E} dx = -\int_{-\infty}^{\infty} \left(\frac{w'_1}{w_1}\right)'_E w_{1E} dx = -\int_{-\infty}^{\infty} \left(\frac{w''_1}{w_1} - \left(\frac{w'_1}{w_1}\right)^2\right)_E w_{1E} dx \\ &= 0 + \int_{-\infty}^{\infty} \ell_E^2 w'_{1E} dx = L^{(2)}_E = \left\langle \ell_E^2 \right\rangle_o ; \end{aligned} \right. \tag{A.4-40}$$

$$\hat{L}^{(2)}_{F:D\ E} \to \hat{L}^{(2)}_{E:E} = \int_{-\infty}^{\infty} \ell_E^2 w_1 dx = L^{(2)}_E; \tag{A.4-41}$$

$$\begin{cases} L^{(4)}_{F:D|E} \to L^{(4)}_{E:E} = \int_{-\infty}^{\infty} (\ell_E^2+\ell_E')^2 w_{1E}dx = \int_{-\infty}^{\infty} \left(\frac{w''_{1E}}{w_{1E}}\right)^2 w_{1E}dx \equiv L_E^{(4)}, \text{ cf.(A.1-19b)} \\ \hat{L}^{(4)}_{F:D|E} \to \hat{L}^{(4)}_{E:E} = \int_{-\infty}^{\infty} (\ell_E^2+\ell_E')w''_{1E}dx = \int_{-\infty}^{\infty} \left(\frac{w''_{1E}}{w_1}\right)_E \left(\frac{w''_{1E}}{w_{1E}}\right) w_{1E}dx = L_E^{(4)} \end{cases} \quad \text{(A.4-42)}, \text{(A.4-43)}$$

$$\begin{cases} L^{(2,2)}_{F:D|E} \to L^{(2,2)}_{E:E} = \int_{-\infty}^{\infty} \ell_E^2 w''_{1E}dx = \int_{-\infty}^{\infty} \left(\frac{w_{1E}}{w_{1E}}\right)^2 \left(\frac{w''_{1E}}{w_{1E}}\right) w_{1E}dx = L_E^{(2,2)} = 2\langle \ell_E^4 \rangle, \\ \qquad\qquad \text{cf. (A.2-16a)} , \qquad\qquad \text{(A.4-44)} \\ L^{(2,2)}_{F:D|E} \to L^{(2,2)}_{E:E} = \int_{-\infty}^{\infty} (\ell_E^2+\ell_E')\ell_E w'_{1E}dx = \int_{-\infty}^{\infty} \left(\frac{w''_{1E}}{w_{1E}}\right)\left(\frac{w'_{1E}}{w_{1E}}\right)^2 w_{1E}dx = L_E^{(2,2)} = 2\langle \ell_E^4 \rangle, \end{cases}$$

(A.4-45)

$$L^{(6)}_{F:D|E} \to L^{(6)}_{E:E} = \int_{-\infty}^{\infty} \left(\frac{w''_1}{w_1}\right)^2_E \left(\frac{w''_{1E}}{w_{1E}}\right) w_{1E}dx = \int_{-\infty}^{\infty} \left(\frac{w''_1}{w_1}\right)^3_E w_{1E}dx = L_E^{(6)},$$

cf. (A.2-29b). (A.4-46)

D. Optimum Distributions for Specified Detector Nonlinearities:

The question here is, given a (threshold) detector structure (A.4-1,2,3), e.g., given F(x), what is the pdf, $w_{1F}(x|F)_o$ for which these detector algorithms are optimum, i.e. are LOBD's and AODA's jointly. This is easily established formally from (A.4-3), since

$$F(x) = \ell_F(x) = \frac{d}{dx} \log w_{1F}(x|F)_o \ , \ (-\infty < x < \infty) \ , \qquad \text{(A.4-47)}$$

which is readily integrated to

$$\boxed{w_{1F}(X|F)_o = Ae^{B\int F(x)dx} = AE^{BG(x)}} \ ; \ A = \int_{-\infty}^{\infty} e^{B\int F(x)dx} dx, \ (A,B > 0), \qquad \text{(A.4-48)}$$

with A the normalizing constant, since w_{1F} is a proper pdf, e.g. $w_{1F} \geq 0$, $w_{1F}(\pm\infty) = 0$ (fast enough that) $\int_{-\infty}^{\infty} w_{1F} dx = 1$. The constant B is chosen to insure that $x^2 = 1$, i.e. x is normalized to the mean intensity $\langle X^2 \rangle$. We remember that $F(x) = -F(-x) = -F(|x|)$, $x < 0$, so that $\int F(x)dx \equiv G(x)$ $[=G(-x)] \leq 0$, all $(-\infty < x < \infty)$, i.e. G is negative, even. We also require that $\lim_{|x| \to \infty} G(x) \to -\infty$ at least as fast as $\log |x|^{1+\eta}$, $\eta > 0+$, so that $\int_{-\infty}^{\infty} (\exp G)dx < \infty$, i.e. $(0<)A < \infty$.

Let us consider two simple but important examples:

(i). $F(x) = -x$: a (simple) correlation detector (A.4-49a)

(ii). $F(x) = -\sqrt{2}\ \mathrm{sgn}\ x$: a "super-clipper" [46] or hard limiter (normalized in accordance with (A.4-50b)). (A.4-49b)

[Other detector characteristics are handled in the same way, cf. [43], [44].] Applying (A.4-49a,b) to (A.4-48) gives directly

(Correlators):

$$w_{1F}(x|F)_o = \frac{1}{\sqrt{2\pi}} e^{-x^2/2} \quad ; \ (\overline{x^2}=1 \text{ (by original normalization)}); \quad A=1/\sqrt{2\pi}\ ,\ B=1\ ; \qquad \text{(A.4-50a)}$$

("superclippers"):

$$w_{1F}(x|F)_o = \frac{1}{\sqrt{2}} e^{-|x|\sqrt{2}} \quad (\overline{x^2}=1, \text{ as required: } A = 1/\sqrt{2},\ B = \sqrt{2}). \qquad \text{(A.4-50b)}$$

As we expect, the optimum noise for correlators in threshold detection is gaussian, while for the "super-clipper" it turns out to be "Laplace" noise, cf. (A.4-50b), [a result obtained by the author about 1967 in ONR studies]. (Note that the addition of a gaussian component in Case (ii), (A.4-49b),

destroys the optimality of the super-clipper.)

Finally, if F is not available but $H(x_i,s_j)$ is specified, we can find F(x) from the fact that $H(x_i,x_i) \equiv h(x_i)^2$ and the consequent Riccati equation from (A.4-3b):

$$F^2(x) + F'(x) = h(x)^2 \ . \tag{A.4-51}$$

For F one solves the associated equation ([41], Sec. 2.15, p. 24)

$$u''(x) - h^2(x)u = 0; \text{ where } F = u'/u \ , \tag{A.4-52}$$

at all non-singular points (of u, u',u") in $-\infty < x < \infty$.

A.4-2. Suboptimum Detectors, I: Simple Correlators and Energy Detectors:

In these important cases, which we have already shown to be LOBD when the interference is gaussian, cf. Sec. A.1-3, we see at once from (A.1-24,25) that in (A.4-1,2) we set

$$F(x) = -x \ ; \ \therefore F' = -1 \quad , \tag{A.4-53}$$

and accordingly from (A.4-32)-(A.4-36) we have for the associated structure and performance parameters (the L's):

$$\begin{aligned} L^{(1)}_{F:E} &= \langle x^2-1 \rangle_o = \overline{x^2}-1 = 0, \text{ cf. (A.4-50a)} \ ; \\ L^{(2)}_{F:E} &= \langle 1 \rangle_o = 1 \ ; \\ \hat{L}^{(2)}_{F:E} &= \langle x^2 \rangle_o = 1 \ ; \\ L^{(4)}_{F:E} &= \langle (x^2-1)^2 \rangle_o = \overline{x^4} - 2\overline{x^2} + 1 = \overline{x^4}-1 \ ; \end{aligned} \tag{A.4-54}$$

$$\hat{L}^{(4)}_{F:E} = \left\langle (x^2-1)'' \right\rangle_o = \left\langle 2 \right\rangle_o = 2 \ ;$$

$$L^{(2,2)}_{F:E} = 2\left\langle 1 \right\rangle_o = 2 \ ; \ \hat{L}^{(2,2)}_{F:E} = -\left\langle (-x^3+x)' \right\rangle_o = \left\langle 3x^2-1 \right\rangle_o = 2;$$

$$L^{(6)}_{F:E} = \left\langle (x^2-1)^{2''} \right\rangle_o = \left\langle 12x^2-4 \right\rangle_o = 8. \qquad \text{(A.4-54) (cont'd.)}$$

Substituting (A.4-53,54) into A.4-1,2; and [A.4-11, A.4-18 for the biases], we get at once

$$B'_{coh} = \log \mu - \frac{1}{2}\sum_i^n \left\langle \theta_i \right\rangle^2 \ ; \ B'_{inc} = \log \mu - \frac{1}{4}\sum_{ij}^n \left\langle \theta_i \theta_j \right\rangle^2 \ ; \qquad \text{(A.4-55)}$$

cross-correlators:

$$g(\underset{\sim}{x})_{coh} = \{\log \mu - \frac{1}{2}\sum_i^n \left\langle \theta_i \right\rangle^2\} + \sum_i^n \left\langle \theta_i \right\rangle x \ ; \qquad \text{(A.4-56a)}$$

auto-correlators:

$$g(\underset{\sim}{x})_{inc} = \log \mu - \frac{1}{4}\sum_{ij}^n \left\langle \theta_i \theta_j \right\rangle^2 + \frac{1}{2!}\sum_i^n (x_i x_j - \delta_{ij})\left\langle \theta_i \theta_j \right\rangle \ ,$$

$$= \{\log \mu - \frac{1}{2}\sum_i^n \left\langle \theta_i^2 \right\rangle - \frac{1}{4}\sum_{ij}^n \left\langle \theta_i \theta_j \right\rangle^2\} + \frac{1}{2!}\sum_{ij}^n \left\langle \theta_i \theta_j \right\rangle x_i x_j \ , \qquad \text{(A.4-56b)}$$

which are precisely our previously derived results (A.1-23), (A.1-24), respectively, for the LOBD's here in gaussian noise.

In the same way, we obtain $\hat{\sigma}_o$ from (A.4-9), (A.4-29), viz.:

$$\hat{\sigma}^2_{o\text{-}coh} \doteq \sum_i^n \left\langle \theta_i \right\rangle^2; \ \hat{\sigma}^2_{o\text{-}inc} \doteq \frac{1}{4}\sum_{ij}^n \left\langle \theta_i \theta_j \right\rangle^2 \{(\overline{x_i^4}-3)\delta_{ij}+2\}, \qquad \text{(A.4-57)}$$

and $\sigma_{o\text{-}(\ )}$ from (A.4-12), and (A.4-31), viz.:

$$\sigma_{o\text{-coh}} \doteq \{\sum_{i}^{n} \langle\theta_i\rangle^2\}^{1/2} \ ; \tag{A.4-58a}$$

$$\sigma_{o\text{-inc}} \doteq \sum_{ij}^{n}\langle\theta_i\theta_j\rangle^2 / (\sum_{ij}^{n}\langle\theta_i\theta_j\rangle^2\ [(\overline{x_i^4}-3)\delta_{ij}+2])^{1/2} \ . \tag{A.4-58b}$$

[Generally $\overline{x_i^4} \geq 1$, so that all variances are positive as required.]

The conditions (A.4-10), (A.4-30) on the maximum "small" values of a_o (>0) permitted to insure $\hat{\sigma}_1^2 \doteq \hat{\sigma}_o^2$ are:

coherent: ($\hat{\sigma}_o^2=\sigma_o^2$):

$$|\sum_{ij}^{n}\langle\theta_i\theta_j\rangle[\langle\theta_i\theta_j\rangle-\langle\theta_i\rangle\langle\theta_j\rangle] \ / \ \sum_{i}^{n}\langle\theta_i\rangle^2 << 1; = 0<<1; \ \langle\theta_i\theta_j\rangle=\langle\theta_i\rangle\langle\theta_j\rangle.$$

Incoherent:

$$|\sum_{ij}^{n}\langle\theta_i^2\rangle\langle\theta_i\theta_j\rangle^2+\sum_{ijk}^{i\neq j\neq k}\{4\langle\theta_i\theta_j\rangle\langle\theta_j\theta_k\rangle\langle\theta_k\theta_i\rangle-2\langle\theta_i^2\rangle\langle\theta_j\theta_k\rangle^2\}$$

$$<< \sum_{ij}^{n}\langle\theta_i\theta_j\rangle^2\{(\overline{x_i^4}-3)\delta_{ij}+2\}.$$

A. The Energy Detector:

The energy detector is a special case of (A.4-2), where now we set

$$F_i \rightarrow F_{ij} = -x_i\delta_{ij} \tag{A.4-60}$$

in (A.4-2), since the energy detector is physically a quadratic device with no memory. We write from (A.4-3b), accordingly

$$g(\underset{\sim}{x})_{inc} = \log \mu + \hat{B}'_{inc} + \frac{1}{2!}\sum_{i}^{n} \langle \theta_i^2 \rangle (x_i^2 - 1) \ , \qquad \text{(A.4-61a)}$$

where the proper bias $\hat{B}'_{inc}$, is from (A.4-18) and (A.4-54), (j=i) now

$$\hat{B}'_{inc} \doteq -\frac{1}{4}\sum_{i}^{n} \langle \theta_i^2 \rangle^2 \ , \qquad \text{(A.4-61b)}$$

so that we can rewrite (A.4-61a) in the equivalent form

$$g(\underset{\sim}{x})_{inc}\Big|_{energy} = \{\log \mu - \frac{1}{2}\sum_{i}^{n}\langle \theta_i^2 \rangle - \frac{1}{4}\sum_{i}^{n} \langle \theta_i^2 \rangle^2\} + \frac{1}{2}\sum_{i}^{n} \langle \theta_i^2 \rangle x_i^2 \ . \qquad \text{(A.4-61c)}$$

The variances $\hat{\sigma}^2_{o\text{-}inc}$ and σ_o^2 are (from (A.4-57), (A.4-58b), on setting $2 \to 2\delta_{ij}$:

$$\hat{\sigma}^2_{o\text{-}inc} \doteq \frac{1}{4}\sum_{i}^{n} \langle \theta_i^2 \rangle (\overline{x_i^4} - 1) \ ; \ \sigma_{o\text{-}inc} \doteq \sum_{i}^{n} \langle \theta_i^2 \rangle^2 / \{\sum_{i}^{n} \langle \theta_i^2 \rangle^2 (\overline{x_i^4} - 1)\}^{1/2} \ . \qquad \text{(A.4-62)}$$

The controlling condition on the maximum value of the input signal, for which $\hat{\sigma}_1^2 \doteq \hat{\sigma}_o^2$, cf. (A.4-30), becomes from (A.4-60) therein:

$$\underline{\hat{\sigma}_1^2 \doteq \hat{\sigma}_o^2}: \quad 4\sum_{i}^{n} \langle \theta_i^2 \rangle^3 / \sum_{i}^{n} \langle \theta_i^2 \rangle^2 (\overline{x_i^4} - 1) << 1. \qquad \text{(A.4-63)}$$

Finally, we observe that for correlators (of which the energy detector is a special case) in the threshold regime, only the fourth-order moments $(\overline{x_i^4})$

(relative to the intensity $\langle X^2 \rangle$, e.g. $\overline{x^2} = 1$) are significant, because of the fundamentally second-order ($\sim x_i x_j$) nonlinearities of the detectors, cf. (A.4-61a). This is in sharp contrast with optimum detectors (LOBD's), which operate against the whole noise pdf (i.e. all moments, when they exist), via $F \to \ell_F(x)$. From the fact that only x_i^4 appears in the argument ($\sim\hat{\sigma}_{o\text{-}inc}$) of the probability measures of performance, rather than the appropriate functional of the entire pdf, indicates that performance of correlation detectors can be very suboptimum vis-à-vis the LOBD's appropriate to the noise in question, as is, of course, well-known [cf. [1a,b], [13], [33], [34] for the original work, employing empirically established statistical-physical models of the real-world EMI environment, cf. Sec. 3.]

A.4-3 Suboptimum Detectors II: Hard Limiters ("Super-clippers" and "Clipper-Correlators"):

Here the detector characteristic is given by (A.4-49b), viz., $F = -\sqrt{2}\ \mathrm{sgn}\ x$, and $\therefore F' = -2\sqrt{2}\ \delta(x-o)$, where the factor 2 represents the weight (2) of the jump at x=0, for the superclipper. From (A.4-39)-(A.4-46) we obtain accordingly (remembering that F is odd and w_{1E} is even) when $F \neq E$:

$$L_{F:E}^{(1)} = \int_{-\infty}^{\infty} [2(\mathrm{sgn}\ x)^2 - \sqrt{2}\ \mathrm{sgn}'x] w_{1E} dx = \{2 - \int_{-\infty}^{\infty} 2\sqrt{2}\ \delta(x-o) w_{1E} dx\}$$

$$= 2(1 - \sqrt{2}\ w_{1E}(0)) \ ; \qquad \text{(A.4-64)}$$

and

$$L_{F:E}^{(2)} = \int_{-\infty}^{\infty} 2\sqrt{2}\ \delta(x-o) w_{1E} dx = 2\sqrt{2}\ w_{1E}(0) \ ; \ \hat{L}_{F:E}^{(2)} = \int_{-\infty}^{\infty} 2\ \mathrm{sgn}^2 x w_{1E} dx = 2 \ ; \qquad \text{(A.4-65a)}$$

$$L_{F:E}^{(4)} = \int_{-\infty}^{\infty} [2(\mathrm{sgn}\ x)^2 - 2\sqrt{2}\delta(x-o)]^2 w_{1E} dx = 4 + 8\delta(x-o) w_{1E}(0) \ ; \ (\mathrm{sgn}\ 0 = 0); \qquad \text{(A.4-65b)}$$

$$\hat{L}^{(4)}_{F:E} = \int_{-\infty}^{\infty}[(\operatorname{sgn} x)^2 - 2\sqrt{2}\,\delta(x-0)]w''_{1E}dx = 0 - 2\sqrt{2}\,w''_{1E}(0); \quad |<\infty| \quad ; \qquad \text{(A.4-65c)}$$

$$L^{(2,2)}_{F:E} = \int_{-\infty}^{\infty} 2\,\operatorname{sgn}^2 x \cdot w''_{1E}(x)dx = \int_{-\infty}^{\infty} w''_{1E}(x)dx = 0 \quad ; \qquad \text{(A.4-65d)}$$

$$\hat{L}^{(2,2)}_{F:E} = -\int_{-\infty}^{\infty}\sqrt{2}[2\operatorname{sgn}^2 x - 2\sqrt{2}\,\delta(x-o)]\operatorname{sgn} x \cdot w'_{1E}(x)dx = 4\sqrt{2}\int_0^{\infty} w'_{1E}(x)dx - 0$$

$$= 4\sqrt{2}\,w_{1E}(0); \qquad \text{(A.4-65e)}$$

$$L^{(6)}_{F:E} = \int_{-\infty}^{\infty}[2\,\operatorname{sgn}^2 x - 2\sqrt{2}\,\delta(x-o)]^2 w''_{1E}(x)dx = 0 - 0 + 8\delta(x-o)w''_{1E}(0)\ . \qquad \text{(A.4-65f)}$$

[When F=E: i.e. $w_{1E}(x)$ is given by (A.4-50b), we have the optimum case in which the receiver is "matched" to the (Laplacian) noise, and we use (A.4-39)-(A.4-46) for the parameters.]

In this case we must discard the singular component of detector structure and of any $L_{F:E}$ [which occurs here when x = 0] when we apply the above results both to the detection algorithm and the evaluation of performance. This is to ensure that detection on a finite sample ($n<\infty$) is not perfect in the presence of finite (positive) noise intensity. Of course, physically, the "super-limiter" characteristic $F(x) = -\sqrt{2}\,\operatorname{sgn} x$) is a mathematical idealization: in actual practice one uses a processing element where $|F'(x)| < \infty$, i.e., there are no infinite slopes, and hence no singularities in the structure or the assocated performance parameters. Accordingly, with the above in mind, we may substitute (A.4-64),(A.4-65) into (A.4-1,2), and (A.4-11,18) for the bias to get

$$B'_{coh} = \log \mu - \sqrt{2}\sum_i^n \langle\theta_i\rangle^2 w_{1E}(o)_i \ ; \qquad \text{(A.4-66a)}$$

$$B'_{inc} = \log \mu - \sum_{i}^{n} \langle \theta_i^2 \rangle (1-\sqrt{2}\, w_{1E}(0)_i) - \frac{1}{4} \sum_{ij}^{n} \langle \theta_i \theta_j \rangle^2 [8 w_{1E}(0)_i w_{1E}(0)_j$$

$$- \{\sqrt{2}\, w''_{1E}(0)_i + 8 w_{1E}(0)_i^2\} \delta_{ij}] \ , \qquad \text{(A.4-66b)}$$

and the algorithms for coherent and incoherent detection, respectively, are thus

coherent:

$$g(\underset{\sim}{x})_{coh} = \{\log \mu - \sqrt{2} \sum_{i}^{n} \langle \theta_i \rangle^2 w_{1E}(0)_i\} + \sqrt{2} \sum_{i}^{n} \langle \theta_i \rangle \operatorname{sgn} x_i \ , \qquad \text{(A.4-67a)}$$

incoherent:

$$g(\underset{\sim}{x})_{inc} = B'_{inc}\Big|_{\text{Eq.(A.4-66b)}} + \sum_{ij}^{n} \langle \theta_i \theta_j \rangle \operatorname{sgn} x_i \operatorname{sgn} x_j \ , \qquad \text{(A.4-67b)}$$

this last where we have omitted the singular term $F'_i \delta_{ij} = -2\delta(x-o)$, which is zero (all $x \neq o$), for the reasons cited above. These algorithms (A.4-67a,b) represent "clipper-correlators": the former a clipper crosscorrelator, the latter, a clipper autocorrelator.

In a similar way we obtain the various $\hat{\sigma}_o$ [from (A.4-9,29)] and σ_o [from (A.4-12-31)], viz.:

$$\hat{\sigma}^2_{o\text{-}coh} \doteq 2 \sum_{i}^{n} \langle \theta_i \rangle^2 \ ; \ \hat{\sigma}^2_{o\text{-}inc} \doteq \sum_{ij}^{n} \langle \theta_i \theta_j \rangle^2 (2-\delta_{ij}) \ , \qquad \text{(A.4-68)}$$

and

$$\sigma_{o\text{-}coh} \doteq 2 \sum_{i}^{n} \langle \theta_i \rangle^2 w_{1E}(0)_i / \Big(\sum_{i}^{n} \langle \theta_i \rangle^2 \Big)^{1/2} \ ; \qquad \text{(A.4-69a)}$$

$$\sigma_{o\text{-inc}} \doteq \frac{\sum_{ij}^{n} \langle \theta_i \theta_j \rangle^2 \{8 w_{1E}(0)_i w_{1E}(0)_j - [\sqrt{2}\, w''_{1E}(0)_i + 8 w_{1E}(0)_i^2]\delta_{ij}\}}{2\{\sum_{ij}^{n} \langle \theta_i \theta_j \rangle^2 (2-\delta_{ij})\}^{1/2}} . \qquad \text{(A.4-69b)}$$

[Since $w''_{1E}(0)_i \leq 0$, $w_{1E}(0)_i > 0$, we see that $\sigma_{o\text{-coh}}$, $\sigma_{o\text{-inc}}$ are always positive, as are $\hat{\sigma}_{o\text{-coh}}$, $\hat{\sigma}_{o\text{-inc}}$, as required for proper variances.]

The conditions (A.4-10), (A.4-30) on the maximum allowed values of the (small) input signal (a_o), to insure $\hat{\sigma}_1^2 \doteq \hat{\sigma}_o^2$ are specifically here

coherent:

$$4 \sum_i \langle \theta_i \rangle^4 w_{1i}(0)_E^2 << \sum_i \langle \theta_i \rangle^2, \qquad \text{(A.4-70a)}$$

when $\langle \theta_i \theta_j \rangle = \langle \theta_i \rangle \langle \theta_j \rangle$ in these coherent cases. We have also

incoherent:

$$\Big| \{ \sum_{ij}' 6 \langle \theta_i^2 \rangle \langle \theta_i \theta_j \rangle^2 w_{1E}(0)_i w_{1E}(0)_j + \sum_{ijk}^{i\neq j\neq k} [w_{1E}(0)_j w_{1E}(0)_k \langle \theta_j \theta_k \rangle$$

$$\cdot \{16 \langle \theta_i \theta_j \rangle \langle \theta_k \theta_i \rangle + 16 \langle \theta_j \theta_k \rangle \langle \theta_i^2 \rangle (1-\sqrt{2}\, w_{1E}(0)_i)\}$$

$$+ 4\sqrt{2} \langle \theta_i^2 \rangle \langle \theta_j^2 \rangle \langle \theta_k^2 \rangle w''_{1E}(0) \{1-\sqrt{2}\, w_{1E}(0)_i\} \delta_{ij}] \Big|$$

$$<< 4 \sum_{ij}^{n} \langle \theta_i \theta_j \rangle^2 (2-\delta_{ij}). \qquad \text{(A.4-70b)}$$

Unlike the (suboptimum) correlation detectors of Sec. A.4-2 above, these clipper-correlators, (A.4-67), are considerably closer to the optimum [42]-[45], because much more than the (second and) fourth moments of the pdf of the interference is employed, viz. the "zero-crossings" of the noise (and signal) via the $\{\text{sgn } x_i\}$. This fact is also exhibited in the arguments of the probability measures of performance, namely (A.4-69a,b) specifically when our real-world noise models (cf. Sec. 3) are employed.

A.4-4 Binary Signals:

The algorithms for binary signals employing suboptimum detectors of Class (A.4-1,2,3) above are readily obtained from the general relations (2.13)-(2.17), esp. (2.15), (2.16). These relations, in turn, are specialized to the important special subclasses of simple correlators [Sec. (A.4-21)] and clipper-correlators [Sec. A.4-3], as given in Sec. 4.2 above. In general, we replace $\langle\theta_i\rangle$ by $\Delta\theta_i^{(21)}$ $(= \langle\theta_i^{(2)}\rangle - \langle\theta_i^{(1)}\rangle$, and $\langle\theta_i\theta_j\rangle$ by $\Delta^{(21)}\theta_i\theta_j = \langle(\theta_i\theta_j)^{(2)}\rangle - \langle(\theta_i\theta_j)^{(1)}\rangle \equiv \Delta\rho_{ij}^{(21)}$ etc., in the "on-off" results. Thus, we have, for these binary signal cases:

A. Simple Correlators:

Eq. (A.4-57):

$$\hat{\sigma}^{(21)2}_{\text{o-coh}} \doteq \sum_i^n \left(\langle\theta_i^{(2)}\rangle - \langle\theta_i^{(1)}\rangle\right)^2; \quad \hat{\sigma}^2_{\text{o-inc}} \doteq \frac{1}{4}\sum_{ij}^n \left[\langle(\theta_i\theta_j)^{(2)}\rangle^2 - \langle(\theta_i\theta_j)^{(1)}\rangle^2\right]$$

$$\cdot\{(\overline{x_i^4}-3)\delta_{ij}+2\}, \quad \left[\langle\theta_i\theta_j\rangle^{(2)} = \langle a_{oi}^{(2)} a_{oj}^{(2)}\rangle \rho_{ij}^{(2)}, \text{ etc.}\right]; \tag{A.4-71}$$

Eqs. (A.4-58):

$$\sigma^{(21)}_{\text{o-coh}} \doteq \left\{\sum_i^n \left(\langle\theta_i^{(2)}\rangle - \langle\theta_i^{(1)}\rangle\right)^2\right\}^{1/2};$$

$$\sigma^{(21)}_{o\text{-}inc} \doteq \sum_{ij}^{n}[\langle(\theta_i\theta_j)^{(2)}\rangle-\langle(\theta_i\theta_j)^{(1)}\rangle]^2/(\sum_{ij}^{n}[\langle(\theta_i\theta_j)^{(2)}\rangle-\langle(\theta_i\theta_j)^{(1)}\rangle]^2$$

$$\cdot\{(\overline{x_i^4}-3)\delta_{ij}+2\})^{1/2} \ . \qquad \text{(A.4-72b)}$$

The "smallness" conditions on the input signals $(a_o^{(1)},a_o^{(2)})$, permitting $\hat{\sigma}_1^2 \doteq \hat{\sigma}_o^2$, are obtained directly from (A.4-59), on making the substitutions indicated above, viz. $\langle\theta_i\rangle \to \langle\Delta\theta_i\rangle = \langle\theta_i^{(2)}\rangle-\langle\theta_i^{(1)}\rangle$, $\langle\theta_i\theta_j\rangle \to \rho_{ij}^{(2)}-\rho_{ij}^{(1)} \equiv \Delta\rho_{ij}^{(21)}$, etc., with $\langle\theta_i^2\rangle \to \langle\theta_i^{(2)}\theta_j^{(2)}\rangle$, and $\langle\theta_i^{(1)}\theta_j^{(1)}\rangle$, $\langle\theta_k\theta_i\rangle \to \langle\theta_k^{(2)}\theta_i^{(2)}\rangle$ etc., in (A.4-59b), cf. (A.2-57).

B. ("Super") Clipper-Correlators:

Eq. (A.4-68):

$$\hat{\sigma}^{(21)2}_{o\text{-}coh} \doteq 2\sum_{i}^{n}[\langle\theta_i^{(2)}\rangle - \langle\theta_1^{(1)}\rangle)^2; \ \hat{\sigma}^2_{o\text{-}inc} \doteq \sum_{ij}^{n}(\langle(\theta_i\theta_j)^{(2)}\rangle-\langle(\theta_i\theta_j)^{(1)}\rangle)^2\{2-\delta_{ij}\} \ ; \qquad \text{(A.4-73)}$$

Eq. (A.4-69):

$$\sigma^{(21)}_{o\text{-}coh} \doteq 2\sum_{i}^{n}[\langle\theta_i^{(2)}\rangle-\langle\theta_i^{(1)}\rangle]\, w_{1E}(0)_i/\{\sum_{i}^{n}(\langle\theta_i^{(2)}\rangle-\langle\theta_i^{(1)}\rangle)^2\}^{1/2} \ ; \qquad \text{(A.4-74a)}$$

$$\sigma^{(21)}_{o\text{-}inc} \doteq \frac{\sum_{ij}^{n}(\langle(\theta_i\theta_j)^{(2)}\rangle-\langle(\theta_i\theta_j)^{(1)}\rangle)^2\{8w_{1E}(0)_i w_{1E}(0)_j-[\sqrt{2}\ w''_{1E}(0)_i+8w_{1E}(0)_i^2]\delta_{ij}\}}{2\{\sum_{ij}^{n}(\langle(\theta_i\theta_j)^{(2)}\rangle-\langle(\theta_i\theta_j)^{(1)}\rangle)^2(2-\delta_{ij})\}^{1/2}} \ .$$

(A.4-74b)

Again, for the "smallness" condition on the input signals $(a_o^{(1)},a_o^{(2)})$ we make the indicated substitutions, $\langle\theta_i\rangle \to \langle\theta_i^{(2)}\rangle-\langle\theta_j^{(1)}\rangle$, $\langle\theta_i\theta_j\rangle^2 \to \langle(\theta_i\theta_j)^{(2)}\rangle^2 - \langle(\theta_i\theta_j)^{(1)}\rangle^2$, etc., in (A.4-70a,b) above. [Specifically, for (A.4-70b) we

replace $\langle \theta_i^2 \rangle$ by $\langle \theta_i^{(2)} \theta_j^{(2)} \rangle$, $\langle \theta_i^{(1)} \theta_j^{(1)} \rangle$ and $\langle \theta_k \theta_i \rangle$ by $\langle \theta_k^{(2)} \theta_i^{(2)} \rangle$, $\langle \theta_k^{(1)} \theta_i^{(1)} \rangle$;
$\langle \theta_i \theta_j \rangle^2 \to \Delta\rho_{ij}^{(21)2}$ etc., cf. (A.2-57).]

APPENDIX A5

$\hat{Q}_n^{(21)}$, $\hat{B}_n^{(21)*}$, $R_n^{(21)*}$ for Incoherent Reception with Binary Symmetric Channels

For binary symmetric channels ($a_o^{(2)}=a_o^{(1)}=a_o$; $p_1=p_2=1/2$) we need to evaluate $\hat{Q}_n^{(21)}$, which appears in the processing gain, and $\hat{B}_n^{(21)*}$, the associated bias, cf. Table 6.1b. We also need $R_n^{(21)*}$, (A.2-61b), to help establish the upper bounds on input signal size (and the equality of $\sigma_{1n}^{(21)*} \doteq \sigma_{on}^{(21)*}$). We shall do this for the basic type of common binary signals: sinusoids of different frequencies, cf. (7.3a), when there is either no fading or slow fading (e.g., $m_{ij} = 1$, cf. (7.7)), in the stationary noise regimes.

The quantities to be evaluated are:

$$\hat{Q}_n^{(21)}{}_{-1} \equiv n^{-1} \sum_{ij}{}' [\rho_{ij}^{(2)}-\rho_{ij}^{(1)}]^2 = \frac{1}{n} \sum_{ij}^{n} [\rho_{ij}^{(2)}-\rho_{ij}^{(1)}]^2 \; ; \tag{A.5-1}$$

$$\hat{B}_n^{(21)*} \equiv -\frac{\overline{a_o^2}^2}{8} \sum_{ij} (\rho_{ij}^{(2)2}-\rho_{ij}^{(1)2})[(L^{(4)}-2L^{(2)2})\delta_{ij}+2L^{(2)2}] \; , \tag{A.5-2}$$

where

$$\rho_{ij}^{(1),(2)} = \langle s_i^{(1),(2)} s_j^{(1),(2)} \rangle = \cos \omega_{o1,o2} (t_i-t_j). \tag{A.5-3}$$

Let us examine $\hat{Q}_n^{(21)}$ and use $T = n\Delta t$; $t_i = i\Delta t = x$, etc., so that we have to a good approximation:

$$\hat{Q}_n^{(21)}{}_{-1} \approx \frac{n}{T^2} \iint_0^T [\cos \omega_{o2}(x-y)-\cos\omega_{o1}(x-y)]^2 dxdy$$

$$= \frac{n}{4T^2} \iint_{-T}^{T} [\cos\omega_{o2}(x-y)-\cos \omega_{o1}(x-y)]^2 dxdy$$

$$= \frac{n}{2T^2}\int_0^{2T}(2T-z)(\cos\omega_{o2}z-\cos\omega_{o1}z)^2dz\ , \qquad (A.5\text{-}4)$$

where we have the identity

$$\iint_{-T}^{T} f(x-y)dxdy = 2\int_0^{2T}(2T-z)f(z)dz\ . \qquad (A.5\text{-}4a)$$

The evaluation of (A.5-4) proceeds directly:

$$\hat{Q}_n^{(21)}\text{-}1 \cong \frac{n}{2T^2}\int_0^{2T}(2T-z)\{1+\frac{1}{2}\cos\omega_{o2}z+\frac{1}{2}\cos\omega_{o1}z-\cos(\omega_{o2}-\omega_{o1})z$$

$$-\cos(\omega_{o2}+\omega_{o1})z\}dz \qquad (A.5\text{-}5a)$$

$$\underset{\sim}{\sim} n\{1+\frac{1}{2T^2}\int_0^{2T}(2T-z)\{\frac{\cos\omega_{o2}z+\cos\omega_{o1}z}{2}-\cos(\omega_{o2}-\omega_{o1})z$$

$$-\cos(\omega_{o2}-\omega_{o1})z\}dz\ , \qquad (A.5\text{-}5b)$$

$$\therefore\ \boxed{\hat{Q}_n^{(21)}\text{-}1 \underset{\sim}{\sim} n\{1+O(1/\omega_{o1}T \text{ or } 1/\omega_{o2}T)\} \underset{\sim}{\sim} n,\ (\omega_{o1,o2}T \sim n \gg 1)\ ,} \qquad (A.5\text{-}5c)$$

as expected. Note that $\hat{Q}_n^{(21)}$ is twice Q_n, (A.2-42e), $n\gg1$, which is to be expected, since here the binary signals have twice as much energy as the "on-off" cases. [With purely incoherent structure $\rho_{ij}^{(\ )} \approx \delta_{ij}$, $\therefore \hat{Q}_n^{(21)} \approx 1$, and and so $\hat{Q}^{(21)}\text{-}1 \doteq 0$, which gives zero processing gain - cf. Table 6.1b. This is also to be expected, since now we have two indistinguishable, equal energy signals, with no coherent structure.]

We proceed similarly with the bias, (A.5-2), which we can write directly here for these symmetrical channels

$$\hat{B}_n^{(21)*} = -\frac{L^{(2)^2}}{4}\overline{a_o^2}^2 \sum_{ij}{}' [\rho_{ij}^{(2)^2} - \rho_{ij}^{(1)^2}]$$

$$= -\frac{L^{(2)^2}}{4}\overline{a_o^2}^2 \sum_{ij}^{n} [\cos^2\omega_{o2}(t_i-t_j) - \cos^2\omega_{o1}(t_i-t_j)] \qquad \text{(A.5-6a)}$$

$$= -\frac{L^{(2)^2}}{8}\overline{a_o^2}^2 \sum_{ij}^{n} [\cos 2\omega_{o2}(t_i-t_j) - \cos 2\omega_{o1}(t_i-t_j)] \qquad \text{(A.5-6b)}$$

$$\simeq -\frac{L^{(2)^2}\overline{a_o^2}^2 n^2}{16T^2}\int_o^{2T}(2T-z)(\cos 2\omega_{o2}z - \cos 2\omega_{o1}z)dz \qquad \text{(A.5-6c)}$$

$$\therefore\ \hat{B}_n^{(21)*} \cong -\frac{L^{(2)^2}\overline{a_o^2}^2 n^2}{32}\left[\frac{\sin^2 2\omega_{o2}T}{(\omega_{o2}T)^2} - \frac{\sin^2 2\omega_{o1}T}{(\omega_{o1}T)^2}\right] = 0, \qquad \text{(A.5-7)}$$

when we sample such that $\omega_{o1}T = \omega_{o1}n\Delta t = k'2\pi$, $\omega_{o2}T = \omega_{o2}n\Delta t = k''2\pi$, or $\Delta t = (2\pi\lambda_1)/\omega_{o1} = (2\pi\lambda_2)/\omega_{o2}$; $\lambda_1 \equiv k'/n$, $\lambda_2 = k''/n$, where k', k'', n ($>>1$) are integers. Thus, $(\lambda_1/\omega_{o1}) = (\lambda_2/\omega_{o2})$, or

$$\boxed{\frac{k'}{k''} = \frac{\omega_{o1}}{\omega_{o2}} = \text{ratio of integers}\ .} \qquad \text{(A.5-8)}$$

<u>This means that one should choose the carrier frequencies f_{o1}, f_{o2}, such that (A.5-8) is satisfied.</u> Otherwise the bias $\hat{B}_n^{(21)*}$ is not strictly zero, although it can be quite small.

APPENDIX A6
Computer Software

In this appendix we simply list the computer programs used for the calculations given in the report and required for similar calculations. The programs are essentially self-explanatory via the comment statements, but some further explanation may be helpful.

The first program given, NORMB, is used to compute the normalization parameter, Ω. The "basic" Class B model is normalized to the rms level of the gaussian portion of the noise process since the 2nd (and other) moments do not exist for the Class B model. In NORMB, the parameter Ω is computed by truncating the Class B model, either at an envelope level of 80 db (on the original scale, gauss rms = 1) or at a level for which the probability of exceedance is 10^{-6}, whichever occurs first. In any particular case, the Ω would be computed by comparison of the Class B model with actual measured envelope data or by other appropriate means. The program NORMB integrates the truncated envelope distribution to obtain the rms level. Since the envelope power is twice the actual noise power, the proper corresponding normalization for the instantaneous amplitude is obtained by using 2Ω. For example, in (3.15a) the parameter Ω_B is given by 2Ω, Ω from NORMB. This program requires the subroutine CONHYP for the confluent hypergeometric function and the function routine GAMMA for the gamma function.

The next programs given are LOBDNA and LOBDNB. The routine LOBDNA computes the LOBD nonlinearity for Class A noise for both the canonical (3.13) and quasi-canonical (3.14) models (Figure 7.1). The routine LOBDNB computes the nonlinearity for Class B noise (3.15) (Figures 7.2a and 7.2b).

The three programs PC1, PC2, and PC3, compute the general performance results and probabilistic controls given on Figure 7.3-7.6. The programs require complementary error function and inverse error function routines given by the function routines CERF and ERFIN.

The programs PARA and PARB compute the detection parameters, processing gains, and bounds for input signal size, Figures 7.7-7.22, for Class A (PARA) and Class B (PARB) noise. The program PARA requires the subroutine FUN1 and FUN2 and the program PARB requires the subroutine FUN.

The program PDVPDS computes the probability of detection compared to the optimum probability of detection results of Figures 7.23a and 7.23b, and the program PEVPES computes the probability of error versus the optimum probability of error characteristics, Figure 7.24.

Finally, the programs WOA and WOB compute the pdf, evaluated at zero, for Class A and Class B noise, Figures 7.25 and 7.26.

In some of the programs SYSTEMC and IRAY are used. This is to suppress an exponent underflow error message for the particular computer used (CYBER 170/750) and are not, in general, required.

```
      PROGRAM NORMB(INPUT,OUTPUT)
C     THIS PROGRAM COMPUTES THE NORMALIZATION FACTOR OMEGA
C     FOR THE TRUNCATED CLASS B MODEL SO THAT THE ENVELOPE RMS
C     VALUE IS EQUAL TO 1. SATURATION(TRUNCATION)IS ASSUMED
C     TO BE AT 80DB(ON ORIGINAL NORMALIZED TO GAUSS POWER
C     SCALE)OR AT P=1.E-6, WHICHEVER OCCURS FIRST.
C     NOTE. THIS PROGRAM NORMALIZES TO THE ENVELOPE RMS. THE REAL
C     NOISE POWER IS ONE HALF THE ENVELOPE POWER. FOR COMPUTATIONS
C     WHICH USE THE INSTANTANEOUS AMPLITUDE PDF, THE PROPER
C     NORMALIZATION IS OBTAINED BY USING 2.*OMEGA, OMEGA BEING
C     THE NORMALIZATION PARAMETER OBTAINED HERE.
      DIMENSION IRAY(6),AALPHA(9),AAA(6)
      DATA IRAY/-1,-1,-1,0,-1,-1/
      DATA AALPHA/0.2,0.4,0.6,0.8,1.0,1.2,1.4,1.6,1.8/
      DATA AAA/0.001,0.01,0.1,0.5,1.0,2.0/
      PRINT 6
    6 FORMAT(1H1)
      DO 80 I=1,9
      ALPHA=AALPHA(I)
      DO 70 J=1,6
      AA=AAA(J)
      SS=0.
      PE2=1.
      DO 60 K=1,25
      E=10.**((-22.+K*4.)/20.)
      PE1=PE2
      SS1=0. $ FN=1. $ SS2=0.
      E2=10.**((-20.+K*4.)/20.)
      DO 40 N=1,25
      FN=FN*N
      CALL CONHYP(1.-N*ALPHA/2.,2.,E2*E2,S,IOVFLW)
      T=(((-AA)**N)/FN)*GAMMA(1.+N*ALPHA/2.)*S
      IF(IOVFLW.NE.1) GO TO 24
      SS2=SS2+T
      GO TO 40
   24 SS1=SS1+T
   40 CONTINUE
      FP=0.
      IF(E2*E2.LT.675.) FP=EXP(-E2*E2)
      PE2=FP-E2*E2*(FP*SS1+SS2)
      SS=SS+E*E*(PE1-PE2)
      IF(PE2.LE.1.E-6) GO TO 64
   60 CONTINUE
   64 RMSS=SS+PE2*E2
      RMS=SQRT(RMSS)
      RMSDB=20.*ALOG10(RMS)
      OMEGA=1./RMSS
      PRINT 7, ALPHA, AA, RMSDB, OMEGA
   70 CONTINUE
   80 CONTINUE
    7 FORMAT(5X,3(1PE9.2,2X),2X,1PE12.5)
      END
```

```
      SUBROUTINE CONHYP(A,B,X,S,IOVFLW)
C.....COMPUTES 1F1(A,B,X) FOR REAL A,B,X
C.....IF X GREATER THAN 741. AN OVERFLOW WILL OCCUR. SEE
C.....COMMENTS BELOW.
      S=1.  $ Y=1.
      IOVFLW=0
      KUNDEF=0
      IF(A.GT.0.)GO TO 101
      K=-A
      ENA=-K-1
      VA=A-ENA
      IF(VA.EQ.1..OR.VA.EQ.0.)GO TO 110
  101 IF(B.GT.0.)GO TO 130
      J=-B
      ENB=-J-1
      VB=B-ENB
      IF(VB.EQ.1..OR.VB.EQ.0.)120,130
  110 KUNDEF=1
      GO TO 101
  120 IF(KUNDEF.EQ.1)PRINT1000,A,B
      IF(KUNDEF.NE.1)PRINT1001,B
      RETURN
  130 IF(KUNDEF.EQ.1)GO TO 10
    5 IF(X.GE.100.) GO TO 60
    6 IF(X.GE.10.) GO TO 10
      NN=100
      GO TO 15
   10 NN=300
   15 IF(KUNDEF.EQ.1) NN=-A+1
      DO 20 N=1,NN
      D=N*((B+N-1.0)**2.)
      Y=(A+N-1.0)*(Y/D)
      Y=Y*(B+N-1.0)
      Y=Y*X
      IF(S.EQ.(S+Y))GO TO 50
      S=S+Y
   20 CONTINUE
   50 RETURN
C.....APPROXIMATES 1F1(A,B,X) FOR REAL A,B,X BY USING THE
C.....ASYMPTOTIC EXPANSION. SEE PAGE 1073, INTRODUCTION
C.....TO STATISTICAL COMMUNICATIONS THEORY, MIDDLETON.
C.....IF X.GE.675. AN OVERFLOW WILL OCCUR FROM EXP.
C.....TO AVOID THIS, THE VARIABLE IOVFLW IS SET TO 1 AND
C.....THE FUNCTION VALUE IS CALCULATED WITHOUT THE EXP(X) FACTOR.
C.....SO THAT THE VALUE RETURNED IS S/EXP(X)
   60 NN=20
      DO 100 N=1,NN
      Y=Y*(B-A+N-1.)*(N-A)
      Y=Y/(N*X)
      IF(S.EQ.(S+Y))GO TO 150
      S=S+Y
  100 CONTINUE
```

```
  150 S=S*(GAMMA(B)/GAMMA(A))*(X**(A-B))
      IF(X.LT.675.)GO TO 190
      IOVFLW=1
      GO TO 200
  190 S=S*EXP(X)
  200 RETURN
 1000 FORMAT(//,1X,* CANNOT EVALUATE EXPRESSION SINCE BOTH*,
     1* A AND B ARE NEGATIVE INTEGERS OR ZERO, A=*,F10.2,* , B=*,
     2F10.2,//)
 1001 FORMAT(//,1X,* BAD VALUE FOR B GIVES INFINITE RESULT FOR S*,
     1 *, B=*,F10.2,//)
      END
```

```
      FUNCTION GAMMA(X)
C     RETURNS THE GAMMA FUNCTION FOR REAL ARGUMENT.
C     NOTE. THE GAMMA FUNCTION IS NOT DEFINED FOR A NEGATIVE INTEGER OR ZER
C     INPUT
C       X = THE REAL ARGUMENT.
C     OUTPUT.
C       GAMMA(X) = THE GAMMA FUNCTION OF ARGUMENT X.
   75 FORMAT(66H GAMMA FUNCTION OF A NEGATIVE INTEGER, OR OF ZERO, IS NO
     1T DEFINED.)
    5 IF(X) 10,80,15
   10 N=-X
      EN=-N-1
      V=X-EN
      IF(V.EQ.1.)80,20
   15 N=X
      EN=N
      V=X-EN
   20 GAMMA=1.+V*(.422784337+V*(.411840251 8+V*(.08157821878+V*
     1(.07423790761+V*(-.0002109074673+V*(.01097369584+V*(-.002466747981
     2+V*(.001539768105-V*(.0003442342046-V*.000067710571 17)))))))))
      IF(EN-2.) 37,25,30
   25 RETURN
   30 N=N-1
      DO 35 I=2,N
      FI=I
   35 GAMMA=GAMMA*(FI+V)
      RETURN
   37 N=2.-EN
      DO 40 I=1,N
      FI=2-I
   40 GAMMA=GAMMA/(FI+V)
      RETURN
   80 PRINT 75
      CALL EXIT
      END
```

```
      PROGRAM LOBDNA(INPUT,OUTPUT)
C     THIS PROGRAM COMPUTES THE LOBD NON-LINEARITY FOR CLASS A
C     NOISE FOR BOTH THE CANONICAL AND QUASICANONICAL MODEL.
C     THE PARAMETERS AA,GAM,ALPHAO,U(FOR MU),SGAM,AND GO ARE INPUTS.
C     THE DERIVED PARAMETERS,DSQ,ALPHA,AND GAMH ARE COMPUTED.
C     PC IS THE CANONICAL NON-LINEARITY AND PQC IS THE
C     QUASICANONICAL NON-LINEARITY.
      DIMENSION IRAY(6),AA(4),GAM(4)
      DATA IRAY/-1,-1,-1,0,-1,-1/
      DATA AA/0.35,0.1,0.01,0.35/
      DATA GAM/5.E-4,0.001,5.E-4,0.1/
      CALL SYSTEMC(115,IRAY)
    6 FORMAT(1H1)
      ALPHAO=0.01
      U=0.
      SGAM=2.
      GO=1.
      PI=3.1415926
      SRPI=SQRT(PI)
      ALPHA=(2.-U)/SGAM
      DSQ=ALPHA/((2.-ALPHA)*(ALPHAO**((2.-ALPHA)*SGAM)))
      D=SQRT(DSQ)
      DO 90 I=1,4
      GAMM=GAM(I)
      GAMH=GAM(I)*DSQ
      A=AA(I)
      PRINT 6
      PRINT 7, GAMM, GAMH, A
      DO 80 J=1,51
      ZDB=-62.+J*2.
      Z=10.**(ZDB/20.)
      ZSQ=Z*Z
      FM=1.
      SIGCO=GAMM/(1.+GAMM)
      SIGQO=GAMH/(1.+GAMM)
      SUMCB=EXP(-ZSQ/(2.*SIGCO))/SQRT(2.*PI*SIGCO)
      SUMCT=SUMCB*Z/SIGCO
      SUMQB=D*EXP(-ZSQ*DSQ/(2.*SIGQO))/SQRT(2.*PI*SIGQO)
      SUMQT=SUMQB*DSQ*Z/SIGQO
      DO 70 M=1,15
      FM=FM*M
      SIGC=(M/A+GAMM)/(1.+GAMM)
      SIGQ=(M/A+GAMH)/(1.+GAMM)
      TCB=(A**M/FM)*EXP(-ZSQ/(2.*SIGC))/SQRT(2.*PI*SIGC)
      TCT=TCB*Z/SIGC
      F=((A*GO)**M)/FM
      TQB=F*D*EXP(-ZSQ*DSQ/(2.*SIGQ))/SQRT(2.*PI*SIGQ)
      TQT=TQB*DSQ*Z/SIGQ
      FN=1. $ SB=0. $ ST=0.
      F1=PI/(2.*GAMMA((3.+ALPHA)/2.)*((M+GAMM*A*DSQ)**(ALPHA/2.)))
```

```
      DO 60 N=1,M
      FN=FN*N
      FMN=1.
      KK=M-N
      IF(KK.EQ.0) GO TO 21
      DO 20 K=1,KK
      FMN=FMN*K
   20 CONTINUE
   21 CMN=FM/(FN*FMN)
      F2=GAMMA((1.+N*ALPHA)/2.)*F1**N
      ARG=ZSQ*DSQ/(2.*SIGQ)
      CALL CONHYP(-0.5*N*ALPHA,0.5,ARG,BS,IOVFLW)
      IF(IOVFLW.EQ.1) GO TO 31
      S=((-1.)**N)*CMN*EXP(-ARG)*F2*BS
      GO TO 32
   31 S=((-1.)**N)*CMN*F2*BS
   32 SB=SB+S
      CALL CONHYP(-0.5*N*ALPHA,1.5,ARG,TS,IOVFLW)
      IF(IOVFLW.EQ.1) GO TO 33
      SS=((-1.)**N)*CMN*(1.+N*ALPHA)*EXP(-ARG)*F2*TS
      GO TO 34
   33 SS=((-1.)**N)*CMN*(1.+N*ALPHA)*F2*TS
   34 ST=ST+SS
   60 CONTINUE
      H=D/SQRT(2.*PI*PI*SIGQ)
      HT=H*Z*DSQ/SIGQ
      SB=F*H*SB
      ST=F*HT*ST
      SUMCB=SUMCB+TCB
      SUMCT=SUMCT+TCT
      SUMQB=SUMQB+TQB+SB
      SUMQT=SUMQT+TQT+ST
   70 CONTINUE
      PC=SUMCT/SUMCB
      PQC=SUMQT/SUMQB
      PRINT 8, ZDB, PC, PQC
   80 CONTINUE
   90 CONTINUE
    7 FORMAT(2X,3(1PE12.5,2X),/)
    8 FORMAT(5X,F5.1,2X,1PE12.5,2X,1PE12.5)
      END
```

```
      PROGRAM LOBDNB(INPUT,OUTPUT)
C     THIS PROGRAM COMPUTES THE LOBD NON-LINEARITY FOR
C     CLASS B NOISE. THE INPUT PARAMETERS ARE ALPHA,AA,AND OMEGA.
C     THE NON-LINEARITY VALUES ARE GIVEN BY ZZ.
      DIMENSION IRAY(6),AALPHA(3),AAA(3),OOMEGA(9)
      DATA IRAY/-1,-1,-1,0,-1,-1/
      DATA AALPHA/0.8,1.0,1.2/
      DATA AAA/0.2,1.0,2.0/
      DATA OOMEGA/2.0087E-4,4.0202E-5,2.0115E-5,9.9889E-4,
     11.9996E-4,1.0000E-4,5.1565E-3,1.0357E-3,5.1816E-4/
      CALL SYSTEMC(115,IRAY)
      DO 80 I=1,3
      ALPHA=AALPHA(I)
      DO 70 J=1,3
      AA=AAA(J)
      OMEGA=2.*OOMEGA(3*(I-1)+J)
C     TO NORMALIZE TO REAL NOISE RMS.
      PRINT 6
      PRINT 7, ALPHA, AA, OMEGA
      DO 60 K=1,25
      ZDB=-65.+K*5.
      Z=10.**(ZDB/20.)
      ZN=Z*Z/OMEGA
      SUM=0. $ FN=1. $ SUM1=0.
      DO 20 N=1,26
      FN=FN*N
      CALL CONHYP(-N*ALPHA/2.,1.5,ZN,S,IOVFLW)
      T=(((-AA)**N)/FN)*GAMMA(.5+N*ALPHA/2.)*S*(1.+N*ALPHA)
      IF(IOVFLW.NE.1) GO TO 14
      SUM1=SUM1+T
      GO TO 20
   14 SUM=SUM+T
   20 CONTINUE
      FP=0.
      IF(ZN.LT.675.) FP=EXP(-ZN)
      TOP=FP*(SUM+1.7724539)+SUM1
      SUMM=0. $ FM=1. $ SUMM1=0.
      DO 40 M=1,26
      FM=FM*M
      CALL CONHYP(-M*ALPHA/2.,0.5,ZN,S,IOVFLW)
      TT=(((-AA)**M)/FM)*GAMMA(.5+M*ALPHA/2.)*S
      IF(IOVFLW.NE.1) GO TO 34
      SUMM1=SUMM1+TT
      GO TO 40
   34 SUMM=SUMM+TT
   40 CONTINUE
      FPP=0.
      IF(ZN.LT.675.) FPP=EXP(-ZN)
      BOT=FPP*(SUMM+1.7724539)+SUMM1
      ZZ=2.*(Z/OMEGA)*TOP/BOT
      PRINT 8, ZDB, ZZ
   60 CONTINUE
   70 CONTINUE
   80 CONTINUE
    6 FORMAT(1H1)
    7 FORMAT(2X,2(F4.1,2X),1PE12.5,/)
    8 FORMAT(5X,F5.1,1PE12.5)
      END
```

```
      PROGRAM PC1(INPUT,OUTPUT)
C     TO COMPUTE THE GENERAL PERFORMANCE CURVES,
C     FIGURES 7.3 AND 7.4, EQUATION 7.13.
      DIMENSION ALPHA(9)
      DATA ALPHA/1.E-1,1.E-2,1.E-3,1.E-4,1.E-5,1.E-6,1.E-8,
     1 1.E-10,1.E-12/
      PRINT 6
    6 FORMAT(1H1)
      DO 20 I=1,25
      SIGDB=-22.+2.*I
      SIG=10.**(SIGDB/20.)
      PE=0.5*CERF(SIG/(2.*SQRT(2.)))
      PRINT 7, SIGDB, PE
   20 CONTINUE
    7 FORMAT(10X,F5.1,2X,1PE12.5)
      PRINT 6
      DO 60 J=1,9
      T1=ERFIN(1.0-2.*ALPHA(J))
      DO 40 K=1,25
      SIGDB=-22.+2.*K
      SIG=10.**(SIGDB/20.)
      T=SIG/SQRT(2.)-T1
      IF(T.LE.0.) GO TO 30
      PD=1.-0.5*CERF(T)
      GO TO 35
   30 T=-T
      PD=0.5*CERF(T)
   35 PRINT 7, SIGDB, PD
   40 CONTINUE
      PRINT 8
   60 CONTINUE
    8 FORMAT(//)
      END
```

```
      PROGRAM PC3(INPUT,OUTPUT)
C     TO COMPUTE THE RESULTS GIVEN ON FIG 7.6, EQ. 7.14.
      DIMENSION PE(13)
      DATA PE/0.4,0.2,0.1,5.E-2,1.E-2,5.E-3,1.E-3,5.E-4,1.E-4,
     1 5.E-5,1.E-5,5.E-6,1.E-6/
      PRINT 6
    6 FORMAT(1H1)
      DO 10 I=1,13
      C=ERFIN(1.-2.*PE(I))
      CDB=10.*ALOG10(C)
      PRINT 7, PE(I), C, CDB
   10 CONTINUE
    7 FORMAT(10X,3(1PE12.5,2X))
      END
```

```
      PROGRAM PC2(INPUT,OUTPUT)
C     TO COMPUTE THE PROBABILISTIC CONTROLS ON DETECTION,
C     FIGURE 7.5, EQUATION 7.14.
      DIMENSION ALPHA(9), PDET(16), P1(9), P2(16)
      DATA ALPHA/1.E-1,1.E-2,1.E-3,1.E-4,1.E-5,1.E-6,
     1 1.E-8,1.E-10,1.E-12/
      DATA PDET/0.02,0.04,0.06,0.08,0.1,0.2,0.3,0.4,0.5,0.6,
     10.7,0.8,0.9,0.95,0.98,0.99/
      PRINT 6
    6 FORMAT(1H1)
      DO 10 I=1,9
      P1(I)=ERFIN(1.-2.*ALPHA(I))
   10 CONTINUE
      DO 20 J=1,16
      P2(J)=ERFIN(ABS(2.*PDET(J)-1.))
      IF(2.*PDET(J)-1..LE.0.)  P2(J)=-P2(J)
   20 CONTINUE
      DO 40 K=1,9
      PC=P1(K)
      DO 30 L=1,16
      PDB=0.
      P=PC+P2(L)
      IF(P.LE.0.) GO TO 29
      PDB=10.*ALOG10(P)
   29 PRINT 7, PC, P2(L), P, PDB
   30 CONTINUE
      PRINT 6
   40 CONTINUE
    7 FORMAT(10X,4(1PE12.5,2X))
      END


      FUNCTION CERF(X)
C     SEE APPROXIMATIONS FOR DIGITAL COMPUTERS
C     BY C. HASTINGS, PRINCETON U. PRESS, 1955,
C     PAGE 169. ALSO IN ABRAMOWITZ AND STEGUN.
C     NOTE, VALID ONLY FOR X.GE.0..
      E=1.0/(1.0+0.3275911*X)
      S=(((((0.940646070*E)-1.287822453)*E+1.259695130)*E-0.252128668)*E
     1+0.225836846)*E
      XSQ=X**2
      EXPFX=0.0
      IF(XSQ.LT.709.0)EXPFX=EXP(-XSQ)
      CERF=S*EXPFX*1.128379167
      RETURN
      END

      FUNCTION ERFIN(Q)
C     COMPUTES THE INVERSE ERROR FUNCTION, USING
C     26.2.23 OF ABRAMOWITZ AND STEGUN.
      P=(1.-Q)/2.
      T=SQRT(ALOG(1./(P*P)))
      X1=2.515517+0.802853*T+0.010328*T*T
      X2=1.0+1.432788*T+0.189269*T*T+0.001308*T*T*T
      XP=T-X1/X2
      ERFIN=XP/(SQRT(2.))
      RETURN
      END
```

```
      PROGRAM PARA(INPUT,OUTPUT)
C     THIS PROGRAM COMPUTES L(2),L(4),L(2,2) AND L(6)
C     FOR VARIOUS COMBINATIONS OF CLASS A NOISE
C     PARAMETERS.
C     THE COHERENT PROCESSING GAIN, PER SAMPLE, IS L(2).
C     THE INCOHERENT PROCESSING GAIN, PER SAMPLE, IS
C     IS A FUNCTION OF L(2),L(4) AND THE SIGNAL PARAMETER QN.
C     THE RATIO OF THE COHERENT AND INCOHERENT PROCESSING
C     GAINS IS ALSO CALCULATED ALONG WITH XO AND YO.
      COMMON/QQQ/A,GAM
      DIMENSION IRAY(6),AA(10),G(7),QN(2)
      DIMENSION PIINC(2),PIDB(2),RATIO(2),RADB(2),YO(2)
      DIMENSION Z1(7),Z2(7),Z3(7),Z4(7)
      DATA AA/1.E-4,1.E-2,0.1,0.5,1.0,2.0,3.0,4.0,5.0,10.0/
      DATA G/1.E-8,1.E-7,1.E-6,1.E-5,1.E-4,1.E-3,1.E-2/
      DATA QN/1.,10./
      DATA IRAY/-1,-1,-1,0,-1,-1/
      CALL SYSTEMC(115,IRAY)
      PRINT 6
    6 FORMAT(1H1)
      DO 80 L=1,10
      A=AA(L)
      DO 70 L1=1,7
      GAM=G(L1)
      SUM1=0.$SUM2=0.$SUM3=0.$SUM4=0.
      DO 50 I=1,36
      BDB=-160.+5.*(I-1)
      CDB=-160.+5.*I
      B=10.**(BDB/20.)
      C=10.**(CDB/20.)
      IF(I.EQ.1) B=0.
      DX=(C-B)/6.
      DO 40 J=1,7
      X=B+(J-1)*DX
      CALL FUN1(X,Z1(J),Z3(J))
      CALL FUN2(X,Z2(J),Z4(J))
   40 CONTINUE
      S1=0.3*DX*(Z1(1)+5.*Z1(2)+Z1(3)+6.*Z1(4)+Z1(5)+5.*Z1(6)+Z1(7))
      S2=0.3*DX*(Z2(1)+5.*Z2(2)+Z2(3)+6.*Z2(4)+Z2(5)+5.*Z2(6)+Z2(7))
      S3=0.3*DX*(Z3(1)+5.*Z3(2)+Z3(3)+6.*Z3(4)+Z3(5)+5.*Z3(6)+Z3(7))
      S4=0.3*DX*(Z4(1)+5.*Z4(2)+Z4(3)+6.*Z4(4)+Z4(5)+5.*Z4(6)+Z4(7))
      SUM1=SUM1+S1
      SUM2=SUM2+S2
      SUM3=SUM3+S3
      SUM4=SUM4+S4
   50 CONTINUE
```

```
      SUM1=2.*SUM1
C     SUM1 IS L(2)
      SUM2=2.*SUM2
C     SUM2 IS L(4)
      SL4DB=10.*ALOG10(SUM2)
      SUM3=2.*SUM3
C     SUM3 IS L(2,2)
      SL22DB=10.*ALOG10(SUM3)
      SUM4=2.*SUM4
C     SUM4 IS L(6)
      SL6DB=10.*ALOG10(ABS(SUM4))
      SL2=SUM1
      SL2DB=10.*ALOG10(SL2)
      XO=SL2/(SUM3/2.-SL2*SL2)
      DO 60 K=1,2
      F=2.*SL2*SL2/SUM2
      PIINC(K)=(SUM2/8.)*(1.+F*(ON(K)-1.))
      PIDB(K)=10.*ALOG10(PIINC(K))
      RATIO(K)=PIINC(K)/SL2
      RADB(K)=10.*ALOG10(RATIO(K))
   60 CONTINUE
      YO(1)=SUM2/ABS(SUM4/2.+6.*SL2*SUM3)
      YO(2)=1./ABS(3.*SUM3/SL2+2.*SL2)
      PRINT 7, A, GAM
      PRINT 8, SL2, SUM2, SUM3, SUM4
      PRINT 9, XO, YO(1), YO(2)
      PRINT 10, PIINC(1), PIINC(2), RATIO(1), RATIO(2)
      PRINT 11, SL2DB, PIDB(1), PIDB(2), RADB(1), RADB(2)
      PRINT 12, SL4DB, SL22DB, SL6DB
   70 CONTINUE
   80 CONTINUE
    7 FORMAT(2X,2(1PE10.3,2X))
    8 FORMAT(5X,4(1PE10.3,2X))
    9 FORMAT(5X,3(1PE10.3,2X))
   10 FORMAT(5X,4(1PE10.3,2X))
   11 FORMAT(5X,5(1PE10.3,2X))
   12 FORMAT(5X,3(1PE10.3,2X),/)
      END
```

```
      SUBROUTINE FUN1(X,Y,YY)
C     THIS SUBROUTINE COMPUTES THE L(2) AND L(2,2) INTEGRANDS
C     FOR CLASS A NOISE.
      COMMON/QQQ/A,GAM
      PI=3.141592654
      SM1=0. $ SM2=0. $ FM=1.
      DO 10 MM=1,26
      M=MM-1
      IF(M.NE.0) FM=FM*M
      SIGSQ=(M/A+GAM)/(1.+GAM)
      T1=((A**M)/FM)*EXP(-X*X/(2.*SIGSQ))/((2.*PI*SIGSQ)**0.5)
      T2=T1/SIGSQ
      SM1=SM1+T1
      SM2=SM2+T2
   10 CONTINUE
      TEMP=X*X*SM2*SM2/SM1
      Y=EXP(-A)*TEMP
C     Y IS THE L(2) INTEGRAND.
      YY=2.*EXP(-A)*TEMP*TEMP/SM1
C     YY IS THE L(2,2) INTEGRAND
      RETURN
      END



      SUBROUTINE FUN2(X,Y,YY)
C     THIS SUBROUTINE COMPUTES THE L(4) AND L(6) INTEGRANDS
C     FOR CLASS A CANONICAL NOISE.
      COMMON/QQQ/A,GAM
      PI=3.141592654
      SM1=0. $ SM2=0. $ SM3=0. $ FM=1.
      DO 10 MM=1,26
      M=MM-1
      IF(M.NE.0) FM=FM*M
      SIGSQ=(M/A+GAM)/(1.+GAM)
      T1=((A**M)/FM)*EXP(-X*X/(2.*SIGSQ))/(SQRT(2.*PI*SIGSQ))
      T2=T1/SIGSQ
      T3=T2/SIGSQ
      SM1=SM1+T1
      SM2=SM2+T2
      SM3=SM3+T3
   10 CONTINUE
      G=X*X*SM3-SM2
      TEMP=G*G/SM1
      Y=EXP(-A)*TEMP
C     Y IS THE L(4) INTEGRAND.
      YY=EXP(-A)*TEMP*G/SM1
C     YY IS THE L(6) INTEGRAND.
      RETURN
      END
```

```
      PROGRAM PARB(INPUT,OUTPUT)
C     THIS PROGRAM COMPUTES L(2),L(4),L(2,2),AND L(6)
C     FOR VARIOUS COMBINATIONS OF CLASS B NOISE
C     PARAMETERS, ALPHA,AA,AND OMEGA.
C     THE COHERENT PROCESSING GAIN, PER SAMPLE, IS L(2).
C     THE INCOHERENT PROCESSING GAIN, PER SAMPLE, IS A
C     FUNCTION OF L(2), L(4) AND THE SIGNAL PARAMETER QN.
C     THE RATIO OF THE COHERENT AND INCOHERENT PROCESSING
C     GAINS IS ALSO CALCULATED ALONG WITH THE BOUNDS XO AND YO.
      COMMON/QQQ/ALPHA,AA,OMEGA
      DIMENSION IRAY(6),AALPHA(9),AAA(6),OOMEGA(54),QN(2)
      DIMENSION PIINC(2),PIDB(2),RATIO(2),RADB(2),YO(2)
      DIMENSION Z1(7),Z2(7),Z3(7),Z4(7)
      DATA AALPHA/0.2,0.4,0.6,0.8,1.0,1.2,1.4,1.6,1.8/
      DATA AAA/0.001,0.01,0.1,0.5,1.0,2.0/
      DATA OOMEGA/6.551E-4,6.564E-5,6.659E-6,1.419E-6,7.683E-7,
     14.502E-7,2.057E-3,2.062E-4,2.067E-5,4.176E-6,2.115E-6,
     I1.085E-6,8.519E-3,8.588E-4,8.598E-5,1.723E-5,8.631E-6,
     34.333E-6,1.078E-1,4.001E-3,4.016E-4,8.037E-5,4.020E-5,
     42.012E-5,7.396E-1,3.069E-2,1.996E-3,3.998E-4,2.000E-4,
     51.000E-4,9.335E-1,3.080E-1,1.026E-2,2.069E-3,1.036E-3,
     65.182E-4,9.572E-1,7.708E-1,1.121E-1,1.438E-2,5.507E-3,
     72.761E-3,9.618E-1,9.099E-1,4.697E-1,1.119E-1,4.993E-2,
     82.133E-2,9.636E-1,9.456E-1,7.584E-1,3.656E-1,2.255E-1,0.0/
      DATA QN/1.,10./
      DATA IRAY/-1,-1,-1,0,-1,-1/
      CALL SYSTEMC(115,IRAY)
      PRINT 6
    6 FORMAT(1H1)
      DO 80 L=1,9
      ALPHA=AALPHA(L)
      DO 70 L1=1,5
      AA=AAA(L1)
      OMEGA=2.0*OOMEGA(L1+6*(L-1))
C     TO NORMALIZE TO REAL NOISE RMS.
      IF(OMEGA.EQ.0.) GO TO 70
      SUM1=0.$SUM2=0.$SUM3=0.$SUM4=0.
      DO 50 I=1,42
      BDB=-160.+5.*(I-1)
      CDB=-160.+5.*I
      B=10.**(BDB/20.)
      C=10.**(CDB/20.)
      IF(I.EQ.1) B=0.
      DX=(C-B)/6.
      DO 40 J=1,7
      X=B+(J-1)*DX
      CALL FUN(X,Z1(J),Z2(J),Z3(J),Z4(J))
   40 CONTINUE
```

```
      S1=0.3*DX*(Z1(1)+5.*Z1(2)+Z1(3)+6.*Z1(4)+Z1(5)+5.*Z1(6)+Z1(7))
      S2=0.3*DX*(Z2(1)+5.*Z2(2)+Z2(3)+6.*Z2(4)+Z2(5)+5.*Z2(6)+Z2(7))
      S3=0.3*DX*(Z3(1)+5.*Z3(2)+Z3(3)+6.*Z3(4)+Z3(5)+5.*Z3(6)+Z3(7))
      S4=0.3*DX*(Z4(1)+5.*Z4(2)+Z4(3)+6.*Z4(4)+Z4(5)+5.*Z4(6)+Z4(7))
      SUM1=SUM1+S1
      SUM2=SUM2+S2
      SUM3=SUM3+S3
      SUM4=SUM4+S4
   50 CONTINUE
      SUM1=2.*SUM1
C     SUM1 IS L(2)
      SUM2=2.*SUM2
C     SUM2 IS L(4)
      SL4DB=10.*ALOG10(SUM2)
      SUM3=2.*SUM3
C     SUM3 IS L(2,2)
      SL22DB=10.*ALOG10(SUM3)
      SUM4=2.*SUM4
C     SUM4 IS L(6)
      SL6DB=10.*ALOG10(ABS(SUM4))
      SL2=SUM1
      SL2DB=10.*ALOG10(SL2)
      XO=SL2/(SUM3/2.-SL2*SL2)
      DO 60 K=1,2
      F=2.*SL2*SL2/SUM2
      PIINC(K)=(SUM2/8.)*(1.+F*(QN(K)-1.))
      PIDB(K)=10.*ALOG10(PIINC(K))
      RATIO(K)=PIINC(K)/SL2
      RADB(K)=10.*ALOG10(RATIO(K))
   60 CONTINUE
      YO(1)=SUM2/ABS(SUM4/2.+6.*SL2*SUM3)
      YO(2)=1./ABS(3.*SUM3/SL2+2.*SL2)
      PRINT 7, ALPHA, AA, OMEGA
      PRINT 8, SL2, SUM2, SUM3, SUM4
      PRINT 9, XO, YO(1), YO(2)
      PRINT 10, PIINC(1), PIINC(2), RATIO(1), RATIO(2)
      PRINT 11, SL2DB, PIDB(1), PIDB(2), RADB(1), RADB(2)
      PRINT 12, SL4DB, SL22DB, SL6DB
   70 CONTINUE
   80 CONTINUE
    7 FORMAT(2X,3(1PE10.3,3X))
    8 FORMAT(5X,4(1PE10.3,2X))
    9 FORMAT(5X,3(1PE10.3,2X))
   10 FORMAT(5X,4(1PE10.3,2X))
   11 FORMAT(5X,5(1PE10.3,2X))
   12 FORMAT(5X,3(1PE10.3,2X),/)
      END
```

```
      SUBROUTINE FUN(X,Y,YY,YYY,YYYY)
C     THIS SUBROUTINE COMPUTES THE L(2)(Y),THE L(4)(YY),
C     THE L(2,2)(YYY),AND THE L(6)(YYYY) INTEGRANDS FOR
C     CLASS B NOISE.
      COMMON/QQQ/ ALPHA,AA,OMEGA
      PI=3.141592654
      ZN=X*X/OMEGA
      FM=1.
      SUM1=SUM2=SUM3=0.
      SUM4=SUM5=SUM6=0.
      DO 20 M=1,26
      FM=FM*M
      CALL CONHYP(-M*ALPHA/2.,0.5,ZN,S,IOVFLW)
      CALL CONHYP(-M*ALPHA/2.,1.5,ZN,SS,IOVLLW)
      CALL CONHYP(-M*ALPHA/2.,2.5,ZN,SSS,IOVFLW)
      T=(((-AA)**M)/FM)*GAMMA(0.5+M*ALPHA/2.)
      T1=T*S
      T2=T*(1.+M*ALPHA)*SS
      T3=T*(1.+M*ALPHA)*(1.+M*ALPHA/3.)*SSS
      IF(IOVFLW.NE.1) GO TO 15
      SUM4=SUM4+T1
      SUM5=SUM5+T2
      SUM6=SUM6+T3
      GO TO 20
   15 SUM1=SUM1+T1
      SUM2=SUM2+T2
      SUM3=SUM3+T3
   20 CONTINUE
      FP=0.
      IF(ZN.LT.675.) FP=EXP(-ZN)
      PT=FP*(SUM1+SQRT(PI))+SUM4
      P1T=FP*(SUM2+SQRT(PI))+SUM5
      P11T=FP*(SUM3+SQRT(PI))+SUM6
      P=PT/(PI*SQRT(OMEGA))
      P1=-2.*X*P1T/(PI*OMEGA**1.5)
      P11=4.*X*X*P11T/(PI*OMEGA**2.5)-2.*P1T/(PI*OMEGA**1.5)
C     P IS PDF OF X
C     P1 IS PDF PRIME
C     P11 IS PDF PRIME PRIME (2ND DERIVITIVE)
      Y=P1*P1/P
      YY=P11*P11/P
      YYY=(2.*P1**4.)/(P**3.)
      YYYY=(P11**3.)/(P*P)
      RETURN
      END
```

```
      PROGRAM PDVPDS(INPUT,OUTPUT)
C     PROGRAM COMPUTES THE CANONICAL PERFORMANCE RESULTS,EQUATION
C     6.50, PROBABILITY OF DETECTION VERSUS OPTIMUM PROBABILITY
C     OF DETECTION, AS FUNCTION OF DEGRADATION FACTOR PHID,
C     FOR A GIVEN FALSE ALARM PROBILITY, ALPHAF.
      DIMENSION ALPHA(2), PHI(7), PDSS(18)
      DATA ALPHA/1.0E-3,1.0E-6/
      DATA PHI/1.,0.5,0.1,0.05,0.01,0.005,0.001/
      DATA PDSS/1.0E-6,5.0E-6,1.0E-5,5.0E-5,1.0E-4,5.0E-4,0.001,
     10.005,0.01,0.05,.1,.5,.6,.7,.8,.9,.95,.98/
      PRINT 6
    6 FORMAT(1H1)
      DO 60 I=1,2
      ALPHAF=ALPHA(I)
      DO 50 J=1,7
      PHID=PHI(J)
      PRINT 7, ALPHAF, PHID
      DO 40 K=1,18
      PDS=PDSS(K)
      T1=ERFIN(1.-2.*ALPHAF)
      T2=ERFIN(ABS(2.*PDS-1.))
      IF(2.*PDS-1..LE.0.) T2=-T2
      T3=SQRT(PHID)*(T2+T1)
      T=T3-T1
      IF(T.LE.0.) GO TO 30
      PD=1.0-0.5*CERF(T)
      GO TO 35
   30 T=-T
      PD=0.5*CERF(T)
   35 PRINT 8, PDS, PD
   40 CONTINUE
      PRINT 9
   50 CONTINUE
   60 CONTINUE
    7 FORMAT(5X,2(1PE10.3,3X),/)
    8 FORMAT(8X,2(1PE10.3,3X))
    9 FORMAT(//)
      END
```

```
      PROGRAM PEVPES(INPUT,OUTPUT)
C     PROGRAM COMPUTES THE CANONICAL PERFORMANCE RESULTS EQUATION
C     6.51, PROBABILITY OF BINARY BIT ERROR VERSUS OPTIMUM
C     PROBABILITY OF ERROR, AS A FUNCTION OF DEGRADATION FACTOR PHID.
      DIMENSION PHI(10),PESS(17)
      DATA PHI/1.0,.9,.8,.7,.6,.5,.4,.3,.2,.1/
      DATA PESS/1.E-6,2.E-6,5.E-6,1.E-5,2.E-5,5.E-5,1.E-4,2.E-4,
     15.E-4,.001,.002,.005,.01,.02,.05,.1,.2/
      PRINT 6
    6 FORMAT(1H1)
      DO 60 I=1,10
      PHID=PHI(I)
      PRINT 7, PHID
      DO 40 J=1,17
      PES=PESS(J)
      PE=0.5*CERF(PHID*ERFIN(1.-2.*PES))
      PRINT 8, PES, PE
   40 CONTINUE
      PRINT 9
   60 CONTINUE
    7 FORMAT(5X,1PE10.3,/)
    8 FORMAT(8X,2(1PE10.3,3X))
    9 FORMAT(//)
      END

      PROGRAM WOA(INPUT,OUTPUT)
C     PROGRAM COMPUTES THE PDF EVALUATED AT ZERO
C     FOR CLASS A NOISE.
      DIMENSION AA(10),G(7)
      DATA AA/1.E-4,1.E-2,0.1,0.5,1.0,2.,3.,4.,5.,10./
      DATA G/1.E-8,1.E-7,1.E-6,1.E-5,1.E-4,1.E-3,1.E-2/
      PI=3.141592654
      PRINT 6
    6 FORMAT(1H1)
      DO 80 J=1,10
      A=AA(J)
       PRINT 7, A
      DO 70 K=1,7
      GAM=G(K)
      SUM=0. $ FN=1.
      DO 60 NN=1,30
      N=NN-1
      IF(N.NE.0) FN=FN*N
      T=((A**N)/FN)*SQRT((1.+GAM)/(N/A+GAM))
      SUM=SUM+T
   60 CONTINUE
      WO=EXP(-A)*SUM/SQRT(2.*PI)
      ARE=4.*WO*WO
      AREDB=10.*ALOG10(ARE)
      PRINT 8, GAM,WO,ARE,AREDB
   70 CONTINUE
      PRINT 9
   80 CONTINUE
    7 FORMAT(5X,1PE10.3,/)
    8 FORMAT(8X,4(1PE10.3,3X))
    9 FORMAT(//)
      END
```

```
      PROGRAM WOB(INPUT,OUTPUT)
C     PROGRAM COMPUTES THE PDF EVALUATED AT ZERO
C     FOR CLASS B NOISE.
      DIMENSION AALPHA(9),AAA(6),OOMEGA(54)
      PI=3.141592654
      DATA AALPHA/0.2,0.4,0.6,0.8,1.0,1.2,1.4,1.6,1.8/
      DATA AAA/0.001,0.01,0.1,0.5,1.0,2.0/
      DATA OOMEGA/6.551E-4,6.564E-5,6.659E-6,1.419E-6,7.683E-7,
     14.502E-7,2.057E-3,2.062E-4,2.067E-5,4.176E-6,2.115E-6,
     I1.085E-6,8.519E-3,8.588E-4,8.598E-5,1.723E-5,8.631E-6,
     34.333E-6,1.078E-1,4.001E-3,4.016E-4,8.037E-5,4.020E-5,
     42.012E-5,7.396E-1,3.069E-2,1.996E-3,3.998E-4,2.000E-4,
     51.000E-4,9.335E-1,3.080E-1,1.026E-2,2.069E-3,1.036E-3,
     65.182E-4,9.572E-1,7.708E-1,1.121E-1,1.438E-2,5.507E-3,
     72.761E-3,9.618E-1,9.099E-1,4.697E-1,1.119E-1,4.993E-2,
     82.133E-2,9.636E-1,9.456E-1,7.584E-1,3.656E-1,2.255E-1,0.0/
      PRINT 6
    6 FORMAT(1H1)
      DO 80 J=1,5
      AA=AAA(J)
      PRINT 7, AA
      DO 70 K=1,9
      ALPHA=AALPHA(K)
      OMEGA=2.0*OOMEGA(6*(K-1)+J)
C     TO NORMALIZE TO REAL NOISE RMS.
      SUM=0. $ FN=1.
      DO 60 NN=1,30
      N=NN-1
      IF(N.NE.0) FN=FN*N
      T=(((-AA)**N)/FN)*GAMMA(N*ALPHA/2.+0.5)
      SUM=SUM+T
   60 CONTINUE
      WO=SUM/(PI*SQRT(OMEGA))
      ARE=4.*WO*WO
      AREDB=10.*ALOG10(ARE)
      PRINT 8, ALPHA,OMEGA,WO,ARE,AREDB
   70 CONTINUE
      PRINT 9
   80 CONTINUE
    7 FORMAT(5X,1PE10.3,/)
    8 FORMAT(8X,5(1PE10.3,3X))
    9 FORMAT(//)
      END
```

FORM **NTIA-29**
(4-80)

U.S. DEPARTMENT OF COMMERCE
NAT'L. TELECOMMUNICATIONS AND INFORMATION ADMINISTRATION

BIBLIOGRAPHIC DATA SHEET

	1. PUBLICATION NO.	2. Gov't Accession No.	3. Recipient's Accession No.
	NTIA Report 83-120		

4. TITLE AND SUBTITLE
Optimum reception in nongaussian electromagnetic interference environments: II. Optimum and suboptimum threshold signal detection in Class A and B noise

5. Publication Date
May 1983

6. Performing Organization Code
NTIA/ITS.S3

7. AUTHOR(S)
David Middleton and A. D. Spaulding

9. Project/Task/Work Unit No.
910 1518

8. PERFORMING ORGANIZATION NAME AND ADDRESS
NTIA/ITS.S3
325 Broadway
Boulder, CO 80303

10. Contract/Grant No.

11. Sponsoring Organization Name and Address
NTIA/DoD
U.S. DEPARTMENT OF COMMERCE BLDG.
Washington, DC

12. Type of Report and Period Covered

13.

14. SUPPLEMENTARY NOTES

15. ABSTRACT *(A 200-word or less factual summary of most significant information. If document includes a significant bibliography or literature survey, mention it here.)*

The general theory of optimum and suboptimum detection of threshold (i.e., weak) signals in highly nongaussian interference environments is developed. Both signal processing algorithms and performance measures are obtained canonically, and specifically for both narrowband and broadband interference environments. Suboptimum systems are also treated and a number of numerical examples are included which illustrate the determination of performance and performance comparisons. An extensive set of appendices contains many of the analytic details developed and presented here as well as the required computational algorithms.

16. Key Words *(Alphabetical order, separated by semicolons)*

Threshold signal detection; optimum threshold detection algorithms; performance measures; performance comparisons; electromagnetic interference environments (EMI); suboptimum detectors; locally optimum and asymptotically optimum algorithms; Class A, B noise; correlation detectors; clipper-correlators; error probabilities; minimum detectable signals; processing gain; bias, EMI scenarios; composite threshold detection algorithms; on-off binary signal detection; non-gaussian noise and interference.

17. AVAILABILITY STATEMENT	18. Security Class. *(This report)*	20. Number of pages
☒ X UNLIMITED.	UNCLASSIFIED	346
☐ FOR OFFICIAL DISTRIBUTION.	19. Security Class. *(This page)* UNCLASSIFIED	21. Price:

☆ U.S. Government Printing Office: 1980—678-495/529